THE EFFECT OF MECHANICAL ACTIVATION ON ENERGETICS AND DISSOLUTION KINETICS OF INDIAN BEACH SAND ILMENITE

THESIS SUBMITTED FOR THE DEGREE OF

DOCTOR OF PHILOSOPHY

IN

METALLURGICAL ENGINEERING

By

C.Sasikumar

DEPARTMENT OF METALLURGICAL ENGINEERING
INSTITUTE OF TECHNOLOGY
BANARAS HINDU UNIVERSITY
VARANASI – 221005
INDIA

Enrolment No.309493 **2009**

CONTENTS

.

.

.

.

.

PREFACE

Mechanical activation is a non-equilibrium process of enhancing the internal energy of solids by mechanical processes such as high energy milling and high strain rate deformation through the accumulation of non-equilibrium defects. The activated solid is a thermodynamically and structurally unstable arrangement of the lattice components, exhibiting increased enthalpy and Gibbs free energy in comparison to the stable crystalline substance. In the mechanical activation process, the non-equilibrium energy is stored in the material as point and line defects, new surfaces and interfaces, volume defects in crystals and through structural rearrangement which can be utilized to reduce the activation energy during subsequent processing. In the present thesis, the effect of the mechanical activation through high energy milling was studied on energetics and the acid dissolution kinetics of Indian beach sand ilmenite samples.

The thesis consists of seven chapters. The salient features of each chapter are described below:

Chapter 1 comprises of introduction and literature survey of mechanical activation process. Various activation processes and distinguishing features of the mechanical activation process are discussed in detail. The manifestations of the stored energy during the mechanical activation process and its applications in subsequent processing are also discussed. Further, the application of the mechanical activation process as a pre-treatment for dissolution of Indian beach sand ilmenite samples is justified.

The literature survey summarizes the history of mechanical activation processes, milling equipments used in mechanical activation process, thermodynamic and kinetic aspects of mechanical activation, energy stored in the material and the effect of mechanical activation on the physical, chemical, structural, thermal and magnetic properties. Further, the use of mechanical activation as pretreatment in various mineral processing techniques is discussed in detail. The literature reported on processing of ilmenite samples also discussed.

.

The objective of the present thesis is described as:

1. To study the effect of mechanical activation process on physico-chemical, structural, thermal and magnetic properties of ilmenite samples.
2. To study the effect of mechanical activation process on energetics of ilmenite samples.
3. To find out effect of mechanical activation on subsequent dissolution behaviour of Indian beach sand ilmenite samples in sulphuric and hydrochloric acids.
4. To make a comparative study of physico-chemical and structural alterations induced by natural weathering and mechanical activation of Indian beach sand ilmenite samples and their effect on subsequent dissolution behaviour.

Chapter 2 describes the materials and experimental details of the present study. The details of the ilmenite samples collected for investigation, milling equipment used for mechanical activation and the experimental techniques used to characterize the energetics, physico-chemical, structural, thermal and magnetic properties of ilmenite samples are given in detail. Further the equipment used for dissolution study and the experimental procedures adopted to study the extent of dissolution are described in details.

The ilmenite concentrate samples used in the present study were collected from beach placer deposits located at Chatrapur, Navaladi, Manavalakurichi and Chavara in India. All the ilmenite samples were subjected to mechanical activation in a Fritsch Pulverisette-5 planetary ball mill having agate bowl and balls (Fritsch GMBH, Germany). The unmilled and activated samples of ilmenite were characterized with various techniques to study the alterations induced by mechanical activation on physico-chemical, structural, thermal and magnetic properties of ilmenite.

The unmilled and activated samples of different ilmenite concentrates were subjected to chemical analysis using conventional and EPMA with Standard Programme Intenational (SPI) mineral standards and on-line ZAF correction procedures. The mineralogical characteristics of the ilmenite

.

samples before milling were studied using a polarized optical microscopy under normal mode of illumination and with crossed nickel prisms. The phase constitution and structural parameters were characterized by X-ray diffraction analysis using Co-Kα radiation at a scan rate of 1^{o}/min. The analysis of line broadening in X-ray diffractograms and the determination of structure and lattice parameters were carried out using the software XRDA (X-ray diffraction analysis 1992ï 93). The variation in particle size distribution, and surface area of the ilmenite samples were investigated using a laser diffraction analyzer and a multipoint BET technique respectively. The changes in morphological and microstructurual characteristics were studied using scanning electron microscopy and transmission microscopy. Thermal and magnetic studies were performed using TG/DTA analyzer and vibrating magnetometer respectively. The energy stored in the material was characterized with energy meter, iso-thermal heat calorimeter, dissolution studies with acids, surface energy measurements using contact angle measurements and strain energy, energy of amorphization using x-ray diffraction techniques.

The ilmenite samples before and after milling were subjected to dissolution in sulphuric acid and hydrochloric acid. The experiments were carried out at various concentrations of sulphuric acid (1.8M, 5.5M, 9.2M and 12.9M) and hydrochloric acid (2.3M, 6.9M, 9.2M and 11.5M molar concentration of HCl) at various temperatures (80-120^{O}C).

Chapter 3 is a compilation of experimental results and discussion on the effect of mechanical activation on physico-chemical, structural, thermal and magnetic properties of the ilmenite samples. The properties studied include mineralogy, chemical composition, ferric to ferrous ratio, particle size and distribution, surface area, morphology, density, defect density, phase constitution, crystallite size, lattice parameters, strain, thermal oxidation, saturation magnetization and coercivity of the ilmenite sample before and after milling.

.

The beach sand deposits obtained from different regions have a significant difference in mineralogy and chemical composition because of the variation in the degree of weathering from the Orissa to Kerala coast. The mineralogical study showed that many ilmenite grains were moderately altered and the alteration appears to proceed along grain boundaries, grain edges, along crystallographic directions and fissures in varying intensity and pattern.

The particle size of Chatrapur ilmenite lies in the range of 100-500 μm in unmilled condition; whereas the particle size of Manavalakurichi ilmenite samples show a range of 12-400 μm. The initial BET surface area is higher for the Manavalakurichi ilmenite sample (6.13 m^2/g) compared to the Chatrapur ilmenite 1.46 m^2/g as it has undergone a higher degree of weathering compared to the Chatrapur ilmenite sample. The particle size decreases exponentially with milling time and reaches a steady state (0.04-15 μm) beyond 90 minutes of activation in both the ilmenite samples.

It was observed that both Chatrapur and Manavalakurichi ilmenite samples reveal smooth sub-rounded to sub-angular particles in unmilled condition. In contrast, the activated sample consists of particles in the submicron to micron range and is predominantly angular in shape caused by fracture of the original particles. The initial density of the Manavalakurichi sample is considerably lower than the Chatrapur sample because of the enhanced weathering. The density of Chatrapur and Manavalakurichi ilmenite samples shows an exponential decrease with the time of milling. The decrease in density can be attributed to the volume enhancement caused both by creation of defects leading to an increase in lattice parameter of the activated samples. The volumetric density of defects created in milling process was derived from the density derived from experimental procedure and theoretical density derived from x-ray diffraction analysis. The volumetric defect density shows an exponential variation with milling time.

The X-ray diffraction analysis of ilmenite samples in unmilled as well as in milled condition indicates predominantly ilmenite (JCPDS No.29-0733)

.

phase. The Chatrapur sample shows the traces of pseudo-rutile (JCPDS No.29-1494) and Hematite (ICDD 24-72) with ilmenite peaks and the pseudo-rutile phase could not be detected after 4 hours of milling indicating fine grained or undergone partial amorphization. The pseudo-rutile peaks are not observed in the Manavalakurichi ilmenite sample because of its likely presence in amorphous form; however, a significant amount of rutile phase (JCPDS No. 21-1276) was observed in both unmilled and activated samples of Manavalakurichi ilmenite. As the activation time increased, line broadening and shifting of the ilmenite peaks as well as the pseudo-rutile and rutile peaks occurred for the Chatrapur and Manavalakurichi samples respectively. The variation of crystallite size and strain with milling time was calculated from the line broadening of the ilmenite reflections using Scherrerôs formula. The crystallite size decreases exponentially with milling time in both the samples of ilmenite. However the non-uniform strain resulting from lattice defects increased exponentially with milling time. The lattice parameters of the ilmenite samples before and after mechanical activation were determined from XRD results using Cohenôs method. Both óaô and ócô parameters increased linearly with milling time. The variation in lattice volume and the uniform strain caused by the expansion of lattice volume was determined for the ilmenite samples subjected to different milling time. It was observed that mechanical activation resulted in a substantial increase in uniform strain and it shows exponential variation with milling time.

Mechanical activation also shows considerable alterations in thermal oxidation characteristics of ilmenite and minor changes in magnetic properties. The rate of oxidation of Fe^{2+} to Fe^{3+} was found to increase with increasing milling time. The unmilled sample shows less than 50% oxidation, however the activated samples show complete oxidation at $850^{O}C$. The magnetization at a field of strength 1200 kA/m found to be decreasing exponentially with milling time. On the contrary, the coercivity of the ilmenite sample showed exponential increase with milling time as there is a considerable variation in crystallite size, grain boundary volume, and structural disorder introduced by milling.

.

Chapter 4 describes the effect of mechanical activation on energetics of ilmenite samples. The results of direct energy measurements obtained using precise power measurement equipment and isothermal calorimetry are analyzed to find out the energy consumption of the mill, energy transferred to the material and the enthalpy of relaxation of defects. Further the indirect energy measurements using various characterization techniques such as, the changes in surface energy, grain boundary energy, strain energy and the energy of amorphization of ilmenite samples by mechanical activation are derived and discussed.

The energy consumption of the mill was studied in absence of material as well as in presence material under identical milling conditions. The energy transferred to the material was derived from the difference in specific energy consumption. The specific energy transferred to the material was found to be about 47.8 wh/mol (160 kJ/mol) for Chatrapur ilmenite subjected to 4 hours of milling. It was found that about 3% of the energy input to the mill was transferred into the material (Chatrapur ilmenite) in 4 hours of milling. The energy input to the mill and the fraction of the energy transferred to the material were measured for the different ilmenite samples obtained from Chatrapur, Navalady, Manavalakurichi and Chavara regions. It was observed that the specific power consumption of the mill as well as the energy transferred to the material under identical conditions of milling increased with increased weathering as the material characteristics were altered by the weathering process. The energy transferred to the material varied in the range of 3 to 8% after 4 hours of milling depending on the degree of alteration induced by weathering.

The relaxation of stored energy immediately after activation was studied in an aqueous medium at room temperature ($27^{O}C$) using an isothermal heat calorimeter. Only a partial relaxation of defects was observed as the relaxation depends on both temperature and time. The enthalpy of relaxation with milling time was derived from the isothermal calorimetric experiments and it was

.

observed that the enthalpy of relaxation of defects shows an exponential increase with milling time.

The variation in surface energy of the material with milling time was studied using contact angle measurements determined from tensiometric analysis. The surface energy of the material increased from 20 mJ/m^2 (10 J/mol) to 50 mJ/m^2 (40 J/mol) by 4 hours of milling of Manavalakurichi ilmenite. Further the fraction of stored energy as grain boundary energy was derived from grain boundary area and the specific grain boundary energy approximation given by Imamura and Senna (1982). The variation of grain boundary area with milling time was derived from the crystallite size measurements and using tetrakaidecahedron configuration of grains. The results show considerable enhancement in grain boundary area with milling time. The grain boundary energy exhibited an exponential increase with milling time. The grain boundary energy of the Manavalakurichi ilmenite sample increased from 10 mJ/m^2 (5 J/mol) to 20 mJ/m^2 (40 J/mol) after 4 hours of milling.

The elastic strain energy induced by mechanical activation was determined using Eshelbyôs equation derived from the theory of elasticity with the assumption that there was no change in shear and bulk modulus of the material during the process of mechanical activation. The strain energy contributed from both uniform strain as well as non-uniform strain showed an exponential variation with milling time. A large part of the stored energy was reflected as strain energy.

The energy required for quasi-amorphization/disordering was determined using the heat of fusion and heat capacity data were derived at room temperature (300K) and the fraction of amorphization derived XRD using integral peak areas by the method described by Ohlberg and Stickler (1969). A large part of the stored energy was also reflected as structural disorder. The energy stored as structural disorder was about 34 and 25 kJ/mol respectively

.

for the Chatrapur and Manavalakurichi ilmenite samples subjected to 4 hours of milling.

The stored energy of the material will be equal to the summation of energy changes contributed by the changes in surface energy, grain boundary energy, strain energy, and energy of amorphization. This was 75 kJ/mol for the 4 hours milled sample of Chatrapur ilmenite and 172 kJ/mol for Manavalakurichi ilmenite.

Chapter 5 discusses the results of experimental study carried out to find the effect of mechanical activation on acid dissolution behaviour of ilmenite samples. The dissolution characteristics in both sulphuric and hydrochloric acids were discussed. The effect of temperature, acid concentration, solid to liquid ratio and mechanical activation were described in detail. The difference in dissolution characteristics of ilmenite in sulphuric and hydrochloric acid are analyzed using Eh-pH measurements. The derivation of kinetic parameters for dissolution of Fe and Ti of mechanically activated ilmenite samples are discussed in details. The effect of surface area and structural disorder on rate constants was analyzed.

The dissolution study in sulphuric acid was carried out for all the ilmenite samples obtained from different regions of the country, both in milled and unmilled condition. The ilmenite samples from the different regions showed different physico-chemical characteristics and their resistance to acid leaching increased with the degree of alteration. However, for all samples it was observed that mechanical activation enhanced the dissolution kinetics in sulfuric acid several folds. The dissolution of Fe and Ti increased monotonically with time of milling and showed a sigmoidal increase with time of leaching. It was also observed that activated ilmenite dissolved incongruently in sulfuric acid i.e., the dissolution behaviour of Fe and Ti was different. The sulfuric acid dissolution kinetics in general conformed to the reaction rate control model. However, in a few cases where hydrolysis set in, the dissolution kinetics conformed initially to the reaction rate control model

.

and for higher leaching times to the shrinking core model where diffusion through the product layer is rate controlling. The activation energies for the dissolution of Fe and Ti were different and decreased monotonically with time of milling. An attempt has been made to correlate the decrease in activation energy to the increase in the energy input to the material through high-energy milling. The relative contribution of the increase in surface area and structural disorder/defects on the enhancement of the dissolution rates has been evaluated.

The effect of the change in phase constitution, particle size distribution, surface area, crystallite size, strain and lattice parameters introduced by mechanical activation on the dissolution kinetics in HCl was also investigated for the altered beach sand ilmenite from Manavalakurichi. The dissolution behavior was found to be different in HCl compared to that in H_2SO_4. For sulfuric acid leaching, the dissolution of Fe and Ti increased monotonically with time of milling and showed a sigmoidal increase with time of leaching, whereas the hydrolysis of titanium occurred in HCl medium, especially for the activated samples at lower acid concentration, lower solid to liquid ratio and higher temperature leading to lower solution recoveries. The dissolution kinetics in HCl prior to hydrolysis conformed initially to the reaction rate control model and for higher leaching times to the shrinking core model where diffusion through the product layer is rate controlling. The activation energies for the dissolution of Fe and Ti decreased with time of milling and were marginally lower in HCl than in H_2SO_4.

Chapter 6 is a comparative study between the effects of natural weathering and mechanical activation on ilmenite samples. The oxidation of ilmenite samples on weathering and mechanical activation is illustrated in this chapter. Further the effect of natural weathering and mechanical activation on physico-chemical, structural parameters and dissolution characteristics were compared.

.

The oxidation state of iron in ilmenite is a good indicator of the degree of weathering; the degree of alteration increased with the ferric to ferrous ratio. It was observed that the ferric to ferrous ratio increases in the order: Chatrapur ï Navaladi ï Manavalakurichi ï Chavara indicating that the Chatrapur sample is least altered and the Chavara sample has undergone maximum alteration. Similar to the weathering process, it is seen that the ferric to ferrous ratio increases with increase in milling time, although the extent of oxidation in mechanical activation is comparatively much lower. It was observed that the physical properties like specific gravity and crystallite size decreased while surface area as well as average pore size increases with increased in both natural weathering and mechanical activation. However the dissolution kinetics differs in natural weathering in comparison to mechanical activation. It was observed that the solubility of iron and titanium in sulfuric acid decreased significantly and their activation energies increased with increased weathering of the samples because of the oxidation of Fe^{+2} to Fe^{+3}. Although the mechanical activation process also resulted in increased ferric to ferrous ratio, the dissolution kinetics was substantially enhanced by the activation process. The enhanced dissolution kinetics in the mechanical activation process is attributed to the increase in strain and defect concentration introduced during the activation process despite the partial oxidation of Fe^{+2} to Fe^{+3}.

Chapter 7 presents the overall conclusions and suggestions for the future work. The summary of conclusions obtained in the experimental study of the effect of mechanical activation on physical, chemical, structural, thermal and magnetic properties are illustrated. The results of energetics of mechanical activation of ilmenite samples are summarized. Further the conclusions obtained in dissolution study of ilmenite samples are presented. The results obtained in the comparative study of natural weathering and mechanical activation is also summarized.

Mechanical activation resulted in substantial increase in structural disorder in addition to the enhancement in surface area because of milling to submicroscopic particles. The apparent density of all the ilmenite samples

.

decreased with milling time, due to the increase in lattice volume arising from the creation of defects. A partial amorphization/disordering of the pseudorutile and hematite phase were observed for the Chatrapur ilmenite sample after 4 hours of milling. The crystallite size of ilmenite samples decreased exponentially with milling time, whereas the non-uniform strain and the uniform strain from lattice volume expansion increased with milling time. In terms of the physico-chemical characteristics, mechanical activation was found to have a similar effect as compared to natural weathering on ilmenite.

The specific power consumption in the planetary mill was found to depend on the degree of alteration of ilmenite. Chatrapur ilmenite: 5865 kJ/mol; Manavalakurichi ilmenite: 6053 kJ/mol. The energy transferred to the material varied in the range of 3.0 to 8.0 % in 4 hours of milling depending on the degree of alteration of the ilmenite. Part of the energy transferred to the material was found to be stored as additional surfaces and interfaces point, line and volume defects, high energy structures and lattice strain. Part of the defect energy stored in the activated ilmenite samples was found to relax much faster. Chatrapur ilmenite and Manavalakurichi ilmenite exhibited 19 kJ/mol and 12 kJ/mol respectively. A large part of the stored energy was reflected as strain energy. The energy stored through additional surfaces and grain boundaries (GB) was much lesser. These are quoted as strain energy: 24 kJ/mol ; Surface energy: 0.01 kJ/mol ;GB Energy 0.02: kJ/mol.

The Ti and Fe in the ilmenite dissolves incongruently and not according to their stoichiometry in the ilmenite phase. Mechanical activation considerably enhanced the dissolution kinetics for both Fe and Ti. However the extent of dissolution decreased with natural weathering as Ti rich phases increased. The dissolution kinetics of ilmenite in hydrochloric acid was marginally favorable compared to that in sulfuric acid. However, the enhanced dissolution of Ti in HCl for the activated sample is affected by the hydrolysis reactions. The dissolution kinetics in HCl (prior to significant hydrolysis) and in H_2SO_4 was found to conform to the reaction rate control model for the initial leaching period and thereafter to the shrinking core model where product layer diffusion

.

is rate controlling. The activation energies for dissolution of Fe and Ti decreases monotonically with milling time. The activation energy for dissolution of Fe and Ti was higher in H_2SO_4 compared to HCl.

The ferric to ferrous ratio increased with both natural weathering and time of milling. Natural weathering resulted in the formation of new Fe^{+3} and Ti-rich phases whereas mechanical activation was found to result only in partial amorphization/disordering of some of the existing phases. The enhanced dissolution kinetics in the mechanical activation process is attributed to the increase in strain and defect concentration introduced during the activation process.

.

ACKNOWLEDGMENTS

The research work presented in this thesis was carried out under the supervision of Dr. S. Srikanth (Scientist-in-Charge, National Metallurgical Laboratory Madras Centre) and Professor N.K. Mukhopadhyay (Department of Metallurgical Engineering, Institute of technology, Banaras Hindu University).

I would like to express my sincere thanks and gratitude beyond words to my supervisors, Dr. S. Srikanth and Professor N.K. Mukhopadhyay, for their expert guidance and constant encouragements through out the entire duration of my Ph.D. work. Dr.S. Srikanth and Professor N.K. Mukhopadhyay have introduced me the area of mechanical activation. Their stimulation and encouragement influenced me to continue research in the area even in difficult situations. Dr.S. Srikanth has shown me insights into the thermodynamics and kinetics of mechanical activation process. Professor N.K. Mukhopadhyay guided me to have a real feel about the characteristics of the material being milled.

I would like to pay my sincere thanks to Prof. Shamsuddin (Head, Department of Metallurgical Engineering, Institute of Technology, Banaras Hindu University), Prof. S.P. Mehrotra (Director NML, Jamshedpur) and Professor R.C. Gupta, Professor S.N. Ojha (Former Head, Department of Metallurgical Engineering, Institute of Technology, Banaras Hindu University) for providing me an all the facilities and all other helpful actions which were necessary for this research work.

I express my gratitude and thanks to Professor P. Ramachanrda Rao (Hon'ble vice chancellor (former), BHU) and Professor S. Lele (Hon'ble Rector (former)) for their needful help and encouragement in carrying out the research work.

I express my sincere thanks and gratitude to Professor S.N. Ojha, Professor Vakil Singh, Professor R.K. Mandal, Professor G.V.S. Sastry, Professor T.R. Mankhand, Mr. Rampada Manna, Dr. N.K.Prasad, and Mr.J.P.

.

Goutam from Department of Metallurgical Engineering, Institute of Metallurgical Engineering, Banaras Hindu University, Dr. G. Bhaskar Raju (Scientist, NML Madras Centre) and Dr. S. Prabhakar (Scientist, NML Madras Centre) for their valuable comments and suggestions.

I acknowledge Dr. T. Sankaranarayanan (Scientist, NML Madras Centre) for his invaluable guidance in chemical analysis. I am grateful to Dr. D.S. Rao and Dr. B.R.V. Narashimman for their invaluable guidance and support in carrying out the mineralogical study and chemical analysis. My special thanks go to Mr. Satendra Kumar (NML MC) for his help in chemical analysis.

I am thankful to Mr. B. Ravikumar for his assistance in carrying out XRD, Dr. Rakesh Kumar, Dr. T.C. Alex and Dr. Sanjay Kumar for assistance in the calorimetric studies and Mr.Swapan Das for help in SEM analysis. My thanks also extended to Dr. P.A. Joy of NCL Pune for the magnetic measurements. I would like to thank Mr. T.P. Yadav (Research Scholar, Department of Physics, Banaras Hindu University) for his extensive help in carrying out TEM studies.

I am thankful to Dr. Santwana Mukhopadhyay (Dept. of Appl.mathamatics, IT-BHU), Dr. S. Subba Rao (Scientist, NML MC), Mr. T.C. Manoharan (Scientist, NML MC), Mr. V. Vijaya kumar (Scientist, NML MC), Mr. R. Gopalakrishnan (Technical Officer), Mr. K. Gopalakrishna (Scientist), Mr. Anand Rao (Scientist, NML MC), Mr. A. Rajkumar (Tech. officer, NML MC), Mr. A. Ramesh (NML MC) and Dr. Niddhi singh, (Scientist, NML MC) for their encouragement and assistance.

I also express my sincere thanks to Dr. M. Muthukumar (Bharathiar University), Mr. Dibyendu Mukherjee (Research Scholar, Dept. of Met.Engg., IT-BHU), Mr. Roushan Kumar (Research Scholar, Dept. of Applied Mathematics, IT-BHU), Mr. M. Kumar (Research Scholar, NML MC), Mr. Laksmipathy Raj (Research Scholar, NML MC) and Mr. Chenna K. Reddy (NML MC) for their precious help in carrying out the research works.

.

I also convey my thanks to all my friends and colleagues at the NML Madras Centre and in the Department of Metallurgical Engineering IT-BHU for their companionship and help.

I am deeply indebted to CSIR for financial support through the award of several fellowships (JRF and SRF) during the period of my research.

I acknowledge Indian Rare Earths Limited, located at Chatrapur, Manavalakurichi, Chavara and Indian Oceanographical Survey limited, Navalady for supplying the ilmenite concentrate samples.

I am indebted to my parents, my teachers and my country. Above all I express my sincere thanks to my supreme father, GOD for providing me the opportunity to do research.

Sasikumar Chandrabalan

.

ABBREVIATIONS AND NOTATIONS

$\breve{U}$	-	fraction of solid material dissolved
β	-	Fraction of dissolution sites on step edges
γ_S	-	Specific surface energy of the material
γ_{gb}	-	Specific grain boundary energy
ε	-	Lattice strain induced during milling
ρ	-	Density of the material
θ_D	-	Angle of diffraction
θ_C	-	Contact angle between the liquid and solid
η	-	The viscosity of the liquid
$\mathring{u}_l$	-	Surface tension of the liquid
μ	-	Shear modulus of the material
K	-	Bulk modulus of the material
$c.\bar{r}$	-	The material constant describing the orientation of micro capillaries and the mean radius in tensiometry
λ	-	Wavelength of the radiation used
ΔA_{GB}	-	Change in grain boundary area
ΔA_S	-	Change in surface area
A_p	-	Pre-exponential factor
A_S	-	Rate coefficient for dissolution at steps
A_T	-	Rate coefficient for dissolution at terraces
B_0	-	Instrumental line broadening
B_t	-	Full width at half maximum (FWHM) intensity of the peak
C	-	Molar concentration of acid
Cp	-	Molar heat capacity at constant pressure
D_M	-	Mean particle diameter
$D_{unmilled}$	-	Mean particle diameter of unmilled sample
D_{milled}	-	Mean particle diameter of milled sample
D_{Cry}	-	Average crystallite size

.

E_{amor}	ï	Energy of amorphization
E_S	ï	Energy coefficient for surface energy
$E_{Ů}$	-	Energy coefficient for lattice strain energy
E_D	ï	Energy coefficient related to reduction of crystallite size
E_{QA}	ï	Energy coefficient for quasi-amorphization
E_Y	-	Youngôs modulus of the starting material
Ea	-	Apparent activation energy of the stable solid prior to activation
Ea^*	-	Apparent activation energy of the activated material
Ea_T	-	Activation energy for dissolution from terraces
$qpEa^*$	-	Change in activation energy of the material
ΔE_M	-	Internal Energy change of the milled material
ΔE_G	ï	Internal Energy change of Grinding Media
E_{latt}	-	Lattice energy of starting material
ΔE_{SE}	-	Change in surface energy of the material
$qpE_{Ů}$	-	Change in elastic strain energy
ΔE_{GB}	-	Change in grain boundary energy
F_r	-	The surface roughness factor
f_{trans}	ï	Fraction of other structural transformations
f_{Amor}	-	Fraction of amorphization
G_M	-	Gibbs free energies of the material in non-activated state
G_M*	-	Gibbs free energies of the material in activated state
ΔG_M	-	Change in Gibbs free energy of the material
H_M	-	Enthalpy of material in non-activated state
H_M*	-	Enthalpy of the material in activated state
H_i	-	Enthalpy required to transfer a lattice element to the i-th state
ΔH_M	ï	Enthalpy change of the material being ground
$\Delta H_{def,rel}$	-	Enthalpy of point, line and surface defects that has short relaxation times
ΔH_G	ï	Enthalpy change of the grinding media
qpH_F	-	Enthalpy of fusion

.

ΔH_{trans} - Enthalpy change associated with other structural transformations

ΔH_{amor} - Enthalpy of amorphization

ΔH_K - Cohesive work of dissolution

ΔH_S - Enthalpy of solvation

ΔH_R - Enthalpy of the reaction

Io - Integral intensity of the non-activated material

Ix - Integral intensity of the activated material

k - The rate constant of the non-activated material

k* - The rate constant of the activated material

L - Average distance between cations in the solid lattice

M_f - Ratio of the rate coefficients for dissolution at steps to the terraces

M - Molar weight of the sample

n - Order of reaction

N_i - N_i is the number of lattice elements in the i-th energy level

N_A - Avogadroôs number

N_G - Number of grains per unit volume

N_S/N_A - The relative number of atoms or ions at the surface

$NÚ/N_A$ - The relative number of atoms or ions in plastically deformed structure

N_{GB}/N_A - The relative number of atoms or ions at the grain boundaries

N_{QA}/N_A - The relative number of atoms or ions in the quasi-amorphous regions

qpP - Change in pressure of the system during activation process

Q - Heat evolved during milling process

R - Gas constant

R_S - Rates of dissolution from steps

R_T - Rates of dissolution from terraces

R_F - Ratio of the rates of dissolution from steps (R_S) and terraces (R_T)

S_M - Entropy of material in non-activated state

S_M* - Entropy of the material in activated state

.

t	-	time
t_{rel}	-	Ratio of the total time for dissolution of a stepped particle relative to the time for dissolution of a spherical particle of the same mass
T	-	Absolute temperature
Uo	ï	Background intensity of non-activated material
Ux	-	Background intensity of activated material
Vo	ï	Unit cell volume before Mechanical Activation
Vi	-	Unit cell volumes after Mechanical Activation
V_{mol}	-	The molar volume of material being milled
ϕV	-	Change in volume during activation process
W	ï	Total Mechanical Work Input into the mill during milling
w_L	ï	Weight of the penetrating liquid
X_A	-	Degree of Amorphization
X_X	-	Degree of crystallinity

.

CHAPTER 1

REVIEW OF LITERATURE

1.1 Introduction

The various forms of energy (kinetic, potential, electromagnetic etc.,) and the mechanisms of conversion of energy from one form to another has always fascinated alchemists, chemists, physicists, engineers and scientists alike from time immemorial. Any form of energy can be converted to any other form of energy: only the extent and efficiency of conversion varies. The process of activation of materials can be described as a treatment involving any form of energy (potential, kinetic or electromagnetic) to enhance the potential energy of the material and resulting in a chemical or physical change. This enhanced non-equilibrium potential energy can be utilized during its subsequent processing (Tkacova, 1989; Balaz, 2000). All forms of energy can be used to enhance the potential energy of a material. Various techniques such as thermal, mechanical, chemical, photochemical, ultrasonic, sonochemical, microwave, and irradiation can be adopted for activating a material. The enhanced potential energy of the material manifests itself as increased specific surface area, increased vacancy and dislocation concentrations, enhanced grain boundary area, structural disorder, a higher energy metastable phase, higher oxidation states, alteration of the bond length/bond angles/bond energy and increased energy level of electrons. However, each activation process has its own characteristics in terms of energy transfer and its efficiency and field of application.

The enhancement in the potential energy of materials using mechanical forces is used for grinding (mechanical milling), alloying (mechanical alloying), chemical transformations (mechano-chemical synthesis), plastic deformation at high strain rates (severe plastic deformation) and non-equilibrium defect and structural energy enhancement (mechanical activation). In the mechanical activation process, the materials are subjected to high energy

.

milling using specifically designed energy intensive mills. Fig 1.1 shows the schematic diagram of mechanical activation process.

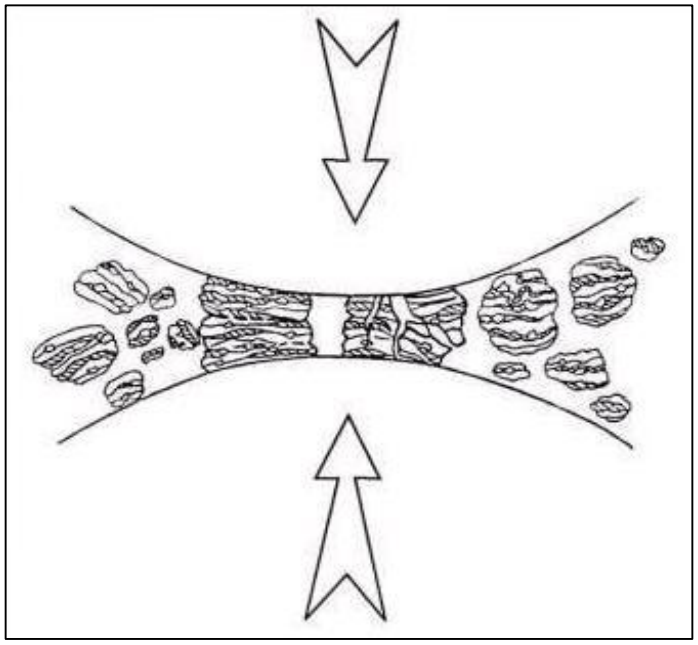

Fig.1.1 Schematic diagram representing mechanical activation process

Mechanical activation is similar to fine grinding of materials; the difference being that the activation effect achieved is over and above the surface area effect achieved in fine grinding. However, there is a limitation for grinding of powder particles, beyond which there is no fragmentation or reduction in particle size. For brittle materials such as minerals, the fracture stress is generally lower than the yield stress and therefore continuous fracturing of surfaces occur as stress is increased. However, as the particle sizes becomes smaller, the fracture stress increases more than yield stress and beyond a critical particle size, the fracture stress is higher than the yield stress resulting in plastic deformation rather than fracture. The repetitive input of mechanical energy into the material increases the concentration of defects and stress field around the defects. The stress field created by mechanical action will be elastic or plastic in nature and it will undergo relaxation in the course of time. However, depending on the time elapsed after activation; relaxation processes are not complete and hence part of the stress is stored in the material.

.

Thus, mechanical activation is interplay between the stress field creation, relaxation and energy stored in the material. There are various micro processes with varying relaxation times occurring during and after the process of high energy milling. The various possible micro processes and their time of relaxation (Balaz, 2000) are shown in Fig.1.2.

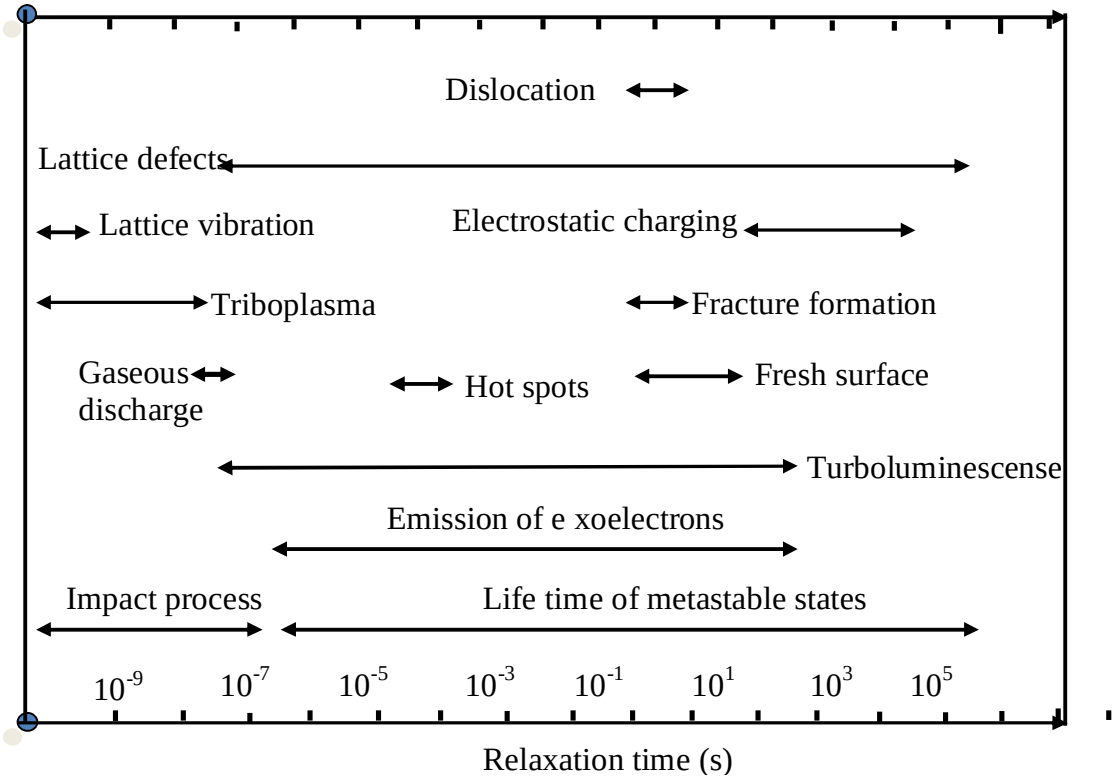

Fig. 1.2: The relaxation time for various effects introduced by mechanical activation (Balaz, 2000).

It is observed that lattice defects, electrostatic charging, turbo luminescence, emission of exo-electrons and fresh surface creation has a longer time of relaxation (10-10^5 secs) compared to the other processes.

Mechanical activation also induces chemical/phase transformations in some of the materials. The fundamental mechanism by which the mechanical work is converted to chemical energy is important for the analysis of mechano-chemistry. There are two schools of thought on this (Thiessen et al, 1967; Boldyrev, 1972). One school (Boldyrev, 1972) assumes that the conversion of mechanical to chemical energy occurs through an intermediate conversion to thermal energy. According to this, mechanochemical reactions proceed at ñhot

.

spotsò at the contact zones where very high temperatures are attained. Another group (Thiessen et al, 1967) proposed a triboplasma model based on the idea that an impact of sufficient intensity results in a quasi-adiabatic energy accumulation. There is also a phonon theory of disintegration of solids based on the release of phonons because of the interaction of the dislocations created by mechanical activation with other dislocations, defects, or grain boundaries (Bretenev et al, 1969). The weakness of all these models is that they consider only one mode of energy dissipation. The various possible energy dissipation processes that can occur when mechanical energy is provided as input into a solid, are shown in Fig.1.3.

Activation of solids is enhancement of its potential energy

- Step diagram for energy dissipation

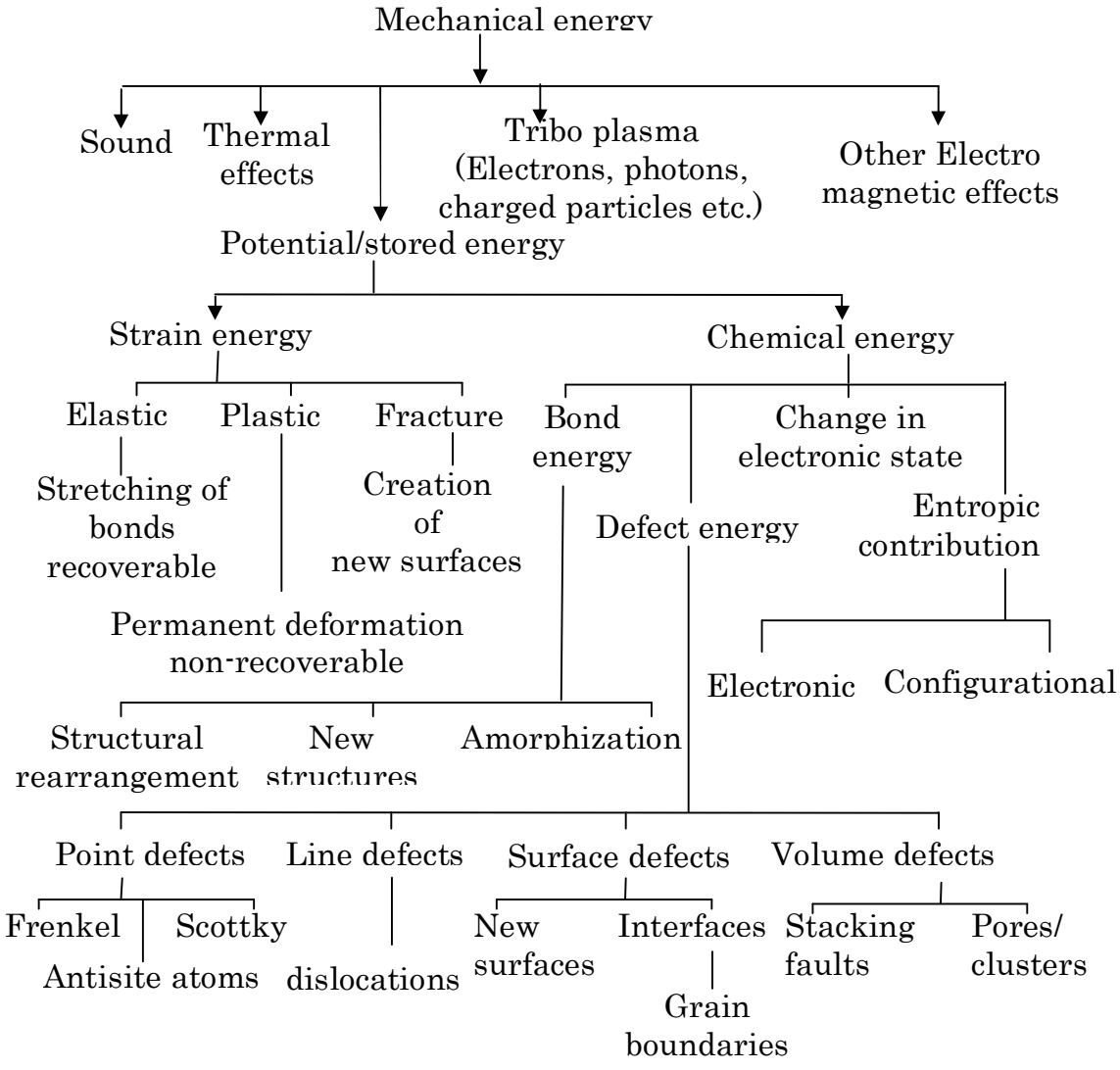

.

Fig. 1.3: The various possible energy dissipation processes that can occur when mechanical energy is input into a solid.

A part of the kinetic energy input or the mechanical work done on the solids through compression, shear and impact results in the creation of fresh surfaces and partial storage in the solid as chemical and strain energy. A large part of the mechanical energy transforms to heat, some gets dissipated as sound and some energy is expended in the various electromagnetic processes. Shear and compressive stresses possibly result in accumulation of structural defects at the surface and in the near-surface layers whereas the impact stresses possibly results in defects that are uniformly distributed through the entire volume of the material. The strain energy stored could be either elastic which is recoverable or plastic, which is irreversible. The lattice defects such as point, line and surface/interface defects such as low angle and high angle grain boundaries enhance the strain energy of the materials. The chemically stored energy can manifest through bond energy changes such as in structural rearrangement, or result in new structures or complete disordering as in amorphization or result in a change in electronic state or Fermi energy. Mechanical stress also results in various emission phenomena. Balaz (2000) and Tkacova (1989) have discussed these in details.

The total mechanical work done during milling as well as the energy that is stored in the materials will depend on the impacting material and their mass, the impact processes occurring and their dynamics as well as the nature of the material being milled and itôs mass. Depending on the mode of transfer of external energy, mechanical activation can be achieved in a variety of mills such as planetary mills, attrition mills, vibratory mill, tumbling mill, jet mill, ball mill etc., both in dry and in wet medium. However, the specific mill power and the specific energy transferred to the solid particles will depend upon the type of mill as well as the grinding medium of milling. For a ball mill, the specific mill power is 30-50 kWt^{-1}, for a vibratory mill it is 250-4500 kWt^{-1}, for an attrition mill it is 900-14000 kWt^{-1} and for the planetary mill it is 9000-

.

36000 kWt^{-1} (Tkacova, 1989). It is estimated that about 5-15% of the specific mill power can be transferred to the material being milled, which redistributes as surfaces and structural defects.

The mechanical activation process causes changes in physical, chemical, and structural properties of the materials. The energy stored in the material is used in further processing. The mechanical activation processes has potential for extensive application in the field of extractive metallurgy of complex and refractory minerals. In metal extraction processes of complex minerals, the leaching/dissolution is the slowest step. The rate of leaching of mineral samples can be considerably enhanced by mechanical activation processes. There are several reports in the literature on the enhancement of dissolution kinetics of various minerals induced by mechanical activation. These have been comprehensively reviewed by Ballaz (2000), Tkacova (1989) and reported a reduction in activation energy and improved rate of leaching in dissolution of Chalcopyrite, Pentlandite, Galena, Sphaleraite, Tetrahedrite, Stibnite, Enargite and gold and silver bearing minerals. Several pilot scale processes based on mechanical activation have also been reported. Pawlek (1977) investigated and patented copper extraction using wet grinding of chalcopyrite. He achieved complete extraction of copper into solution in 30 minutes of activation-leaching. The leaching of mechanically activated chalcopyrite concentrate was tested on an industrial scale in the LURGI-MITTERBERG process (Turke et al., 1978). The leachability of copper increased from 20% to 96% with an energy input of 300 $kWht^{-1}$. The ACTIVOX^{TM} process was developed in Australia to enhance the bacterial oxidation of sulphide minerals (Angov, 1993). Using this process the recovery of nickel was extended from 50% to 97% by mechanical activation. Further the processes IRIGETMET (Mullov et al., 1979), SUNSHINE (Anderson et al., 1993) and METPROTECH (Liddell and Dunne, 1988) were developed on pilot scale and industrial scale to enhance the leachability of gold using mechanical activation treatment.

India is endowed with large resources of ilmenite with an estimated reserve of around 278 million tons amounting to 20% of the total world

.

reserves. Fig. 1.4 shows the coastal regions of Indian subcontinent, where ilmenite occurs in beach placer deposits (Dwivedy, 1999; Mukherjee, 2000).

Fig. 1.4 Locations of Coastal regions of India, where ilmenite occurs as a placer deposit.

Other than being a major resource for the paint and pigment industry and for titanium metal and alloys, ilmenite finds application in plastics, welding-rod coatings, and ceramic industries and in production of synthetic rutile. A major part (94%) of the ilmenite is used in pigment production. The common method used for the production of pigment grade TiO_2 is the chloride process (Murty et al, 2004; Becher, 1963) and sulfate process (Mukherjee, 2000). About 40% of the worldôs and 50% of Indiaôs pigment grade TiO_2 production is through the sulfate route (Mukherjee, 2000). However, the kinetics of dissolution of ilmenite is the slowest step in ilmenite processing. Several methods have been proposed for the enhancement of the dissolution rate of ilmenite. Reduction and/or oxidation pretreatment followed by leaching with acids/bases as well as direct pressure leaching of ilmenite concentrate

.

have been reported (Sinha, 1973; Sinha, 1979; Farrow and Ritchie, 1987; Walpole, 1997; Balderson and McDonald, 1999; Natziger and Elger, 1987; Ogasawara and Velso de Araiya, 2000; Jayasekera et al, 1995; Balaz, 2003). Methods involving high temperature and high-pressure increases the cost of operation and imposes stringent safety requirements.

The influence of mechanical activation on the subsequent dissolution of mineral samples has recently attracted attention (Duncan and Metson, 1982a, 1982b; Tkacova and Balaz, 1996; Balaz, 1996; Balaz et al,1992; 1996; Welham and Llewellyn, 1998; Amer, 2000; Welham, 2001; Amer, 2002; Boldyrev, 2006). In the present thesis, the Indian beach sand ilmenite samples were subjected to mechanical activation and the enhancement in kinetics of dissolution was investigated in detail with hydrochloric and sulphuric acids. The beach sand ilmenite grains alter by natural weathering and oxidation phenomena giving rise to many altered phases (Suresh Babu et al, 1994). In some respects, it may be expected that the mechanical activation process at ambient conditions can simulate the natural weathering/alteration process occurring on a geological time scale. Subsequently the dissolution behavior of ilmenite may be altered by the oxidation process. Therefore, a comparative study was carried out to analyze the similarities in the effects of natural weathering/alteration and mechanical activation on the physico-chemical characteristics of the Indian beach sand ilmenites and their subsequent acid dissolution behavior.

1.2 Historical background

The activation of materials using mechanical energy dates back to the Stone Age. Mechanical energy was used on flint stones to make fire. During the period of Aristotle (371-286 BC), (John, 1774; Takacks, 2000) his student Theophrastus wrote a book titled ñOn Stones or de lapidusò which described the production of mercury from cinnabar using mechanical energy. The metal (mercury) is reported to have been obtained from mercury sulphide (native cinnabar) through grinding in a brass mortar with a brass pestle in the presence of vinegar. The mechanochemical reaction can be written as (Balaz, 2003)

.

$$HgS + Cu \rightarrow Hg + CuS \quad \text{.....(1.1)}$$

$$\Delta G = 4817 - 26.982\ T\ J;\ \ \Delta G_{300K} = -3278\ J$$

The first systematic investigation on the effect of mechanical energy on materials was made by an American chemist Carey Lea (1892; 1893; 1894). He published papers on the decomposition of gold, silver, platinum and mercury halides using mechanical energy. In his work, he clearly differentiated the mechanically activated reactions from thermally activated reactions. During the same period, Oswald (1887) wrote a book titled ôText book on general chemistryô in which he classified various methods for the stimulation of chemical reactions and introduced the term ñmechanochemistryò. This term refers to the chemical reactions initiated or pre-activated by mechanical energy. Immediately following that, the studies on the solid state reactions induced by mechanical energy was initiated in Russia by Flavickij (1909). He studied the effect of mechanical energy on the reactivity of powder particles. Later, the investigations were continued at different universities of Russia with a scope of development of a method for qualitative analysis of ores and minerals (Boldyrev et al, 1953), to improve the shock sensitivity of explosives (Sukhikh, 1947) and in production of polymers (Russanov, 2000 and 2002). In Germany, mechanical action is described as trituration and Parker (1914; 1918) carried out a detailed investigation on the chemical reactions induced by trituration. The method of trituration was later applied to qualitative analysis of natural mixtures in geology (Isakov, 1950). In 1920ôs the research study of mechanochemistry on organic macro molecules (Wanetig, 1922; 1925; 1927) attracted the attention of many authors. During 1940 to 1950, research studies were carried out on mechanically induced phase transformations on minerals (Clark and Rovan, 1941). Peter (1962) carried out a systematic study on mechanochemical reactions and proposed that all kinds of solid-state reactions can be observed during milling, beginning with simple decomposition reactions and ending with complicated syntheses from multicompartmental systems. During 1960ôs, many experimental techniques were developed to study the effect of mechanical energy on solid state systems (Rebinder, 1947; Karasev et

.

al.,1953; Schaider and Tetzner, 1961; Cottrell, 1964; Kodakov and Rebinder, 1966; Kubo, 1968). Subsequently, many researchers have contributed to the development of mechanochemistry and mechanical activation processes (Lin et al., 1975; Boldyrev and Avvakumov, 1971; Butyagin, 1971; Thiessen et al, 1967; Boldyrev, 1972; Stroiizdat Tallin, 1977; Heegn, 1979;1986; 1987; Tkacova, 1989; Balaz, 2000; Boldyrev and Tkacova, 2000, Suryanarayana, 2004, Boldyreva, 2003).

Mechanochemistry found industrial utilization in the second half of the last century and has since been used for several applications (Balaz, 2000; Tkacova, 1989; Boldyrev, 2006; Aresta et al., 2005, Mehrotra, 2006; Suryanarayana, 2001; Balaz, 2001). The most common applications include hydrometallurgical processing of minerals (Balaz,2000; Kulebakin, 1988; Turke et al., 1978), acid-free production of fertilizers from natural phosphates (Boldyrev, 1977; Chaikina, 2002), production of pure metals, materials for hydrogen storage, magnetic materials, catalyst, sensors, oxide dispersion strengthened (ODS) super alloys, nanostructured materials, synthesis of novel phases, solders, carbides, nitrides and silicides (Balaz, 2001; Suryanarayana, 2001;2004). Today, mechano-chemical methods are actively employed in pharmaceutics for the production of medicines (Shaktshneider and Boldyrev, 1993; 1999; Boldyreva, 2003; Boldyrev, 2004), in production of pigments and cosmetics (Gregoreva et al., 2003), in processing of organic wastes including poly , bromo- and chloro- containing aromatics (Zhang et al., 2002) and in extraction of phenol from aqueous solution (Lapids et al., 1998).

The application of mechanical energy to chemical processes has several variations and is referred in the literature by various terms: mechanical alloying (MA), high energy milling (HEM), reactive milling (RM), mechano-chemical processing (MCP) and mechanical activation (Suryanarayana, 1999; 2004). The milling process carried out with the aim of mixing powders of different metals, alloys or compounds are termed as mechanical alloying (MA). Material transfer is involved in this process to obtain a homogeneous alloy. Whereas milling of pure metals, intermetallics, or prealloyed powders, which has

.

uniform composition are termed as mechanical milling (MM) (El-Eskandarany et al., 1990). The destruction of long-range order in intermetallics to produce either a disordered intermetallic or an amorphous phase has been referred to as mechanical disordering (MD) (Weeber et al, 1986). There is no material transfer in mechanical milling (MM), and mechanical disordering (MD), as the homogenization is not required. The objective of these processes is, reduction of particle size or structural deformation. The mechanical milling is also referred as mechanical grinding (MG) by some of the authors. Generally the term grinding is used where mainly shear stresses and chip formation is involved and the term milling is used where complex triaxial stresses as hydrostatic stress are involved (Jang et al., 1975).

Some of the investigators often used the terms mechanochemical processing (MCP), mechanochemical synthesis, or mechano-synthesis which refers to the milling process in which chemical reaction and phase transformation takes place due to application of mechanical energy. Researchers often used the term mechano chemical reaction (MCR) to refer to the chemical reaction induced by mechanical milling and reaction milling (RM) to refer to the solid state reactions induced by milling process. On the other hand the term mechanical activation refers to the milling process where there is no chemical reaction involved. The materials are been activated to a high energy state by structural disordering caused by mechanical activation.

Ostwald defined mechanochemistry as ña branch of chemistry dealing with the chemical and physico-chemical changes of substances in all states of aggregation (Flavickij, 1902).ò Later, Huttig (1943) postulated that mechanochemistry includes only release of lattice bonds without formation of any new substances. In the 80ôs, Heinicke (1984) carried out several investigations on mechano-chemical reactions and proposed that it is possible to carry out reactions that are not feasible by equilibrium thermodynamics. He defined mechano-chemistry as: ña branch of chemistry which is concerned with chemical and physico-chemical transformations of substances in all states of aggregation produced by the effect of mechanical energyò.

.

The first study on the effect of mechanical activation on the thermodynamic properties of solids was initiated by Huttig (1943). He defined the activated state to be a thermodynamically and structurally unstable configuration at all temperatures below the melting point. However the term ómechanical activationô was first introduced by Smekal in 1942. He defined mechanical activation as a process of increasing the reaction ability of a substance which remains unchanged. If there is a change in composition or structure of the material, then it is called ómechanochemical reactionô. This definition is solely based on the observed effect. The observations of Peters et al., (1962) show that the transformations due to mechanical stress of material are accompanied by chemical reaction.

Butjagin (1984) considered mechanical activation from three aspects: structural disordering, structural relaxation, and structural mobility. Under real conditions, all the three factors simultaneously affect the reactivity of a solid. He defined mechanical activation as an increase in reaction ability due to the changes in solid structure. However, structural relaxation plays an important role in the reactivity of solids. Ljachov (1994) described mechanical activation as a state slowly changing with time. He proposed a generalized relaxation curve for activated solids. He discussed that various parts of the curve correspond to the different processes with different times of relaxation. Based on the time of relaxation, the processes were classified as short-lived and long-lived. The process which has a very short time of relaxation has no effect on reactivity of the solid. Only the processes with longer relaxation times have an influence on the reactivity of the solid. The effect of mechanical activation is relaxed as heat, fresh surfaces, aggregation, recombination, adsorption, imperfections and chemical reactions between adjoining particles. Thus, mechanical activation is a multi-step process with changes in energetic parameters and the accumulation of energy within the solid.

Juhasz (1974) classified the various processes during mechanical activation as primary and secondary processes. The primary processes include increase in internal energy, surface energy, surface area and decrease in

.

coherence energy of solids. The secondary process includes aggregation, adsorption and recrystallization.

Malcanov et al., (1988) investigated the various stages during the mechanical activation process and grouped them into four major steps. In the first step the stress is less than the strength limit of the solid. In crystalline substances, the atoms are deflected from the normal position. The crystal lattice is disordered and the intermolecular, interatomic, and interionic distances as well as angles of orientation alter. In the second step, new surfaces are created. Mechanical energy input to the material is transformed into surface energy and the energy state of the solid changes. In the third step, energy is accumulated at surface and interface layers. There is a significant change in the structure and properties of the solid. In the fourth step, the solid loses its original identity and turns into a substance having different structure, properties and composition.

1.3 High energy milling equipments

In general the milling devices can be classified into three categories based on the objective of combination process (Boldyrev et al., 1996) as coarse grinding, fine grinding and mechanical activation. The size reduction is the prime aim in coarse grinding and fine grinding or fine milling operations. The term fine grinding is used for size reduction below 100 µm and ultra fine grinding for particles below 10 µm (Bolyrev, 1983; Balaz, 2000). However the objective of mechanical activation processes is not the size reduction, but to create structural changes, which enhance the reactivity of the substances (Boldyrev, 1983). Thus the milling equipment used for mechanical activation must have sufficient energy intensity to create the structural changes in the materials. Boldyrev (1996) described two conditions for activation to take place i.e. the particles should have a size lesser than tough-brittle transition and the stress-intensity of the mills used for activation, should be higher than that of tough-brittle transition. Otherwise the activation is not possible only the size reduction occurs. The milling equipment used for mechanical activation are generally termed as high energy milling equipment.

.

There are various types of stresses are involved in high energy milling devices. The main types of stresses responsible for effective grinding includes compression, shear (attrition), impact (stroke) and impact (collision) (Heinicke, 1984). In general the ball mill, planetary mill, vibration mill, attritor or stirring ball mill, pin mill and roll mills are used in high energy milling processes. The principle of operation and stress intensity of some of the mills used for mechanical activation are described below.

1.3.1 Ball mill

Fig 1.5 shows the schematic diagram of ball mill used for high energy milling of materials (Suryanarayana, 2004; Balaz, 2008).

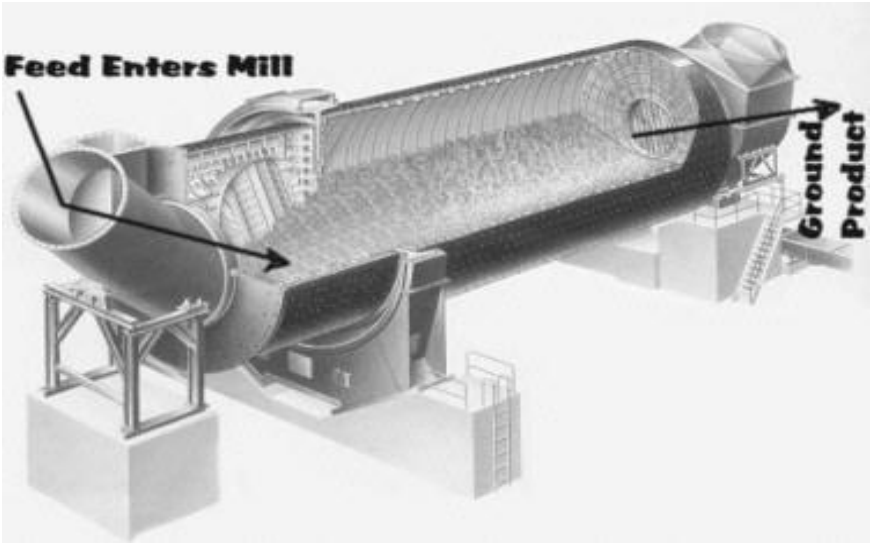

Fig. 1.5 Schematic diagram of ball mill used for high energy milling operations.

In ball mills a rotating cylinder, partially filled with grinding media is used for grinding the materials. There are many types of grinding media used in ball mills, each material have its own specific properties and advantages. In general ceramic balls, flint pebbles and stainless steel balls are used for milling operations. In grinding flammable materials the grinding materials made of lead, antimony, brass or bronze are used. To avoid contamination of iron and to

.

mill materials with high corrosive nature, the grinding materials made of ceramic materials such as alumina and silica are used.

The material to be ground is filled with the grinding media and made to rotate around a horizontal axis. An internal cascading effect reduces the material to a fine powder. Industrial ball mills can operate continuously fed at one end and discharged at the other end. The grinding works on principle of critical speed. The critical speed can be understood as that speed after which the steel balls start rotating along the direction of the cylindrical device. Thus cause no grinding further. In general the mills are operated at 65 to 75 percentage of the critical speed. Compression stress and impact stress acting between the colliding balls and ball and powder, powder particles and walls of the cylinder are the prime stresses in milling operations.

Many authors have used ball mills for mechanical activation, mechanochemical synthesis and mechanical alloying. Welham and Llewellyn (1998), Welham (2001) and Chen (1993, 1999) had used ball mills for mechanical activation of mineral samples and mechanochemical synthesis of rutile from ilmenite.

1.3.2 Vibration mill

Fig. 1.6 shows the photograph of typical vibration mill used in high energy milling processes (Suryanarayana, 2004; Balaz, 2008). A cylindrical tube type vessels filled with grinding media is used for milling operation. The vibrating mill consists of two or three tubes driven by a motor. About 70 to 80 percentages of the tubes are filled with grinding media. In general balls, cylpebs and grinding rods are used as grinding media. If the grinding is iron-free, balls or cylpebs of aluminium oxide are used. The grinding media are held up at the outflow heads by separating discs to ensure that only the ground material can flow out.

The feed material is filled with the grinding media and cylinder tubes are vibrated in a circular or elliptical direction. The feed material and the grinding media constantly receive impulses from the circular or elliptical

.

vibrations in the body of the mill. The grinding action is produced by continuous head-on collisions of the grinding media. Continuous feeding is carried out by vibrating feeders, rotary valves or conveyor screws. In general for mechanical activation purposes batch type milling is carryout.

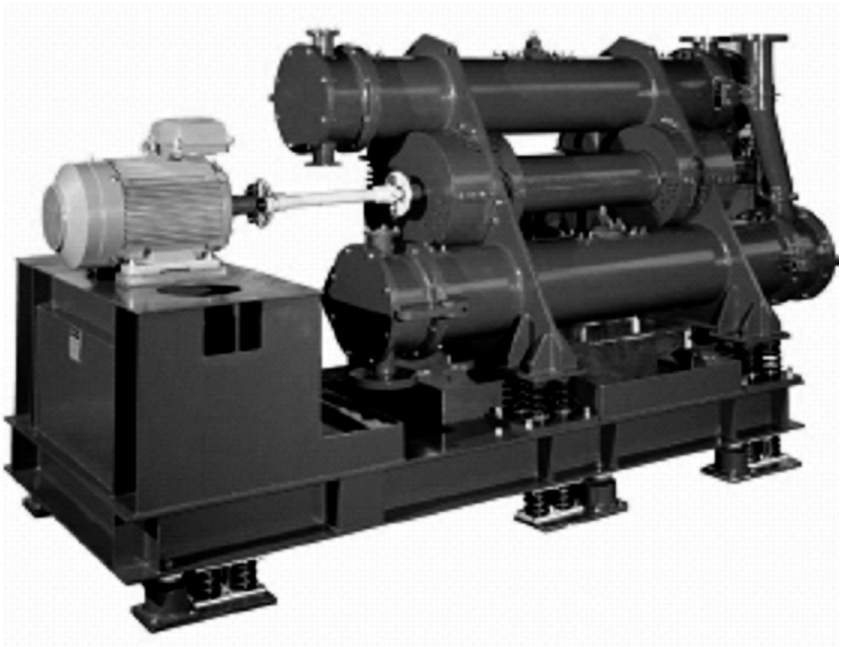

Fig.1.6 Photograph of typical vibration mill used for high energy milling of materials.

Bernhardt and Heegn (1976), Husemann et al., (1976), Balaz (1981), Heegn (1989), Tkacova et al., (1993) and Balaz et al., (2004; 2005) had used vibration mills for mechanical activation and synthesis of nano-sized materials. According to Bernhardt and Heegn (1976), the quantity of the feed and amplitude of vibration mill are the important factors for mechanical and mechanochemical activation. Recently Gock et al., (1996, 1998, 1999) introduced new concept of vibrating mills working in eccentric mode. These mills can be vibrated in elliptical, circular and linear directions. The amplitude and rotation speed of the mills are increased by these concepts, thus lead to higher activation.

1.3.3 Attritor

Fig. 1.7 shows the schematic diagram of attritors used for fine milling and ultrafine grinding of materials (Suryanarayana, 2004; Balaz, 2008). The

.

attritors are made of a cylindrical chambers and revolving shaft having multiple impellers as shown in figure. The attritors are also referred as stirred ball mills. The impellors are used to energize the grinding media. The grinding media includes various materials: through-hardened carbon steel, aluminum oxide, chrome steel steatite, 440C stainless steel, tungsten carbide, zirconium silicate, silicon nitride, zirconium oxide (MgO or Y2O3 stabilized) and silicon carbide are used for grinding operation. The high density media give better results. For efficient milling the media should be denser than the material to be ground and in wet milling operation the highly viscous materials require media with higher density to prevent floating. The impellers used for grinding also have different shapes like flat discs and discs with various geometric openings and concentric rings. The unique feature of attritor is that the power input is used directly for agitating the media to achieve grinding unlike other milling processes where the power is used for rotating or vibrating a large, heavy tank in addition to the media.

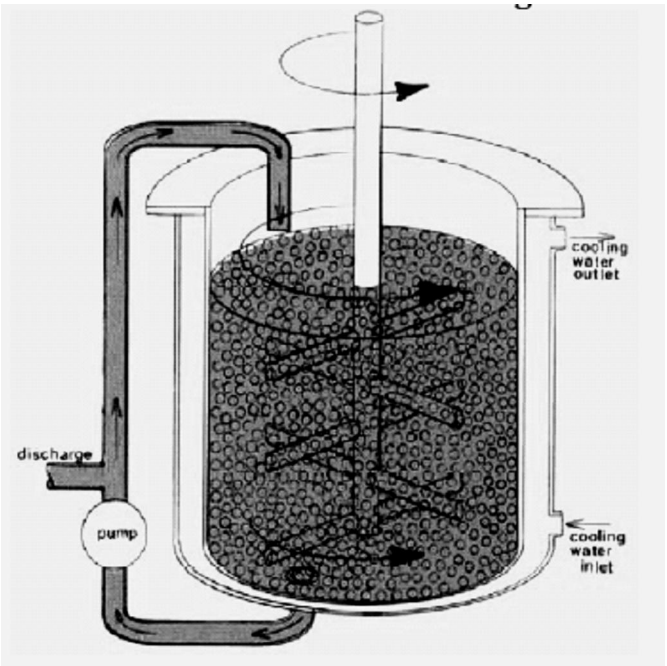

Fig.1.7 Schematic diagram of attritor mill used for high energy milling of materials.

.

The shaft revolves at very high speed and there is a constant impinging of impellors on grinding media. Further shearing action is created by the spinning action of balls moving in different directions. The impact and shear stresses acting on the materials grind the particles to finer size. In wet milling the shear stress is also created by the liquid medium used for grinding. In dry milling operations better milling was achieved by an expanded moving bed of media. This condition is described as kinematic porosity. The final products achieved by attritors are generally spherical in shape compared to other impact-type milling equipment. The arritors are also versatile to operate under a broad range of conditions. i.e. the type, size and amount of grinding media, milling speed and feed rate of raw material can be adjusted according to the requirements.

In addition to communition, attritors also showed efficient blending, especially for blending of dissimilar materials. However, Heegn et al., (1974) demonstrated that the vibration mills are adventurous in comparision to the attritors for creating structural disorder. Extensive amorphization was achieved in vibration milling of strontium ferrite, whereas there is only specific surface area not in crystallinity was achieved by attrition milling. Balaz (2008) documented the differences in vibration and attrition milling. There was a great difference observed in both the structural disordering. These differences are due to the difference in milling environment and ball dimensions (Boldyrev, 1983).

1.3.4 Pin mill or Centrifugal impact mill

Figure 1.8 shows the photograph of typical pin mill used in fine grinding of materials (www.sturventevantinc.com). The pin mills or centrifugal impact mills consist of a rotor assembly, to which a radial arrangement of steel pins are mounted, at a definite, calculated spacing. This rotor turns at a very high rotational speed, of the order of 5000 rpm. Between each radial set of pins, a stator assembly is mounted. This is basically a stationary metal ring, with slots at regular intervals. The product is introduced to the pin mill at the shaft axis; Centrifugal forces accelerate the material and launch it into the impact zone

.

where the material strikes the pins and stator assembly at random. This cycle is randomly repeated, and the particles are bounced back to the centre of the rotor, and the process is repeated. Thus finer particles are produced. The desired particle size distribution is obtained by controlling the rotor speed. Varying the rotor speed between a few hundred rpm up to 5400 rpm provides the flexibility to use the machine as a coarse grinding or de-agglomerating unit as well as a fine grinding mill.

Fig.1.8 shows the photograph of Centrifugal mill used for ultra fine grinding of materials.

1.3.5 SPEX mill

The SPEX mills used for high energy milling of materials is shown in fig. 1.9 (Balaz, 2008). The SPEX mills are also referred as mixer mills and shaker mills.These mills are recently developed in USA. In SPEX mills the material to be milled is mixed with grinding media in a container. The containers are usually cylindrical and the grinding media is generally balls. Sometimes rods, cylinders, or other shapes also used. The container with the materials and grinding media is made to swing energetically back and forth several thousand times. The back and forth motion is combined with a lateral motion at the end. Since there is larger amplitude (50 mm) involved and clamp movement (1200 rpm) is extremely rapid, the balls develop high grinding

.

forces. Thus the spex mills often used for high energy milling and mechanical alloying purposes (Koach 1993).

Fig.1.9 Photograph of SPEX mill used in high energy milling processes.

1.3.6 Planetary ball mill

The planetary ball mills consist of a grinding bowls fixed eccentrically on sun wheel (fig. 2.1). The direction of movement of the sun wheel is opposite to that of the grinding bowls in the ratio of 1:2 or 1:2.5. The grinding bowls with material and balls rotate around their own axis on a counter-rotating supporting disc. The charge inside the bowls rotates around the mill axis and revolves around its own axis as planets. Thus the mills are named as planetary mill. The centrifugal forces caused by the rotation of the grinding bowls and supporting discs work on the contents of the grinding bowls. The force resulting from rotation of the grinding bowl when the mill is started causes the rotating balls to rub against the inside wall of the bowl thus crushing the material. The material is primarily crushed by the high-energy impact of grinding balls together with friction between the balls and the wall of the grinding bowl. At a certain point in time the stronger centrifugal force of the supporting disc causes the grinding material and balls to separate from the inner wall of the grinding bowl. The grinding balls cross the bowl at high

.

speeds impacting with the grinding material on the opposite wall, creates size reduction by impact.

The planetary mill had been extensively used in Russia for the studies on mechanical activation (Golosov 1971; Molcanov et al., 1988; Molconov and Jusupov, 1981; Avvkumov, 1986). The energy densities of these mills are 100-1000 times of other conventional mills (Fokina et al., 2004). Recently a planetary mill of continuous feeding of grinding material was manufactured (Kochnev, 1992; Kochnav and Simakin, 1994). Industrial planetary mills with 3 to 5 tones of powder per hour are available commercially (http:/www.ttd.spb.ru). This type of mill has been used for the present study. The details are given in chapter 2.

1.4 Energetics of mechanical activation processes

The effect of mechanical treatment on metals was investigated by Tamman (1929). He observed that about 5-15% of the total energy input is stored or accumulated inside the metals when subjected to mechanical treatment. In mechanically activated solids, the energy is stored as lattice defects (point, line, surface and volume defects), strain, enhanced surface area, enhanced grain boundaries, structural alteration and the stored energy is responsible for the enhanced reactivity of the activated substances. The activated state can be characterized by an excess Gibbs energy, ΔG_M (Tkacova, 1989):

$$\Delta G_M = G_M^{\ *} - G_M \qquad (1.2)$$

where $G_M^{\ *}$ and G_M are the Gibbs energies of the activated and non-activated states respectively. If sufficient time is not provided for relaxation, the activated solid will have non-zero entropy even at absolute zero temperature. It was found that the frozen in entropy may reach up to 40 percent of the melt (Meyar, 1977). Using the Gibbs-Helmholtz equation, the free energy change for the activated process can be given as:

$$\Delta G_M = \left(H_M^* - H_M\right) - T(S_M^* - S_M) \qquad (1.3)$$

.

where H_M and H_M* represents the enthalpy change of the unmilled material and material in activated state respectively and S_M and S_M* is the corresponding entropy change. Thus the useful stored energy available for conversion can be characterized by the enhanced free energy of the activated material. The enhanced energy of the activated solid can be determined through various means:

1.4.1 From the law of energy conservation

From the 1st law of thermodynamics, assuming that no work is done against external pressure and ignoring energy dissipation through sound and electromagnetic processes, the grinding work, W during the mechanical activation process can be expressed as (Tkacova,1989):

$$W = \Delta H_M + \Delta H_G - (-Q) \quad \text{.....(1.4)}$$

where ΔH_M and ΔH_G are the change in the enthalpy of the material being ground and the grinding media respectively and Q is the reversible energy released as heat. Therefore, ΔH_M can be determined through total energy measurements of the mechanical work done W and calorimetric measurements of the change in enthalpy of the grinding media ΔH_G and the heat liberated Q respectively. Schellinger and Lalkala (1951) and Schellinger (1952) carried out experiments by placing the ball mill inside a calorimeter. The effective grinding work was found to be 10 to 20 percent of the energy input. In some of the grinding systems equipped with modern apparatus the effective work was found to be 25-35% during the initial stage of grinding (Tkacova, 1989).

1.4.2 From heat of dissolution using calorimetry

The enthalpy change of activated material can be determined by calorimetric experiments, provided the material both in the normal and mechanically activated state dissolves completely in aqueous or non-aqueous media. The enthalpy of dissolution is obtained using exothermic substitution reactions which yield a water-soluble product. The overall enthalpy of the dissolution process (ΔH_M) is expressed as (Tkacova,1989).

.

$$\Delta H_M = \Delta H_K - \Delta H_S - \Delta H_R \quad \text{.....(1.5)}$$

where ΔH_K is the heat consumed to overcome the cohesive forces when the substance is transferred to the solution, (i.e cohesive work of dissolution), ΔH_S is the solvation enthalpy, and ΔH_R is the enthalpy of the reaction. The solvation enthalpy (ΔH_S) and the enthalpies of the reaction (ΔH_R) of an activated material and stable material are equal, provided there is no mechanochemical reaction. However, there will be a difference in the enthalpy of cohesive work of dissolution between the activated (ΔH_K^*) and stable material (ΔH_K^*). The cohesive work of dissolution is (ΔH_K) decreased by structural defects. Thus $\Delta H_K^* < \Delta H_K$. The difference between the enthalpy of dissolution of the activated (ΔH^*) and stable form (ΔH) of the same substance is positive. This difference represents the excess enthalpy of the activated material ΔH_M and is equal to the effective work of mechanical activation W (Tkacova,1989):

$$W = \Delta H^* - \Delta H = \Delta H_K - \Delta H_K^* = \Delta H_M \quad \text{..... (1.6)}$$

Since the enthalpy change introduced by activation is derived from the difference in two large enthalpy components, the uncertainty associated with this method would be expected to be large. Further, the above equation is valid only for solids that are completely soluble under the experimental conditions. However all the materials may not be completely soluble under the experimental conditions where relaxation processes are absent and hence the equation can be rewritten as (Tkacova,1989):

$$\Delta H_M = Q/M \quad \text{..... (1.7)}$$

where Q is the heat of dissolution of the solid substance and M is the amount of solid dissolved under the experimental conditions. The amount of solid dissolved in the stable and the activated form are different and this has to be considered while deducing the enthalpy of the activated solid.

.

1.4.3 From statistical thermodynamics

The macroscopic change in enthalpy of the activated solid is because of various micro effects such as increase in surface area, grain boundary area, lattice strain, and quasi-amorphization. Based on the equations of statistical thermodynamics, the enthalpy of the macroscopic state may be expressed as the sum of the enthalpies of microscopic states (Tkacova,1989):

$$H = \sum_{i=1}^{m} N_i H_i \quad \text{é .(1.8)}$$

where for a solid, N_i is the number of lattice elements in the i-th energy level and H_i the enthalpy required to transfer a lattice element to the i-th state, or in other words

$$H = \left(\frac{N_S}{N_A}\right)E_S + \left(\frac{N\varepsilon}{N_A}\right)E_{\text{Ü}} + \left(\frac{N_D}{N_A}\right)E_D + \left(\frac{N_{QA}}{N_A}\right)E_{QA} \text{é é é é é é .é é} \quad (1.9)$$

Where N_A is the Avogadroôs number, E is the energy coefficient and subscripts s, *ε,D,* and *QA* denote free surface area, lattice strain, reduction of crystallite size and quasi-amorphization respectively. The relative number of atoms or ions at the surface (N_P/N_A), in plastically deformed structure (N_D/N_A), at the grain boundaries (N_B/N_A) and in the quasi-amorphous regions (N_Q/N_A) can then be calculated from experimental determination of specific surface area, lattice strain, crystallite size and the amount of the amorphous phase. The molar surface energy ε_P is in turn deduced from the surface energy and the lattice strain energy ε_D can be assessed from the compressibility factor. Assuming that the state of the species at the grain boundaries and the quasi-amorphous regions is similar to the melt, molar heats of fusion can be substituted for ε_B and ε_Q.

The energy contributions to new surface formation, crystallite disintegration and quasi-amorphization were studied by Merva et al.(1973), Sheng et al., (1999), Chakk et al.,(1994) and Sharma and Suryanarayana (2008). Tkacova (1979 and 1989) summarized their results of individual energy

.

contribution and overall enthalpy change of some minerals (Quartz, Magnetite, Kaolinite and Calcite) subjected to activation in various mills (ball mill, vibratory mill, attritor and disintegrator). The energy contributions were in the range of 1-4 % by formation of new surface, 7.5 -22% by crystallite disintegration and 70-90 % by quasi-amorphization. A very high value of surface energy (20 %) was achieved in kaolinite mineral sample subjected to activation in vibratory mill. The overall energy input into the material determined theoretically was found to be 12 - 30 kJ/mol in various mills and the experimental value of heat of dissolution was in the range of 2-17 kJ/mol for quartz, magnetite and calcite mineral samples. The overall enthalpy change determined theoretically as well as the heat of dissolution was maximum (52-350 kJ/mol) with kaolinite mineral sample milled in vibratory mill and attritor.

Ermilov et al. (2002) proposed an equation to evaluate the stored energy in the material from X-ray diffraction data using the relation

$$\Delta E_M = |V_o - V_i| E_{latt} + 6E_{surf} V_{mol}\left(\frac{1}{D_I} - \frac{1}{D_0}\right) + \frac{2}{3} E_Y \left(\varepsilon^2_{milled} - \varepsilon^2_{unmilled}\right) V_{mol} \quad \text{.....(1.10)}$$

where ΔE_M (kJ/mol) is the energy stored during activation; Vo and Vi are unit cell volumes before and after MA, respectively; E_{latt} (kJ/mol) is the lattice energy of starting material; E_{surf} (kJ/mol) is the surface energy of starting material; D_i and D_0 (m) are the sizes of the coherently scattering domain in activated and starting materials respectively; V_{mol} (m^3) is the molar volume of starting material; E_Y (GPa) is Youngôs modulus of the starting material; and ε^2_{milled} and $\varepsilon^2_{unmilled}$ are the root mean square (rms) microstrains in the activated and starting materials respectively. The energy stored in the material by mechanical activation was determined from lattice energy and atomization energy (Bogatyreva and Ermilov, 2008) of the material before and after milling The energy stored in SiO_2 by mechanical activation was in the range of 25-95 kJ/mol at different milling conditions.

.

1.4.4 From kinetics of dissolution

1.4.4.1 Activation energy of dissolution

Zelikman et al.(1975) described that the breaking of bonds in the crystalline lattice of the materials by mechanical activation brings about a decrease in activation energy and increase in the rate of leaching. The decrease in activation energy (φE^*) can be described as

$$\Delta Ea^* = Ea - Ea^* \quad \text{.....(1.11)}$$

Where Ea is the apparent activation energy of the stable solid prior to activation, Ea^* is the apparent activation energy of the activated material. Normally $Ea > Ea^*$. The decrease in activation energy in activated materials was observed in many reactions (Balaz, 2000; Tkacova,1989; Welham, 1997; Welham, 2001; Welham and Llewellyn, 1998; Balaz and Briancin, 1993; Balaz et al., 1995; Balaz, 2003; Chun Li,2006; Bin Liang et al., 2005). Balaz et al (1995), studied the decomposition reaction of pyrite subjected to mechanical activation in a planetary mill, and showed that the activation energy reduced from 87 kJ/mol to 53 kJ/mol in 30 minutes of activation. The apparent activation energy of mechanically activated tetrahedrite reduced from 30kJ/mol to 18kJ/mol in 20 minutes of milling. Chun Li et al (2006) studied the effect of milling on the dissolution of ilmenite and showed a decrease in activation energy from 47.5 to 38 kJ/mol.

1.4.4.2 Rate constant of dissolution process

The rate constant of the activated material (k*) can be described as

$$k^* = k.\exp\left(\Delta Ea^* / RT\right) \quad \text{.....(1.12)}$$

k, R and T stand for the rate constant of leaching for the non-activated material, gas constant and reaction temperature respectively. In general $k^* > k$, i.e. the rate of leaching of activated material is greater than that of non-activated material. Here, it is assumed that the stored energy is fully released during the dissolution process, the reaction mechanism and path is identical during the

.

leaching of the activated and non-activated solids and further that the decrease in activation energy is of the same magnitude as the difference in enthalpy of the stable and activated solid. This method ignores the relaxation processes occurring during the process of dissolution. Under actual conditions, the energy stored in the solid will be significantly more than the difference in activation energy of the solid in the activated and non-activated states. Welham and Llewellyn (1998) have reported an eightfold increase in the dissolution rate of ilmenite in sulfuric acid even at ambient pressure through mechanical activation.

Senna (1989) has carried out a detailed investigation on the effect of physicochemical changes on dissolution kinetics of mineral samples. He has demonstrated that a plot of rate constant normalized by surface area against the applied energy of activation changes according to the mechanism of the reaction. If the normalized rate constant (k/S_i) does not vary with the applied energy of activation then the surface area is effective in enhancing the reaction rate and insensitive to the structural changes. On the other hand, if the surface area normalized rate constant (k/S_i) decreases with applied energy, the effective surface area is lesser than the measured physical surface area. In the third case if the normalized surface area (k/S_i) increases with applied energy then the reaction rate enhancement is attributed to both surface area and structural imperfections.

1.5 Effect of mechanical activation on physico-chemical and structural properties of solid

Mechanical activation has a significant influence on the physical, chemical, and structural properties of the solid materials. The changes in physico-chemical properties of activated solids depends on various parameters (Sherif El-Eskandarany et al, 1991): the milling equipments used for activation (vibratory mill, attrition mill , planetary mill, jet mill); shape of grinding media (balls, rods or other shapes); materials of grinding tools (stainless steel, tungsten carbide, zirconium oxide, aluminium oxide, silicon nitride); grinding mode (dry or wet); ball-to-activated material size ratio, ballï to-activated

.

material weight ratio; temperature of milling; milling speed; time of activation and the material being activated.

The solids subjected to activation are reported in the literature to undergo various micro and macro processes (Heegn, 1979 and 1987; Fernandez-Bertan, 1999; Tromans and Meech, 1999 and 2002; Balaz, 2000; Tkacova,1989; Kalinkin et al., 2003, Pourghahramani, 2006). The various effects reported to be observed in the material are:

- Repeated deformation, fragmentation, and cold welding leading to disintegration and fracturing of powder particles, formation of new surfaces and enlargement of surface area, surface aggregation and surface oxidation.
- Material abrasion
- Plastic deformation and disordering of crystal structure (lattice distortions), the formation of various lattice defects such as point, line, surface and volume defects etc, electronic defects and amorphization. All of these result in an increase of dislocation density, lattice strain and crystallite size
- Phase transformation in polymorphic materials
- Emission of photons and electrons
- Stimulation of lattice oscillations and local heating of solids
- Electrostatic charge-discharge processes
- Change in magnetic properties
- Chemical reactions, decomposition, ionic changes, oxidation-reduction reactions and complex formation.

In general, the effect of mechanical activation can be classified as changes in physical, chemical, structural, thermal, mechanical, magnetic, and electronic properties of the solid materials.

1.5.1 Effect of mechanical activation on physical properties

Some of the physical properties that re altered during the process of mechanical activation are: particle size, particle morphology, surface area,

.

microstructural changes, optical properties, density, surface energy and melting point (Balaz, 2000; Tkacova, 1989; Kalinkin et al., 2003).

The primary effect of grinding is communition of powder particles. The fragmentation of particles depends on the material properties such as fracture toughness of the material, flaw size, and size of the powder particles (Schonert, 1982 and 1990). However there is a limit to the reduction of particle size beyond which there is no fracture and the particles will undergo only plastic deformation. Further milling beyond the critical size results in activation of the material (Boldyrev et al., 1996). In general, the particle size decreases exponentially with the time of activation (Balaz, 2000; Tkacova, 1989; Welham and Llewellyn, 1988). The particle size shows an increasing trend if there is an agglomeration during the activation process.

Juhász and Opoczky (1990) studied the changes in morphology of the particles subjected to mechanical activation. The morphology of the powder particles are greatly influenced by the mechanical activation process. The various possible morphological changes introduced by mechanical activation can be described qualitatively using the definition of particle shape prepared by British Standard Institute (Allen, 1981; Kaye, 1981). The particle shapes are classified as acicular, angular, crystalline, dendritic, fibrous, flaky, granular, irregular, modular and spherical. The ductile materials in general (metals) show flaky and plate-like morphology while the brittle materials (minerals) show angular and sub angular grains upon mechanical milling. The change in morphology of the powder particles has a strong influence on the reactivity of the solid materials. Tromans and Meech (2002) analyzed the conjoint effects of particle size and micro-topography on the overall mass dissolution behavior of fine particles. They suggested that microtopography-enhanced dissolution can be significant for surface-controlled leaching reactions exhibiting high activation energies (>70kJ/mol) and for low particle sizes (<1 μm). They derived an expression for the differential dissolution at the step edges of a particle in comparison to that at the terraces through a parameter t_{rel} defined as

.

the ratio of the total time for dissolution of a stepped particle relative to the time for dissolution of a spherical particle of the same mass (of diameter D_M).

The significant effect of mechanical activation is the increase in the specific surface area of the material being activated. Many investigations on the effect of specific surface area (BET surface area) on mechanical activation show an exponential variation with time of milling or energy input into the material (Balaz,2000; Tkacova, 1989; Welham and Llewellyn, 1998). In most of the materials, the specific surface increased from 2-8 m^2/g to 12-15 m^2/g by dry milling in atmospheric condition (Balaz,2000; Tromans and Meech, 2002). Higher value of surface area was achieved in some of the materials by wet milling. About 20-60 m^2/g was achieved by wet milling of some sulphide minerals (Balaz,2000; Tkacova,1989; Avvakumov, 1986). Further, the extent of change in surface area depends on the type of mill and other milling conditions. The specific surface area starts declining in some of the materials after certain period of activation indicating that the powder particles are being agglomerated on activation (Balaz, 1997; Balaz, 2000; Kalinkin et al., 2003).

1.5.2 Effect of mechanical activation on structural properties

The structural properties of the material: the crystal structure, unit cell parameters, and lattice volume and density of the materials can be altered by mechanical activation (Balaz, 2000; Tkacova, 1989; Suryanarayana et al., 2001). It is possible to create a defective structure with high concentration of non-equilibrium defects (Boldyrev, 1979). The defects include vacancies, interstitials, dislocations, new surface, low angle and high angle grain boundaries, stacking faults, pores and voids and disordering. In other words the mechanical energy is stored in the form of lattice defects and other structural imperfections. As the concentration of defects increases, the energy accumulated in the solid increases. Balaz and Tkacova studied the structural disorder of chalcopyrite subjected to mechanical activation in an attritor and showed that the degree of crystallinity varies in the range of 40-90% depending upon the milling conditions. Quasi-amorphous or amorphous regions are formed by structural disorder of the material during grinding (Balaz, 2000;

.

Tkacova, 1989; Suryanarayana, 2001). There are many studies on mechanically induced amorphization of materials (Berg and Sljapina, 1975; Asadov, 1975). Balaz (1997) studied the degree of amorphization of chalcopyrite, pyrite, tetrahedrite, galena, sphalarite and cinnabar with milling time using x-ray diffraction analysis and showed 5-60% of amorphization in various mineral samples. The mechanical activation also changes the crystallite size of the material. The variation of crystallite size of the material with milling time was studied by various authors (Balaz, 2000; Tkacova, 1989; Welham and Llewellyn, 1998) Further, it is also possible to induce polymorphic transformations through the mechanical activation process i.e. transformation of one crystal structure into another without change in chemical composition (Gock, 1978; Avvakumov, 1979;Balaz, 1985). For instance, the transformation of Ŭ phase (tetragonal) into ɓ phase (cubic) was observed by mechanical activation of chalcopyrite (CuFeS2) (Schort and Steward, 1957; Avvakumov, 1979, Imamura and Senna, 1982). The transformation of cinnabar from trigonal (Ŭ-HgS) to cubic structure (ɓ-HgS) was also observed by mechanical activation (Senna, 1985; Boldyreva, 2003). Avvakumaov (1979) postulated that the high local pressures and temperatures at the contact surface of mechanically activated particles as well as the presence of volume defects are responsible for phase transformations. In general, the phases transformed by thermal activation will have lower density, whereas the mechanically induced phase transformations show phases with higher density. For example, zinc sulphide (ZnS) exits in two forms, i.e. as cubic sphalerite and hexagonal wurtzite. Mechanical activation of wurtzite brings about a transformation to sphalerite, however the activation of sphalarite results only in its amorphization (Dachille and Roy, 1961; Zeto and Roy, 1969). The authors postulated that the driving force behind this transformation is the motion of dislocations in the activated solid. Changes in bond angles and bond lengths were also noticed by some of the authors (Buyanov, 1987; Molchanov et al., 2000).

.

1.5.3 Effect of mechanical activation on chemical properties

Another significant feature of mechanical activation is the induction of chemical reactions in some of the materials. Solid state reactions ranging from polymorphic transitions to decomposition reactions were possible by mechanical activation processes (Thiessen, 1970; Schrader and Werner, 1975; Bade and Hoffmann, 1996). In general, the mechanical activation processes accelerates the reaction rate, increases the conversion levels, reduces the pressure and temperature required for the reactions and induces mechano-chemical transformations and mechanical alloying. For example, the degree of decomposition of jadeite into nepheline and albite does not exceed 10% under the action of hydrostatic pressure at 350^0C, whereas it increases up to 60% under the simultaneous action of pressure and shear at the same temperature (Boldyrev, 2006). Boldyrev (2006) classified the mechanically induced chemical reactions into solid-gas, solid-liquid and solid-solid reactions.

1.5.3.1 Effect of mechanical activation on solid-gas reactions

Mechanical activation enhances the adsorption of gases on solid surfaces and their subsequent reactions. The enhanced reactivity of solids found application in enhancing the catalytic activity of metals and oxides (Keller, 1955; Koach, 1995; Grigorĉeva and Boldyrev, 1995; Grigorĉeva, et al., 1997). The diffusion of gas molecules is also enhanced by the mechanical activation process. Thus, the kinetics of oxidation, nitridation, hydrogenation, and carboxylation of materials were enhanced by the mechanical activation process (Boldyrev,2006). As examples, mechanical activation found application in synthesis of nickel carbonyl, methylchlorosilane, SiN, and TiN (Grigorĉeva, et al., 1997; Eckert, 1992). Thermodynamically forbidden reactions are reported to be possible by the mechanical activation process, for example, the oxidation of gold by carbon dioxide (El-Eskandarany, 1992).

1.5.3.2 Effect of mechanical activation on solid - solid reactions

Promotion of the solid state reaction is one of the primary advantages of mechanical activation. Chemical reactions that occur in solid state avoids the

.

use of solvents which has a great benefit from environmental point of view and in reducing the pressure, temperature and cost of operation. In the extraction of gold, the highly toxic process of amalgamation can be eliminated by mechanical activation (El-Eskandarany, 1992). Mechanical alloying is another common solid state reaction classified under mechano-chemical reactions. Mechanical activation has been used for the synthesis of crystalline and quasi-crystalline intermetallic phases, meta-stable phases, solid state amorphization (Zhao et al., 1999, Manna et at, 2004) and mechanochemical synthesis (Murty et al., 1998; Suryanarayana et al., 2001). Alloys of Al-Cu, Cu-Zn Ti-Al, Al-Si are reported to have been prepared by mechanical milling (Suryanarayana et al., 2001). Quasi-crystalline phases $Al_{65}Cu_{20}Co_{15}$, $Al_{65}Cu_{20}Fe_{15}$, and $Al_{65}Cu_{20}Mn_{15}$ and amorphous phases $Al_{88}Y_2Ni_6Fe_4$, Al-50 Zr, $BiFeO_3$, Co-33B, Co-Nb, Co-25Ti have been synthesized by planetary milling for 30 to 60 minutes. Chen (1997 and 1998) observed that the ilmenite phase converts to metastable pseudo-rutile ($Fe_2Ti_3O_9$) and γ-Fe_2O_3 during the process of mechanical activation in air and oxygen.

1.5.3.3 Effect of mechanical activation on solid-liquid reactions

The effects of mechanical activation on solid-liquid systems are used extensively in pharmaceuticals and hydrometallurgy. In pharmaceuticals, mechanical activation is used for enhancing the effectivity, absorption and solubility of poorly soluble medicines (Huttenrauch and Fricke, 1985; Dubinskya, 1989; Shakhtshneider and Boldyrev, 1993) and in hydrometallurgy, mechanical activation used to increase the efficiency of leaching of ores and minerals (Duncan and Metson, 1982a&b; Tkacova, 1989; Tkacova and Balaz, 1988; 1996; Balaz, 1996; Welham and Llewellyn, 1998; Amer, 2000; Welham, 2001; Amer, 2002; Balaz, 2003, Chun Li, 2006;) in both acids and alkalis. As an example mechanical activation of bauxite has been reported to significantly affect its dissolution kinetics (Rakeshkumar et al., 2004 & 2005a). In the commercial Bayerôs process adopted at National Aluminium Company, India for the purification of alumina (predominantly gibbsite), the ore is digested in NaOH at 100-150^{o}C to form soluble sodium aluminate and the insolubles such

.

as Fe_2O_3, SiO_2 and TiO_2 is left behind in the residue (red mud). The alumina and soda losses to the red mud are about 15-20% and 3-5% respectively. However, when the alumina is mechanically activated for a short time (~30 min) in an attrition mill, subsequent digestion under similar conditions yielded much higher recovery of Al_2O_3 (90-95%) and lower loss of NaOH (0.5-0.6). It was observed that the Gibbsite phase is progressively amorphized during mechanical activation yielding better solution recoveries of Al_2O_3. In an interesting analysis, Rakesh kumar, et al.,(2005b) observed that mechanical activation significantly altered the reactivity of blast furnace slag . The attrition milled slag hydrated in a much shorter time without any chemical activator. The hydration product resulting from the attrition-milled slag was also unique and showed higher crystallinity. The overall increase in the dissolution rates with mechanical activation is in addition to that resulting from an increase in surface area because of several factors such as structural disorder (Tkacova et al., 1993), enhanced strain (Amer, 2000), amorphization of mineral particles (Barton and McConnel, 1979;), preferential dissolution of select crystal faces (Duncan and Metson, 1982 a&b), micro-topography (Tromans and Meech,1999 & 2002), and formation of new phases more amenable to leaching (Tkacova and Balaz, 1996; Welham, 2001).

1.5.4 Effect of mechanical Activation on thermal and magnetic properties

The effects of mechanical activation on thermal and magnetic properties of mineral samples were reported by some of the authors (Berg et al., 1975; Boldyrev, 1972; Tkacova, 1989; Balaz, 2000; 2008). The mechanical activation altered the temperature of phase transformation, decomposition (Kalinkin et al, 2003) , reduction, oxidation, calcinations, and roasting of mineral samples (Balaz,2000; Boldyrev,2006). As an example the decomposition temperature of Chalcopyrite reduced from $900^{O}C$ to $500^{O}C$ by 7 minutes of mechanical activation in atmospheric air (Kulebakin, 1983). The oxidation temperature of Galena (PbS) reduced from $660^{O}C$ to $520^{O}C$ by 30 minutes of mechanical activation. Further the rate decomposition of Chalcopyrite, Cinnabar,

.

Arsenopyrite is enhanced by mechanical activation. The reduction in melting point also observed some of the metal samples (Mehrotra, 2007).

The magnetization behavior of materials also enhanced by mechanical activation process (Ding et al., 1996; Tkacova et al., 1996, Sepelak et al., 1999; Sepelak et al., 2003). The high field magnetization irreversibility, the variation of Nell temperature with the grain size, a high coersivity, and altered (reduced or enhanced) magnetic moments in comparison to bulk materials have been observed in activated ferromagnetic spinals. The effect of mechanical activation on magnetic behavior of materials found applications in catalysis, ferrofluids and information storage.

1.6 Effect of mechanical activation on the processing of ilmenite

In general, the beneficiation of ilmenite falls into two categories: namely beneficiation up to synthetic rutile using either a high temperature reduction smelting process to produce a titania rich slag and subsequent acid leaching or high temperature roasting treatment followed by magnetic separation and selective rusting of the iron in ammoniacal solution such as in the Becher process, or selective leaching of iron in HCl as in Benelite and Murso processes (Mukherjee, 2000). The other alternative is the direct production of pigment grade TiO_2. Some workers have also used direct reductive leaching (using iron) of the ilmenite concentrate (Mahmoud et al., 2004). A common method used for the direct production of pigment grade TiO_2 from ilmenite is the chloride process, which involves chlorination of ilmenite, synthetic rutile or the titania rich slag produced by electrothermal smelting and subsequent separation of iron and titanium chlorides by distillation (www.altairnano.com). Other methods for production of pigment grade TiO_2 involves direct leaching of ilmenite with acids at atmospheric or high pressure resulting in dissolution of iron and titanium in the solution followed by hydrolysis of TiO_2 from the acid leach liquor in the case of the sulfate process and solvent extraction in the case of the Altair process (Afifi, 1994; Abdel-Aal et al., 2000).

The direct acid leaching processes employs mainly sulfuric acid leaching. In the sulfate process, ilmenite concentrate is digested in concentrated

.

sulfuric acid in the temperature range of 150-180^{O}C to dissolve titanium and iron. The dissolved Ti is precipitated as hydrous TiO_2 by preferential hydrolysis of the leach solution. However, the kinetics of dissolution of ilmenite in sulfuric acid is slow (10 to 12 hours per batch), costly and the by-product ferrous sulfate is less marketable and poses an environmental hazard (US Environmental production Agency). Because the regeneration of sulfuric acid from ferrous sulfate is cumbersome, the sulfate process generates waste as much as two times the product weight, which necessitates expensive treatment for neutralization before disposal of the waste. In recent times, there has been some advancement to the sulfate process such as converting the iron sulfate to marketable iron oxide, recycling of the waste acid and an improved market for gypsum. In the recently developed Altair process involving digestion with concentrated hydrochloric acid followed by solvent extraction, the acid can be regenerated and the by-product iron oxide has a market value. The hydrochloric acid leaching process can also be rendered selective for iron under controlled process conditions (Eh and pH). The sulfate process is presently making around 40% of the worldôs TiO_2 pigments.

Several investigators have studied the dissolution behavior of ilmenite in hydrochloric acid (Jackson and Wadsworth, 1976; Hussein et al., 1976; Tsuchida et al.,1982; Sinha, 1984; Lanyon et al., 1999; Olanipekun,1999; Van Dyk et al., 2002) and sulfuric acid (Judd and Palmer, 1973; Imahashi and Takamatsu, 1976; Barton and McConnel, 1979; Hishasi, 1982; Han et al., 1987; Liang et al., 2005; Li et al., 2006). Their studies deal with the effect of stirring speed, particle size, temperature, acid concentration, and acid-to-ilmenite ratio on the kinetics of dissolution of ilmenite in hydrochloric and sulfuric acids. Van Dyk et al. (2002) have summarized the results obtained by hydrochloric acid leaching. They studied the leaching mechanism of ilmenite with hydrochloric acid and showed that the dissolution of ilmenite follows initially a chemical reaction controlled mechanism and later a diffusion controlled mechanism as the Ti-(IV) fines produced by hydrolysis reaction precipitate inside the pores of the unleached particles. Studies on leaching

.

behavior of ilmenite with sulfuric acid showed that the chemical reaction at the particle surface was the rate-limiting step and a value of 64 kJ/mol was estimated for the activation energy based on the dissolution of iron (Han et al., 1987).

Several methods have been proposed for the enhancement of the dissolution rate of ilmenite. Reduction and/or oxidation pretreatment followed by leaching with acids/bases as well as direct pressure leaching of ilmenite concentrate have been reported (Sinha, 1973; Barton and McConnel, 1979; Sinha, 1979; Farrow and Ritchie, 1987; Natziger and Elger, 1987; Jayasekera et al., 1995; Walpole, 1997; Ogasawara and Velso de Araiya, 2000). Addition of certain additives was also found to enhance the dissolution rate of ilmenite. Investigation on reductive leaching of ilmenite ore in hydrochloric acid showed that addition of iron powder reduces the ferric ion, which results in enhanced dissolution of ilmenite and subsequent precipitation of TiO_2 (Mahmoud et al., 2004). Addition of iron powder to enhance the dissolution rate is limited to hydrochloric acid. Methods involving high temperature and high-pressure increases the cost of operation and imposes stringent safety requirements.

Considerable enhancement in dissolution rates of mechanically activated ilmenite in sodium hydroxide solution at elevated temperatures (200^oC) and high oxygen pressures (4.1MPa) was also observed (Amer, 2002). Welham and Llewellyn (1998) have reported an eightfold increase in the dissolution rate of ilmenite in sulfuric acid even at ambient pressure through mechanical activation. They have used conventional ball mill and carried out experiments for periods in excess of 100 hours. Modern high-energy mills may result in imparting high energy to the material in a short time.

1.7 Objectives of the present study

The objective of the present thesis is :-

1. To study the effect of mechanical activation process on physico-chemical, structural, thermal and magnetic properties of Indian beach sand ilmenite samples

.

2. To study the effect of mechanical activation on energetics of ilmenite samples.
3. To find out the effect of mechanical activation on subsequent dissolution behaviour of ilmenite samples in sulphuric and hydrochloric acids.
4. To make a comparative study of physio-chemical and structural alterations induced by natural weathering and mechanical activation of Indian beach sand ilmenite samples and their effect on subsequent dissolution behaviour.

.

CHAPTER 2

EXPERIMENTAL PROCEDURES

2.1 Materials

The ilmenite concentrate samples used in the present study were collected from Indian Rare Earths Limited (IREL) located at Chatrapur in Orissa, Navaladi and Manavalakurichi in Tamilnadu and Chavara, in Kerala regions. The samples were derived from the placer deposits along the eastern coast stretching from Orissa to Kerala. The beach sand deposits were beneficiated to ilmenite by magnetic and gravity concentration techniques. However, there is a significant difference in chemical composition and mineralogy of these ilmenites arising because of the variation in the degree of weathering from the Orissa to Kerala coast.

2.2 Mechanical activation

A Fritsch Pulviresette-5 planetary mill having agate bowl and balls (Fritsch GMBH, Germany) was employed for the mechanical activation of the ilmenite mineral samples. The pulverizer was coupled with a high sensitive power meter to measure the energy input into the mill during the milling operation. The bowl and balls used for milling was of agate to avoid contamination of iron while milling. Figure 2.1 shows the photograph of the planetary mill coupled with the energy meter used for the mechanical activation experiments. For each milling experiment, fifteen agate balls of 20 mm diameter (160 g) were used in each bowl. The samples (40 g in each batch) were subjected to dry milling in ambient atmosphere. The ore to ball ratio in the bowl was maintained at a ratio of 1:4 by weight for all the experiments. Milling was carried out at 200 rpm for all the batch experiments. No other additives were used during the milling. The samples were activated in the planetary mill for 30, 90, and 240 minutes in separate experiments. Putsov et al (2001) and Suryanarayana (2004) report a steady state increase in the temperature (60-600^{0}C) of the container wall in planetary milling. However the milling speed reported in their papers are very high (630-1090 rpm), and at low

.

speed (680 rpm) the temperature rise is expected to be less than 200^0C. Hence, in our experiments the milling was carried out at low speed (200 rpm) to minimize thermal relaxation in the material and further the milling was interrupted every 30 minutes and subjected to air cooling. The milling experiments were carried out in a cyclic mode (i.e. the direction of rotation was changed every 15 minutes) to minimize the aggregation of powder samples and their sticking to the bowls and for effective transfer of energy into the material. At the completion of milling, the contents of the bowl were thoroughly cleaned and dried before the next milling experiment.

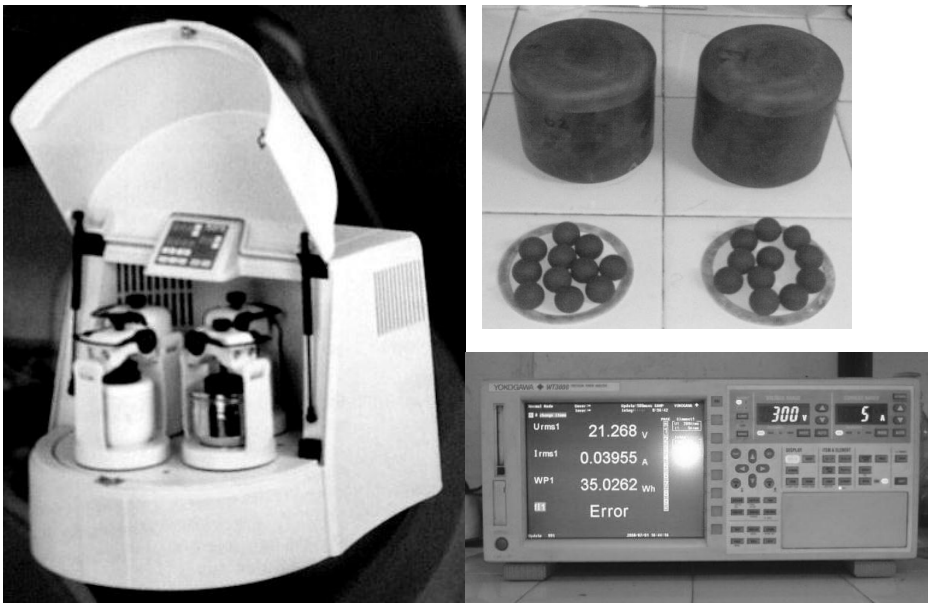

Fig.2.1. Photograph of planetary pulverizing mill (Fritsch GMBH, Germany), energy meter (WT 3000, Yokogawa) and agate bowls & balls used for mechanical activation of ilmenite samples.

2.3. Precise power measurement

The total electrical energy input to the pulverizing mill was measured using a high precision energy meter (YOKOGAWA, Japan WT3000) with sensitivity better than 0.01wh. The time, voltage, current and power consumed by the mill can be continuously measured and recorded simultaneously (every 30 seconds) using memory devices attached to the power meter. The energy meter was connected in parallel with the pulverizing mill to ensure that only

.

the power input to the mill is measured. The power consumption of the mill during intermediate cooling stages was subtracted from the measured value.

2.4 Characterization

2.4.1 Chemical analysis

The ilmenite samples were subjected to bulk chemical analysis. About 0.2 g of the sample was completely dissolved in hydrochloric acid (18.8 M) using a microwave digester (Microwave Accelerated Reaction System MAR5). The microwave digester is provided with eight numbers of reaction vessels; hence the unmilled and activated (30, 90 and 240 min) samples of a single batch could be digested simultaneously. The samples were transferred to the reaction vessel and 25 ml of hydrochloric acid (9.2 M) was added. The temperature (150^0C), pressure (50 Pa) and time (20 min) of digestion were fixed for microwave digestion. The temperature of the reaction vessels were controlled using a temperature probe (PRT-300). The pressure inside the reaction vessel was monitored and controlled by an electronic pressure sensor (ESP-500 plus). The experiments were continued until the samples dissolved completely. After dissolution, the solution was filtered and subjected to chemical analysis by Atomic Absorption Spectrophotometry, UV Spectrophotometry, titration and gravimetric techniques using standard methods (Vogel, 1989).

An Atomic Absorption Spectrophotometer, AAS (Model GBC Avanta) was first employed for the analysis of the filtrate for the elements Fe, Al, Si, Mg, Mn, V, Cr, Ca, and P. However, Ti could not be analyzed with AAS since it had a very low range of sensitivity. Further, the dilution enhances the errors in measurement. The Ti content was determined using an UV visible Spectrophotometer (Shimadzu, Japan, Model No.160A). In acidic medium, titanium (IV) solution produces a yellow colour when treated with hydrogen peroxide. The intensity of the colour is proportional to the amount of Ti in the solution. The intensity is measured at a wavelength of 410 nm using UV spectrophotometer. A comparison is made with a standard titanium (IV)

.

sulphate solution. About 10 ml of the solution was used for each Ti analysis. Phosphoric acid (H_3P0_4) was added to the solution to neutralize the influence of Fe present in the solution. About 10 ml of 3% hydrogen peroxide (H_2O_2) was added into the solution and the intensity measured. The concentration of Fe^{+2} and Fe^{+3} ions were determined using a titration technique. The solution was titrated with potassium dichromate ($K_2Cr_2O_7$) solution (0.1N). Sodium diphenylaminesulphonate was used as an indicator. Iron (II) in the solution shows colourless to violet coloration at the end point. The concentration of Fe^{+3} ions were determined from total iron and Fe^{+2} ion concentration. The percentage of silica in the in the ilmenite samples were determined by gravimetry. All the elements were assumed to exist in the ilmenite sample as oxides.

2.4.2 EPMA analysis

A JEOL, Super Probe JXA-8600 model electron microprobe operating with a current setting of $2x10^{-8}$ A, with Standard Programme International (SPI) mineral standards and using on-line ZAF correction procedures was used for experimental investigation. The composition of the individual ilmenite grains were measured at the centre and at the edges.

2.4.3 Optical microscopy

The mineralogy and microstructural analysis of unmilled samples were carried out using a polarized optical microscope (LEITZ orthoplan, Germany). The samples were analyzed both under normal mode of illusion and with crossed nickel prisms. A qualitative analysis of the various minerals, oxides and other phases present were carried out by optical microscopy. An attempt was made to estimate the extent of alteration of the various ilmenite samples using microscopic analysis. However the activated samples of ilmenite could not be analyzed using an optical microscope because of their fine particle size.

2.4.4 XRD analysis

The effect of mechanical activation on the phase constitution, unit cell

.

parameters, crystallite size, and strain were analyzed by x-ray powder diffraction technique and line broadening analysis using standard methods reported in the literature (Cullity, 2001). The x-ray diffraction measurement was carried out using Siemens D-500 diffractometer. The samples were analyzed with Co-K_α radiation (λ=1.79026 A) at a scan rate of 1^o/min. The diffraction data was obtained using the software DIFFRAC-AT connected with the instrument.

2.4.5 Particle size analysis

The particle size distribution of the ilmenite samples before and after milling was determined using a laser diffraction analyzer (CILAS 1180, France). The instrument has a particle size measurement range of 0.04 to 2500 εm. All the particle size measurements were carried out in an aqueous medium. The particles were dispersed in water and stirred ultrasonically to avoid agglomeration of powder particles. About 100mg of ilmenite sample was used for each measurement.

2.4.6 BET Surface area analysis

The surface area of the ilmenite samples prior to and after mechanical activation was determined using a multipoint BET technique (Micrometrics ASAP 2020). The technique is based on the physical adsorption of helium gas molecules on a solid surface at 77 K (Brunauer et al., 1938). The instrument has a surface area measurement range from 0.001 to 3000 m^2/g. A high vacuum option provided in the instrument was used to measure small surface areas. The specific surface area was derived from the measured data using the software available (ASAP 2020) with the equipment

2.4.7 SEM analysis

The unmilled and activated ilmenite samples were characterized using a JEOL JSM 840A scanning electron microscope to study the microstructure and morphological changes introduced by mechanical activation. The samples were

.

prepared with fine carbon coating and the experiments are carried out in the back-scatter electron imaging mode at 14 kV.

2.4.8 TEM analysis

The TEM microscopic analysis ilmenite samples prior to milling and after milling were carried out with Philips, CM-12 Transmission Electron Microscope operating at 150 kV. The samples were carefully prepared with holey carbon coated grids for experimental investigation. The samples before milling and after 30, 90 and 240 minutes of milling were analyzed with both bright field, dark field illumination. The selected area diffraction patterns (SAED) were also obtained to find out the variation in crystallite size, nano phases and amorphization characteristics of various phases existed in the microstructure.

2.4.9 Thermal analysis

The ilmenite samples before and after milling were subjected to thermal analysis using a simultaneous TG/DTA analyzer (Seiko, Japan, Model No. 320). The experiments were carried out in static air atmosphere. About 50 mg of the sample was used for each experiment. α-alumina was used as a reference material. A dynamic measurement in the temperature range of 35 to 800^{o}C at a heating rate of 10^{o}C/min was adopted.

2.4.10 Calorimetric experiments

To estimate the enthalpy associated with the defects, the heat evolved or absorbed by the unmilled as well as the milled ilmenite samples was measured during the process of relaxation of defects in an aqueous solution using a high precision isothermal heat calorimeter (THERMOMETRIC, TAM AIR) with a sensitivity of 0.1 mW. To accelerate the relaxation process, a dilute acid solution was used. It was earlier confirmed through leaching and chemical analysis that no dissolution of ilmenite occurs at such dilute concentration during the timescale of the calorimetric experiment. The experiments were carried out at room temperature (25^{0}C). The differential power between the

.

sample and an alumina reference was continuously recorded for 6 hours. No changes were observed in the power vs time plots beyond 4 hours. The heat evolved or absorbed was determined from the time integral of the power *vs* time plot. The instrument has a facility to load several samples simultaneously. Thus the unmilled and activated samples (30, 90, and 240 min) were subjected to the measurements simultaneously.

2.4.11 Density measurement

The density of ilmenite samples before and after activation determined using picnometric analysis using MICROMETRIX 2000. The reactor vassal is filled with He gas and the volume of the vessel is determined in blank condition as well as with material. The volume of the material is determined from the difference in volume occupied by He molecules at a given pressure. The density of the material is determined using the weight and volume of the samples.

2.4.12 Surface energy measurement

The specific surface energy of the unmilled and activated ilmenite samples was derived using the contact angle of solid liquid surface measured by the capillary rise method (using KRUSS Tensiometer K100). The capillary rise through a packed bed of the bulk powder measured by the increase in weight as a function of time is correlated to the advancing contact angle between the liquid and solid through the Washburn (1921) equation:

$$\frac{w_L^{\,3}}{t} = \frac{\left[(c.\bar{r})P^2(\pi R^2)\right]\rho^2\gamma_L\cos\theta_C}{2\eta} \qquad \text{.....(2.1)}$$

where w_L is the weight of penetrating liquid, γ_L is the surface tension of the liquid, r is the mean radius of capillary bundle, ρ is the density of measuring liquid, ţ is the relative porosity, R is the inner radius of measuring tube, θ_C is the advancing contact angle, η is the viscosity of liquid, t is the time of flow, c is the constant i.e., tortuosity factor and (c.r) is the empirical constant depending on particle size and packing density.

.

If the viscosity and surface tension of the liquid are known, the advancing angle (contact angle) can be determined from knowledge of the material constant (c.r). The material constant was determined through a calibration experiment using a completely wetting liquid (n-hexane). The measurements were carried out with five liquids: n-Hexane, formamide, water, di-chloromethane, ethelene glycol. The specific surface energy of the ilmenite samples was determined using the Owens, Wendt, Rabel and Kaelble method. In this method the polar and disperse fractions of the surface energy was derived from the contact angle data of various liquids using the following equation (Owens and Wendt , 1969)

$$\frac{1+\cos\theta_C.\sigma_L}{2\sqrt{\sigma_L^D}} = \sqrt{\sigma_S^P}\sqrt{\frac{\sigma_L^P}{\sigma_L^D}} + \sqrt{\sigma_S^D} \quad \text{.....(2.2)}$$

Where $\mathring{u}_S$ and $\mathring{u}_L$ are the surface tension of solid and liquid respectively. P and D refer to the polar and dispersive components.

2.4.13 Magnetic measurement

The magnetic behavior of the unmilled and activated ilmenite samples were studied using a EG&G PAR 4500 vibrating sample magnetometer. The initial magnetization and hysterisis curves of the ilmenite samples were obtained at room temperature, (300 K). Magnetic hysterisis loops were obtained up to 15 koe, were carried out in tightly packed powders of the ilmenite sample in unmilled and activated condition.

2.5 Leaching eperiments

Fig.2.2 shows the line diagram of leaching equipment used for the dissolution experiments with single reactor. Four 250 ml pyrex glass reactors equipped with a thermometer, mechanical stirrer and a reflux condenser were used for leaching of unmilled and mechanically activated samples of ilmenite concentrate. The four reactors were filled with the respective acid of four different concentrations (1.8M, 5.5M, 9.2M and 12.9M for H_2SO_4 and 2.3M, 6.9M, 9.2M and 11.5M molar concentration for HCl). The reactors were heated simultaneously in a single liquid paraffin bath. A resistance heated hot plate

.

with temperature control and power regulation (Powerstat) was used to heat the reactors to the required temperature. A thermometer was fitted to one of the openings. The temperature during the leaching experiments was constant and could be controlled within $\pm 1^{O}C$. Leaching temperatures in the range of 50-95^{o}C was used for HCl and temperatures in the range of 80-120^{o}C was used for H_2SO_4 (except for leaching in 1.8M H_2SO_4 wherein the temperature range was 70-95^{o}C).

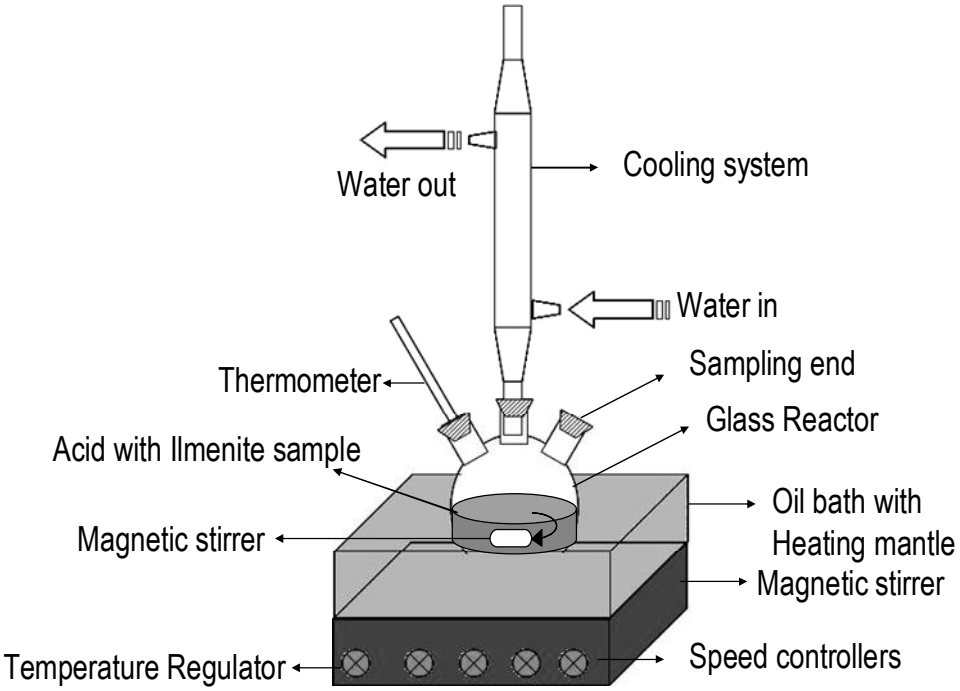

Fig.2.2. Line diagram of leaching equipment (with a single reactor) used for the dissolution experiments.

The leaching experiments were carried out with a solid to liquid ratio of 1:10, and 1:100. Several sulfuric and hydrochloric acid leaching experiments on both, the unmilled as well as the 240 minutes milled samples were also carried out with a solid to liquid ratio of 1:100. Although from the viewpoint of fundamental kinetic analysis, a solid to liquid ratio of 1:100 is desirable, a S:L ratio of 1:10 is more realistic from an industrial and scale up point of view. The reactors were filled with 100 mL of acid solution of the specified composition, preheated to 40^{0}C and 10 g of solid samples (1g in the case of S:L being 1:100) were added to each of the reactor. The bath was subsequently heated rapidly to

.

the experimental temperature where it was held isothermally. The time required for reaching the experimental isothermal temperature after the addition of solid sample was between 5 to 10 minutes. Unmilled, 30, 90 and 240 minutes activated samples were adopted for the leaching studies. Stirring was carried out using a Teflon-coated magnetic stirrer to keep the ilmenite particles suspended in the leachant. The leaching experiments were carried out isothermally and 3 ml of the solution from each reactor were withdrawn at different time intervals for the chemical analysis. The leach solutions drawn for analysis were filtered and made up to 100 mL in a standard flask. The Fe content in the solution was determined using atomic absorption spectrophotometer (Model GBC Avanta) and the Ti content was determined using a UV spectrophotometer (Shimadzu, Japan, Model No.160A). Calibration using standard solutions was done prior to the analysis. After the completion of the leaching experiment, the reactors were quenched in water to stop further dissolution and immediately filtered. The leach residues after filtration were washed thoroughly and dried in sunlight and in an oven at 105^{o}C for four hours, weighed and the mass loss determined. The leach residues were subjected to x-ray diffraction analysis (Siemens D-500 diffractometer) to identify the intermediate phases formed during leaching.

The Eh (redox potential) and pH of the solution was measured at the beginning (prior to heating) and end of each experiment (after quenching) at ambient temperature. The redox potential was measured using a calomel electrode and the measured potentials were converted to that of a standard hydrogen electrode. The instrument was calibrated before every measurement with a buffer solution of pH 4. The Eh and pH measurements were made for all the leaching experiments.

.

CHAPTER 3

EFFECT OF MECHANICAL ACTIVATION ON PHYSICO-CHEMICAL STRUCTURAL, THERMAL AND MAGNETIC PROPERTIES OF ILMENITE

3.1 Chemical and mineralogical characteristics

The chemical compositions of the ilmenite concentrate samples used in the present study are given in Table 3.1.

Element	Chatrapur	Navaladi	Manavalakurichi	Chavara
TiO_2	50.55	51.20	55.10	60.10
FeO	34.20	33.50	20.30	10.50
Fe_2O_3	12.30	12.70	19.90	26.30
Al_2O_3	0.45	0.46	0.80	0.70
SiO_2	0.70	0.81	1.50	0.75
MgO	0.72	0.73	1.00	0.40
MnO	0.54	0.35	0.40	0.40
V_2O_5	0.23	0.22	0.22	0.15
Cr_2O_3	0.05	0.05	0.08	0.13
CaO	0.05	0.18	0.08	0.15
P_2O_5	0.03	0.02	0.12	0.20

Table 3.1: Bulk chemical analysis of the altered ilmenite samples used in the present study

The microphotographs of the raw (unmilled) ilmenite concentrate samples obtained from Chatrapur and Manavalakurichi regions are displayed in Figs. 3.1a and 3.1b respectively. The ilmenite occurs mostly as sub-rounded to sub-angular grains marked by numerous surface pits, etch marks/grooves and crescentic pits as seen in the photomicrograph. Reflected light microscopic studies of the samples suggest that ilmenite is the major phase in both the samples. In addition to the ilmenite phases, traces of primary hematite are noticed in the Chatrapur sample. The Manavalakurichi ilmenite sample shows

.

varying amounts of leucoxene (altered rutile) as well as some coarse grains of primary rutile in addition to the ilmenite.

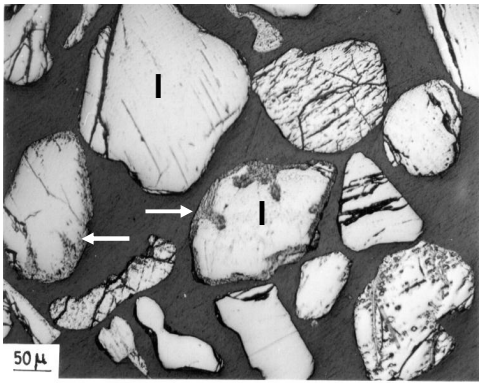

Fig.3.1 a

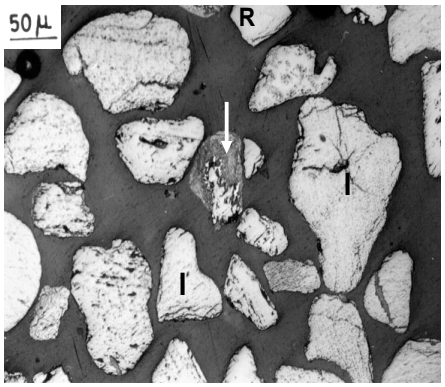

Fig. 3.1 b

Fig 3.1a: Microphotograph of Chatrapur ilmenite sample in unmilled condition under reflected light. Some of the ilmenite grains are unaltered (I) while some grains are altered along the margins and cleavage planes (as shown by arrow mark)

Fig. 3.1b: Microphotographs of the Manavalakurichi ilmenite sample in unmilled condition showing rutile grains (R) and alteration products (as shown by arrow marks) along with ilmenite concentrate (I).

Many ilmenite grains are moderately altered in both the concentrates and the alteration appears to have proceeded along grain boundaries, grain edges, and fissures. The alteration of the grains has occasionally resulted in an amorphous to crypto- or microcrystalline mass resembling leucoxene and pseudo-rutile. Similar petrological characterization results were also reported by Acharya et al. (1999), for beach sand ilmenite of Chatrapur and Manavalakurichi regions respectively. The intensity and mode of alteration varied from grain to grain and was neither uniform nor continuous. The distribution of altered ilmenite in the sample was estimated to be around 10% in Chatrapur ilmenite and 12% in Manavalakurichi ilmenite. The results of the electron microprobe analyses of altered ilmenite at the rim and core, ilmenite, ilmo-hematite, leucoxene and pseudo-rutile are presented in Tables 3.2 and 3.3 for the Chatarpur and Manavalakurichi ilmenite samples respectively.

.

Compounds	Ilmenite*	Altered ilmenite		Pseudo-rutile formed from ilmenite
		Unaltered core *	Altered rim*	
FeO	46.11	46.62	N.D.	N.D.
Fe_2O_3	N.D.	N.D.	2.43	0.75
TiO_2	51.48	50.21	81.63	92.81
MgO	0.87	0.49	0.57	0.18
Al_2O_3	0.11	0.05	3.51	1.59
MnO	0.61	0.31	0.11	0.03
Cr_2O_3	0.10	0.30	0.25	0.14
ZnO	0.04	0.08	0.05	0.01
SiO_2	-----	------	5.58	2.40
V_2O_5	0.27	0.27	0.45	0.51
BaO	0.25	0.35	0.41	0.43
CaO	0.01	0.01	0.04	0.03
K_2O	-----	-----	0.05	0.13
Na_2O	0.15	0.04	0.12	-----
Total	99.94	98.73	95.20	98.99

Table 3.2: EPMA analysis of the Chatrapur ilmenite sample and its associated phases (in wt.%). [1]

Compounds	**Ilmenite***	**Altered ilmenite**	
		Unaltered core *	**Altered rim***
FeO	42.72	45.76	N.D.
Fe_2O_3	N.D.	-----	3.77
TiO_2	53.38	52.69	89.63
MgO	1.51	0.03	0.03
Al_2O_3	0.50	0.41	1.78
MnO	0.85	0.48	0.01
Cr_2O_3	0.05	0.02	0.21
SiO_2	-----	------	1.92
CaO	0.01	0.01	0.14
K_2O	-----	-----	0.01
Na_2O	-----	0.38	0.59
Total	99.02	99.78	98.09

Table 3.3: EPMA of Manavalakurichi ilmenite sample and altered ilmenites (in wt.%) [1]

* Average of two grains; "-----" not detected; N.D. = Not determined.

.

Titania content as well as the ferric to ferrous ratio in the Manavakurichi sample is higher than that of the Chatrapur beach placer ilmenite of Orissa coast, suggesting a higher degree of weathering for the Manavalakuruchi ilmenite. Other workers (Bary et al., 1984; Suresh Babu and Mohan Das, 1999) have also made similar observations on the weathering of Manavalakurichi ilmenite.

3.2 Particle size and surface area

The variation of particle size and particle size distribution with milling time is shown in Fig 3.2a and 3.2b for Chatrapur and Manavalakurichi ilmenite samples respectively.

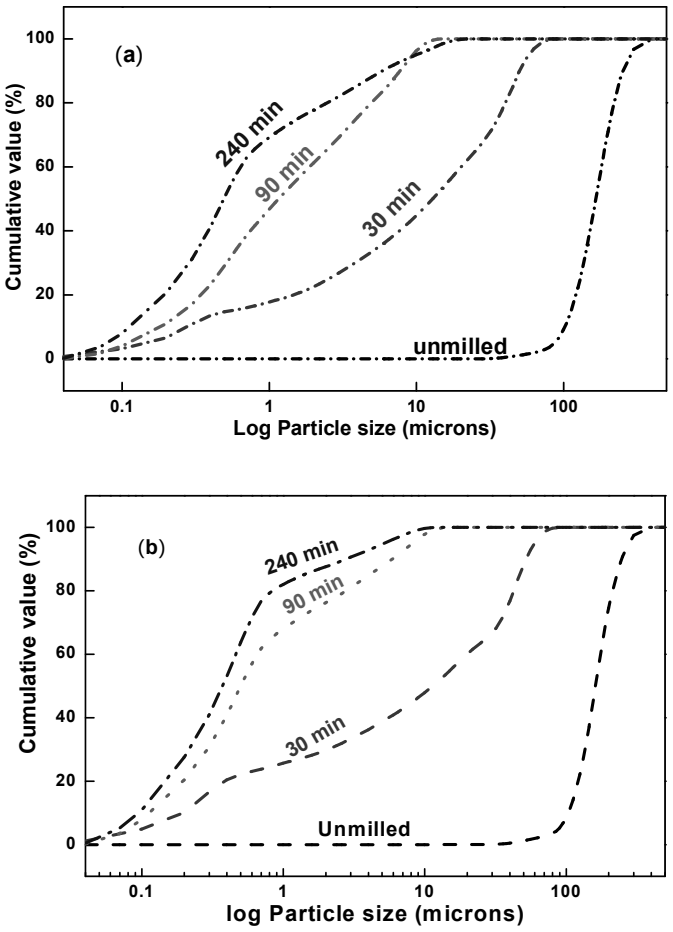

Fig.3.2: Particle size distribution as a function of milling time for (a) Chatrapur and (b) Manavalakurichi Ilmenite samples.

.

The particle size of Chatrapur ilmenite lies in the range of 100-500 μm in unmilled condition; whereas the particle size of Manavalakurichi ilmenite samples show a range of 12-400 μm. The initial BET surface area is higher for the Manavalakurichi ilmenite sample (6.13 m^2/g) compared to the Chatrapur ilmenite 1.46 m^2/g (Suresh babu et al., 1994). The larger initial surface area for Manavalakurichi ilmenite sample can be attributed to the higher degree of weathering compared to the Chatrapur ilmenite sample. The particle size decreases exponentially with milling time and reaches a steady state (0.04-15 μm) beyond 90 minutes of activation in both the ilmenite samples. A plot of the variation of mean particle size and surface area with milling time is shown in Fig. 3.3 for Chatrapur and Manavalakurichi ilmenite samples.

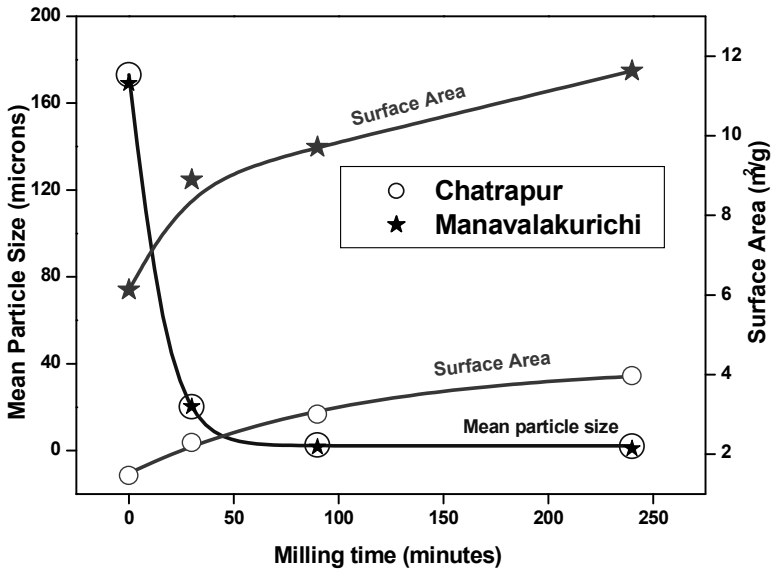

Fig.3.3: Variation of mean particle size and surface area of Chatrapur and Manavalakurichi ilmenite samples with milling time.

The mean particle size of both the ilmenite samples decreases exponentially and reaches a value of ~1 μm in 4 hours of milling. However, there is a distinct variation in surface area of the ilmenite samples before and after milling. The Manavalakurichi ilmenite sample shows higher surface area (12 m^2/g) compared to Chatrapur ilmenite sample (4 m^2/g) in 4 hours of

.

milling. The defects and fissures created by milling increased the surface area of activated samples.

3.3 Morphology

The change in morphology of the ilmenite samples subjected to mechanical activation was studied using scanning electron microscopy. The SEM microphotographs in the back-scattered electron-imaging mode of the Chatrapur and Manavalakurichi ilmenite samples in unmilled condition and after 30 and 90 minutes of milling are shown in figs 3.4(a,b,c), and fig 3.5(a,b,c) respectively.

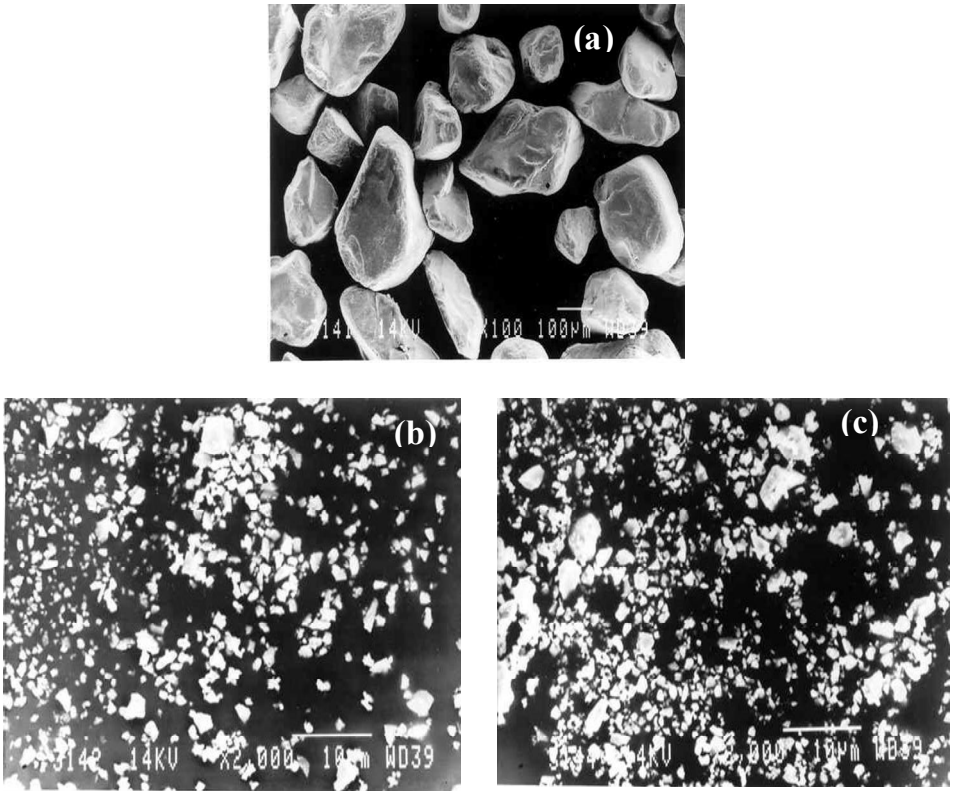

Fig 3.4: SEM Microphotograph of Chatrapur ilmenite samples in (a) unmilled (b) 30 minutes milled and (c) 90 minutes milled condition.

It is observed that both Chatrapur and Manavalakurichi ilmenite samples reveal smooth sub-rounded to sub-angular particles in unmilled condition. The unmilled samples show particles in the size range of 100-500 μm. In contrast, the activated sample consists of particles in the submicron to micron range and

.

is predominantly angular in shape caused by fracture of the original particles. Some of the particles in the activated sample are rounded, probably resulting from a combination of abrasion of the edges and physical deformation during milling (Welham and Llewellyn, 1998). The ilmenite samples subjected to 30 and 90 minutes milling shows particles in the size range of 0.04-80 μm and 0.04-15 μm respectively.

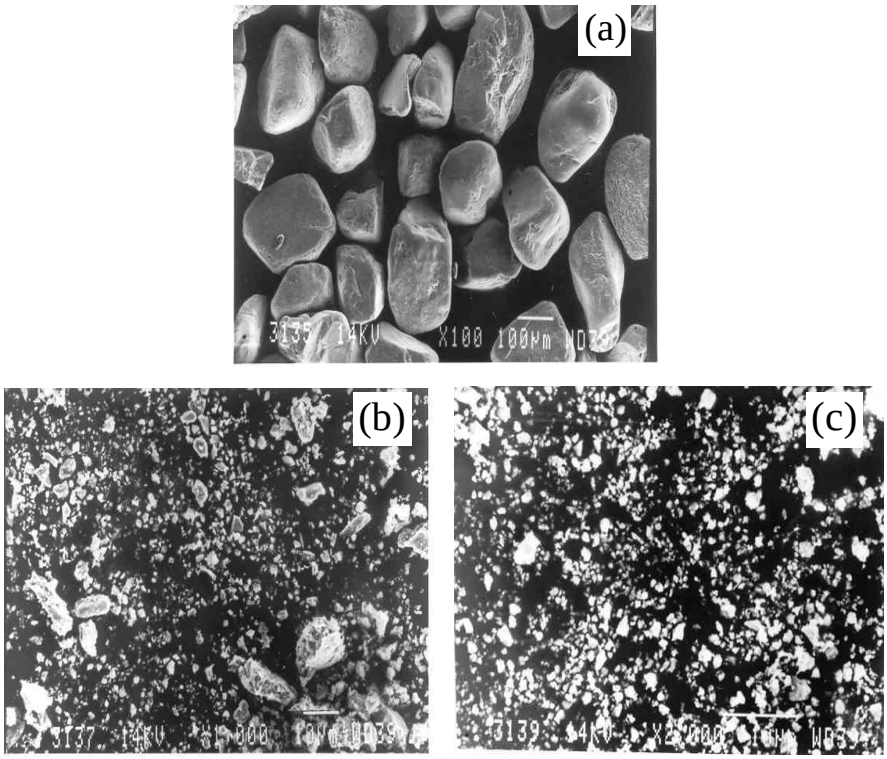

Fig 3.5: SEM Microphotograph of Manavalakurichi ilmenite samples in (a) unmilled (b) 30 minutes milled and (c) 90 minutes milled condition.

The particle size of the Manavalakurichi ilmenite samples shows finer particles after milling compared to Chatrapur ilmenite.

3.4 Density and volumetric density of defects

The variation in the density of the Chatrapur and Manavalakurichi ilmenite samples with milling time is shown in Fig 3.6. The initial density of the Manavalakurichi sample is considerably lower than the Chatrapur sample because of the enhanced weathering. The porosity in ilmenite samples were enhanced by natural weathering process (Suresh babu et al., 1999). The density

.

of Chatrapur and Manavalakurichi ilmenite samples shows an exponential decrease with the time of milling. The decrease in density can be attributed to the volume enhancement caused both by creation of defects as well as the increase in lattice parameter of the activated samples.

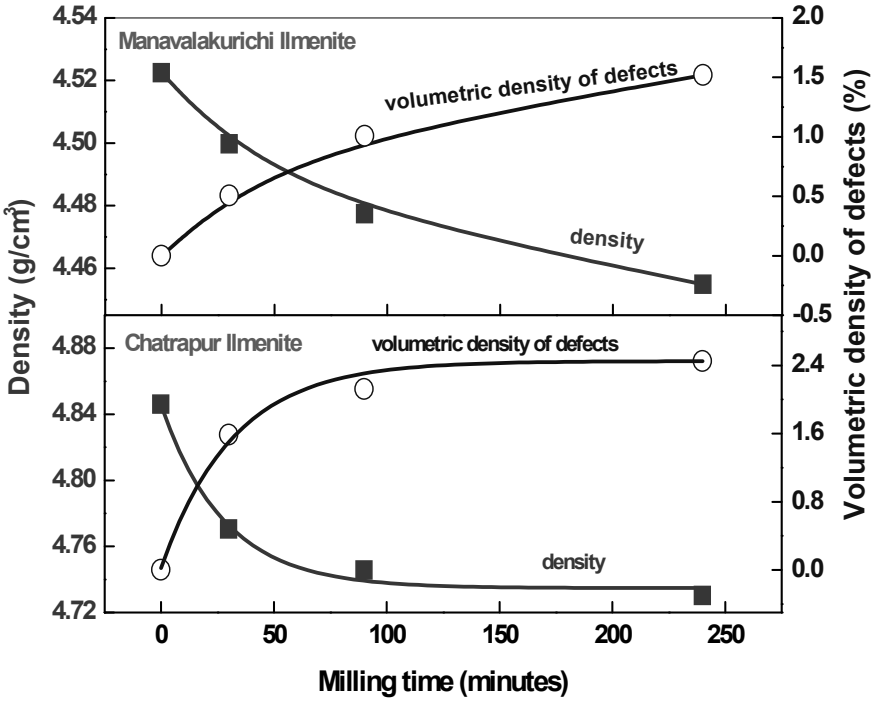

The volume of defects ($\Delta V_{DEFECTS}$) created during milling was derived using the values of experimental density and theoretical density derived from x-ray diffraction technique as:

$$\Delta V_{DEFECTS} = M_{V,EXP} - M_{V,Calc.(XRD)} = \frac{W_M}{\rho_{EXP}} - \frac{W_M}{\rho_{XRD}} \quad .....(3.1)$$

where $M_{V,\ Exp}$ and $M_{V,\ Calc}$ are the molar volume of the ilmenite samples determined from experimental procedure and xrd density calculations respectively. W_M, ρ_{Exp} ρ_{XRD} are the molecular weight, experimental density and theoretical density derived from xrd of the ilmenite samples respectively. The variations of volumetric density of defects created during milling are shown in Fig.3.6 for Chatrapur and Manavalakurichi ilmenite samples. It is observed that the volumetric density of defects created by mechanical activation increase exponentially with milling time.

.

3.5 Crystalline phase transformation and amorphization

The X-ray diffractogram of the Chatrapur and Manavalakurichi ilmenite samples in unmilled condition and for various times of activation are depicted in Figs.3.7 and 3.8 respectively.

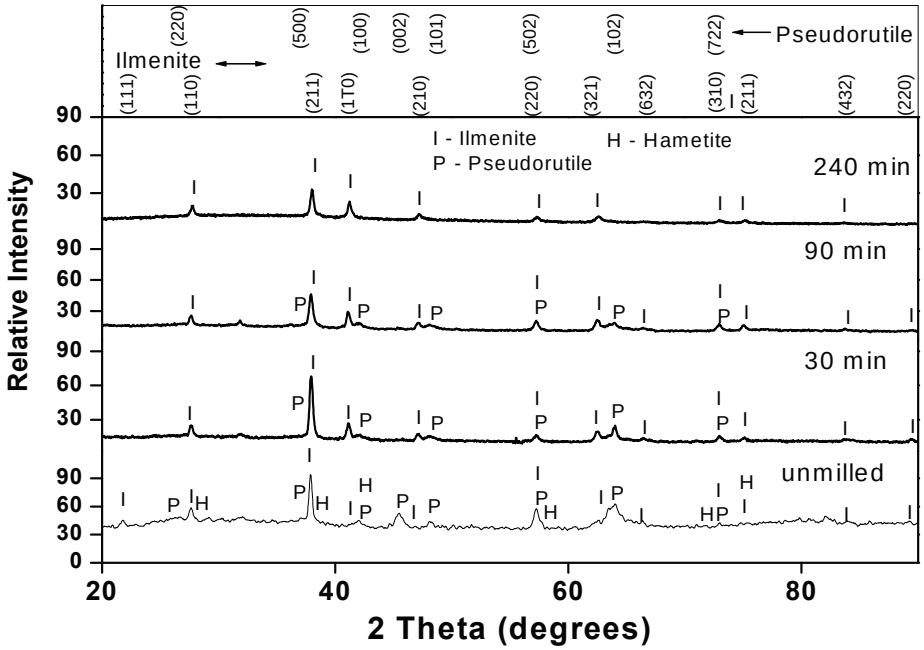

Fig.3.7: XRD of the unmilled, 30 min, 90 min and 240 min milled samples of Chatrapur Ilmenite

The XRD of both the ilmenite samples in unmilled as well as in milled condition indicates predominantly ilmenite (JCPDS No.29-0733) phase. The Chatrapur sample shows traces of pseudo-rutile (JCPDS No.29-1494) and Hematite (ICDD No.24-72) with ilmenite peaks. The pseudo-rutile peaks are not observed in the Manavalakurichi ilmenite sample because of its likely presence in amorphous form; however, a significant amount of rutile phase (JCPDS No. 21-1276) was observed in both unmilled and activated samples of Manavalakurichi ilmenite. As the activation time increased, line broadening and shifting of the ilmenite peaks as well as the pseudo-rutile and rutile peaks occurred for the Chatrapur and Manavalakurichi samples respectively. However after 30 minutes of milling the Hematite peaks were observed in XRD diffractogram and for 240 minutes of activation, only the ilmenite phase was found to be present and the pseudo-rutile phase could not be detected in

.

the Chatrapur ilmenite sample indicating quasi-amorphization of these phases or exist as very fine grained material.

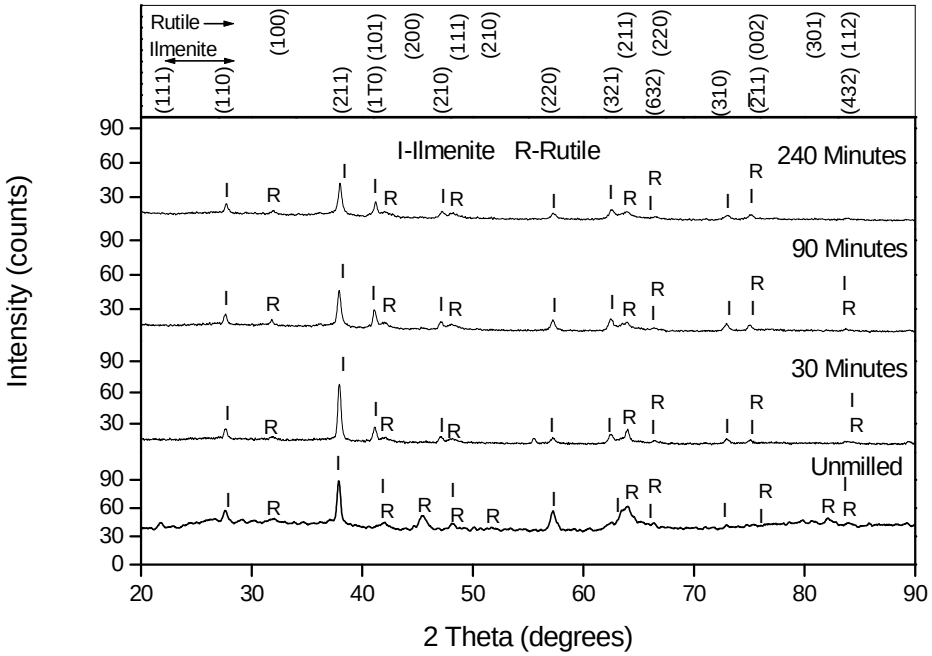

Fig.3.8: XRD of the unmilled, 30 min, 90 min and 240 min milled samples of Manavalakurichi Ilmenite

Suresh Babu and Mohan Das (1999) have earlier studied the weathering characteristics of ilmenite from Chatrapur (Orissa). They observed that the ilmenite from Chatrapur does not contain pseudorutile or rutile as a significant phase and instead they detected hematite in small quantities, both by XRD and Mössbauer spectroscopy. Acharya et al. (1999) also studied the mineralogical features of ilmenite of Chatrapur coast and reported the presence of ilmenite, hematite and altered ilmenite (leucoxene). The Chatrapur sample used in the present study contained traces of pseudorutile. However, with increasing times of activation, the pseudo-rutile phase becomes amorphized. The pseudo-rutile peaks completely disappear after four hours of activation. On the contrary, Chen (1997) observed complete conversion of ilmenite to metastable $Fe_2Ti_3O_9$ (pseudorutile) and γ-Fe_2O_3 phases after hundred hours of ball milling in air. Chen (1997) and Welham (1997) in an independent study did not observe any phase change even after 200 hours of grinding when the mechanical activation of ilmenite was carried out in vacuum.

.

3.6 Crystallite size and strain

The variation of crystallite size and strain with milling time was calculated from the line broadening of the ilmenite reflections using Schererôs formula. The equation describing Hall Williamson method for separation of crystallite size and strain can be written as

$$B = \left[\frac{0.9\lambda}{D_{Cry}\ Cos\ \theta_D} \right] + \left[4\varepsilon \tan \theta_D \right] + B_0 \ldots\ldots\ldots \quad \ldots\ldots(3.2)$$

where, B_t is the full width at half maximum (FWHM) intensity of the peak, λ the wavelength of the radiation used, D_{Cry} is the average crystallite size, ε the lattice strain, θ the diffraction angle and B_0 is the instrumental line broadening. Fig. 3.9 shows the Hall Williamson plot of Chatrapur and Manavalakurichi ilmenite samples illustrating broadening with milling time.

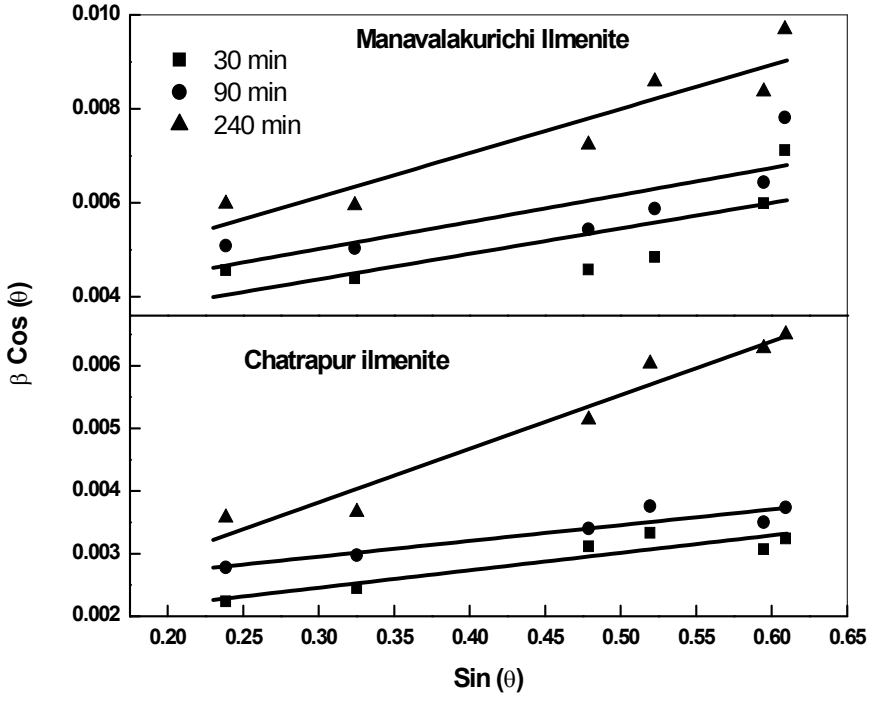

Fig. 3.9: Williamson Hall plot of Chatrapur and Manavalakurichi ilmenite samples illustrating broadening with milling time.

The crystallite size and strain were calculated for the unmilled and the activated samples from the line broadening data for the six most intense

.

reflections for ilmenite using Williamson Hall method. The broadening from other phases (Pseudo-rutile, Hematite and rutile) as well as the broadening caused by instrumental factors were carefully analyzed and deduced from the total broadening. The line broadening caused by only ilmenite peaks were taken into consideration for determining the crystallite size and strain values. The variation of crystallite size and strain with milling time is shown in Fig. 3.10 for both Chatrapur and Manavalakurichi Ilmenite samples.

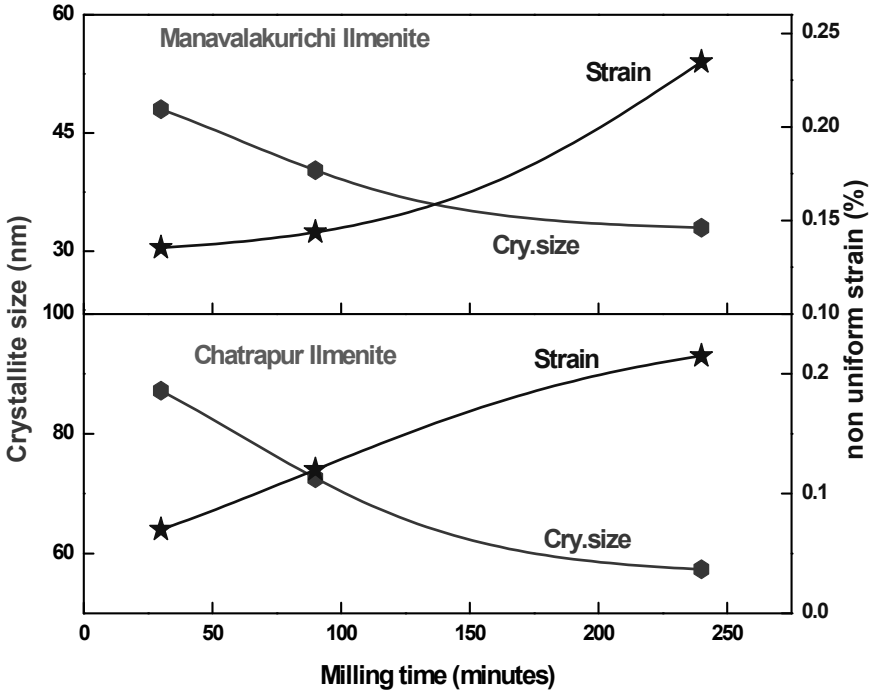

Fig.3.10: Variation of crystallite size and strain of Chatrapur and Manavalakurichi Ilmenite samples with milling time.

The crystallite size decreases exponentially with milling time in both the samples of ilmenite. However there is a difference in the behavior of strain with time of milling for the Chatrapur and Manavalakurichi samples. The lattice strain increases more or less linearly for Chatrapur ilmenite sample and exponentially for Manavalakurichi ilmenite sample with milling time.

The results of crystallite size derived from x-ray line broadening were verified using TEM microscopy. The TEM micrograph of Charapur and Manavalakurichi ilmenite samples, revealing the details of crystallite size, nano

.

phases and selected area diffraction pattern (SAED) are shown in Fig. 3.11 (a b) and 3.12 (a,b,c and d) respectively.

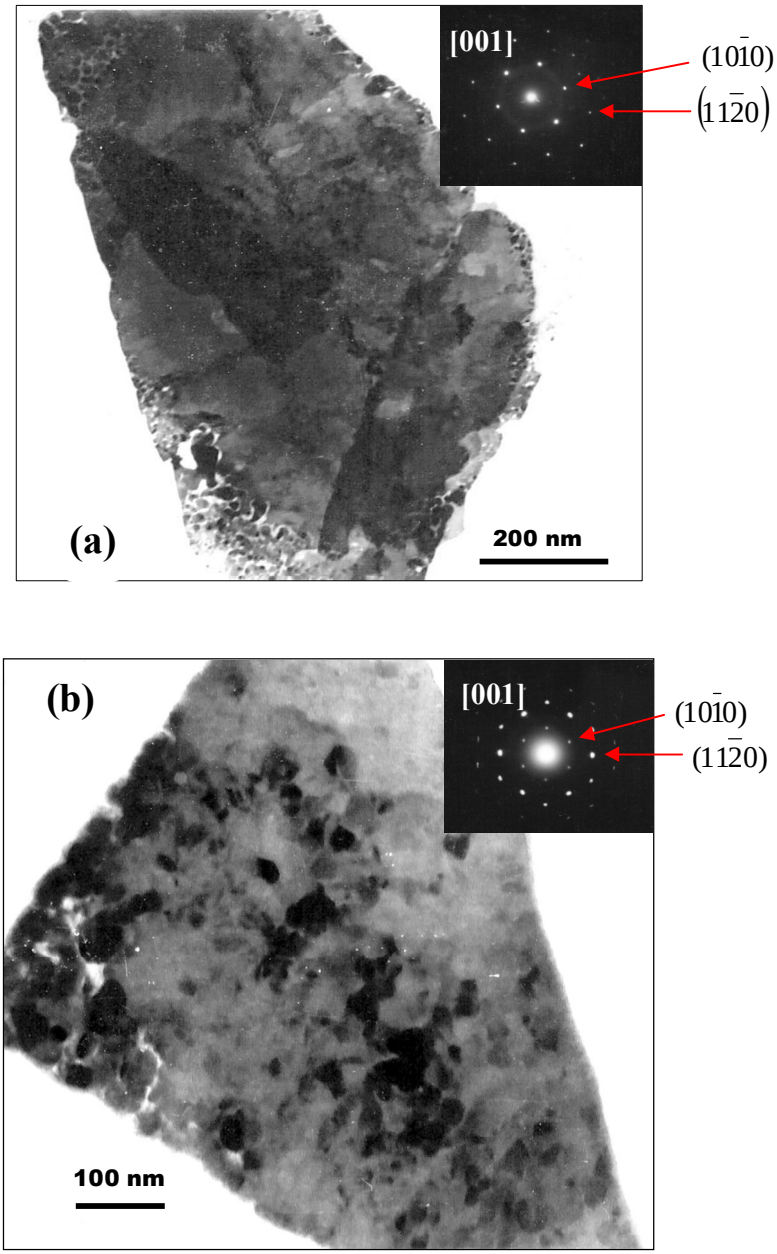

Fig 3.11: TEM Micrograph of Chatrapur ilmenite samples in (a) unmilled (b) 240 minutes milled milled condition showing the variation in crystallite size by milling. The selected area diffraction patterns (SAED) are also shown in the images.

.

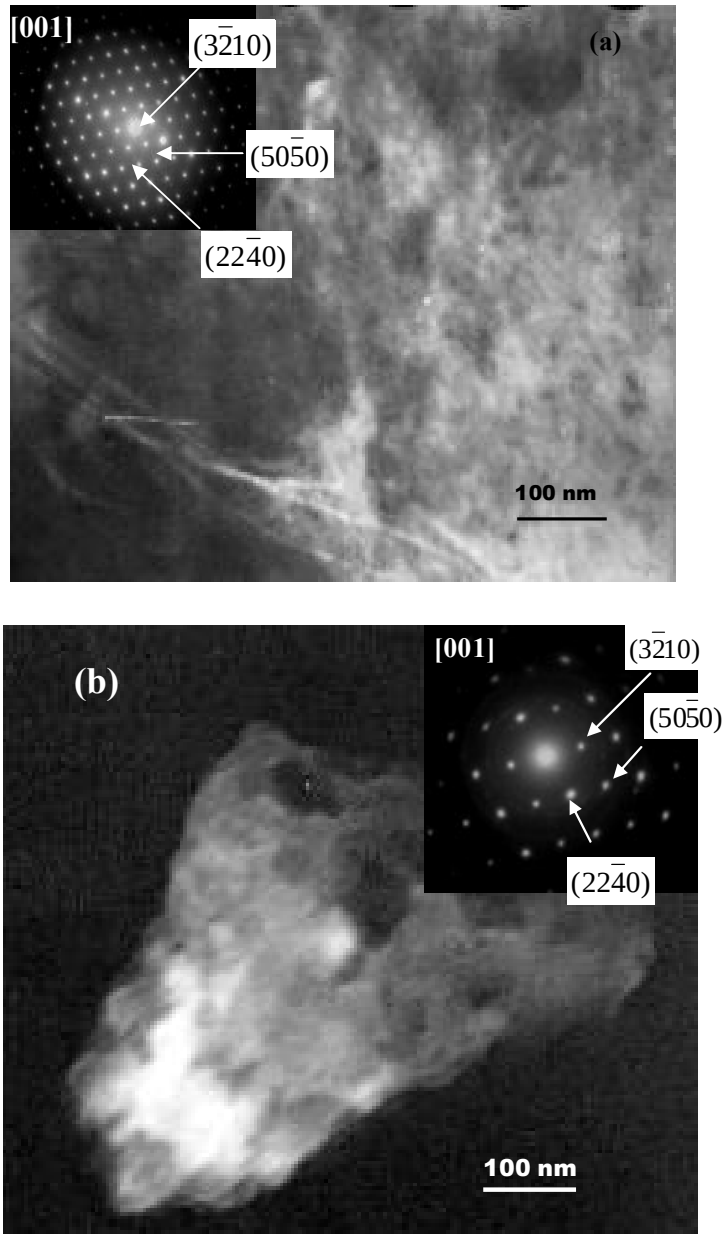

Fig 3.12: TEM Micrograph of Manavalakurichi ilmenite samples in (a) unmilled (b) 30 minutes milled condition showing the variation in crystallite size by milling and diffraction pattern.

.

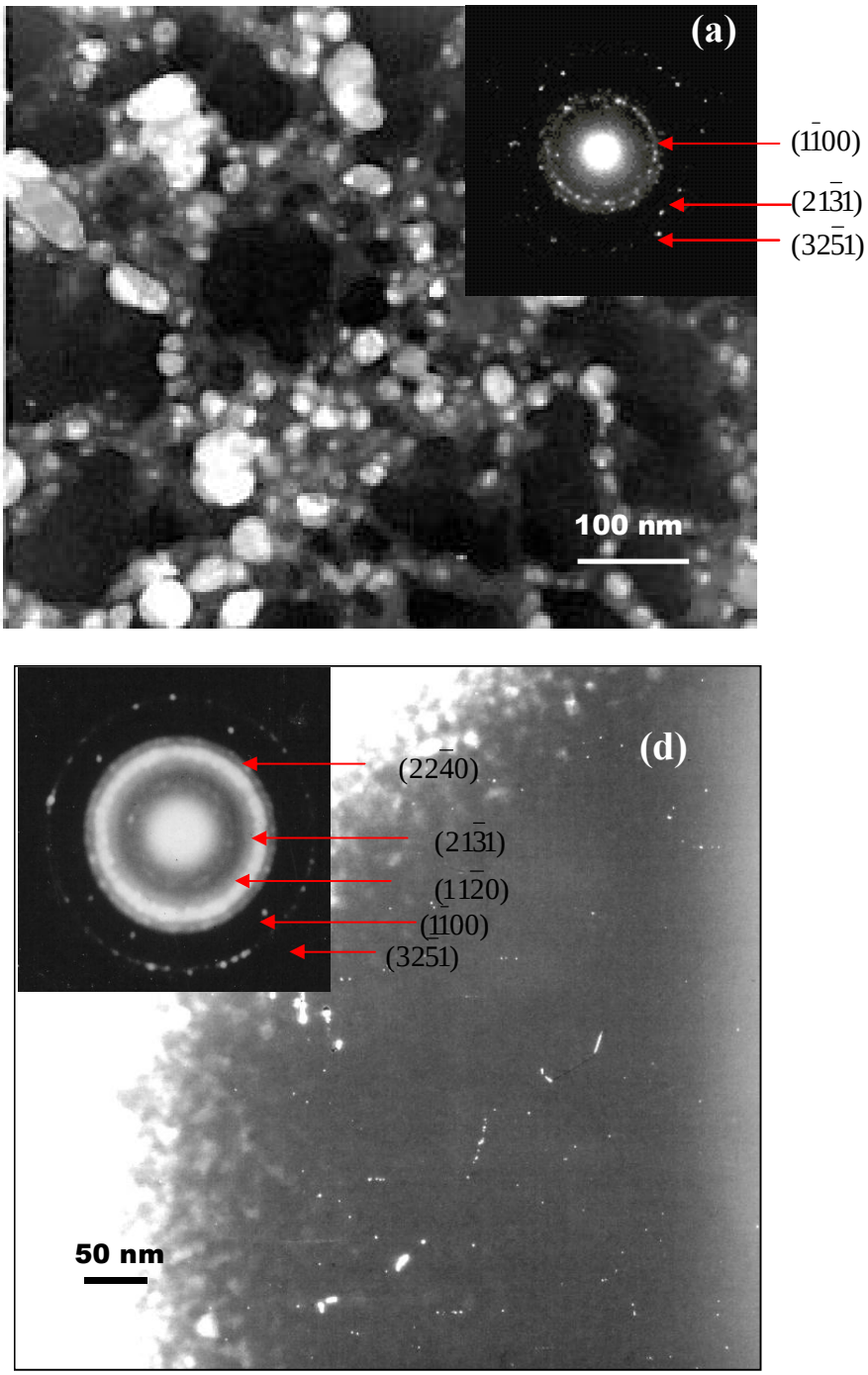

Fig 3.12: TEM Micrograph of Manavalakurichi ilmenite samples subjected to (c) 90 minutes (d) 240 minutes of milling showing very fine grained material after 4 hours of milling.

.

It is observed that the crystallite size of unmilled samples were in the range of 40 to 170 nm (fig. 3.11 a), whereas after 4 hours of milling the crystallite size reduces to 20 to 80 nm (3.11 b) for Chatrapur ilmenite samples. The mean crystallite size was found to be 130 nm in unmilled sample and it was found to be 90 nm, 70 nm and 55 nm in the samples subjected to 30, 90 and 240 minutes of milling. The crystallite size varied exponentially with milling time and the results were comparable with that of the results obtained from x-ray diffraction analysis. The electron diffraction analysis shows hexagonal structure of ilmenite phase before and after milling. However the diffraction pattern shows a very fine grained structure after milling.

The Manavalakurichi ilmenite samples (fig 3.12) shows the crystallite size in the range of 30 90 nm in unmilled condition and 15 to 40 nm after 4 hours of milling. The mean crystallite size was found to be 70, 40, 35 and 25 nm in unmilled sample and 30, 90 and 240 minutes milled samples respectively. The diffraction showed a fine grained material even in unmilled condition compared to Chatrapur ilmenite sample. This variation in unmilled samples can be attributed to the extent of weathering in Manavalakurichi ilmenite sample. The Manavalakurichi ilmenite sample also shows porosity in the sample caused by weathering process. The electron diffraction analysis shows a hexagonal structure of ilmenite in unmilled and after 30, 90 minutes of milling. However the sample subjected to 240 minutes of milling has very fine nano crystals as observed from the ring pattern of the ilmenite sample. The quasi-amorphization of ilmenite or rutile phases was observed in the milled sample as there it is difficulty in detecting the minor constituents. The figure 3.12 c shows the rutile grains with ilmenite sample. It was observed that the particle size of the rutile grains were higher that that of ilmenite grains after milling. It can be attributed to the higher fracture toughness of the rutile phase compared to ilmenite phase.

.

3.7 Grain boundary area

The crystallite size of the ilmenite samples determined by XRD line broadening analysis as well as TEM techniques showed an exponential decrease with milling time indicating an increase in grain boundary area with milling time. The grain boundary area was determined using the crystallite size of the ilmenite sample obtained using XRD line broadening analysis. The crystallites were assumed to have a tetrakaidecahedron configuration and the grain boundary area was calculated from the average crystallite sizes using the expression (Suryanarayana, 2004):

$$\Delta A_{GB} = N_G * 47.569 * (D_{Cry}/3)^2 \quad \text{.....(3.3)}$$

where N_G is the number of grains per unit volume and D the average crystallite size of the ilmenite sample. The` number of grains per unit volume (N_G) was derived from the volume of tetrakaidecahedron crystal as follows

$$V = 8\sqrt{2}(0.377D)^3 = 0.606D^3 \quad \text{.....(3.4)}$$

Where V is the volume of a tetrakaidecahedral crystal and the number of grains per unit volume is described as

$$N_G = \frac{M_V}{V} \quad \text{.....(3.5)}$$

Where Mv is the molar volume of the material. The variation of grain boundary area with milling time is shown in fig.3.13.

.

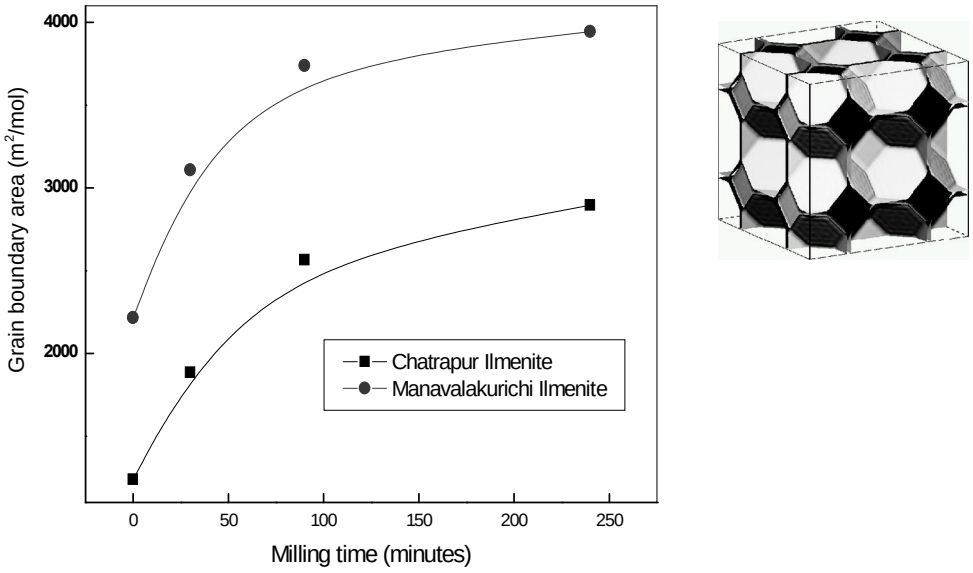

Fig.3.13: Variation of grain boundary area with milling time for Chatrapur and Manavalakurichi ilmenite samples determined from crystallite size measurements.

3.8 Lattice parameters

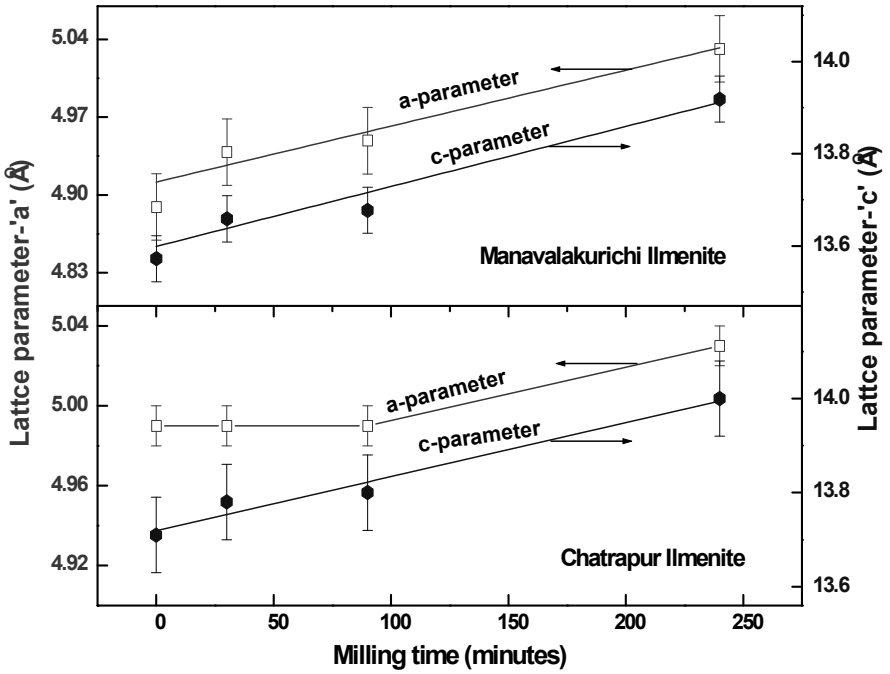

Fig.3.14: Variation of lattice parameters óaô and ócô with milling time for Chatrapur and Manavalakurichi Ilmenite samples.

.

The lattice parameters of the ilmenite samples before and after mechanical activation were determined from XRD results using Cohenôs method (Cullity, 2001). The variation in lattice parameter of the unit cell with time of milling is shown in fig. 3.14 for Chatrapur and Manavalakurichi ilmenite samples.

It is observed that the unit cell parameters (rhombohedra structure) óaô and ócô of both the ilmenite samples (Chatrapur and Manavalakurichi) increase marginally (within the limits of uncertainty) with time of activation.

It was observed that there is negligible distortion in óaô parameter of Chatrapur ilmenite until 90 minutes of activation. About 0.8% distortion was observed in 4 hours of mechanical activation. The ócô parameter increases continuously from 30 to 240 min of mechanical activation and shows a distortion of about 2.0% in the 4 hours activated sample indicating larger distortion in the ócô parameter compared to the óaô parameter. However, the lattice distortion in Manavalakurichi ilmenite is different from that of Chatrapur ilmenite. The distortion of both óaô and ócô parameters are approximately same (about 2.5%) in the Manavalakurichi ilmenite sample. Further, the lattice distortion is higher compared to Chatrapur ilmenite. This variation in lattice distortion can be attributed to a more loose structure for Manavalakurichi ilmenite caused by weathering. The reason for the small increase in lattice parameter in this study upon mechanical activation is not clear. Welham and Llewellyn (1998) did not observe any significant variation in lattice parameters until 25 hours of ball milling. They observed a decrease in óaô parameter after 25 hours of milling and there is no change in ócô parameter in their study. Earlier high pressure studies on crystal structure of ilmenite (Barry et al., 1984) showed a 0.6% reduction in óaô parameter and 1.2% in ócô parameter of the unit cell at a pressure of 4600 MPa.

3.9 Degree of partial amorphization/disordering

The degree of disorder of the ilmenite samples upon activation were evaluated from the extent of amorphization determined from XRD using integral peak areas by the method described by Ohlberg and Stickler (1962).

.

This partial amorphization is often referred as XRD amorphization in literatures (Tkacova, 1989; Balaz, 2000; Balaz, 2008).

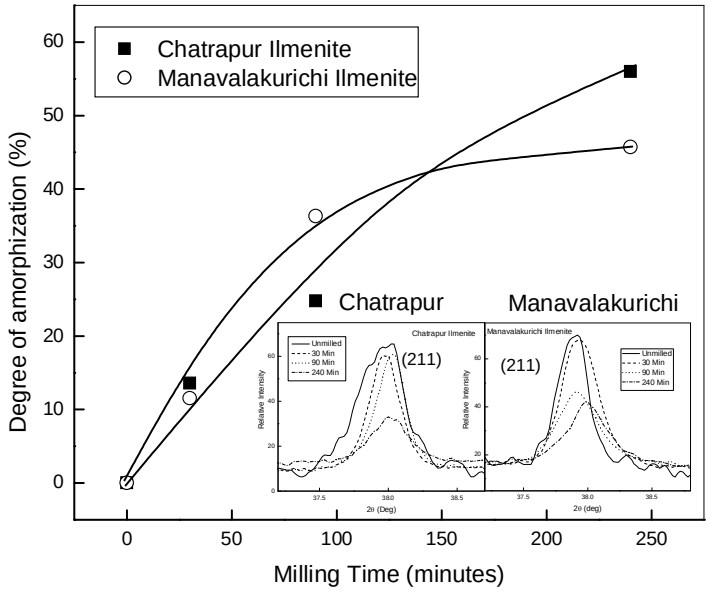

Fig.3.15: Degree of partial amorphization/disordering of Chatrapur and Manavalakurichi Ilmenite samples with milling time. (Inside figures illustrating structural disorder of Chatrapur and Manavalakurichi ilmenite at (211) plane)

The equation describing the degree of crystallinity (X) of a material compared with the non-activated sample can be written as

$$X_X = \left(\frac{Uo}{Ux}\right)\left(\frac{.Ix}{Io}\right) \quad \text{.....(3.6)}$$

Where Uo and Ux denote the background intensity of non-activated and activated samples respectively and Io and Ix are the integral intensity of the non-activated and activated samples respectively. The degree of partial amorphization/disordering, A is a complementary value of crystalline phase. It is defined as:

$$X_A = 100 - X \quad \text{.....(3.7)}$$

The variation in degree of partial amorphization/disordering computed from the integral peak intensity of the ilmenite in unmilled condition as well as in milled

.

condition. The degree of amorphization of Chatrapur and Manavalakurichi ilmenite samples with time of milling is shown in figure 3.15.

It is observed that the degree of amorphization increases exponentially with the time of activation. In contrast to other results (surface area, lattice disorder and defect density introduced by activation) the degree of amorphization is more in Chatrapur ilmenite sample compared to Manavalakurichi ilmenite. The amount of pseudorutile present in Chatrapur ilmenite sample is more than Manavlakurichi ilmenite sample and the psedorutile phase found to amorphize more easily by mechanical activation process.

3.10 Thermogravimetry (TG)

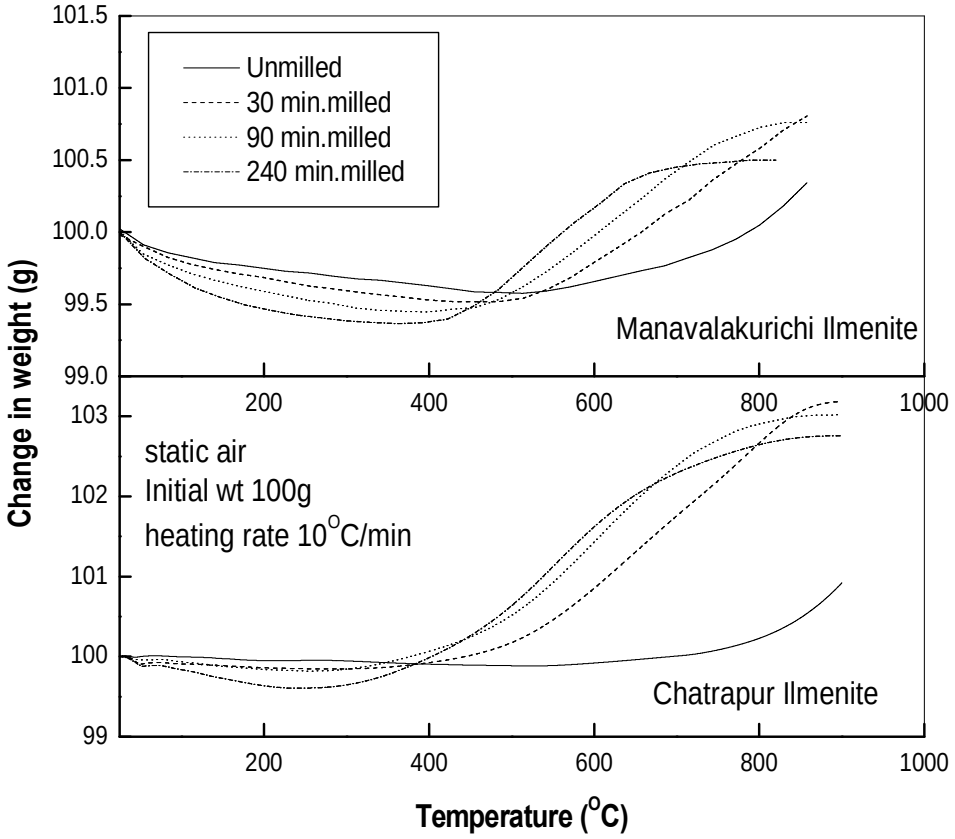

Fig.3.16: TG results showing change in weight of the unmilled and milled samples of Chatrapur and Manavalakurichi Ilmenite with increasing temperature.

.

The results of the thermogravimetric experiments of the unmilled and milled ilmenite samples in static air are depicted in Fig.3.16 for Chatrapur and Manavalakurichi ilmenite. The initial weight loss is due to the release of bound moisture and the subsequent weight gain is due to the oxidation of $FeTiO_3$ (Fe^{2+}) to $Fe_2Ti_3O_9$ (Fe^{3+}) (Suresh Babu et al.,1994; Suresh Babu and Mohan Das,1999). It is seen that the oxidation kinetics is considerably enhanced by mechanical activation in both the samples; complete oxidation is achieved in ambient air by 850^{o}C for the activated samples. The rate of oxidation of Fe^{2+} to Fe^{3+} was found to increase with increasing times of activation whereas, the extent of oxidation decreases with time of activation for activated samples. The TG results of the Chatrapur ilmenite shows a steady state weight gain of ~3.5% for 30 minutes of activation and about 2.8% weight gain for 4 hours of activation indicating partial oxidation of Fe^{2+} to Fe^{3+} during mechanical activation itself. The unmilled sample shows less than 50% oxidation. The x-ray diffractogram of the head sample and 4 hours milled samples of Chatrapur ilmenite quenched from 850^{o}C is shown in Fig. 3.17 (a and b).

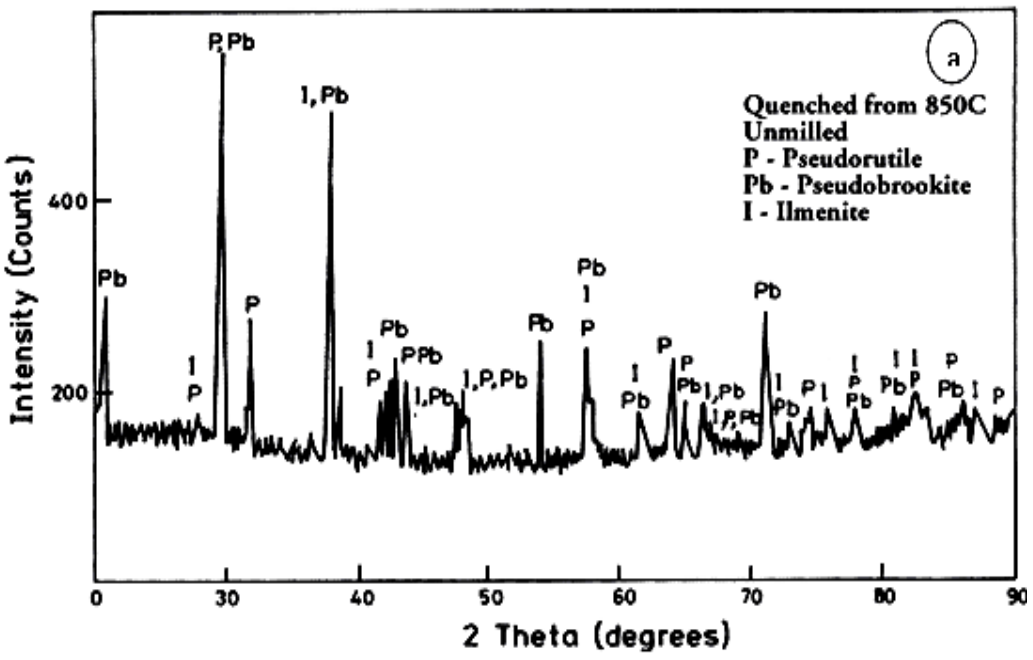

Fig.3.17a: X -ray diffraction pattern of the unmilled sample of Chatrapur ilmenite quenched from 850^{o}C.

.

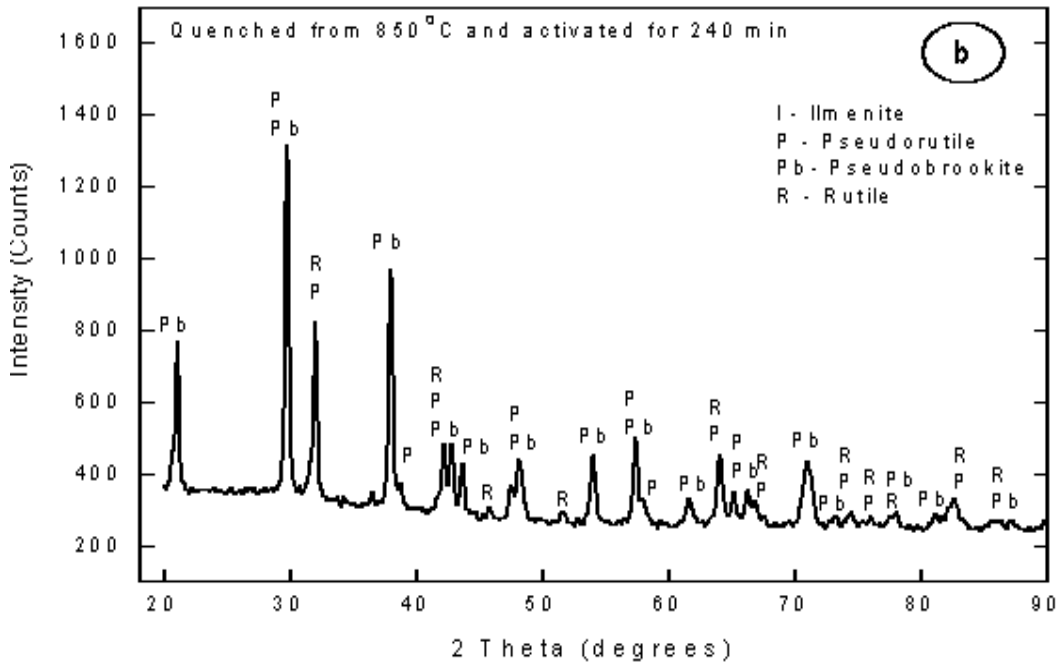

Fig.3.17b: X -ray diffraction pattern of the 4 hours milled sample of Chatrapur ilmenite quenched from 850^{o}C.

The activated samples show the presence of only pseudorutile, rutile and pseudobrookite phases and the ilmenite phase is completely absent at 850^{o}C whereas the unmilled sample under the same conditions shows considerable presence of unoxidized ilmenite in addition to pseudorutile and pseudobrookite. The Manavalakurichi ilmenite shows lesser oxidation both in unmilled and activated conditions compared to Chatrapur ilmenite since the unmilled sample itself is partially oxidized because of the higher degree of weathering i.e. part of the oxidation of Fe^{2+} to Fe^{3+} has occured by natural weathering.

3.11 Magnetic properties

The hysteresis curves for unmilled and milled (30, 90 and 240 min) samples of Manavalakurichi ilmenite at room temperature are shown Fig.3.18.

.

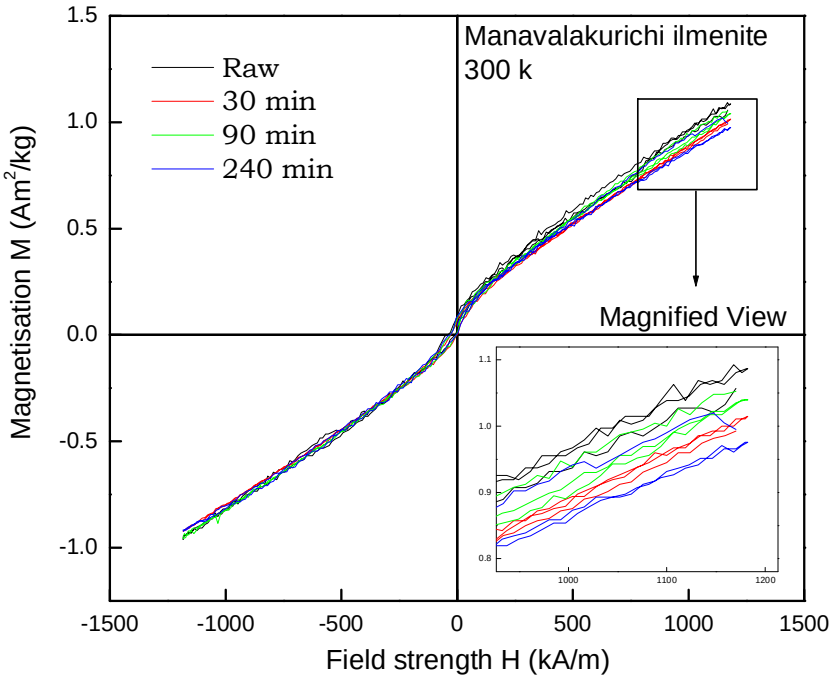

Fig.3.18: Hysteresis loops for unmilled and milled (30, 90 and 240 min) samples of Manavalakurichi Ilmenite showing the effect of milling on the shape of demagnetization curve.

It is observed that the magnetization for the milled as well as the unmilled samples does not saturate upto a field of strength 1200 kA/m. However there is a slight variation in magnetization of unmilled and milled samples at maximum field strength. A variation in coersivity of the ilmenite samples was also observed in milled and unmilled samples. Fig. 3.19 shows the variation of magnetization at maximum field strength (1200 kA/m) and coersivity of Manavalakurichi ilmenite with milling time.

The results show a continuous decrease of the magnetization with milling time. The magnetization at maximum filed of strength 1200 kA/m was found to be 1.08 Am^2/kg for unmilled sample and 0.98 Am^2/kg for the 4 hours milled sample of Manavalakurichi ilmenite; i.e., about 10% decrease in magnetization is observed in 4 hours of milling. This is due to the structural disorder of ilmenite caused by mechanical activation (Ding et al, 1996; Sepelak et al., 2003). On the contrary, the coercivity (Hc) of the ilmenite sample

.

increases with milling time and reaches a steady state after 90 minutes of milling.

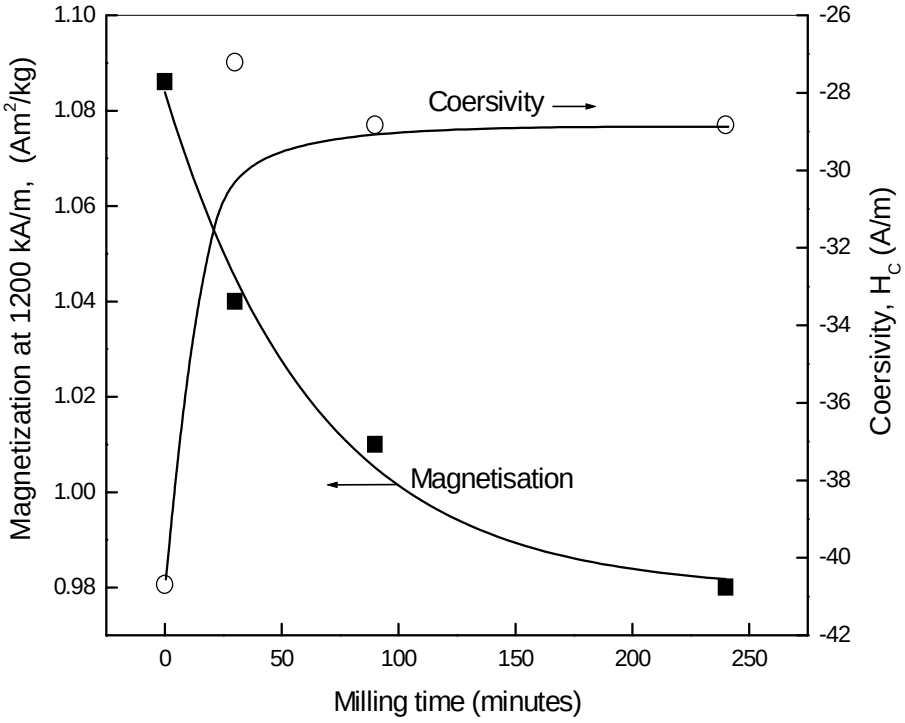

Fig.3.19: Variation of magnetization at a field of strength 1200 kA/m and coersivity (Hc), with milling time for Manavalakurichi ilmenite sample.

The coercivity in unmilled sample is about -40.6 kA/m and -28.7 kA/m for the 4 hours activated sample. The higher coercivity of the milled sample is because of smaller crystallite size, increase in the grain boundary volume, and structural disorder introduced by milling (Ding et al, 1996; Sepelak et al., 1999; Ehrhardt et al., 2003; Sepelak et al., 2003; Rabanal et al., 2003; Shenoy and Joy, 2004).

3.12 Conclusions

1. The morphology of particles changed from sub-rounded to sub angular particles in the raw samples to angular particles upon milling.The particle size decreased exponentially from an initial size range of 100-500 μm with time of activation and remained constant in the range of 0.04 to 15 εm beyond 90 min of activation.

.

2. The BET absorption surface area also showed an exponential variation with milling time and a maximum surface area of 11.6 m^2/g was achieved for Manavalakurichi ilmenite sample in 4 hours of milling.
3. The apparent density of all the ilmenite samples decreased with milling time, partly due to the increase in lattice volume arising from the creation of defects.
4. Significant amount of structural disorder was also observed on mechanical activation.A partial amorphization or a much fined grained phases of the hematite and pseudorutile was observed for the Chatrapur Ilmenite sample after 30 minutes and 4 hours of planetary milling respectively.
5. The ilmenite phase also showed substantial disordering (referred as xrd amorphization in literatures) and the degree of xrd amorphization exhibited an exponential variation with time of milling.
6. The crystallite size of ilmenite samples decreased exponentially with milling time, whereas the non-uniform lattice strain showed a linear increase. The crystallite sizes and the lattice strain varied in the range of 57-131 nm and 0.14ï 0.47% for Chatrapur ilmenite sample and 38-90 nm and 0.17-0.23% for Manavalakrichi ilmenite sample in 4 hours of mechanical activation.
7. The oxidation kinetics was also found to be considerably enhanced by mechanical activation, the rate of oxidation increasing with increasing time of activation. However, complete oxidation (~3.5%) of Fe^{+2} to Fe^{+3} was achieved in ambient air at $850^{O}C$ for the activated samples, less than 50% oxidation occurred in the unmilled sample.
8. The magnetic properties of Manavalakurichi ilmenite showed small variations upon mechanical activation. The magnetization of ilmenite at maximum field strength decreased with milling time; however the coercivity of ilmenite samples increased with milling time as the variation in crystallite size and structural disorder was enhanced by mechanical activation process.

.

CHAPTER 4

ENERGETICS OF THE MECHANICAL ACTIVATION PROCESS

Energy balance

The energy stored by the mechanical activation process increases the internal energy of the material. The energy balance for the mechanical activation process (occurring without a change in chemical composition) can be deduced from the 1st law of thermodynamics. The mechanical work done (or the total mechanical energy input) during the process (W) is given as (Tkacova, 1989):

$$W = \Delta E_M + \Delta E_G - (-Q) \quad \text{é é é é ..é é é é é .é é é é é é é é é ...(4.1)}$$

where, Q is the heat evolved, ΔE_M and ΔE_G is the internal energy change of the milled material and grinding media respectively. Although the stored energy in the material can be determined from independent measurements of the total work done, the energy change of the grinding media and the heat evolved during the process, these experiments are tedious and the uncertainties of measurement large. Equation (4.1) assumes that the energy lost through sound and electromagnetic processes are negligible.

Since no work is done against external pressure, the change in internal energy can be assumed to be the change in enthalpy and thus the internal energy increase in the material can be written as:

$$\Delta E_M = f_{Def.rel}\Delta H_{Def.rel} + \gamma_S.\Delta S.M + \gamma_{GB}.\Delta A_{GB}.M + \varepsilon.\Delta E_\varepsilon + f_{Amor}.\Delta H_{Amor} + f_{Trans}.\Delta H_{Trans} \quad .....(4.2)$$

where, $\Delta f_{def,rel}$ is the fraction of point, line and surface defects that has short relaxation times, $\Delta H_{def,rel}$ is the enthalpy of relaxation, ΔS - change in surface area during milling; γ_s - specific surface energy of material; M - molar weight of the sample , ΔA_{GB} - change in grain boundary area; γ_{GB} - specific grain boundary energy; ε - lattice strain induced during milling; ΔE_ε - strain energy; f_{amor} - fraction of amorphization; ΔH_{amor} - enthalpy of amorphization; f_{trans} -

.

extent of other structural transformations; ΔH_{trans} - enthalpy change associated with other structural transformations.

Only the structural excitation processes that have large relaxation times have been considered in Eq. (4.2). Further, it is assumed that the energy lost or gained by the material through electromagnetic processes are negligible. The energy contributed by the point and line defects is not described separately and is measured indirectly from the strain measurement. It is virtually impossible to precisely measure separately the various contributions given in Eq. (4.2). However, as seen from Eq. (4.2), the total effects can be broadly divided into that resulting from an increase in surface area and energy on milling and the rest of the parameters result from structural effects. For mechano-chemical activation, the energetics associated with the change in chemical composition has to be separately included.

4.2 Direct energy measurements

4.2.1 Precise power measurements

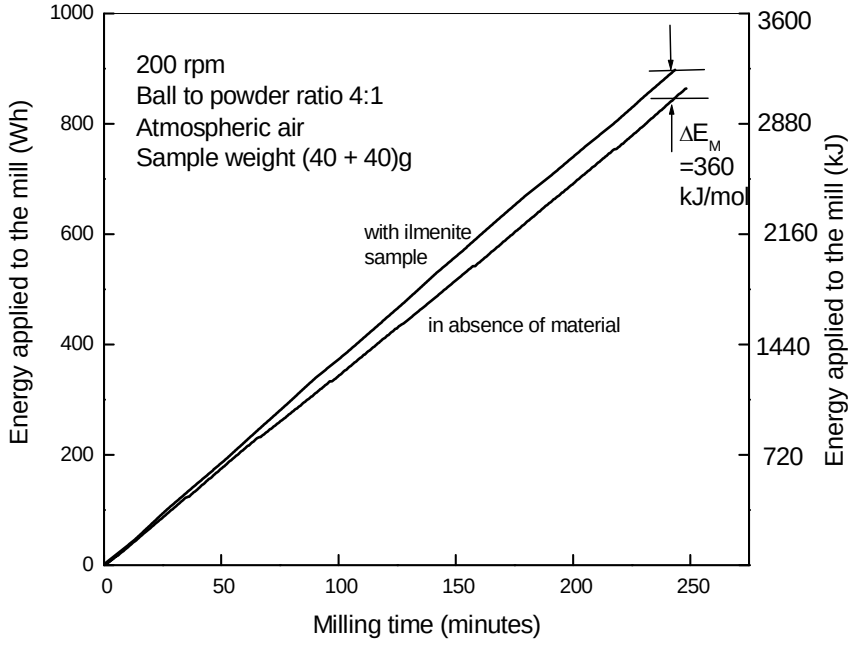

Fig.4.1: Variation of energy applied to the mill with milling time with (Manavalakurichi ilmenite sample) and without material.

.

The energy transferred to the material (ΔE_M) was studied by measuring the energy input into the pulverizing mill with material and in absence of the material (all the other conditions remaining same) using a high precision energy meter. Figure 4.1 shows a plot of applied energy as a function of milling time describing the milling in no load condition and with Manavalakurichi ilmenite sample under identical conditions. It was observed that the energy consumption of the mill (30 balls of net weight 320g at a mill speed of rpm) in 4 hours of milling was 835.2 wh (3006.7 kJ) in absence of material and 887.9 wh (3196.4 kJ) with 80 g material (Manavalakurichi Ilmenite) and under identical milling conditions. The specific energy transferred to the material was found to be about 100.1 wh/mol (360 kJ/mol) for Manavalakurichi ilmenite subjected to 4 hours of mechanical activation i.e., about 6% of the energy input to the mill was transferred into the material (Manavalakurichi ilmenite) in 4 hours of mechanical activation.

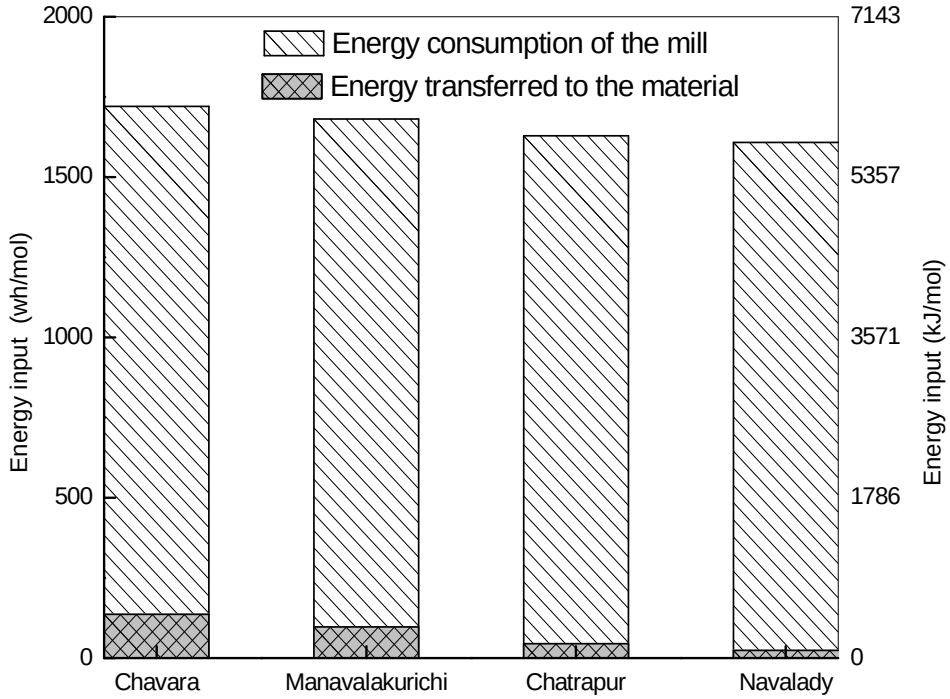

Fig.4.2: Energy input into the mill and fraction of energy transferred into various ilmenite samples obtained from Chavara, Manavalakurichi, Chatrapur and Navalady in 4 hours of milling.

.

The energy input to the mill and the fraction of the energy transferred to the material were measured for the different ilmenite samples obtained from Chatrapur, Navalady, Manavalakurichi and Chavara regions. Figure 4.2 shows the energy input to the mill and the amount of energy transferred to the different ilmenite samples subject to different degrees of weathering.

It was observed that the total energy input to the mill as well as the energy transferred to the material under identical conditions of milling increased with increased weathering i.e., followed a decreasing order as Chavara ï Manavalakurichi ï Chatrapur- Navalady ilmenite. The decrease of energy input into the mill and the energy transferred into the material can be attributed to the decrease in fracture toughness of the material induced by the weathering process. Tromans and Meech (2004) made a similar observation with different mineral samples subjected to ball milling. They suggested that the increase in energy consumption is caused by the increase in fracture toughness of the material. In the present case, the variation in fracture toughness of ilmenite samples are caused by difference in chemical composition (TiO_2, FeO and Fe_2O_3), degree of weathering and particle size/surface area of the material. The energy consumption of the mill with Chavara and Manavalakurichi ilmenite samples are higher as it has higher rutile, TiO_2 phases and finer particles compared to the other two samples. It was observed that the energy transferred into the various ilmenite samples varied between 3.0 to 8.0% in 4 hours of mechanical activation. These results are comparable with the study of Tamman (1929) who showed that about 5-15% energy is stored in materials subjected to mechanical activation process.

4.2.2 Isothermal calorimetry

The enthalpy change of the material (ΔH) subjected to mechanical activation process can be written as follows (Tkacova,1989)

$$\Delta H = \Delta E + P\Delta V + V\Delta P \quad \text{.....(4.3)}$$

Assuming that there is no change in pressure during the activation process and neglecting the work done against external pressure ($P\Delta V$) during the

.

mechanical activation process, the change in internal energy (ΔE) can be assumed to be the change in enthalpy:

$$\Delta H = \Delta E \quad \text{.....(4.4)}$$

In the process of mechanical activation, the energy is stored in the material through increased surfaces, enhanced grain boundaries, increased defect density (point, line, stacking faults and volumetric defects), structural transformation to higher energy structures including disordering. The stored energy is subsequently released by various relaxation processes (Tkacova, 1989; Balaz, 2000). At equilibrium, the activated material would have undergone complete relaxation to its original equilibrium state and the enthalpy of relaxation will be equal to the energy stored in the material. However, during the time scale of the calorimetric experiment only partial relaxation of defect occurs and the extent of relaxation depends both on temperature and time. The relaxation kinetics for the various micro-processes (fig.1.2) given by Balaz (2000) indicates that the point, line and surface defects relax within 10-1000 secs whereas, structural and surface area relaxation requires much higher times (Heinicke, 1984). The timescale of the calorimetric experiment at room temperature is expected to correspond to the energy of relaxation of the point, line and surface defects.

Fig.4.3 shows the variation of power as a function of time in the calorimeter from the unmilled and activated ilmenite samples in aqueous medium at room temperature (27^{O}C). The enthalpy of relaxation was derived from the area under the curve after 7 hours of relaxation. Fig.4.4 shows the variation of enthalpy of relaxation with milling time. It is observed that the enthalpy of relaxation increases exponentially with time of activation; it was 13 kJ/mol for the Chatrapur ilmenite sample and 16 kJ/mol for the Manavalakurichi ilmenite sample subjected to 4 hours of milling.

.

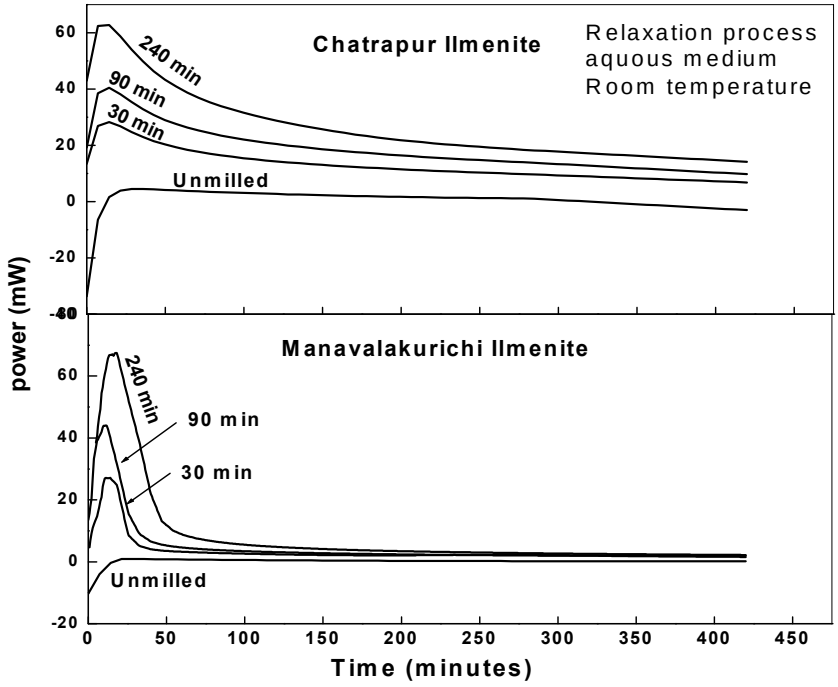

Fig.4.3: Variation of power as a function of time in the calorimeter from the unmilled and activated ilmenite samples in aqueous medium at room temperature (27^{O}C).

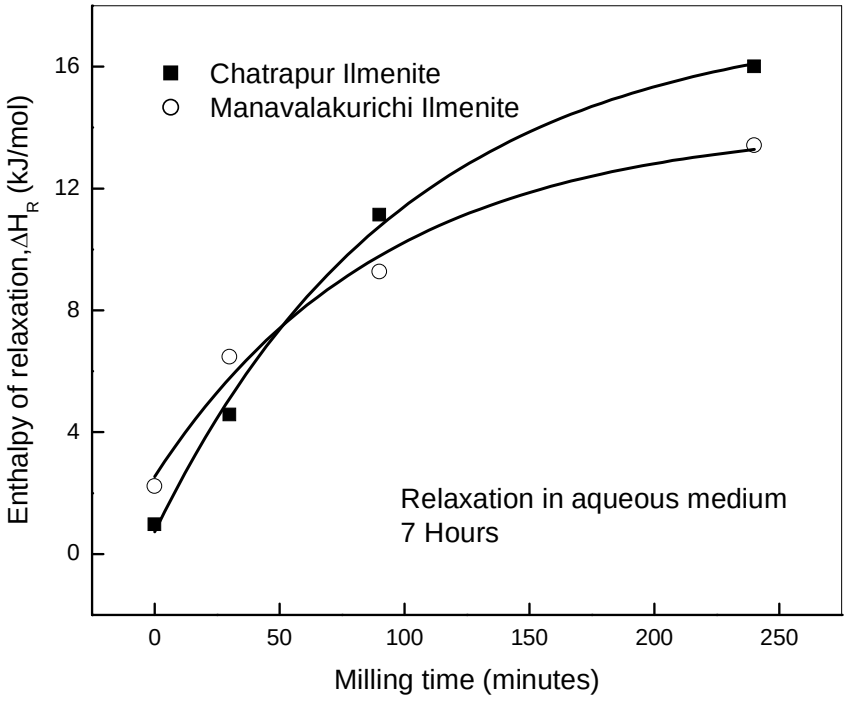

Fig.4.4: Variation of enthalpy of relaxation of Chatrapur and Manavalakurichi Ilmenite samples with milling time.

.

4.3 Indirect energy measurements

The mechanical energy input into the material is stored and distributed in various forms such as enhanced surface energy, strain energy, grain boundary energy, amorphization energy and other structural transformations leading to higher energy structures. The energy stored in the material in the above forms can in principle be determined using various characterization techniques as discussed below. However, the uncertainty associated with these measurements is large and several of these methods are indirect measurement techniques.

4.3.1 Surface energy

The increase in surface energy (ΔE_{SE}) of the material by mechanical activation can be estimated from surface area and specific surface energy measurements using the following equation.

$$\Delta E_{SE} = \gamma_S . \Delta S . M \quad \text{.....(4.5)}$$

where γ_S is the specific surface energy of the material, Δs is the increase in surface area by mechanical activation and M is the molar weight of the sample. The variation of surface energy of Chatrapur and Manavalakurichi ilmenite with milling time is shown in Fig. 4.5.

The surface energy increases linearly with the time of activation. The surface energy of the material increases from 25 mJ/m^2 (11 J/mol) to 45 mJ/m^2 (37J/mol) by 4 hours of planetary milling. The surface energy measurements showed higher values for Manavalakurichi ilmenite samples in unmilled and milled condition as it has a higher surface area (fig.3.3). A surface area of 11.6 m^2/g was achieved in 240 minutes of planetary milling of Manavalakurichi ilmenite.

The increase in surface energy per unit mass (ΔE_{SE}) can also be calculated theoretically from the equation derived by Tromans and Meech (2004) as:

.

$$\Delta E_{SE} = \frac{6Fr\gamma_S}{\rho}\left[\frac{1}{D_{Milled}} - \frac{1}{D_{Unmilled}}\right] \approx \frac{6Fr\gamma_S}{\rho Df} \quad \text{.....(4.6)}$$

where ρ is the mineral density (gm^{-3}), γ_S is the fracture surface energy (Jm^{-2}), F_r is the surface roughness factor (>1) allowing for non-spherical morphology of milled particles D_{Milled} and $D_{ummilled}$ are the average diameter of the material in milled and unmilled conditions respectively. Fig 45 shows the variation of calculated values of surface energy determined from data derived in this study using the equation of Tromans and Meech (2004).

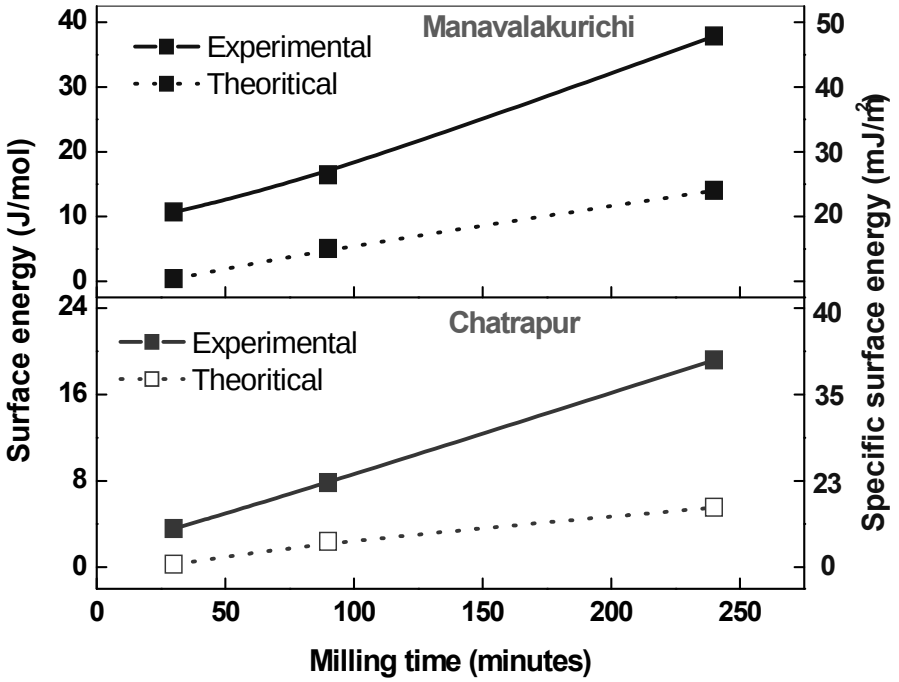

Fig.4.5: Variation of surface energy of Chatrapur and Manavalakurichi ilmenite samples with milling time.

It is observed that the theoretical values are somewhat lower than the experimental values. The porosity and surface defects caused by mechanical activation were not taken into account in the theoretical calculations.

4.3.2 Grain boundary energy

The energy stored in the material through enhanced grain boundaries can be given as:

.

$$\Delta E_{GB} = \gamma_{GB}.\Delta A_{GB}.M \quad \text{.....(4.7)}$$

where γ_{GB} is the specific grain boundary energy , ϕA$_{GB}$ is the change in grain boundary area of the material by mechanical activation and M is the molar weight of the sample. The grain boundary area was determined using the crystallite size of the ilmenite sample obtained using XRD line broadening analysis. The crystallites were assumed to have a tetrakaidecahedron configuration and the grain boundary area was calculated from the average crystallite sizes. The variation of grain boundary area of the ilmenite as a function of milling time is shown fig. 3.13.

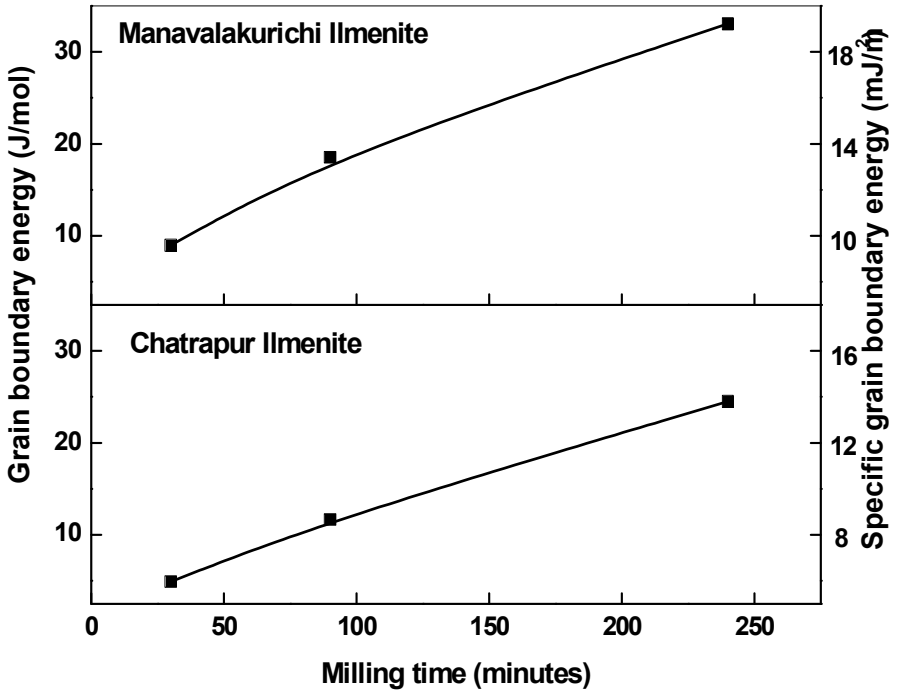

Fig.4.6: Variation of grain boundary energy with milling time for Chatrapur and Manavalakurichi ilmenite samples determined from surface energy measurements.

A considarble enhancement in grain boundary area was observed by milling. The specific grain boundary energy of the ilmenite samples were derived from the approximations given in earlier literaturs. In general, the specific grain boundary energy is approximately 40% of the specific surface energy (Imamura and Senna, 1982). Using this approximation of specific grain

.

boundary energy, the grain boundary energy per unit mass of the ilmenite samples was derived. Fig. 4.6 shows the variation of grain boundary energy of Chatrapur and Manavalakurichi ilmenite samples with milling time.

The grain boundary energy of the ilmenite sample increased to 24.5 J/mol (14.8 J/m^2) in Chatrapur ilmenite sample and 33 J/mol (19 mJ/m^2) in Manavalakurichi ilmenite sample after 4 hours of mechanical activation.

4.3.3 Strain energy

The elastic strain energy induced by mechanical activation was determined using Eshelbyôs equation derived from the theory of elasticity (Senna, 1985)

$$E_{\varepsilon} = \frac{18\mu K\varepsilon^2}{4\mu + 3K} \quad \text{é ..é} \quad (4.8)$$

where μ is the shear modulus of the material, and K is the bulk modulus of the material. The strain energy was calculated with the assumption that there was no change in shear and bulk modulus of the material during the process of mechanical activation. The bulk modulus and shear modulus of ilmenite were taken to be 174 GPa and 90 GPa respectively (Liebermann, 1976; Tromans and Meech, 2001). The elastic strain induced by mechanical activation was obtained from the XRD line broadening measurements of six most intense reflections. The variation of strain energy corresponding to uniform strain as well as non-uniform strain of the ilmenite samples with time of milling is illustrated in Fig.4.7.

.

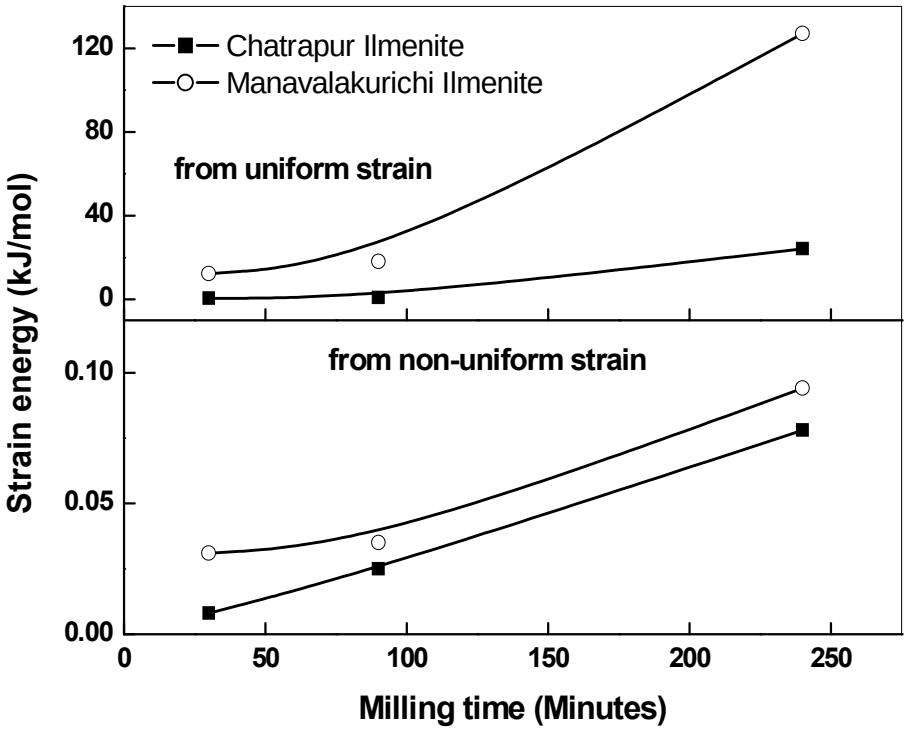

Fig.4.7: Variation of strain energy of Chatrapur and Manavalakurichi ilmenite samples with milling time.

The strain energy derived from non-uniform strain as well as the uniform strain varied exponentially with milling time. The 4 hours activated sample showed total elastic strain energy of 24 kJ/mol for the Chatrapur ilmenite sample and 127 kJ/mol for Manavalakurichi ilmenite sample.

4.3.4 Energy of partial amorphization /disordering

The energy of partial amorphization/disordering of the ilmenite samples were determined using the following equation

$$E_{amor} = \Delta H_F . f_A \quad \text{.....} \quad \text{.....} \quad \text{.....} \quad \text{.....} \quad \text{.....} \quad \text{.....} \quad (4.9)$$

where ΔH_F is the enthalpy of fusion at the reduced temperature of activation and f_A is the fraction of amorphization. The enthalpy change associated with the transformation can be written as

.

$$\Delta H^{T}_{Cryst \rightarrow Amor} = \Delta H^{MP}_{F} - \int_{MP}^{T} \Delta Cp dT \quad \text{.....(4.10)}$$

where

$$\int_{MP}^{T} \Delta Cp dT = \int_{MP}^{T} \left[Cp_{liquid} - Cp_{solid} \right] dT \quad \text{.....(4.11)}$$

$$= \left[a(T - T_{MP}) + b(T^2 - T_{MP}^2) + c\left(\frac{1}{T} - \frac{1}{T_{MP}}\right) \right]_{Liquid} - \left[a(T - T_{MP}) + b(T^2 - T_{MP}^2) + c\left(\frac{1}{T} - \frac{1}{T_{MP}}\right) \right]_{Solid} \quad \text{..(4.12)}$$

where a, b, and c are the thermodynamic constants used for deriving the Cp data of ilmenite in solid and liquid state. The thermodynamic constants (a, b, and c) of ilmenite in solid state were obtained using the software FACTSAGE (Version 5.0).

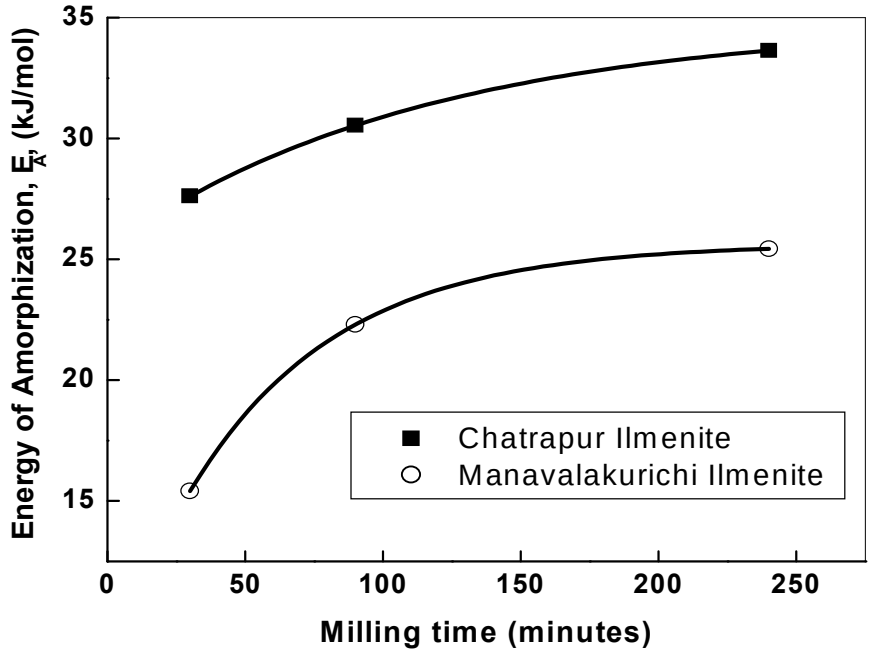

Fig.4.8: The plot of energy of amorphization of Chatrapur and Manavalakurichi ilmenite samples with milling time.

However the Cp data of ilmenite in liquid is not available in the FACTSAGE database. Thus the Cp data of ilmenite in liquid state was derived by kopp-numann rule using the Cp data of FeO and TiO_2 in liquid state (Kellog, 1967). The heat of fusion and heat capacity data were derived at room

.

temperature (300 K) and the fraction of amorphization was derived from integral intensity of xrd peak reflections (Ohlberg, and Strikler, 1962). The typical broadening of ilmenite at (112) reflection and the variation of energy of amorphization with milling time are illustrated in Fig.4.8. It was observed that the energy of amorphization increases exponentially with time of activation. The 4 hours activated samples shows about 25 kJ/mol for Chatrapur ilmenite and 33 kJ/mol for Manavalakurichi ilmenite.

4.3.5 The stored energy of the material

Time of Milling	Energy applied to the mill	Energy transferred to the material (ΔE_M)	Energy lost in breakage of bonds	Manifestation of stored energy in different forms				
				Surface (ΔE_{SE})	Grain boundary (ΔE_{GB})	Elastic strain (ΔE_U)	Amorphization (ΔE_A)	Defects with short relaxation times ($\Delta H_{Def.Rel}$)
Minutes	kJ/mol	kJ/mol	kJ/mol	J/mol	J/mol	kJ/mol	kJ/mol	kJ/mol
Chatrapur ilmenite sample								
30	751.1	43.0	5.8	2.9	4.9	0.5	27.6	9.7
90	2196.0	78.4	32.9	5.8	11.7	0.7	30.5	13.9
240	5865.3	162.3	85.1	15.1	24.5	24.3	33.6	19.3
Manavalakurichi ilmenite sample								
30	742.0	25.6	4.0	25.2	9	6	10.4	5.14
90	2241.0	115.6	81.0	30.5	18.58	9.1	18.3	7.14
240	6048.0	359.7	195.1	47.8	33.07	127	25.4	12.07

Table 4.1 Summary of energy measurements in Chatrapur and Manavalakurichi ilmenite samples subjected to planetary milling

The stored energy of the material will be equal to the summation of energy changes contributed by change in surface energy, grain boundary energy, strain energy, and energy of amorphization. This was 96 kJ/mol for the 4 hours milled sample of Manavalakurichi ilmenite. Table 4.1 shows the summary of energy measurements obtained with direct and indirect

.

measurements. The histogram showing the energy distribution in Chatrapur and Manavalakurichi ilmenite samples subjected to 4 hours of planetary milling is illustrated in fig.4.9 and 4.10 respectively.

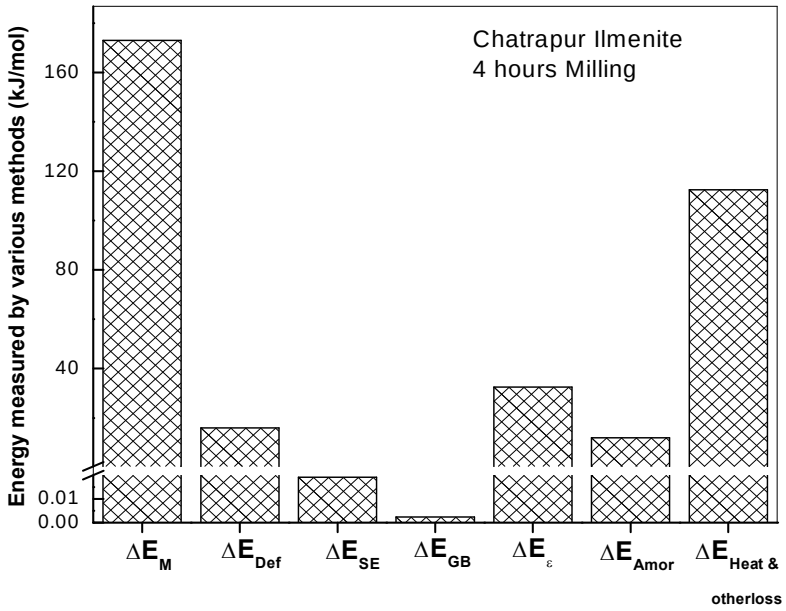

Fig. 4.9: The histogram showing the energy distribution in Chatrapur ilmenite sample subjected to 4 hours of planetary milling.

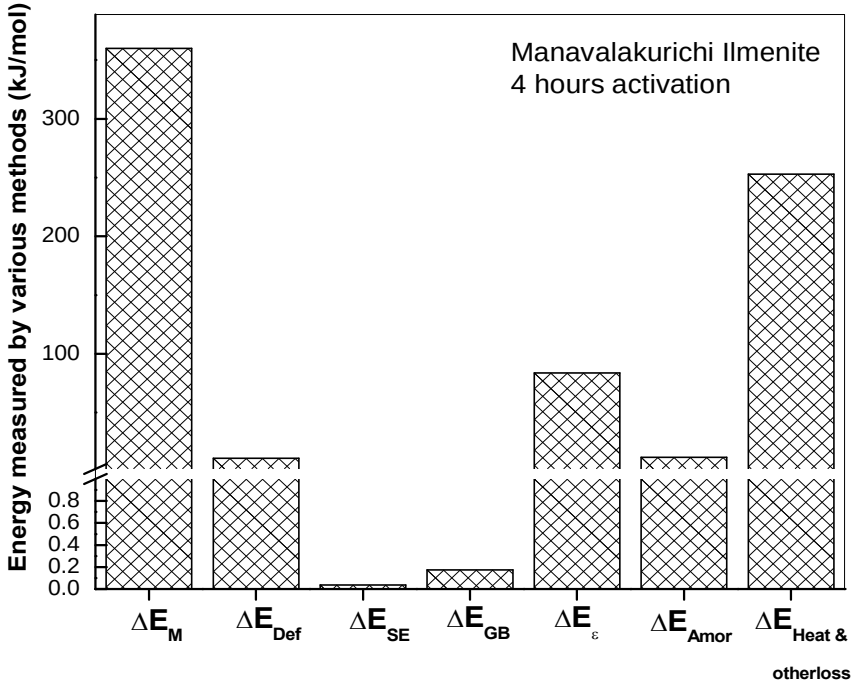

Fig. 4.10: The histogram showing the energy distribution in Manavalakurichi ilmenite subjected to 4 hours milling in a planetary mill.

.

It was observed that a major part of the energy is stored as strain energy and structural disorder; whereas the extent of energy stored in point and line defects, additional surfaces, grain boundaries were comparatively lower. It was observed that large part (about 60%) of energy transferred to the material losses during mechanical activation. The energy losses include friction, heat, and sound energy (Suryanarayana, 2004; Putsov et al., 2001).

4.4 Conclusions

1. The specific power consumption in the planetary mill was found to depend on the degree of alteration of ilmenite. For Chatrapur ilmenite, which was least altered, the specific power consumption was 5865 kJ/mol (10,740 wh/kg). The corresponding energy consumption in 4 hours of milling (milling of 80 g of ilmenite with 30 agate balls of net weight 320 g at a mill speed of 200 rpm)of Chavara ilmenite, which was most altered was 6193 kJ/mol (11,340 wh/kg).
2. It was observed that the energy transferred to the material varied in the range of 3 to 8.0 % in 4 hours of milling in a planetary mill depending on the degree of alteration of the ilmenite. The specific energy transferred derived from milling with material and a blank run under identical conditions was found to be 162 kJ/mol in 4 hours of milling for Chatrapur ilmenite and 360 kJ/mol for Manavalakurichi ilmenite.
3. It was deduced that more than half of this measured difference in energy was actually expended in the breakage of the bonds in the material, which was released mainly as heat and only the remaining energy was truly stored within the material. This energy was found to be stored in additional surfaces and interfaces, point, line and volume defects, high energy structures and non-uniform strain.
4. A large part of the stored energy was reflected as strain energy (24 and 127 kJ/mol respectively for the Chatrapur and Manavalakurichi ilmenite samples) and structural disorder (34 and 25 kJ/mol respectively for the Chatrapur and Manavalakurichi ilmenite samples respectively).

.

5. Part of the defect energy stored in the activated ilmenite samples was found to relax much faster. This component determined from calorimetric studies was found to be 19 kJ/mol for Chatrapur ilmenite and 12 kJ/mol for Manavalakurichi ilmenite sample subjected to 4 hours of mechanical activation.

6. The energy stored through additional surfaces and grain boundaries was found to be much lesser. The surface energy increased from 19 mJ/m^2 (2 J/mol) to 37 mJ/m^2 (15 J/mol) in the Chatrapur ilmenite and from 25 mJ/m^2 (11 J/mol) to 48 mJ/m^2 (40 J/mol) for the Manavalakurichi ilmenite in 4 hours of planetary milling. The grain boundary energy varied in the range of 8-15 mJ/m^2 (5-25 J/mol) in Chatrapur ilmenite and 10-19 mJ/m^2 (9-33 J/mol) in Manavalakurichi ilmenite sample.

.

CHAPTER 5

EFFECT OF MECHANICAL ACTIVATION ON DISSOLUTION KINETICS OF ILMENITE

5.1 Dissolution in sulfuric acid

The extent of dissolution of Fe and Ti in the unmilled as well as mechanically activated samples of Chatrapur ilmenite and Manavalkurichi ilmenite were studied with various concentrations of sulfuric acid (1.8M, 5.5M, 9.2M and 12.9M) at different temperatures (80, 95 and 120^{o}C). At 1.8 M the expreiments were carried out at 70, 80 and 95^{0}C to reduce the mass loss at higher temperature. A few typical dissolution plots of iron as well as titanium (in unmilled and activated samples at 9.2M H_2SO_4) are depited in Figs. 5.1 (a-d) and 5.2 (a-d) for Chatrapur and Manavalakurichi ilmenite samples at 80^{O}C and 120^{O}C respectively.

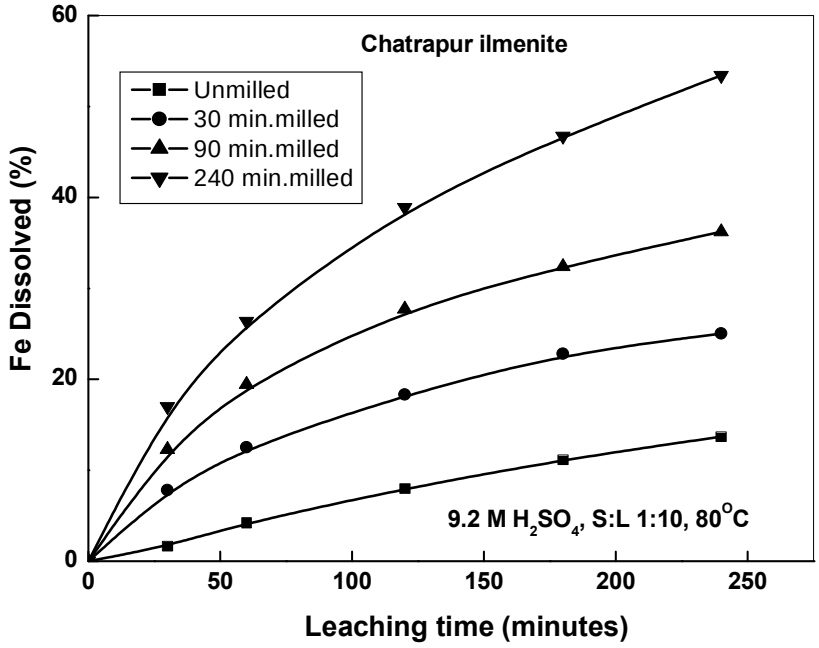

Fig.5.1 a: Variation of dissolution of Fe in unmilled and milled (30,90 and 240 min) samples of Chatrapur ilmenite with leaching time at an acid concentration of 9.2M H_2SO_4, at 80^{0}C.

.

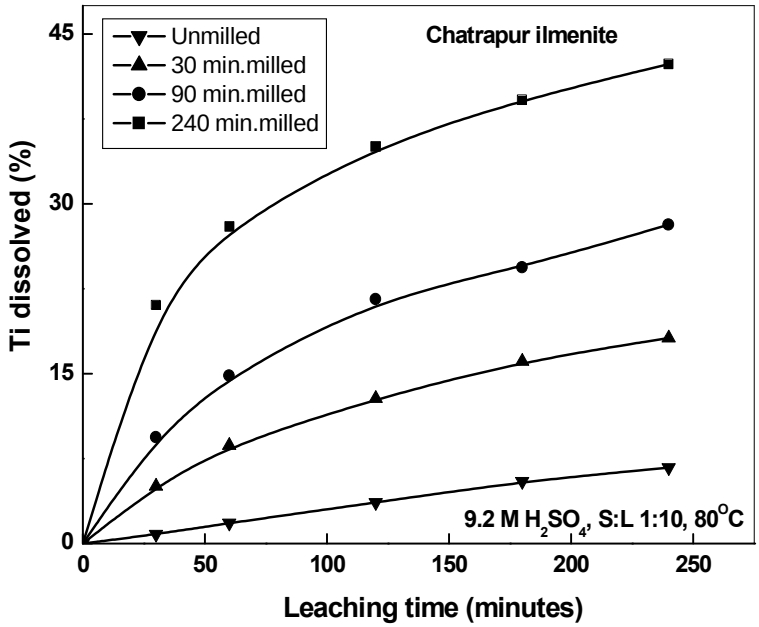

Fig.5.1 b: Variation of dissolution of Ti in unmilled and milled (30,90 and 240 min) samples of Chatrapur ilmenite with leaching time at an acid concentration of 9.2M H_2SO_4, at 80^0C.

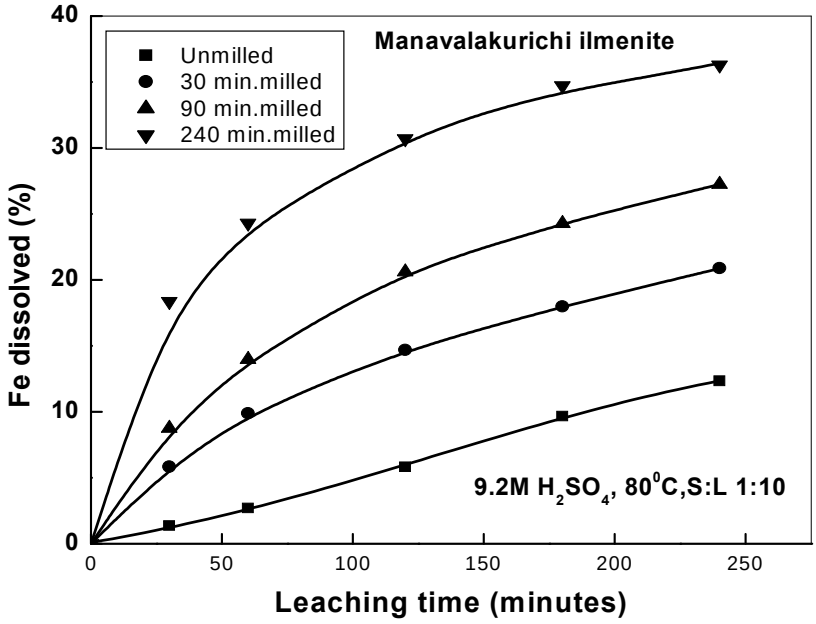

Fig.5.1 c: Variation of dissolution of Fe in unmilled and milled (30,90 and 240 min) samples of Manavalakurichi ilmenite with leaching time at an acid concentration of 9.2M H_2SO_4, at 80^0C.

.

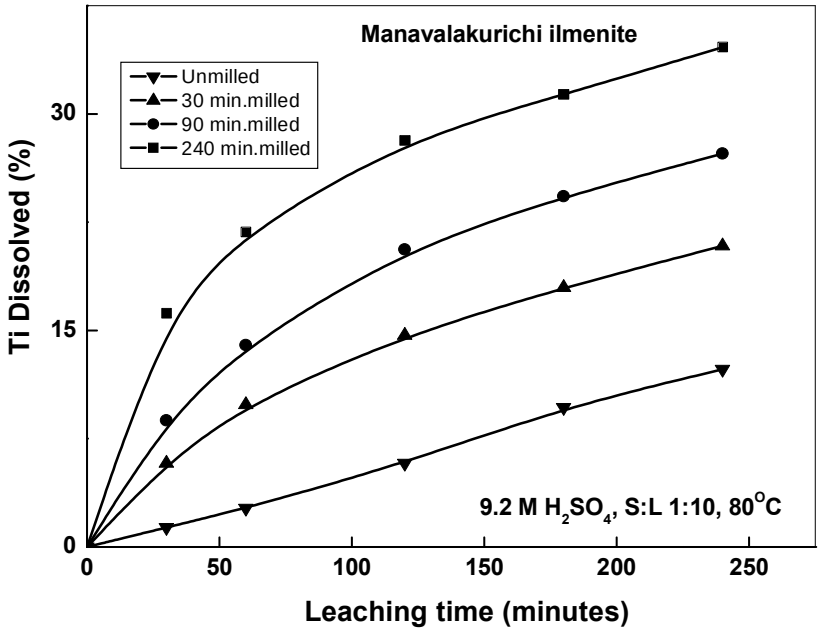

Fig.5.1 d: Variation of dissolution of Ti in unmilled and milled (30,90 and 240 min) samples of Manavalakurichi ilmenite with leaching time at an acid concentration of 9.2M H_2SO_4, at 80^0C.

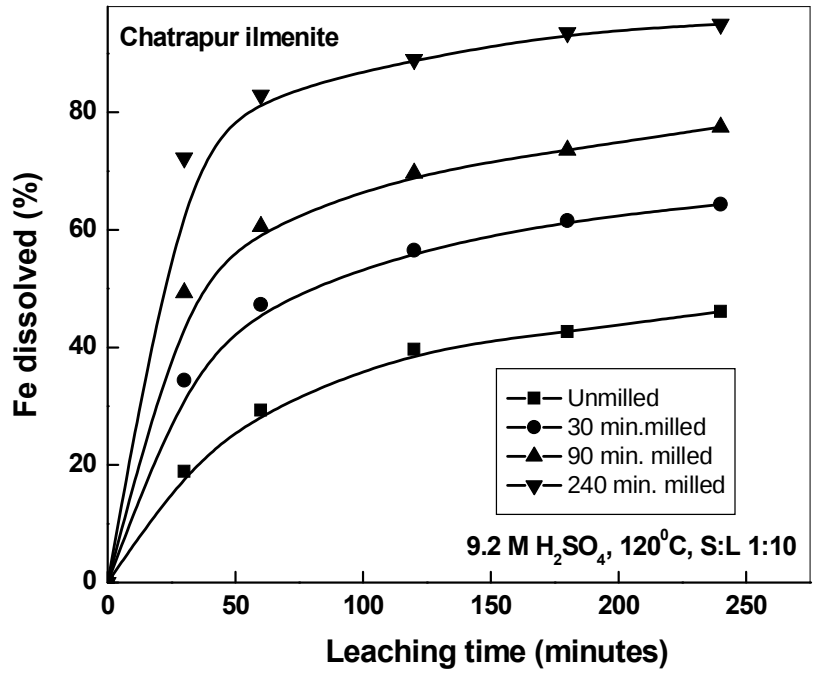

Fig.5.2 a: Variation of dissolution of Fe in unmilled and milled (30,90 and 240 min) samples of Chatrapur ilmenite with leaching time at an acid concentration of 9.2M H_2SO_4, at 120^0C.

.

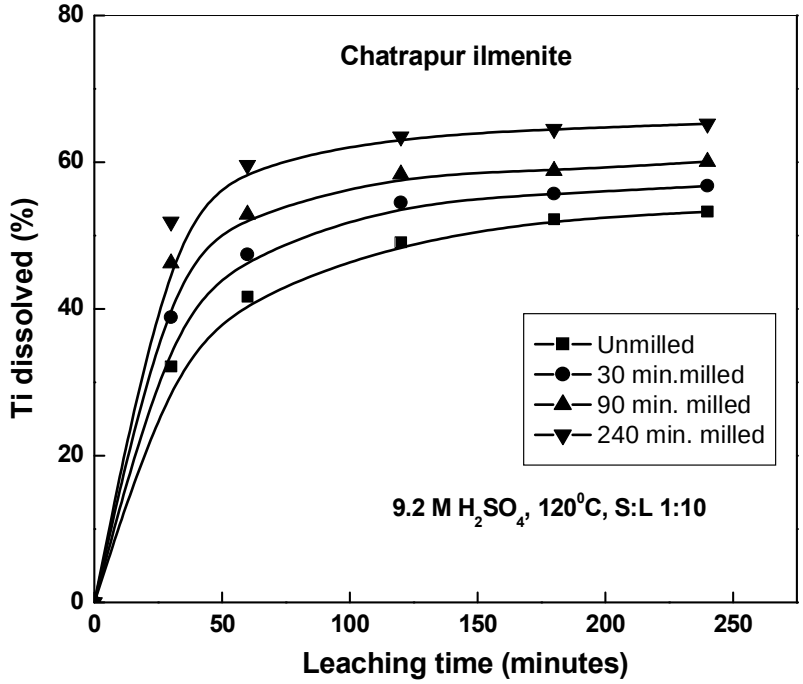

Fig.5.2 b: Variation of dissolution of Ti in unmilled and milled (30,90 and 240 min) samples of Chatrapur ilmenite with leaching time at an acid concentration of 9.2M H_2SO_4, at 120^0C.

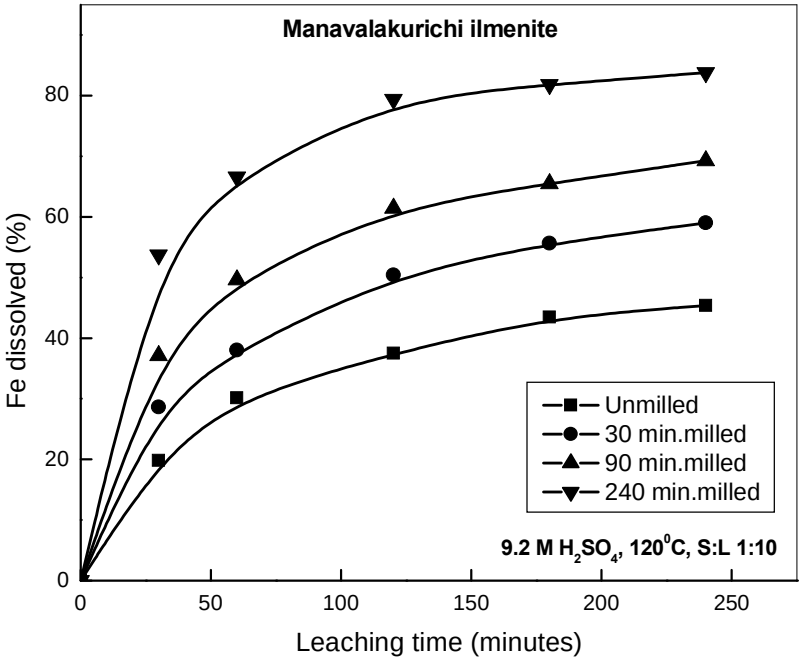

Fig.5.3 c: Variation of dissolution of Fe in unmilled and milled (30,90 and 240 min) samples of Manavalakurichi ilmenite with leaching time at an acid concentration of 9.2M H_2SO_4, at 120^0C.

.

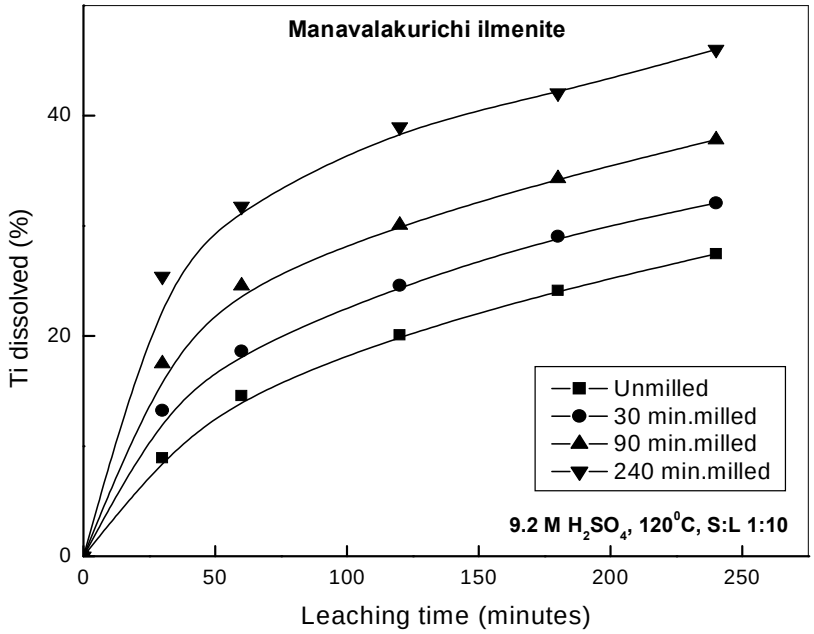

Fig.5.2 d: Variation of dissolution Ti in unmilled and milled (30,90 and 240 min) samples of Manavalakurichi ilmenite with leaching time at an acid concentration of 9.2M H_2SO_4, at 120^0C.

The leaching behavior for both Ti and Fe shows an exponential increase with leaching time at all leaching temperatures in the range 80-120^{o}C and for all times of activation. The rate of leaching is initially higher after which it decreases. Although mechanical activation enhances the dissolution kinetics for both Fe and Ti, it is observed that for the activated samples, the Ti and Fe in the ilmenite dissolves differentially and not according to their stoichiometry in the ilmenite phase. The maximum dissolution of Ti is restricted to 65% whereas, in excess of 90% Fe could be dissolved from Chatrapur ilmenite samples activated for 240 minutes and leached at 120^{o}C for four hours. It is seen that the dissolution rates for iron shows a higher increase with both activation time and leaching temperature in comparison to Ti. The enhanced rates of dissolution of Fe in comparison to Ti in the activated samples can be attributed to the increased oxidation of ilmenite to pseudo-rutile and its subsequent quasi-amorphization. Both, oxidation of iron and amorphization are likely to promote the dissolution reaction. Another reason for the differential dissolution behaviour of Fe and Ti in sulfuric acid may be related to their

.

solvation mechanism. Casey (1995) has proposed that the dissolution of minerals follows a mechanism similar to which ligand exchange occurs around dissolved metal complexes. Casey also suggested that to stabilize the ions in aqueous solutions, many transition metals have six co-ordinating H_2O ligands in their primary solvation sphere. The dissolution reaction of ilmenite is given as (Kelsall and Robbins 1990, Cservenyak et al., 1995):

$$FeTiO_3 + SO_4^{2-} + 4H^+ = Fe^{2+} + TiO.SO_4 + 2H_2O \quad (5.1)$$

Although the solvated Fe^{2+} cation retains the normal six-fold co-ordination of H_2O ligands, the solvated $Ti^{4+}(H_2O)_6$ cation is unstable. However, ligand exchange leads to the formation of a stable $Ti^{4+}(OH^-)_2(SO_4^{2-})(H_2O)_3$, which is equivalent to the oxysulphate complex in Eq. (5.1) (Tromans and Leach, 1999). The energetics of solvation of Fe^{2+} and Ti^{4+} is therefore expected to be different. The enhanced rate of dissolution of Fe in comparison to Ti at higher leach temperatures indicates higher activation energy for the dissolution of iron in comparison to titanium.

Despite an increase in surface area, the extent of dissolution of both iron and titanium decreased in the manavalakurichi ilmenite compared to Chatrapur ilmenite. About 90% Fe and 65% Ti dissolved in the case of the unmilled Chatrapur sample in four hours of leaching at 120^oC compared to 45% of Ti and 80% Fe in the case of the unmilled manavalakurichi sample under the same conditions. The decrease in dissolution with increase can be attributed to the phase changes introdued by weathering (discussed in chapter 6).

5.1.1 Effect of acid concentration

The effect of acid concentration, on dissolution of Fe and Ti were investigated with Manavalakurichi ilmenite sample. The variation of the maximum dissolution of Fe and Ti of Manavalakurichi ilmenite sample at 120^OC with acid concentration is shown in Fig.5.3.

.

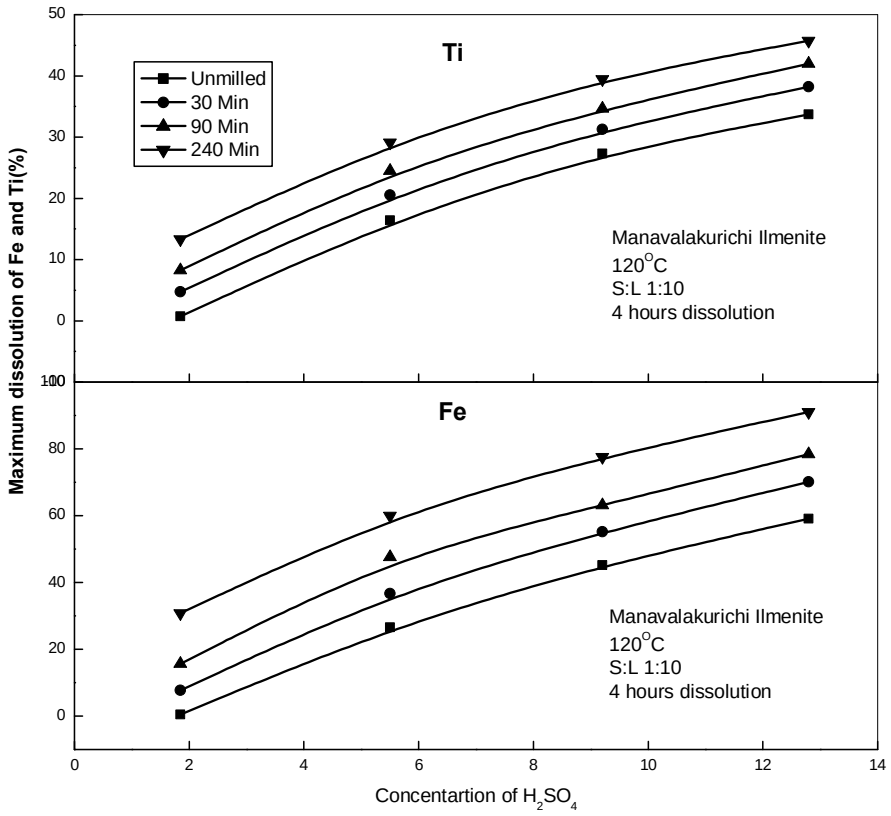

Fig.5.3 The effect of acid concentration on maximum dissolution of Fe and Ti of Manavalakurichi ilmenite subjected to 0, 30, 90 and 240 minutes of milling.

The dissolution of Fe and Ti shows an exponential variation with the concentration of acid. A maximum dissolution of 30% Fe and 13% Ti in the solution was achieved with 1.84 M sulfuric acid and about 91% Fe and 46% Ti was achieved with 12.87M sulfuric acid for the 240 minutes activated sample of Manavalakurichi ilmenite within 4 hours of leaching. The effect of concentration of sulphuric acid on dissolution kinetics of ilmenite was investigated by many authors (Imahashi and Takamatsu,1976; Han et al, 1987). Han et al. (1987) carried out a detailed investigation on the kinetics of dissolution of beach sand ilmenite (Southern Thailand) with acid concentration in unmilled condition. The maximum dissolution of iron achieved was about 50% at 115^0C at 18.8 M H_2SO_4 for a particle size range of 9ï 14 µm. However the systematic reduction of acid concentration by mechanical activation is not reported anywhere.

.

5.1.2 Effect of dissolution temperature

The variation of maximum dissolution of Fe and Ti with temperature of dissolution is shown in Fig.5.4 for Chatarpur and Manavalakurichi ilmenite samples.

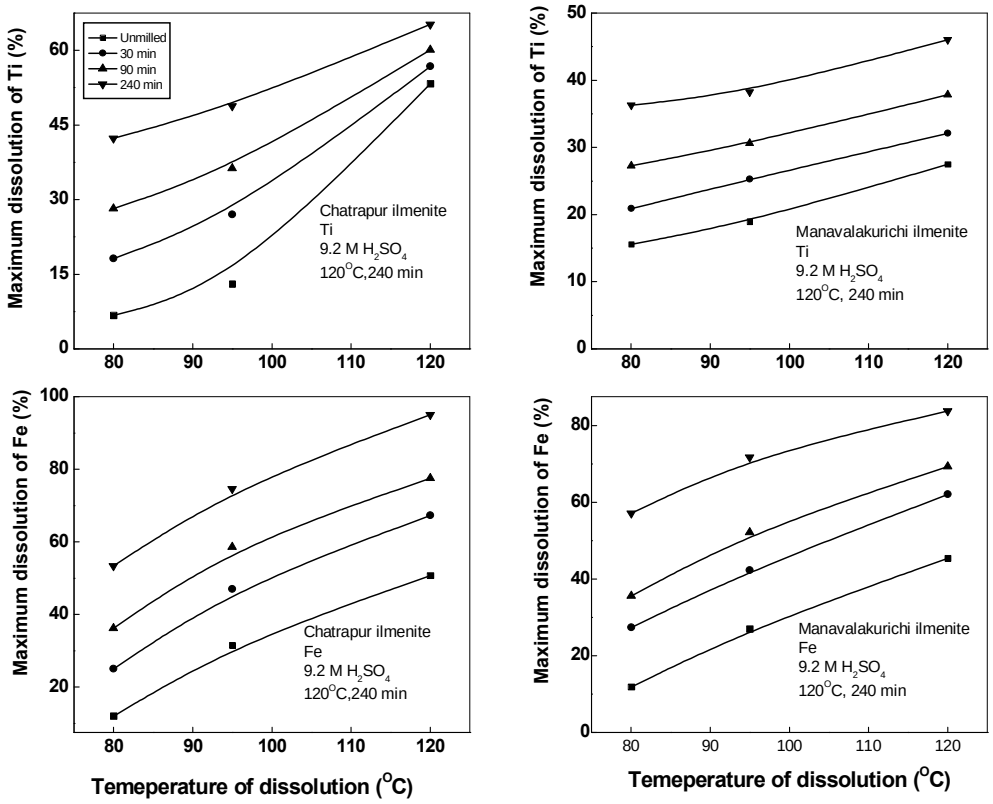

Fig.5.4 The effect of temperature of dissolution on maximum dissolution of Fe and Ti of Chatarpur and Manavalakurichi ilmenite samples at an acid concentration of 9.2M H_2SO_4.

The dissolution of Fe and Ti in both unmilled and activated samples increases exponentially with tempearture of dissolution. About 43% of Ti and 53% of Fe could be dissolved at 80^{o}C , however more than 65% of Ti and 90% of Fe could be dissolved at 120^{o}C in four hours of leaching of Chatrapur ilmenite (4 hours activated) at an acid concentration of 9.2M. Under identical conditions, the Manavalakurichi ilmenite shows dissolution of t 36% of Ti and 57% of Fe at 80^{o}C and 46% of Ti and 83% Fe at 120^{o}C.

.

5.1.3 Effect of solid to liquid ratio

The dissolution behavior of unmilled and activated samples of ilmenite was studied at a solid to liquid ratio of 1:10 and 1:100. The dissolution plots of Fe and Ti in unmilled and activated samples of Chatarpur and Manavalakurichi ilmenite at a solid to liquid ratio of 1:100 is depicted in Fig. 5.5.

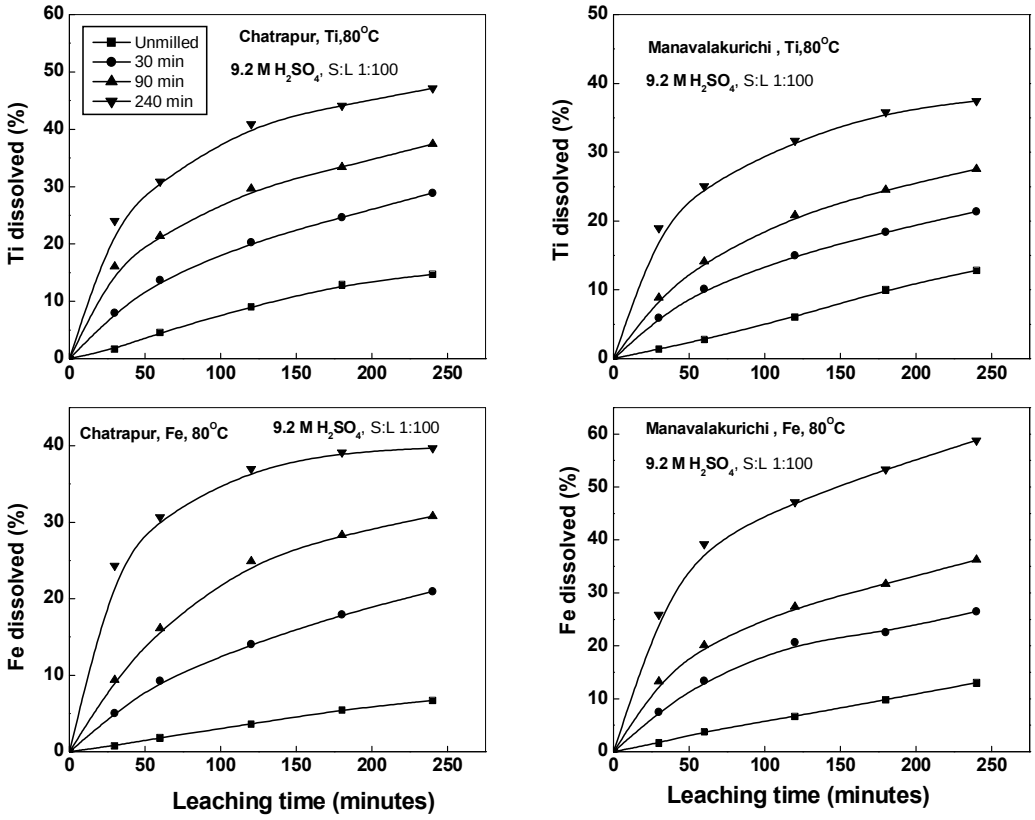

Fig.5.5: The dissolution plot of Fe and Ti at a solid to liquid ratio of 1:100 in 9.2 M H_2S0_4 for the unmilled and activated samples of Chatrapur and Manavalakurichi ilmenite at 80^{O}C.

No differences were noticed in the leaching behavior of the unmilled and activated samples when the leaching was carried out at a solid to liquid ratio of 1:100. Hence all the experiments were carried out at a solid to liquid ratio of 1:10, a value commonly used in industrial leaching set ups. No hydrolysis reaction was observed in the case of sulfuric acid leaching at the temperatures and acid concentrations used in this study (a small amount of hydrolysis occurred for the activated sample when leached at 120^{o}C for

.

prolonged times). Chun Li et al (2006) studied the effect of ore/acid ratio on dissolution of Ti from ilmenite and reported a small variation in dissolution with solid to liquid ratio. However the variation observed by them was within the limits of experimental uncertainty.

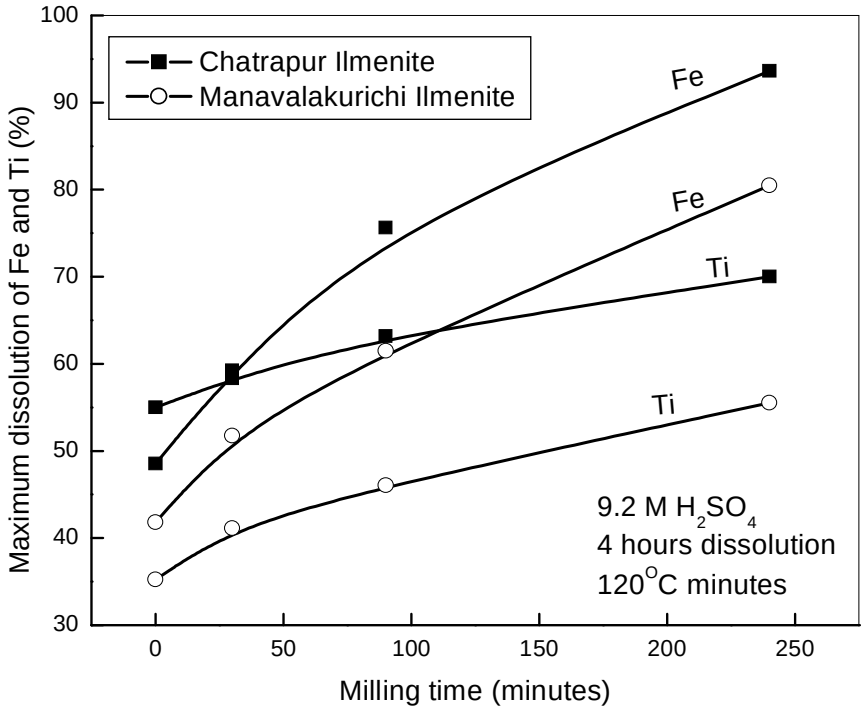

5.1.4 Effect of mechanical activation

Fig.5.6 The effect of mechanical activation on maximum dissolution of Fe and Ti of Chatrapur and Manavalakurichi ilmenite samples at an acid oncentration of 9.2M H_2SO_4

The kinetics of dissolution of both Fe and Ti increased significantly with time of activation. The mechanical activation increases the rate of dissolution as well as the maximum dissolution of Fe and Ti at all the acid concentrations and temperatures used in the present study. The rate of dissolution increases exponentially with time of activation during the initial period of dissolution (<60 min), thereafter decreases with time indicating that the effects of mechanical activation are relaxed. It is also observed that the period of relaxation decreases with increasing temperature and acid concentrations. The

.

initial rate of dissolution (Fe and Ti) of activated samples increases about 2 to 8 times as that of unmilled samples. A similar dissolution behaviour was observed by Welham and Llewellyn (1998) on mechanically activated ilmenite (100 hours of ball milling).

The variation of maximum dissolution of Fe and Ti in 9.2 M H_2SO_4 depicted in Fig.5.6 for Chatrapur and Manavalakurichi ilmenite samples as a function of time of activation. The dissolution of Fe and Ti increases exponentially with time of activation. The Chatrapur ilmenite shows 49% of Ti and 55% of Fe in solution before activation and 65% of Ti and 90% of Fe after activation when dissolved in 9.2M H_2SO_4 at 120^OC. At the same condition, Manavalakurichi ilmenite shows 35% of Ti and 49% of Fe in unmilled condition and 55% of Ti and 85% Fe after 4 hours of milling.

The overall increase in the dissolution rates with mechanical activation is in addition to an increase in surface area a result of several factors such as structural disorder (Balaz et al., 1996), enhanced strain (Balaz, 2000), amorphization of mineral particles (Tkacova et al., 1993), preferential dissolution of select crystal faces (Barton and McConnel, 1979 and Duncan and Metson, 1982), micro-topography (Tromans and Meech, 1999 and 2002) and formation of new phases more amenable to leaching (Welham, 2001 and Tkacova et al., 1996).

5.1.5 Residue analysis

The XRD for some of the leach residues corresponding to sulfuric acid leaching of milled and unmilled samples of Chatrapur ilmenite concentrates are given in Fig.5.7.

In the case of unmilled samples of Chatrapur ilmenite, the leach residue contains only ilmenite and some pseudorutile in unleached condition, whereas it contains a mixture of ilmenite and rutile when leached for 4 h at 120^oC. It appears that the iron of the ilmenite is selectively leached resulting in a titanium-enriched rutile phase in the residue. However, in case of the activated samples, in addition to the unleached ilmenite and the transformed rutile, iron

.

titanium sulfate appears to precipitate from the solution especially for longer leaching times.

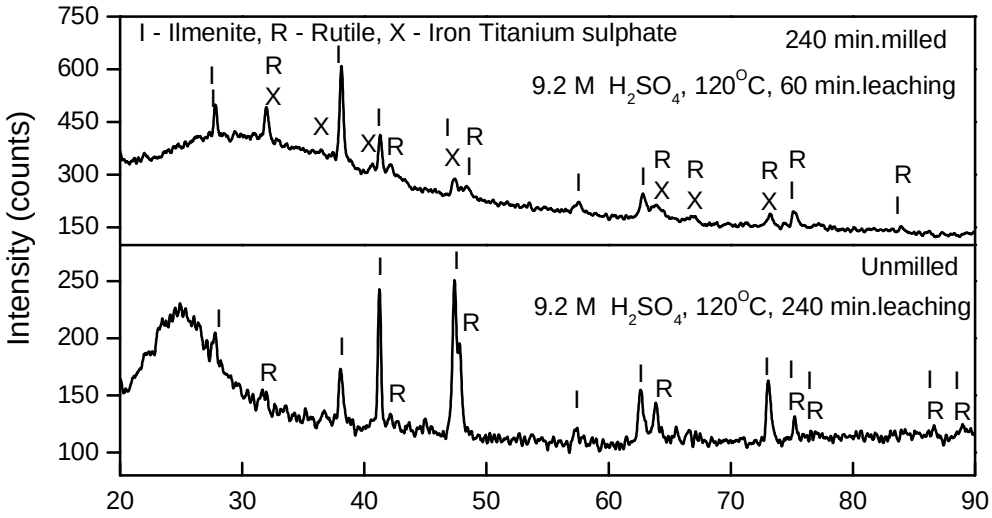

Fig.5.7: XRD of leach residue of Chatrapur ilmenite samples in unmilled condition and planetary milled for 240 minutes and leached in 9.2M H_2SO_4 at 120^oC.

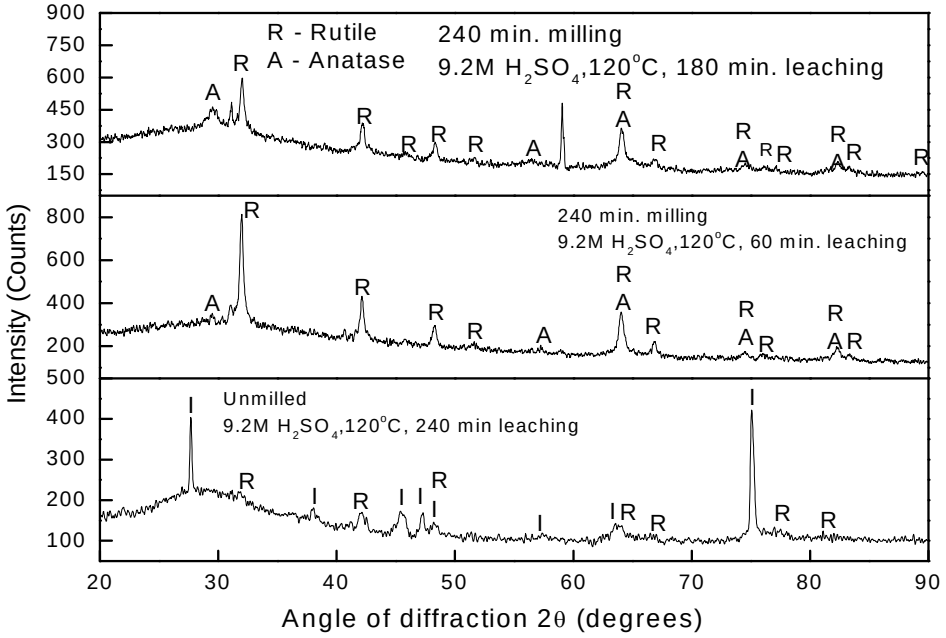

Fig 5.8 XRD of leach residue of Manavalakurichi ilmenite samples in unmilled condition and planetary milled for 240 minutes and leached in 9.2M H_2SO_4 at 120^oC.

.

The XRD for some of the leach residues corresponding to sulfuric acid leaching of Manavalakurichi ilmenite are given in Fig.5.8. Some undissolved ilmenite and rutile are observed in the leach residue for the unmilled sample. However the no ilmenite peaks were observed in activated sample even after in 1 hours of leaching. The titanium-enriched phase was resulted from selective dissolution as well as earlier weathering process. The leach residue of the activated sample shows anatase phase in addition to rutile possibly formed from hydrolyzed products.

5.1.6 Eh-pH measurements

Fig 5.9 shows the Eh-pH diagram for Ti-H_2SO_4-H_2O systems at 25^oC reported by Vaughan and Alfantazi, (2004) and the experimental range of variation of Eh-pH in the present study.

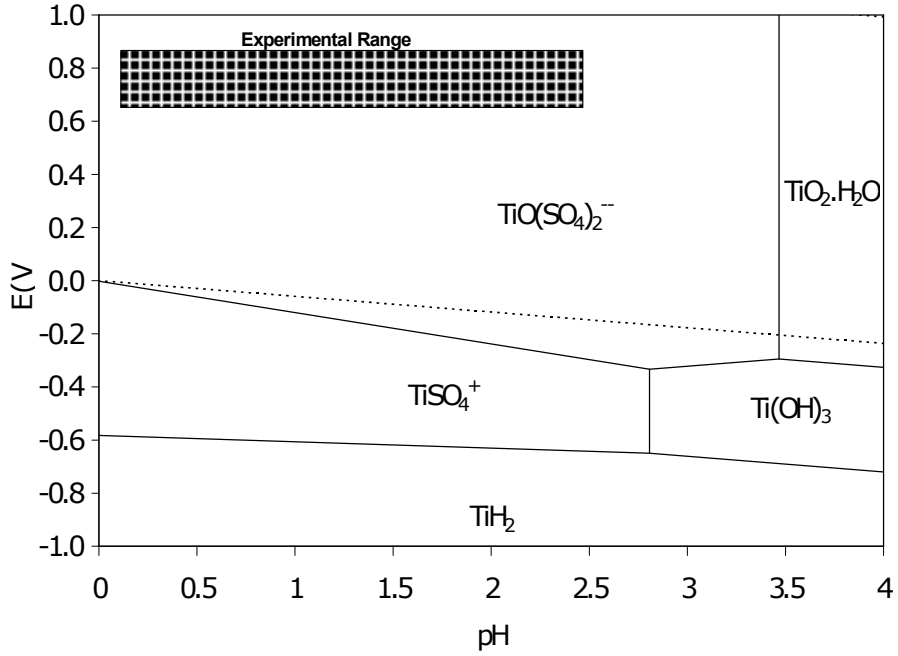

Fig.5.9: The Eh-pH diagram for Ti-H_2SO_4-H_2O systems at 25^oC (Vaughan and Alfantazi, 2004.) and the experimental range of variation of Eh-pH in the present study (Marked by shaded area).

The redox potential and pH during leaching (monitored at the beginning and end of the leaching experiment at ambient temperature) showed small variations. Depending on the initial acid concentration, the increase in pH

.

during the leaching experiment was less than 0.8 and the redox potential varied between 0.68 to 0.85 V for H_2SO_4 leaching. Figure 5.9 shows the range of experimental values of redox potential and pH observed during the leaching measurement.

5.1.7 Kinetic modeling

5.1.7.1 Derivation of kinetic parameters

Initial kinetic analysis of the dissolution behavior of Ti indicated that none of the common kinetic models (power law, diffusion models, phase boundary reaction, Avrami-Erofeev equation, autocatalysis models etc.) (Anderson et al., 1999 and Vyazovkin and Wight, 1999) could satisfactorily explain the results. Application of the model-free iso-conversional method (Vyazovkin and Wight, 1999; Sewry and Brown, 2002) however indicated that the activation energies were constant within the limits of uncertainty for various extent of conversion. However, the main problem with the application of the model-free iso-conversional method in the present case was that the range of conversions for Ti were limited especially at lower temperatures and kinetic parameters other than the activation energy cannot be determined by this method. A non-linear least squares minimization technique (Varhegyi et al., 2001) was therefore employed for the determination of the kinetic parameters for the dissolution of both Ti and Fe. It was observed that the dissolution kinetics of Fe and Ti from ilmenite in H_2SO_4 does not conform totally to either the reaction rate control or the product layer diffusion control mechanism. Therefore, an attempt was made to describe the initial leaching kinetics using the reaction rate control model and the latter stage of dissolution using the shrinking core model wherein diffusion through the product layer is rate controlling. The experimental kinetic data agreed reasonably well with this mechanism of chemical reaction rate control in the initial stage and product diffusion layer in the later stage with correlation coefficients varying from 0.95 to 0.99. This approach has earlier been used by Welham and Llewellyn (1998) to describe the leaching kinetics of activated ilmenite. The kinetic rate equation for an isothermal leaching reaction can be written as:

.

$$\frac{d\alpha}{dt} = k.C^n f(\alpha) = A_P \exp\left(\frac{-E}{RT}\right).C^n f(\alpha) \quad \text{.....(5.2)}$$

Where α is the fractional conversion, k is the rate constant (min^{-1}), A is the pre-exponential factor E is the activation energy (kJ/mol), R the gas constant (kJ. $mol^{-1}.K^{-1}$), C is the acid concentration (mols) and T the absolute temperature (K). dα/dt represents the rate of dissolution and f(α) represents the kinetic model which is a functional of time. Assuming that the acid concentration does not change during the course of the leaching experiment (in the present study, the variation of pH during the course of the leaching experiment was small), integration of Eq. (5.2) yields:

$$g(\alpha) = \int_0^{\alpha} \frac{d\alpha}{f(\alpha)} = k.C^n.t = A_P \exp\left(\frac{-E}{RT}\right).C^n t \quad \text{.....(5.3)}$$

At t=0 ; α=0 and t=t ; α=α

for a duration t, if the rate constant is fixed then $A_P \exp\left(\frac{-E}{RT}\right).C^n$ may be taken as constant or independent of time.

For the reaction rate control mechanism, g(Ŭ) can be given by:

g(Ŭ) = 1-(1-Ŭ)$^{1/3}$é é é é é é é é é ..é é é é é é é é é é é (5.4)

and for the product layer diffusion control shrinking core model, g(Ŭ) is written as follows

$$g(\alpha) = 1 - \frac{2}{3}\alpha - (1-\alpha)^{2/3} \quad \text{.....(.5.5.)}$$

A representative plot showing conformity of the experimental data to initially a reaction rate control mechanism and later to the shrinking core model is shown in Fig.5.10.Simultaneous evaluation of all the kinetic parameters (A, E and n) can be made using a least square minimization technique (Varhegyi et al., 2001). An object function (OF) for the minimization can be written as:

.

$$OF = \sum_{j=1}^{M} \sum_{i=1}^{N_j} \left[g(\alpha) - A \exp\left(\frac{-E}{RT}\right).C^{n}t \right]^{2} / N_j \quad \text{.....} \quad (5.6)$$

Where, M is the number of experimental data sets and N_j is the number of points in the j^{th} experimental curve. The kinetic parameters A, E and n were determined by simultaneous evaluation of all sets of isothermal experimental data as a function of time for all the acid concentrations by minimization of the object function (OF) using a numerical technique.

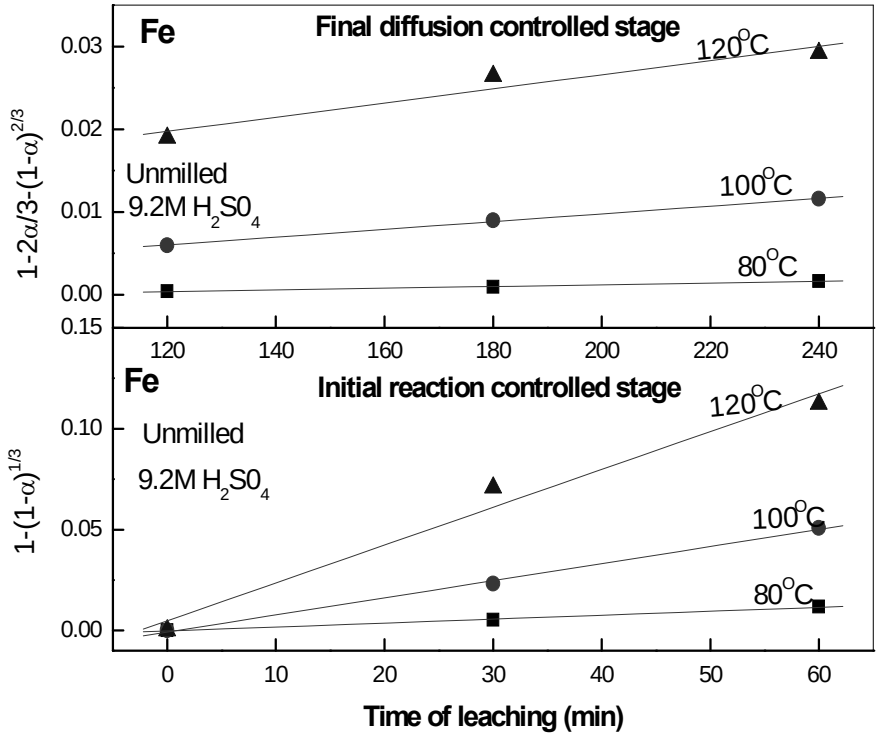

Fig.5.10 Fitting of experimental data of Fe (unmilled, Manavalakurichi ilmenite, 9.2M H_2SO_4,) with suitable kinetic model.

The calculated activation energies for the dissolution of Fe and Ti in the initial and later stages in H_2SO_4 are given as a function of milling time in 5.11. The order of reaction with respect to acid concentration was found to be the same 1.5 for H_2SO_4. The enhanced rate of dissolution of Fe in comparison to Ti indicates higher activation energy for the dissolution of titanium in comparison to iron.

.

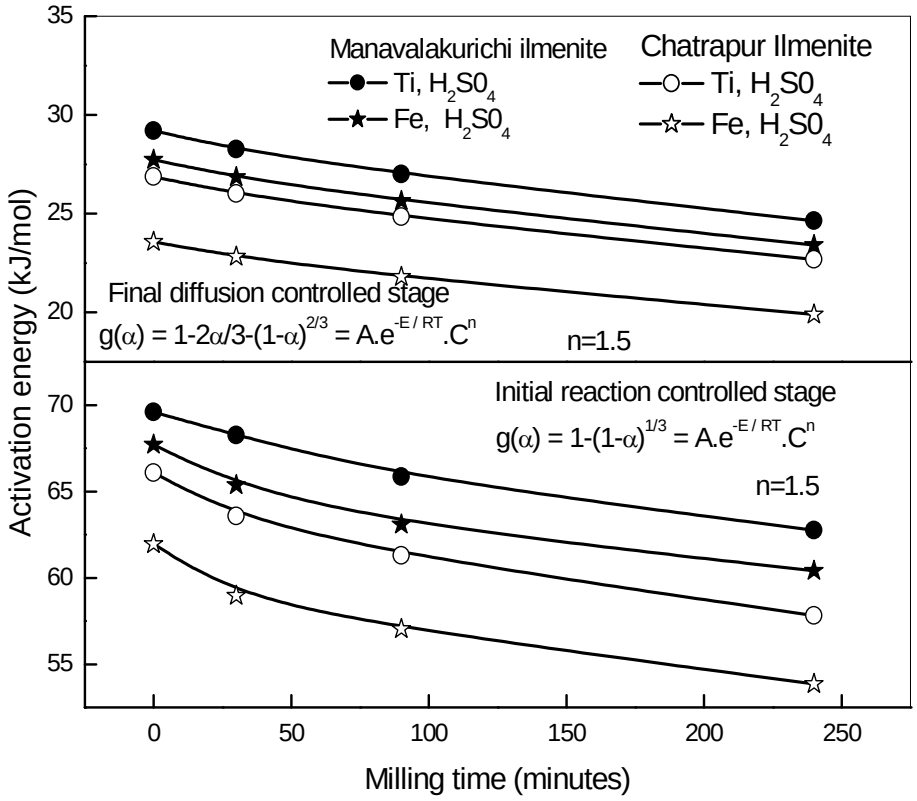

Fig.5.11 Variation of activation energy for the dissolution of Fe and Ti in the initial and later stages in H_2SO_4 for Chatrapur and Manavalakurichi Ilmenite.

The values of the activation energies derived in this study compares well with that reported in the literature (Han et al., 1987, Welham and Llewellyn, 1998). Han et al.,(1987) determined an activation energy of 64.4 kJ/mol for the dissolution of ilmenite in sulfuric acid in the temperature range 88 ï 115^{o}C. None of the above studies report the effect of mechanical activation on the activation energy values for the dissolution of ilmenite. Welham and Llewellyn (1998) reported apparent activation energy of 70 kJ/mol for the chemically controlled stage of dissolution of mechanically activated ilmenite in sulfuric acid in the temperature range 80 ï 120^{o}C. They have not considered the dissolution kinetics of Fe and Ti separately. They observed that the activation energy decreases with milling time for up to one hour after which they increase marginally.

.

5.1.7.2 Effect of microtopography on rate of dissolution

Tromans and Meech (1999, 2002) analyzed the conjoint effects of particle size and micro-topography on the overall mass dissolution behavior of fine particles. They suggested that microtopography-enhanced dissolution can be significant for surface-controlled leaching reactions exhibiting high activation energies (>70kJ/mol) and for low particle sizes (<1 μm). They derived an expression for the differential dissolution at the step edges of a particle in comparison to that at the terraces through a parameter t_{rel} defined as the ratio of the total time for dissolution of a stepped particle relative to the time for dissolution of a spherical particle of the same mass (of diameter D_M). Assuming that the fraction of steps in the spherical particle is zero, their equation reduces to:

$$t_{rel} = \frac{2L}{3\beta D_M}\left[\frac{\beta - \beta R_F}{\beta R_F + (1-\beta)}\right] + 1 \quad \text{.....} \quad \text{.....} \quad \text{.....} \quad (5.7)$$

Where L is the average distance between cations in the solid lattice, β is the fraction of dissolution sites on step edges and,

$R_F = R_S/R_T$ = ratio of the rates of dissolution from steps (R_S) and terraces (R_T)

$$R_F = M_f \exp\left(\frac{0.2E_T}{RT}\right) \text{..... ....} (5.8)$$

where

$M_f = A_S/A_T$ [ratio of rate coefficient for dissolution at steps (A_S) to that at terraces (A_T)] ≈ 2, Ea_T is the activation energy for dissolution from terraces

The calculated values of $1/t_{rel}$ using Eq.(5.7) as a function of mean particle diameter (D_M) for the dissolution of both Ti and Fe at different temperatures and two representative values of β (10^{-2} and 10^{-4}) corresponding to the expected range for mechanically activated minerals are shown in Fig. 5.12 .

.

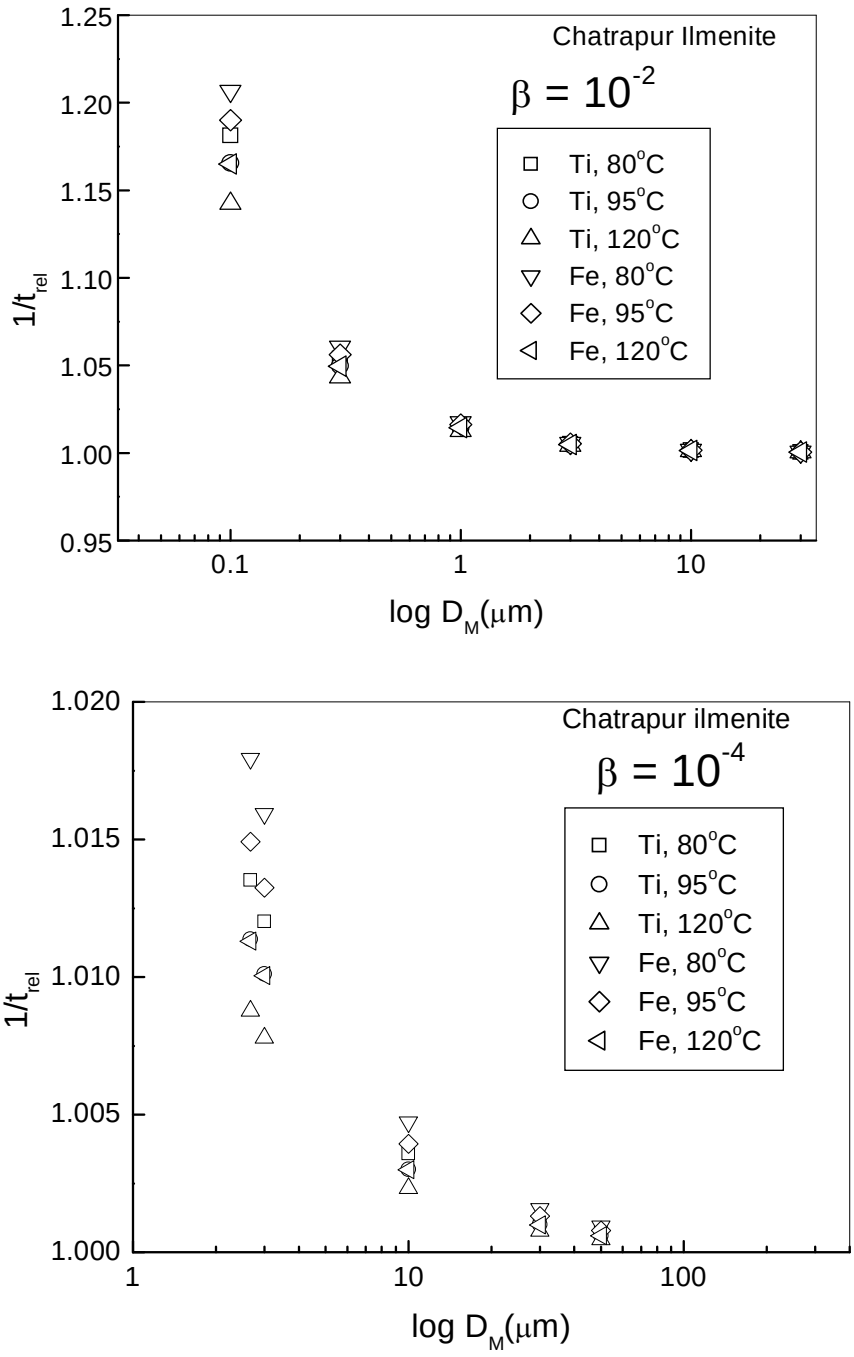

Fig.5.12:Variation of relative particle dissolution rate ($1/t_{rel}$) with mean particle diameter Computed from micro topography model: a) For $\beta = 10^{-2}$ (α_m is the fraction of dissolution sites on step edges

The activation energy values derived for the unmilled sample was used for E_T in Eq. (5.7). It is seen that if the fraction of dissolution sites on step edges (β) is of the order of 10^{-2}, the dissolution at the step edges is likely to be

.

faster by about 20-25% than at the terrace sites. However, for lower values of β, the effect of microtopography on the dissolution kinetics is insignificant. The effect of temperature and the nature of cation (Fe^{2+} or Ti^{4+}) on t_{rel} calculated using the microtopography model was found to be minimal. The experimental results on the dissolution of both Ti and Fe show much faster rates than that predicted by the microtopography model and increases with both time of activation and temperature of dissolution. As mentioned earlier, microtopography is only one of the several factors to be considered and contributes only to a fraction of the total energy stored in an activated mineral.

5.1.7.3 Effect of surface area and structural disorder on rate of dissolution

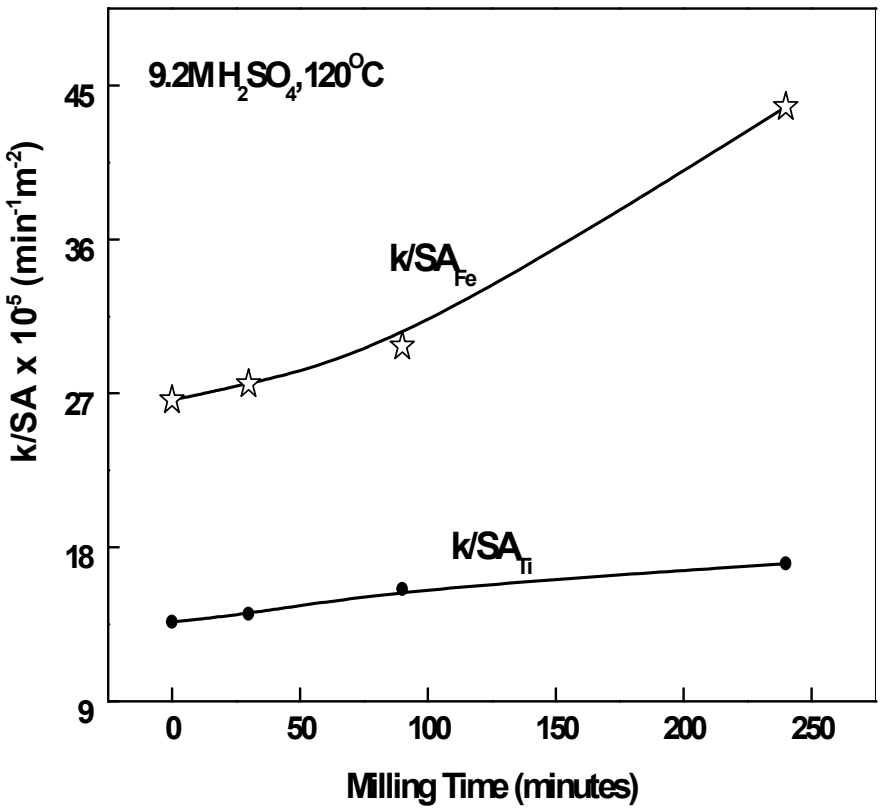

Fig 5.13: Variation of the surface area normalized rate constant for dissolution of Fe with milling time for Manavalakurichi ilmenite sample.

The enhancement in the leaching kinetics because of mechanical activation can arise because of increased surface area or structural disordering or both. Senna, (1989) and Balaz (2000) has summarized some of the methods

.

used to separate the effects of surface area and structure during the mechanical activation process. A method commonly used to determine whether surface area or structural parameters are predominant for the reactivity is to plot the surface area normalized rate constant against the applied energy during activation (Balaz, 2000; Balaz and Balassaova 1994). If the surface area normalized rate constant does not vary with the applied energy, the reaction rate may be considered to be insensitive to structural changes. An increase in the surface area normalized rate constant with the applied energy can be considered to be a result of structural imperfections introduced during the process of mechanical activation. A plot of the surface area normalized rate constant (derived from the reaction rate control parameters) as a function of milling time (or applied energy) for sulfuric acid leaching is given in Fig. 5.13 for Manavalakurichi ilmenite sample. It is observed that the surface area normalized rate constant increases continuously with milling time underlining the effect of structural disordering during mechanical activation.

5.2 Dissolution in hydrochloric Acid

The unmilled and 240 minutes milled samples of Manavalakurichi ilmenite were subjected to dissolution studies at various temperatures (50, 60, 70, 80 and 95^{o}C) and concentrations (2.29M, 6.87M, 9.17M and 11.46M) of HCl. The typical dissolution plots of Fe and Ti at 9.2 M and 11.5M of HCl for unmilled and activated samples are presented in Figs. 5.14 (a-d) and 5.15 (a-d) respectively.

.

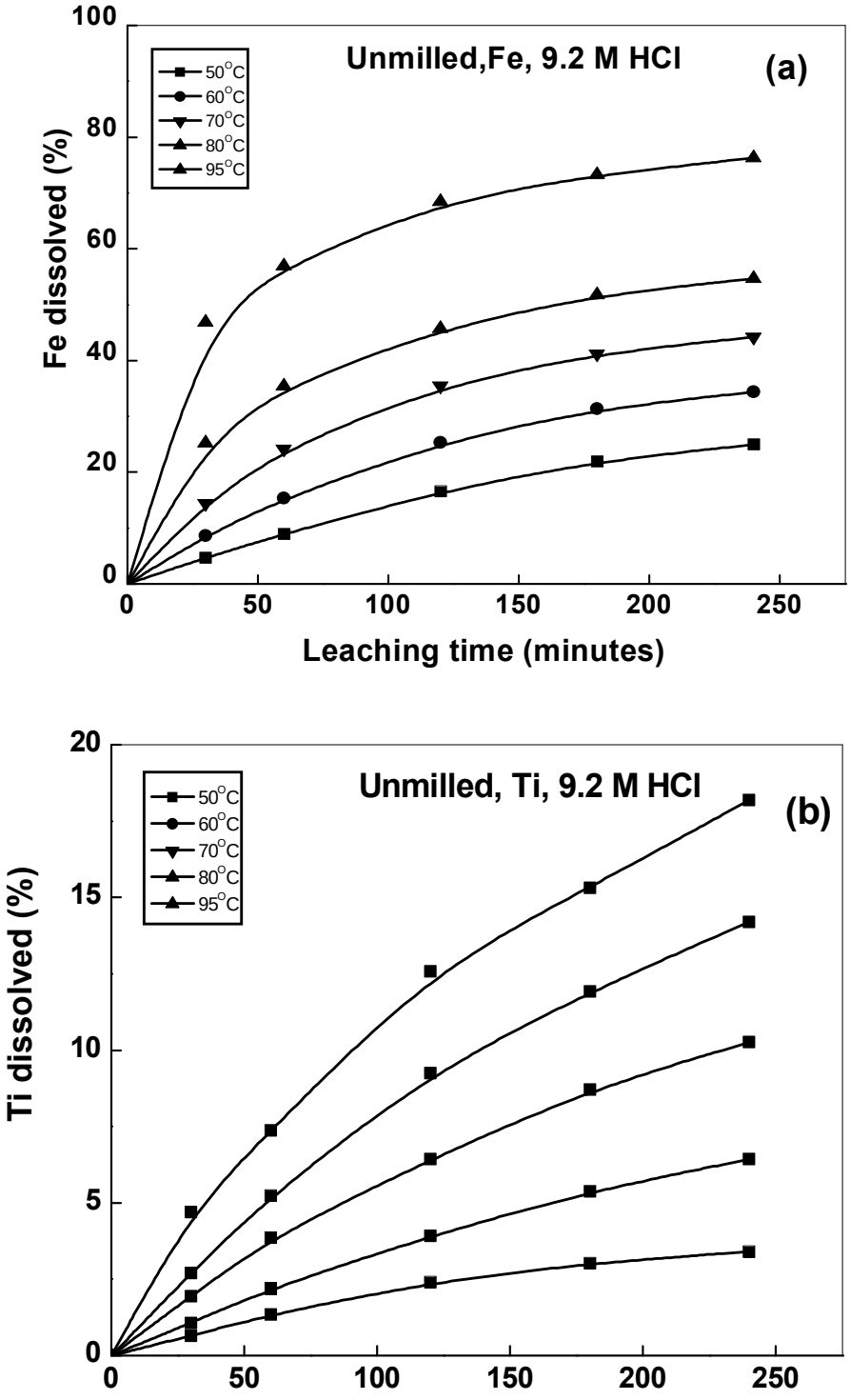

Fig.5.14: Dissolution plots of (a) Fe and (b) Ti in 9.2M HCl for the unmilled sample of Manavalakurichi ilmenite with leaching time at a temperature range of 50-95^{O}C.

.

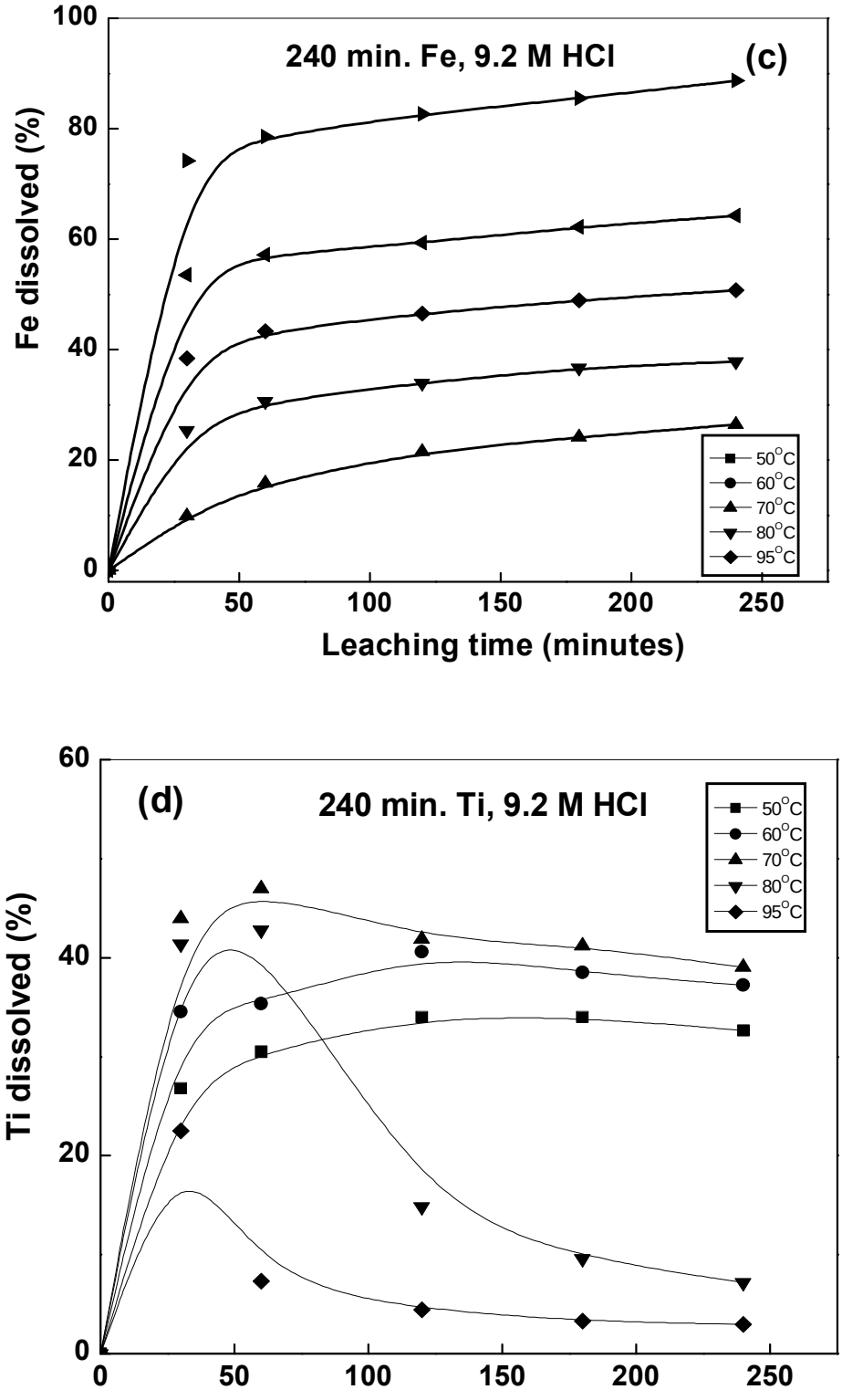

Fig.5.14: Variation of dissolution of (c) Fe and (d) Ti in 9.2M HCl for 240 minutes milled samples with leaching time at a temperature range of 50-95^{O}C.

.

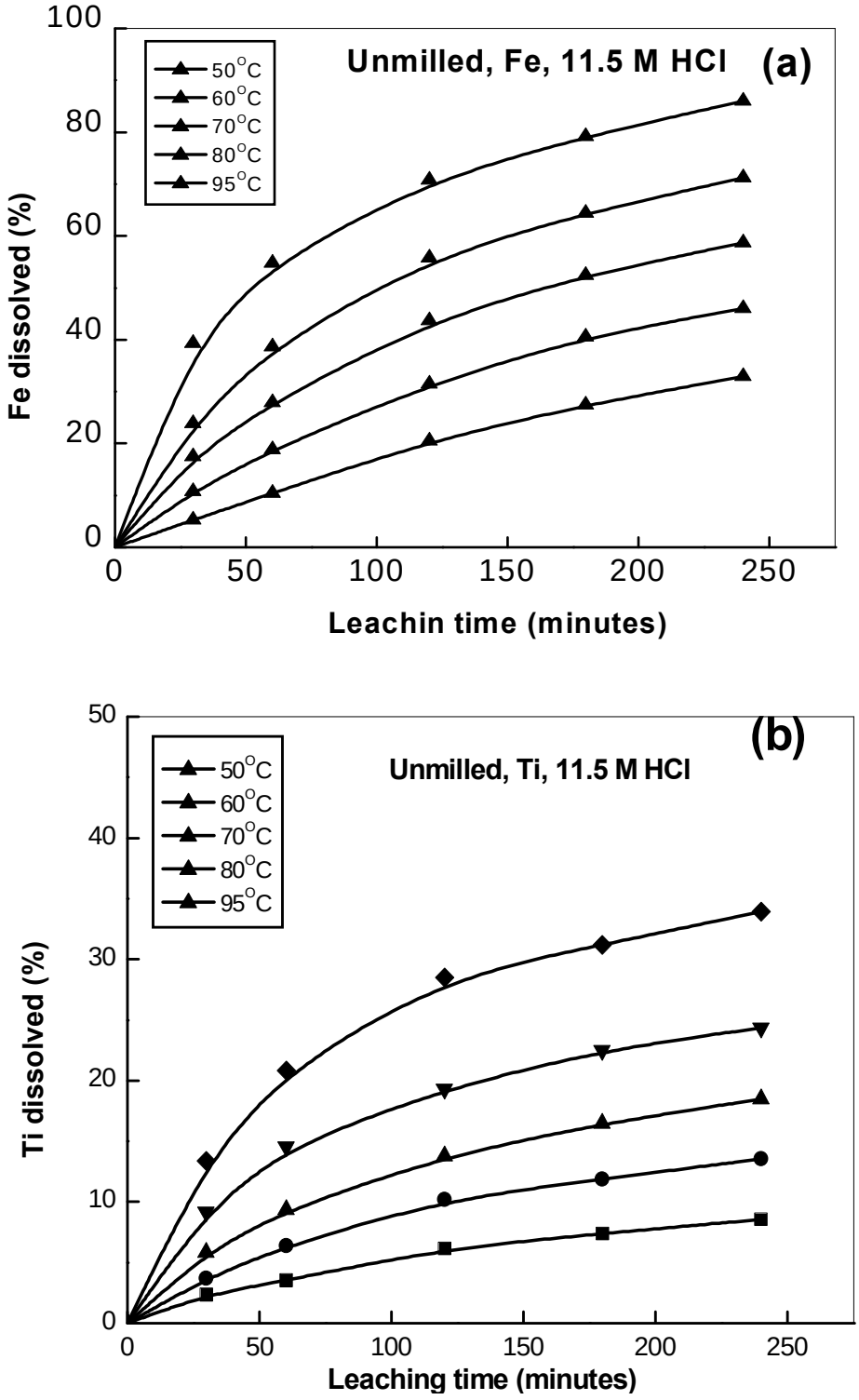

Fig.5.15: Dissolution plots of (a) Fe and (b) Ti in 11.5 M HCl for the unmilled sample of Manavalakurichi ilmenite with leaching time at a temperature range of 50-95^{O}C.

.

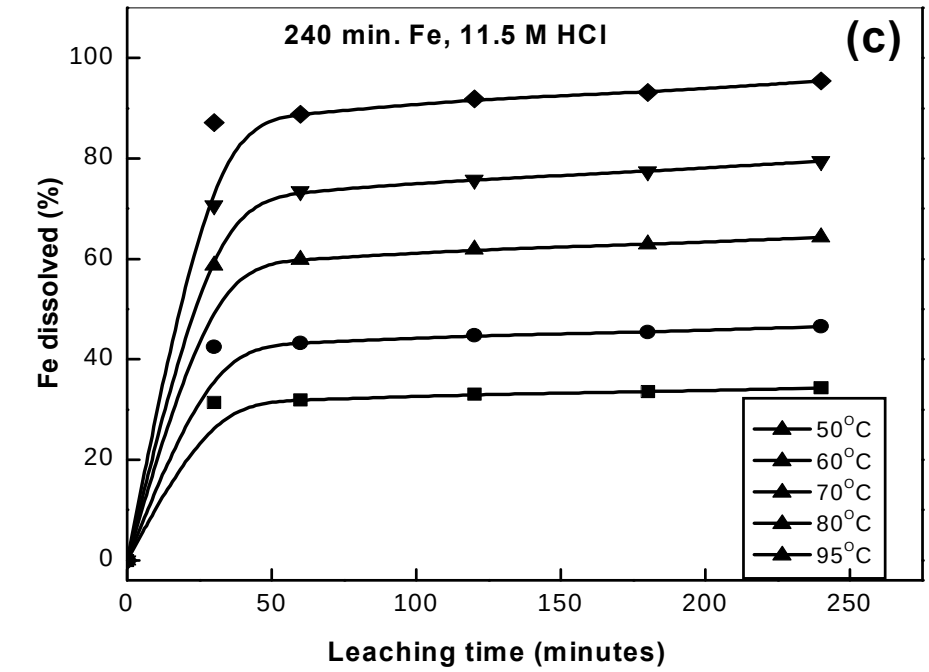

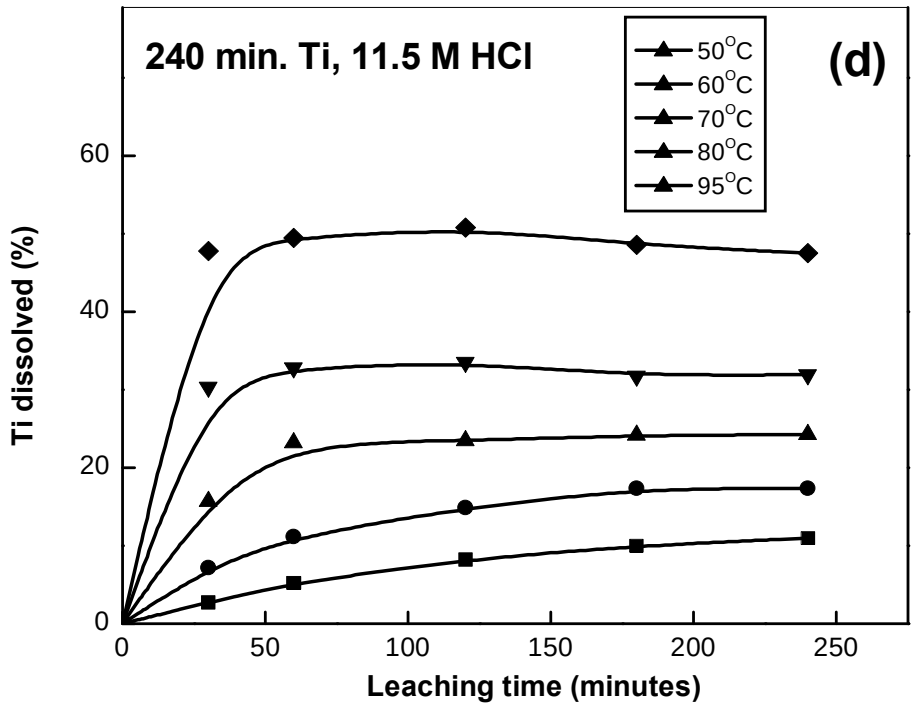

Fig.5.15: Dissolution plots of (c) Fe and (d) Ti in 11.5 M HCl for the 240 minutes milled sample of Manavalakurichi ilmenite with leaching time at a temperature range of 50-95^{O}C.

.

The leaching behavior of Fe and Ti in the unmilled sample shows a monotonic increase with time at all leaching temperatures in the range 50-95^{o}C for all the molar concentrations of hydrochloric acid tested. The differential dissolution of Fe and Ti was enhanced further in hydrochloric acid compared to sulphuric acid. It is observed that the dissolution kinetics of ilmenite in hydrochloric acid appears to be more favorable compared to that in sulfuric acid. Dissolution of up to 46% Ti and 65%Fe (9.2 M HCl at 80^{o}C) could be achieved on the mechanically activated samples (240 min milling) using hydrochloric acid as leachant in 60 minutes of leaching. The extent of dissolution of both Fe and Ti in the activated samples is several times higher than in the unmilled samples. However, the enhanced dissolution of Ti is affected by the hydrolysis and precipitation reactions that set in at higher temperatures and lower acid concentrations for prolonged periods of hydrochloric acid leaching, especially for the activated samples. Fig 5.15 shows the dissolution of Fe and Ti of Manavalakurichi ilmenite sample in unmilled and 240 minutes activated condition at various temperatures in 11.5 M HCl. It was observed that the hydrolysis reaction of Ti in activated sample was considerably reduced at higher acid concentration (11.5 M HCl).

5.2.1 Effect of acid concentration

Figure 5.16 shows the variation of the maximum dissolution of Fe and Ti with increasing acid concentration at 95^{O}C. The extent of dissolution of Fe and Ti increased with the acid concentration. The hydrolysis and precipitation of TiO_2 were in general not observed for the unmilled sample for all the concentrations used in the present study. However in the case of the activated sample, hydrolysis of Ti ions occur especially at lower acid concentration (<8 M HCl). The color of the leach solution also changed from black to brown as the leaching proceeds and precipitates of white TiO_2 were clearly visible in the solution for lower acid concentrations. The effect of acid concentration on ilmenite dissolution was investigated by earlier studies ((Jackson and Wadsworth, 1976; Hussein et al., 1976; Van Dyk et al., 2002). However, the

.

effect of concentration of HCl on mechanically activated ilmenite samples has not been reported.

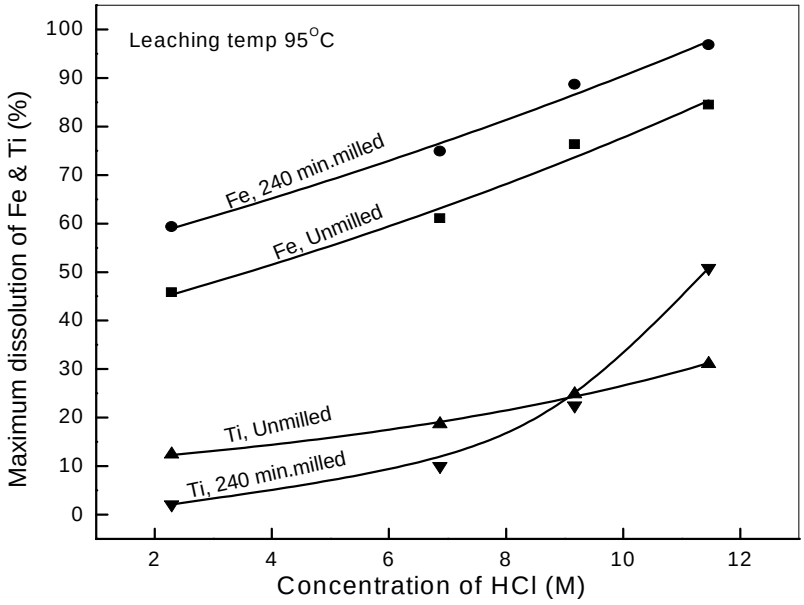

Fig.5.16: Variation of maximum dissolution of Fe and Ti with increasing concentration of HCl at 95^{O}C.

5.2.2 Effect of temperature

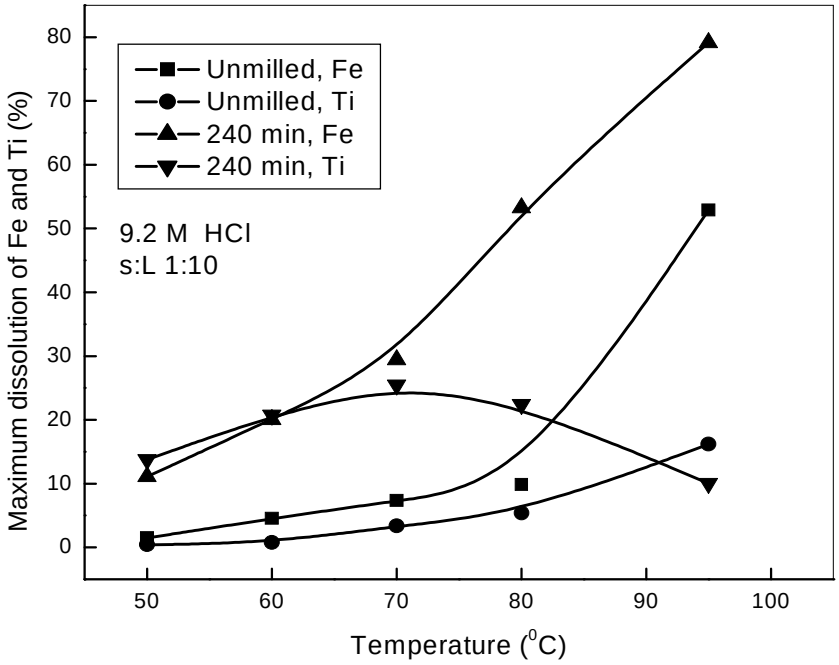

Fig.5.17: Variation of maximum dissolution of Fe and Ti with increasing temperature at 9.2M HCl.

.

The variation of maximum dissolution of Fe and Ti with temperature at 9.17 M HCl is delineated in Fig.5.17 for Manavalakurichi ilmenite. The dissolution of both Fe and Ti increases exponentially with temperature and the hydrolysis reaction is not observed for unmilled sample at all the temperatures. However, the Ti ions are found to be hydrolyzed in activated samples at higher temperatures (>70^{o}C). Thus the quantity of Ti in the solution decreases with temperature for activated samples beyond 70^{O}C and with low acid concentrations.

5.2.3 Effect of solid to liquid ratio

The dissolution plots of Fe and Ti carried out at a solid to liquid ratio of 1:100 in 9.2M of HCl is shown in Fig.5.18.

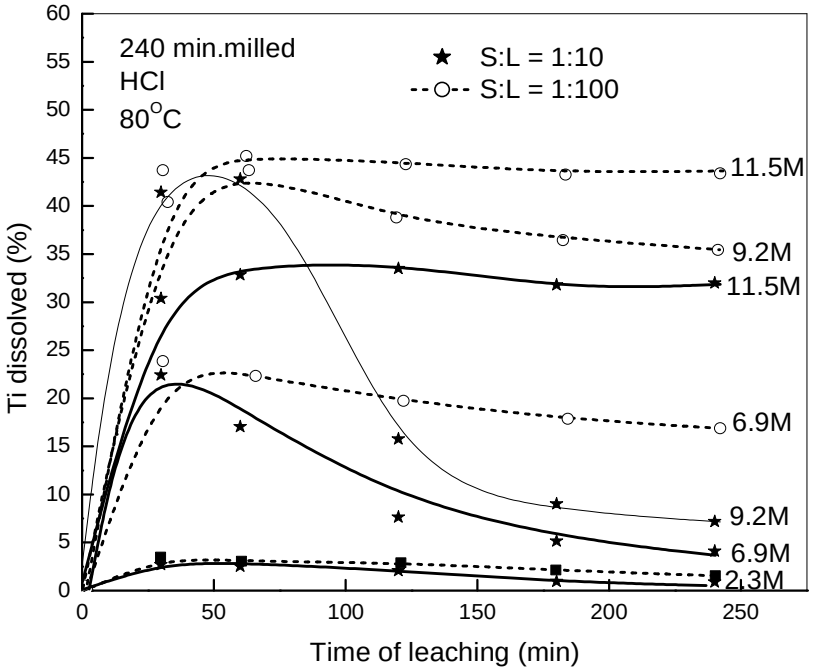

Fig.5.18: The plot showing the dissolution of Ti at a solid to liquid ratio of 1:10 and 1:100 at 80^{0}C for Manavalakurichi ilmenite sample (4 hours activated) subjected to dissolution at various concentrations of HCl.

It was observed that there is no significant enhancement in dissolution of Fe and Ti when higher solid to liquid ratio (1:100) was used. However the hydrolysis reaction of Ti is reduced at a solid to liquid ratio of 1:100.

.

5.2.4 Effect of mechanical activation

The effect of mechanical activation on the maximum dissolution of Fe and Ti of Manavalakurichi ilmenite is depicted Fig.5.19.

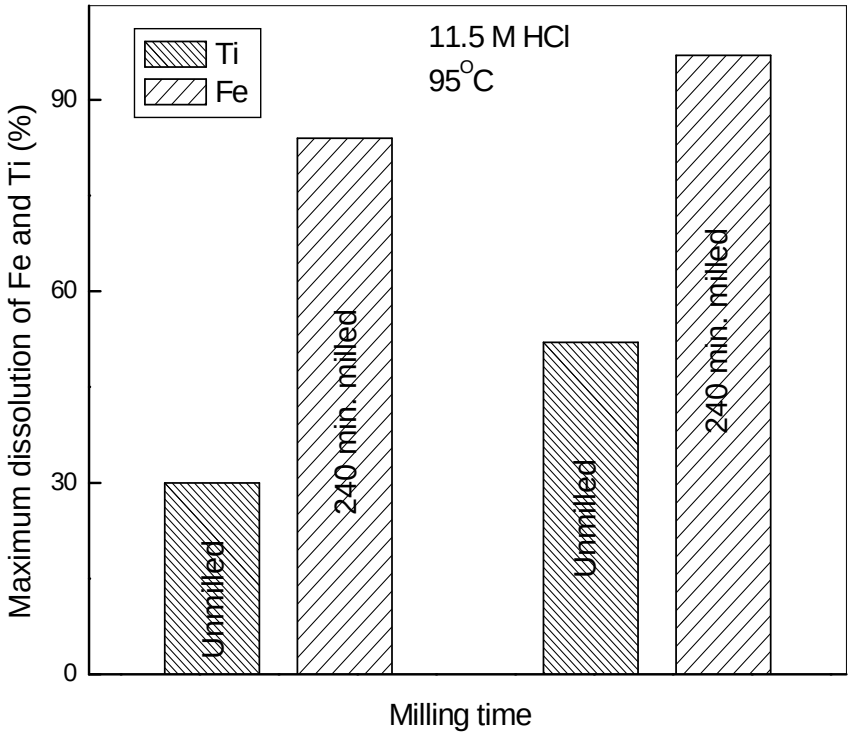

Fig.5.19: The effect of mechanical activation on maximum dissolution of Fe and Ti in Manavalakurichi ilmenite sample in 11.5 M HCl at 95^{O}C .

A considarable enhancement in dissolution of both Fe and Ti was observed in hydrochloric acid leaching of mechanically activated ilmenite sample. The increase in dissolution of Fe and Ti in activated sample depends on the concentration of acid and leaching temperature. In fact the initial rate of dissolution is higher than that of dissolution in sulphuric acid. However the dissolution of Ti is affected by precipitation reaction in activated samples. The activated sample shows about 50% dissolution of Ti within one hour at 95^{O}C using 11.46M HCl whereas the unmilled sample shows about 35% of Ti dissolution in 4 hours of leaching at 95^{O}C for the same acid concentration. The enhanced acid dissolution of Fe and Ti from ilmenite in the mechanically activated samples is attributed to an increase in surface area as well as the non-uniform strain introduced by the defects. Further, the other variables

.

contributing to the enhancement in dissolution are discussed in the earlier section on the effect of mechanical activation on sulphuric acid dissolution.

5.2.5 Residue analysis

The particle size distribution of a representative leach residue from HCl leaching of unmilled as well as activated sample is shown in Fig. 5.20.

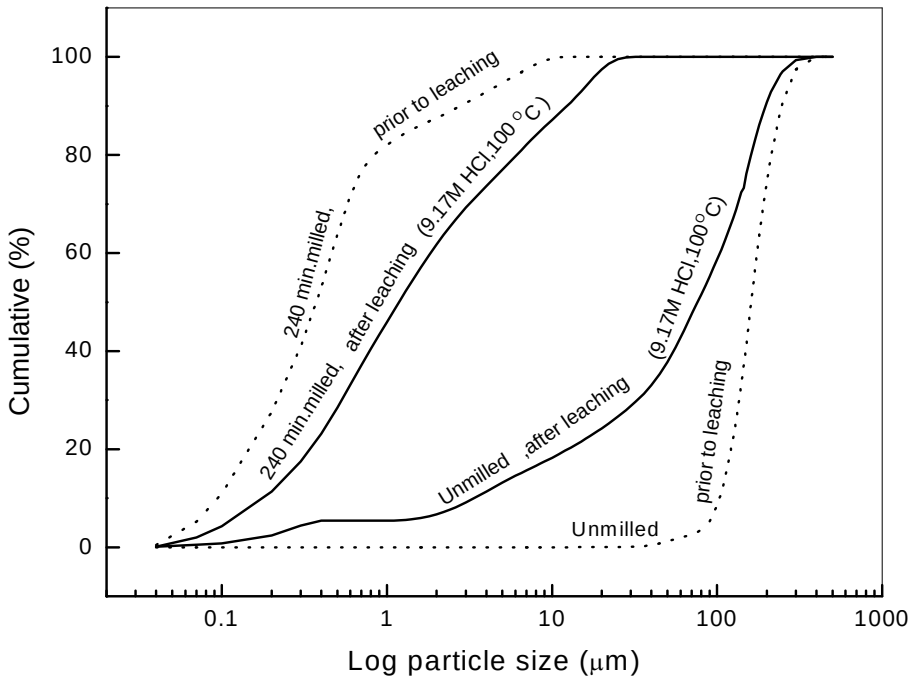

Fig.5.20: Particle size distribution of HCl leach residues of Manavalakurichi ilmenite sample.

The particle size analysis of the leach residues corresponding to the activated sample shows an increase in mean particle size as well as the particle size distribution after leaching. The change in particle size distribution after leaching can be attributed to the complete dissolution of the fine particles leaving behind the coarser particles and the agglomeration of the hydrolyzed products. The XRD for some of the leach residues corresponding to HCl leaching are presented in Fig.5.21.

.

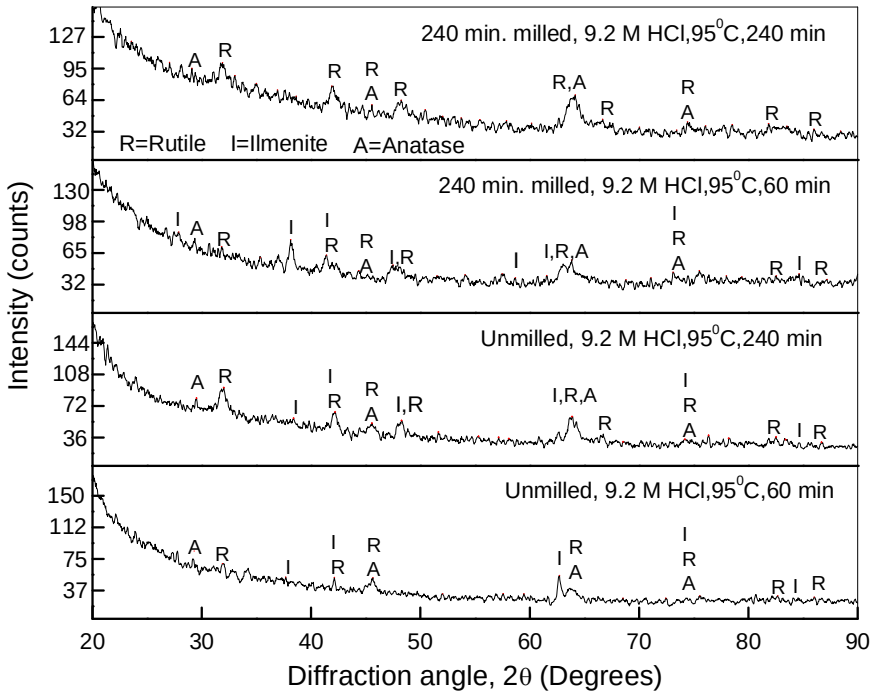

Fig.5.21 X-RAY diffractogram of HCl leach residue of unmilled sample and 240 min. Milled sample

Although the ilmenite phase is more or less leached within 2 hours of leaching with 9.2M HCl at 95°C, the dissolution of the leucoxene/rutile phase was found to be insignificant even after 4 hours of leaching. The minor amount of anatase phase observed in the leach residues has possibly formed from the products of hydrolysis and precipitation.

5.2.6 Eh--pH measurements

The redox potential and pH during leaching (monitored at the beginning and end of the leaching experiment at ambient temperature) showed small variations. Figure 5.20 shows the Eh-pH diagram for Ti-HCl-H_2O systems at 25°C reported by Vaughan and Alfantazi (2004) and the experimental range of variation of Eh-pH in the present study.

.

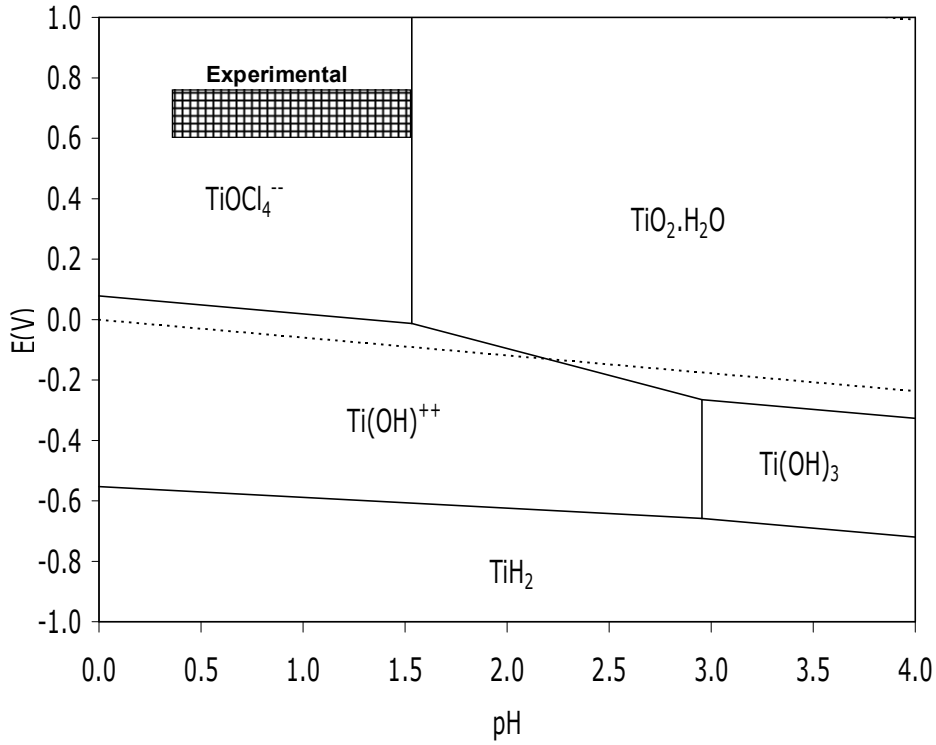

Fig5.22: The Eh-pH diagram for Ti-HCl-H_2O systems at 25^{o}C (Vaughan and Alfantazi, 2004) and the experimental range of variation of Eh-pH in the present study.

The relative leaching behavior of Ti in H_2SO_4 and HCl can be analyzed using the Eh-pH diagrams for these two systems. The Eh-pH diagram for the Ti-SO_4^{--}-H_2O system at 25^{o}C taken from a recent study of Vauhgan and Alfantazi, (2004) is shown in Fig. 5.9. It is seen that Ti dissolves in sulfuric acid over a wide range of oxidation potentials, as $TiO(SO_4)^{2\delta}$ between ï 0.2 to 1.0 V and up to pH of 3.5 and as $TiSO_4^+$ between ï 0.6 to ï 0.2 V and pH up to 2.75. At higher pH (>3.5), Ti precipitates as $Ti(OH)_3$ under reducing conditions and as $TiO.H_2O$ at oxidizing conditions. It is therefore clear that titanium in sulfuric acid solution is stable at low temperatures without the possibility of undergoing hydrolysis except at high pH. The measured redox potentials and pH during sulfuric acid leaching of the unmilled and activated samples lie within the solubility range predicted by the Eh-pH diagram. The Eh-pH diagram for the Ti-Cl^--H_2O system at 25^{o}C taken from the recent study of

.

Vauhgan and Alfantazi, (2004) is shown in Fig.5.20. It is seen that Ti dissolves in HCl as $TiOCl_4^-$ only under oxidizing conditions and in a very limited range of pH (up to ~1.5). At lower oxidation potentials, they hydrolyze to form $Ti(OH)^{++}$ and at higher pH they precipitate as $TiO_2.H_2O$ at higher oxygen potentials and as $Ti(OH)_3$ at lower oxidation potentials. This implies that titanium in hydrochloric acid solution can be destabilized at reducing conditions and at lower acid concentration even at ambient temperature. The phase stability boundaries in the Eh-pH diagram will change at higher temperatures. However, data on the Gibbs energy of formation of the various species in the Ti-Cl-H_2O and Ti-SO_4-H_2O systems at higher temperatures are not available in the literature. The measured pH and redox potentials during leaching in dilute HCl in the present study was found to be at the border of the dissolution/ hydrolysis regions where some hydrolysis can occur. In the present study, it is observed that the hydrolysis reaction of Ti (IV) in hydrochloric acid was enhanced by mechanical activation of ilmenite concentrate before leaching. This may be attributed to enhanced kinetics of the hydrolysis reaction than because of any thermodynamic consideration.

5.2.7 Kinetic modeling

The procedure adopted for derivation of kinetic parameters for dissolution of Fe and Ti is described in section 5.1.7. The dissolution of Fe and Ti of ilmenite follows a two stage mechanism in hydrochloric acid as in sulphuric acid. Therefore, the activation energy of dissolution was derived using the reaction rate control model for the initial stage of dissolution and using the shrinking core model for the later stage of dissolution.

For the reaction rate control mechanism, g(Ŭ) can be given by:

$$g(Ŭ) = 1-(1-Ŭ)^{1/3} \quad (5.9)$$

and for the product layer diffusion control shrinking core model, g(Ŭ) is written as

$$g(\alpha) = 1-\frac{2}{3}\alpha-(1-\alpha)^{2/3} \quad (5.10)$$

.

The calculated activation energies for the dissolution of Fe and Ti in HCl in the initial stage are given Fig.5.21 for unmilled and 240 minutes milled samples of Manavalakurichi ilmenite.

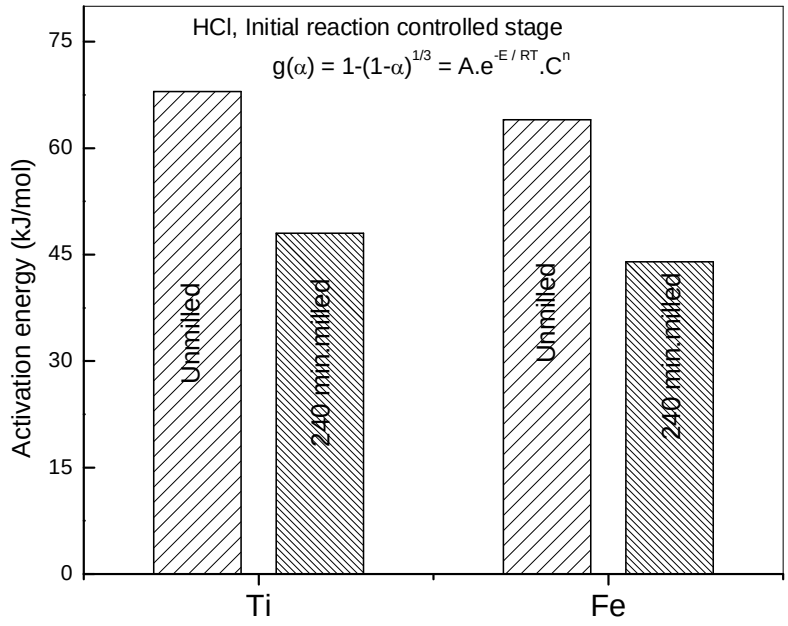

Fig.5.21: The effect of mechanical activation on activation energy of dissolution of Fe and Ti in hydrochloric acid during initial reaction controlled stage.

In comparision to sulphuric acid the kinetics of dissolution of Fe and Ti was considerably enhanced in hydrochloric acid. The order of reaction with respect to acid concentration was found to be the same (1.5) as H_2SO_4 for HCl suggesting that the reaction mechanism is same in both the cases. For the 1st stage of sulfuric acid leaching, the activation energy for the dissolution ranged from 48 to 68 kJ/mol for Fe and 51 to 70 kJ/mol for Ti. For hydrochloric acid leaching the activation energy during the 1st stage of dissolution was 45 to 64 kJ/mol for Fe and 48 to 68 kJ/mol for Ti.. The activation energy for dissolution of Fe and Ti is somewhat higher in H_2SO_4 compared to HCl. The activation energy for dissolution of Fe and Ti also showed a considerable decrease with milling time. About 20 kJ/mol was reduced by 4 hours milling of ilmenite sample. Hishashi et al.,(1982) determined apparent activation energies of 81.2 kJ/mol for titanium and 73.2 kJ/mol for iron dissolution for the leaching of

.

ilmenite ore with highly concentrated hydrochloric acid (11.3 to 11.6 M) at temperatures of 30 ï 80^{o}C. However the activation energy values of Fe and Ti of ilmenite samples in activated condition have not been reported in earlier studies.

The effect of surface area and structural deformation on dissolution rate of activated samples was studied by the method described by balas (2000) and Senna (1989). The surface area normalized rate constant of Fe and Ti dissolved in 9.2M of HCl is shown in fig.5.22 for unmilled and 4 hours milled sample of Manavalakurichi ilmenite.

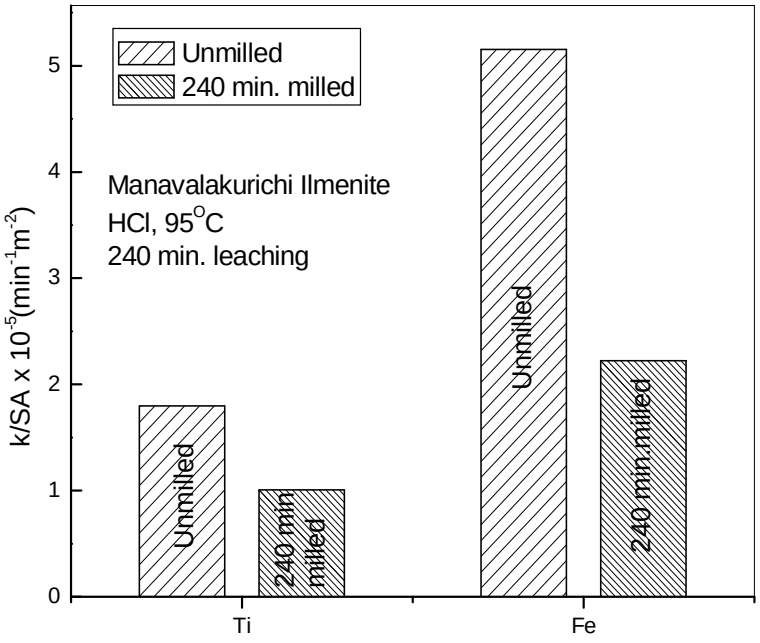

Fig.5.22 : The variation of surface area normalized rate constant of Fe and Ti with milling time for Manavalakurichi ilmenite dissolved in 9.2M HCl.

The rate constant was considerably enhanced by milling; further the rate of dissolution of Fe and Ti is higher that of H_2SO_4 dissolution. Earlier investigations on hydrochloric acid leaching of ilmenite (Jackson and Wadsworth, 1976; Hussein et al., 1976; Tsuchida et al.,1982; Sinha, 1984; Lanyon et al., 1999; Olanipekun, 1999; Van Dyk et al., 2002) yield slower kinetics of dissolution compared to that obtained in the present study on mechanically activated ilmenite.

.

5.3 Conclusions

1. Although mechanical activation considerably enhanced the dissolution kinetics for both Fe and Ti, it was observed that the Ti and Fe in the ilmenite dissolves incongruently and not according to their stoichiometry in the ilmenite phase.
2. The maximum dissolution of Fe and Ti in the Chatrapur ilmenite was restricted to 20-65% in the unmilled condition whereas, in excess of 90% Fe and % Ti could be dissolved (120^{o}C, 4 h leaching) from ilmenite samples subjected to 240 minutes of milling.
3. For Manavalakurichi ilmenite, the maximum dissolution Fe and Ti in unmilled condition was restricted to 20-30% and 25-50% respectively, whereas, in excess of 80-90% Fe and 50-65% Ti could be dissolved (120^{o}C, 4 h leaching) for ilmenite samples activated for 240 min.
4. The dissolution kinetics of ilmenite in hydrochloric acid was marginally favorable compared to that in sulfuric acid. However, the enhanced dissolution of Ti in HCl for the activated sample is affected by the hydrolysis and precipitation reactions that set in at higher temperatures and lower acid concentrations for prolonged periods of leaching.
5. The dissolution kinetics HCl (prior to significant hydrolysis) and in H_2SO_4 is found to conform to the reaction rate control model for the initial leaching period and thereafter to the shrinking core model where product layer diffusion is rate controlling.
6. The activation energy for dissolution of Fe and Ti (in Manavalakurichi ilmenite) was higher in H_2SO_4 (68 and 70 kJ/mol respectively) compared to HCl (64 and 68 kJ/mol respectively). The activation energies for dissolution of Fe and Ti also showed a monotonic increase with time of milling.

.

CHAPTER 6

A COMPARATIVE STUDY OF NATURAL WEATHERING AND MECHANICAL ACTIVATION

6.1 Alterations of ilmenite induced by natural weathering

Natural ilmenites are seldom pure. The beach sand ilmenite grains alter easily by natural weathering and oxidation phenomena giving rise to many altered phases. Ilmenite alteration is essentially the oxidation of iron resulting in enrichment of titanium dioxide and subsequently leading to the formation of leucoxene, rutile or anatase. The commonly accepted ilmenite alteration mechanism given in the literature (Temple, 1966; Grey and Reid, 1975; Morad and Aldahan, 1982; Frost et al, 1983; Anand and Gilkes, 1984; Suresh Babu et al., 1994; Chaudhuri, J.N.B., Newesely, H., 1990, Rao et al, 2005) is:

Ilmenite	Ÿ	Pseudorutile	Ÿ	leucoxene or Rutile / Anatase	+ Hematite
$Fe^{2+}TiO_3$		$Fe_2^{3+}Ti_3O_9$		TiO_2	Fe_2O_3
Hexagonal		Hexagonal		Tetragonal	Hexagonal

During the first stage alteration of ilmenite, the ferrous content decreased and ferric as well as titania contents increased. The oxidation and leaching processes occurring during the alteration also enhance the porosity of the ilmenite grains. Subsequently, the Fe^{2+} is completely oxidized to Fe^{3+} to form the pseudo-rutile phase, which has the same crystal structure as ilmenite. Further alteration causes the gradual collapse of the hexagonal structure and its recrystallisation into the tetragonal structure of rutile (Suresh Babu et al., 1994). In addition to the change in crystal structure, alteration enhances the surface area and porosity, reduces the crystallite size of the ilmenite and may also result in partial amorphization. The effect of alteration has significant implications in the industrial processing of TiO_2 (Suresh Babu et al., 1994). All the downstream metallurgical processes vary widely with respect to their degree of alteration. Studies on the influence of weathering on the high

.

temperature reduction characteristics of three different varieties of ilmenites was carried out by Gupta et al., (1988) who concluded that the rate of reduction and size of iron particles decreases with increased alteration. The said studies also reveal that the reduction of stoichiometric ilmenite is faster than pseudorutile. Chernet (1999) studied the Australian beach sand ilmenite concentrates and derived four different ilmenite products with varying degree of oxidation from it by Frantz electromagnetic separator. She studied the dissolution behavior of these weathered ilmenites in sulfuric acid and concluded that the solubility decreases with increasing TiO_2 content (i.e., with increasing alteration). Similar systematic studies on the effect of alteration/weathering of Indian ilmenites have not been reported in the literature.

6.2 Alteration of ilmenite induced by mechanical activation

During the past decade, there has been considerable interest on the effect of mechanical activation on the physico-chemical properties of minerals and their subsequent dissolution behavior (Chernet, 1999; Balaz, 2000; Duncan and Metson, 1982a,b; Tkacova, 1996). Mechanical activation under ambient conditions results in oxidation, phase transformations, increased surface area, structural defects, strain and changes in the surface characteristics of minerals (Duncan and Metson, 1982a&b; Balaz, 1996; Balaz et al, 1996; Balaz, 2000; Amer, 2000; Welham, 2001). In some respects, it may be expected that the mechanical activation process at ambient conditions can simulate the natural weathering/alteration process occurring on a geological time scale. It is considered interesting to compare the effects of natural weathering/alteration and mechanical activation under ambient conditions. Although the effect of mechanical activation on the enhancement in dissolution rates of ilmenites in sodium hydroxide solution (at 200^{o}C and oxygen pressures of 4.1MPa) (Amer, 2002) as well as in sulfuric acid has been reported (Welham and Llewellyn, 1998), a comparative study between weathering and mechanical activation has so far not been reported in the literature.

.

6.3 Alteration in chemical characteristics:

The bulk chemical compositions of all the natural ilmenite samples used in this study (Chatrapur, Navalady, Manavalakurichi and Chavara) are reported in Table 3.1. The oxidation state of iron in ilmenite is a good indicator of the degree of weathering (Gibb et al., 1969); the degree of alteration increasing with the ferric to ferrous ratio. The variation in the Fe^{+3}/Fe^{+2} ratio with the degree of alteration for the natural ilmenite samples from the different coasts of India used in the present study as well as with time of activation is given in Fig.6.1 and 6.2.

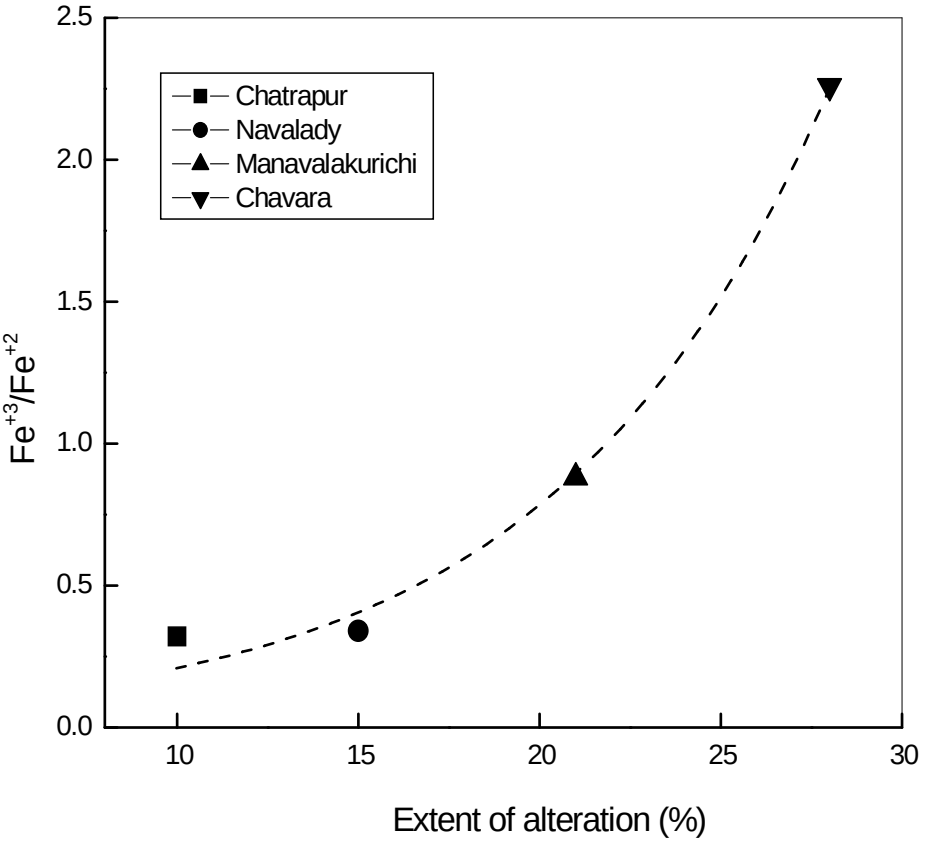

Fig.6.1: Variation of ferric to ferrous ratio with extent of alteration of minerals.

.

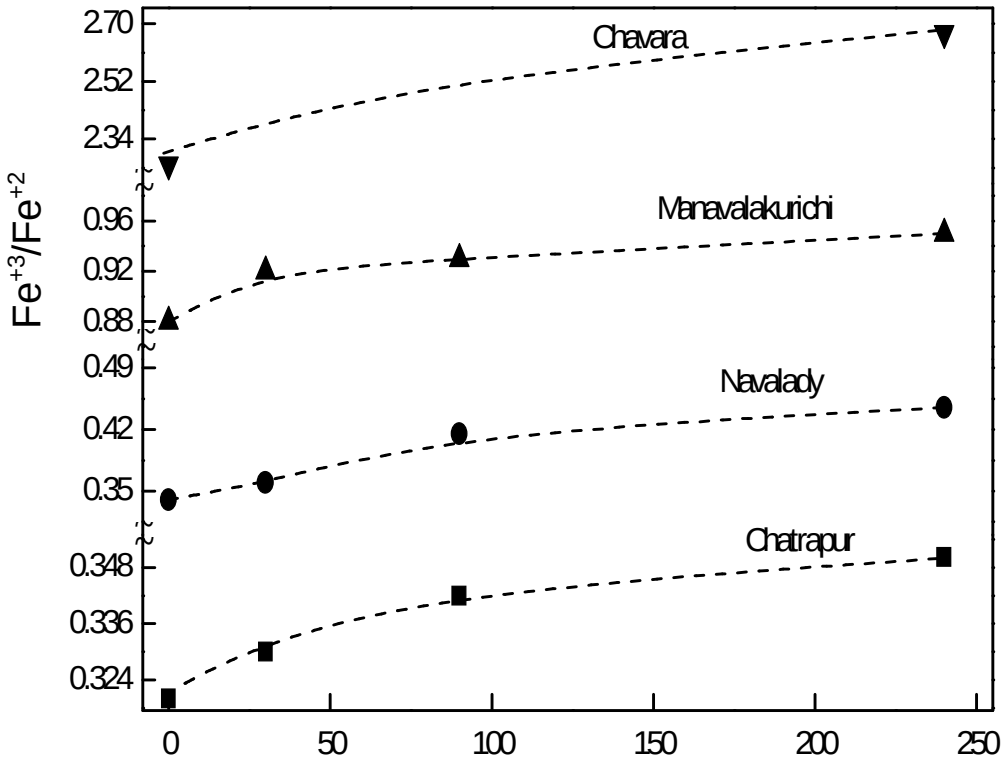

Fig.6.2: Variation of ferric to ferrous ratio with milling time for various ilmenite samples.

It is seen that the ferric to ferrous ratio increases in the order: Chatrapur ï Navaladi ï Manavalakurichi ï Chavara indicating that the Chatrapur sample is least altered and the Chavara sample has undergone maximum alteration. There is a corresponding decrease in the TiO_2 content. Similar observations were also made by other workers for Chatrapur, Manavalakurichi and Chavara ilmenite samples (Suresh Babu et al., 1994; Suresh Babu and Mohandas, 1999). Similar to the weathering process, it is seen that the ferric to ferrous ratio increases with increase in time of activation, although the extent of oxidation in mechanical activation is comparatively much lower.

.

6.4 Alteration in mineralogical characteristics

Representative micrographs of the various ilmenite concentrates collected from the different coasts (Chatrapur, Navalady, Manavalakurichi and Chavara), which are subjected to varying degree of alteration/oxidation are depicted in Figs.6.3a-d.

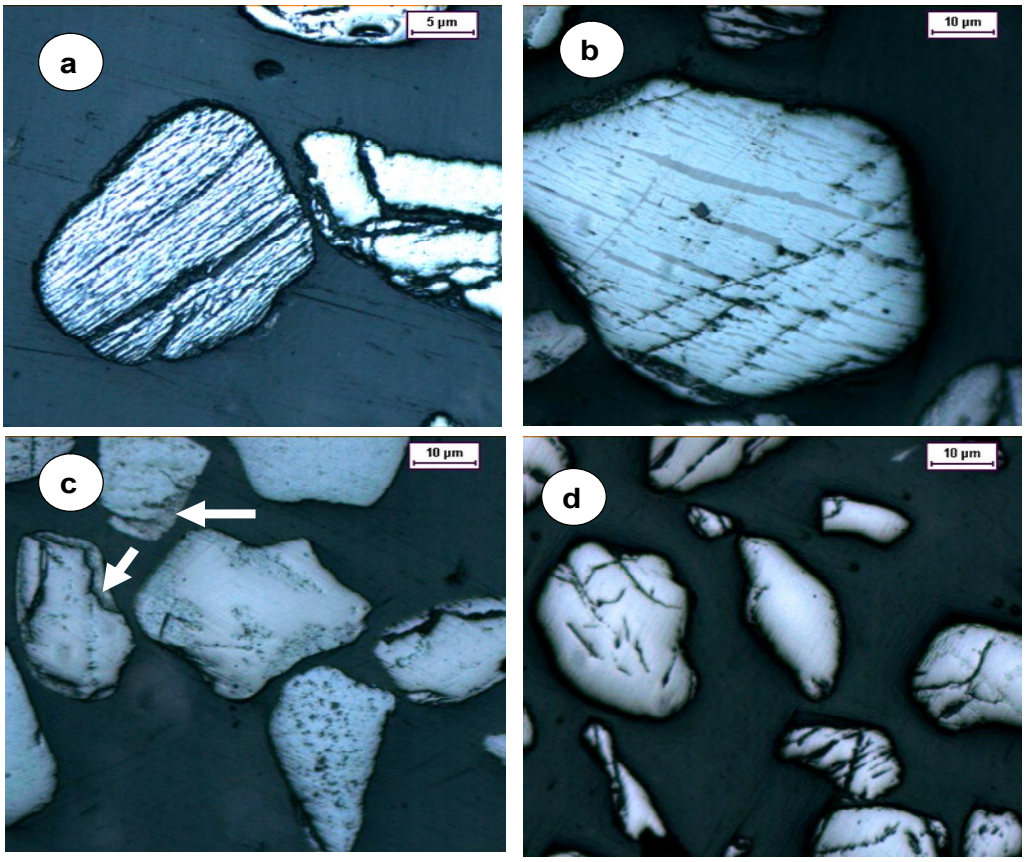

Fig.6.3: a. Photomicrograph of Navalady ilmenite (showing various shapes and sizes of ilmenite grains), b.Chatrapur ilmenite (showing ex-solution layers of primary hematite and ilmenite, c. Manavalakuruchi ilmenite (showing alteration along grain boundaries (shown by arrows)), and d.Chavara ilmenite (showing alteration of ilmenite grain along crystallographic directions) subjected to different degree of weathering.

All the ilmenite samples were found to occur mostly as sub-rounded, elongated (oval) to sub-angular (some what irregular) grains. Micro-morphological features noticed on the ilmenite grains include numerous surface pits, etch marks/ grooves and crescentic pits. Reflected light microscopic

.

studies suggest that unaltered ilmenite is the dominant phase in all the four samples along with varying amounts of alteration products. Mixtures of altered as well as unaltered phases were present in many of the single grains. The various phases in each sample were confirmed using EPMA. In addition to the ilmenite and altered ilmenite phases, the presence of traces of primary hematite (not formed by alteration) was noticed in the case of the Chatrapur sample. In the other samples (especially Manavalakurichi and Chavara), varying amounts of leucoxene were noticed. When altered, ilmenite changes directly or through the intermediate products to leucoxene/rutile. Many ilmenite grains were moderately altered and the alteration appears to proceed along grain boundaries, grain edges, along crystallographic directions and fissures in varying intensity and pattern. The alteration of the ilmenite grains occasionally results in an amorphous to crypto- or microcrystalline mass resembling leucoxene and pseudo-rutile/leucoxene. The intensity and mode of alteration varied from grain to grain and was neither uniform nor continuous. The weathering process occurs due to atmospheric exposure on a geological time scale and involves gradual erosion, oxidation and leaching out of ferrous ion. Leucoxene/rutile and hematite (secondary) are the eventual end products but the process goes through several intermediate stages, the prominent one being the formation of pseudo-rutile. Precise quantitative estimates of the extent of alteration in the weathered samples has been done by using polarized light microscopy, the results of which are given in Table 2.

Table 6.1: A quantitative estimate of the degree of alteration of the ilmenite samples by light microscopy

Sample	Mineralogy
Chatrapur	90% Ilmenite; 10% altered ilmenite.
Navaladi	85% ilmenite, 15% altered ilmenite
Manavalakurichi	79% Ilmenite, 12% altered ilmenite and 9% of leucoxene/rutile
Chavara	77% Ilmenite, 10% altered ilmenite and 13% leucoxene/rutile

.

Chaudhuri & Newesely (1990) and Mucke and Chaudhuri (1991) discussed the transformation of ilmenite to leucoxene during the alteration process. The alteration starts with the continuous removal of the soluble ferrous ion and the electrostatic charge is balanced by oxidizing the remaining iron to ferric form. Ferrous ion is totally oxidized on the formation of pseudorutile. Further removal of ferric iron is compensated for by addition of OH^- to the mineral lattice.

6.5 Alteration in physical and structural characteristics:

The X-ray diffractograms of the different ilmenite samples (Chatrapur, Navalady, Manavalakurichi and Chavara) subjected to varying degrees of alteration are delineated in Fig. 6.4.

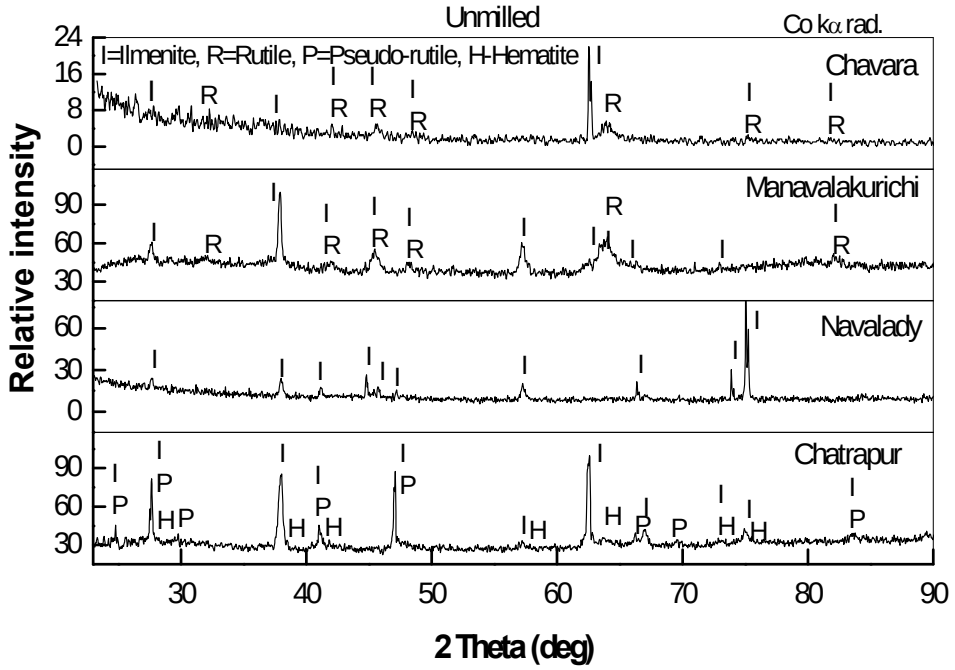

Fig.6.4: X-ray diffractograms of the altered ilmenite concentrates collected from the different locations.

As indicated by the optical microscopic study, ilmenite is the major phase in the XRD patterns (JCPDS No. 29-0733) of all the samples. Small amounts of pseudo-rutile and hematite phases are observed in the Chatrapur sample whereas pseudo-rutile phase could not be observed in the XRD of all

.

the other samples, possibly because of amorphization of this phase. The Navalady sample shows the presence of only the ilmenite phase in the XRD whereas the Manavalakurichi and Chavara samples show the presence of significant amounts of the leucoxene/rutile phase (JCPDS 21-1276) in addition to the ilmenite phase. The ilmenite phase in the Chavara sample shows a higher degree of amorphization.

The X-ray diffractograms of all the ilmenite samples (Chatrapur, Navalady, Manavalakurichi and Chavara) subjected to 240 minutes of planetary milling are delineated in Fig.6.5.

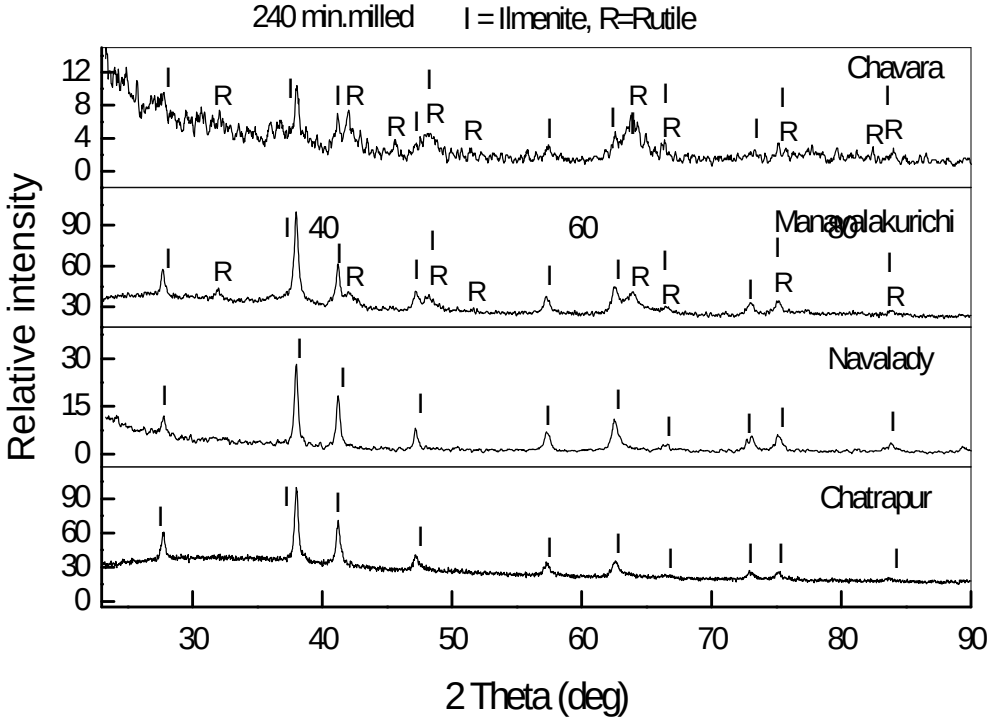

Fig.6.5: X-ray diffractograms of the activated ilmenite samples.

Ilmenite (JCPDS No. 29-0733) appears to be the major phase in all the activated samples although significant amorphization of the ilmenite phase is noticeable in the Manavalakurichi and Chavara samples. The minor amount of the pseudo-rutile phase noticed in the Chatrapur sample prior to activation appears to have amorphized during milling. The Manavalakurichi and Chavara samples show the presence of the leucoxene/rutile phase even after mechanical activation.

.

The XRDs of the naturally weathered as well as the mechanically activated samples shows significant peak broadening. A Williamsonï Hall plot (B Cos θ Vs Sin θ) was used to determine the crystallite size and strain effects from the line broadening analysis. The broadening caused by other phases and instrumental factors were carefully analyzed and deduced from the total broadening.

The variation of crystallite size and pore size determined with BET technique with increasing Fe^{+3}/Fe^{+2} ratio of the naturally weathered ilmenite samples is given in Fig.6.6

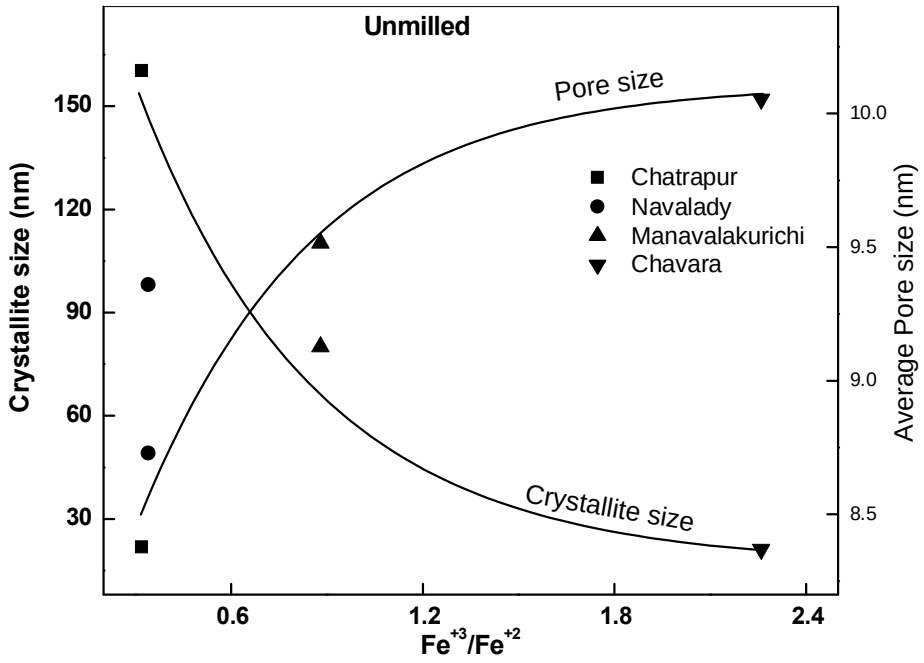

Fig. 6.6 Variation of crystallite size and average pore size determined fro BET technique with increasing Fe^{+3}/Fe^{+2} ratio for the altered ilmenite samples.

The crystallite size decreases exponentially with the extent of alteration. However, there is no increase in strain in the naturally weathered samples. The average pore size determined using a BET surface area analyzer for the naturally altered samples is also depicted in Fig. 6.6. The average pore size increased with the degree of alteration characterized by the Fe^{+3}/Fe^{+2} ratio. The variation of crystallite size and strain with the milling time for various ilmenite

.

samples are shown in fig.3.10. Although the mechanically activated ilmenite samples show a similar trend in crystallite size, decreasing with increasing time of activation, unlike for the naturally altered samples, there is an additional increase in non-uniform strain with increasing time of activation.

The variation of particle size distribution in the naturally altered and mechanically activated ilmenite samples is depicted in Figs. 6.7.

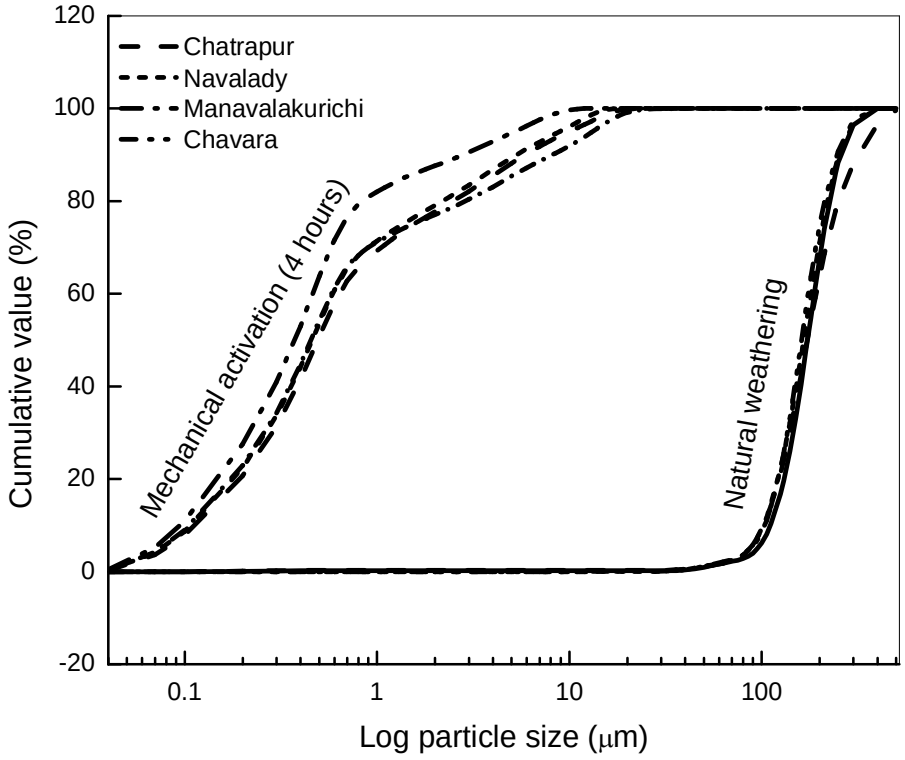

Fig.6.7: Variation of particle size distribution of the natural weathered and mechanical activated ilmenite samples from the various locations.

The particle size distribution shows an exponential variation in both naturally weathered as well as in the mechanically activated ilmenite samples. It is seen that the particle size distribution does not vary much in the naturally altered samples but decreases exponentially with time of mechanical activation.

The results of the surface area and density as a function of the degree of alteration of the natural ilmenite samples are given in Fig.6.8.

.

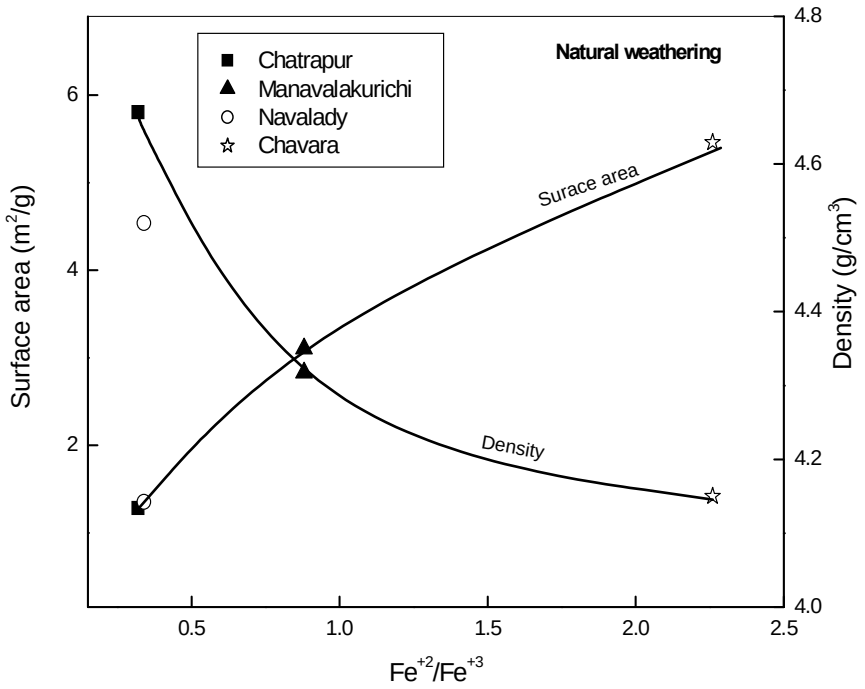

Fig.6.8: Variation of surface area and density of natural weathered ilmenite samples.

Though, the mean particle size of all the four ilmenite samples remain more or less same, an increase in the surface area as well as average pore size and decrease in specific gravity is observed with increase in the degree of alteration characterized by the Fe^{+3}/Fe^{+2} ratio. The increased surface area may be attributed to the development of internal surfaces due to micro-cracks and porosity formed during the alteration / weathering process.

The variation of surface area and density of Navalady and Chavara ilmenite samples with milling time is given in fig.6.9. The variation of surface area of Chatrapur and Manavalakurichi ilmenite with milling time is given in 3.3. It was observed that the surface area of all the four ilmenite samples increase with the milling time. The increase in surface area in the activated samples is much higher than the increase in surface area observed during the alteration of these ilmenite samples. The density of the ilmenite samples shows a decreasing trend with milling time. This decrease in density was caused by volumetric defects introduced into the material by milling. The volumetric density of defects introduced by milling is discussed in chapter 3.

.

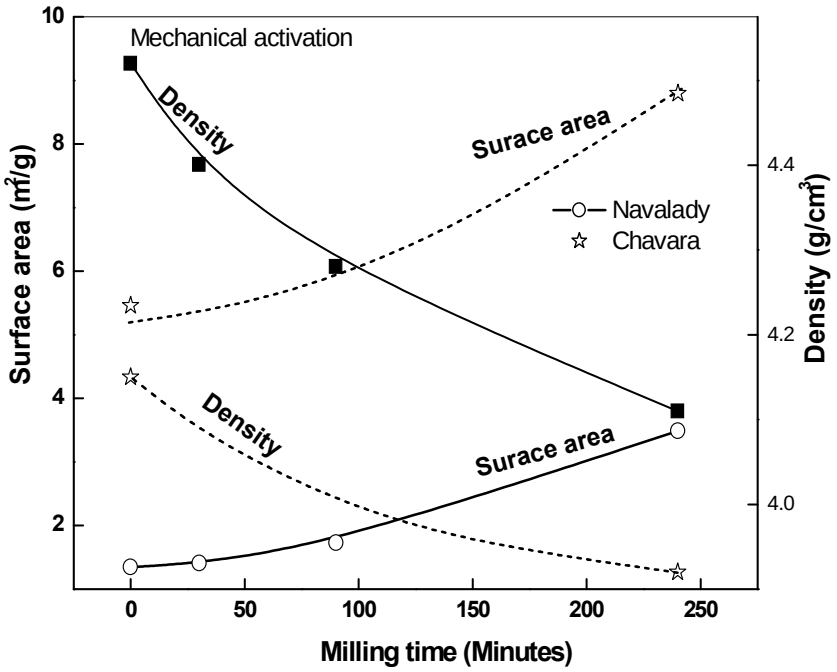

Fig.6.9: Variation of surface area and density of natural weathered and mechanical activated ilmenite samples from the various locations.

6.6 Alteration in dissolution characteristics:

The extent of dissolution of Fe and Ti in 9.2 M sulfuric acid, for the various ilmenite concentrate subjected to different degree of alteration as well as mechanically activated samples at different temperatures (60, 80, 100 and 120^{o}C) with varied leaching times was studied. A typical plots showing the varation of dissolution iron as well as titanium in ilmenite samples subjected to different degree of weathering at 120^{o}C are depicted in Fig. 6.10.

.

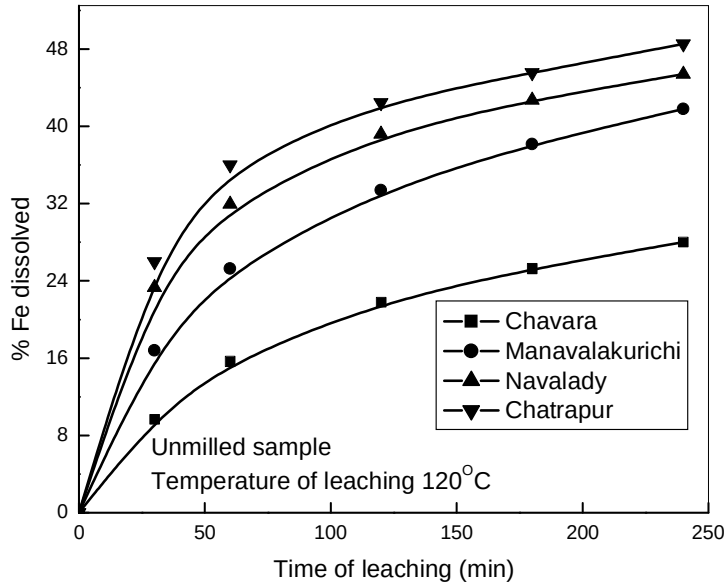

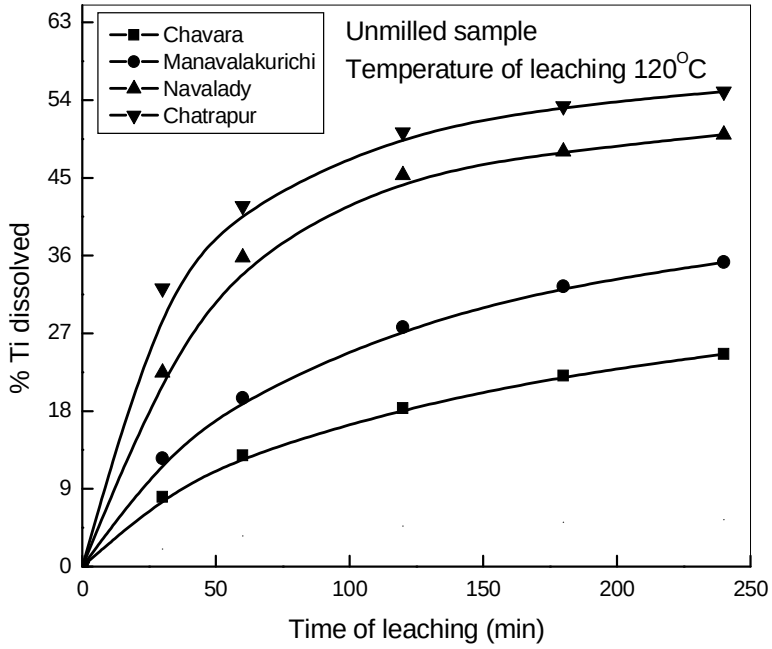

Fig.6.10: Variation of dissolution of Fe and Ti with time of leaching at $120^{O}C$ for the ilmenite samples subjected to different degree of alteration in 9.2 M sulfuric acid.

The vaiation in dissolution charateristics of Fe and Ti in mechanically activated samples of different ilmenite samples at $120^{0}C$ in 9.2M sulfuric acid are given in fig. 6.11.

.

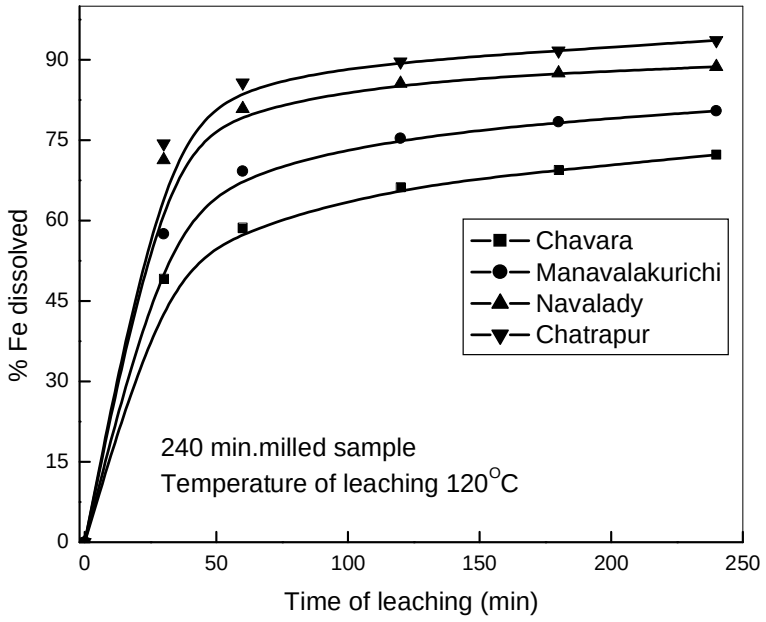

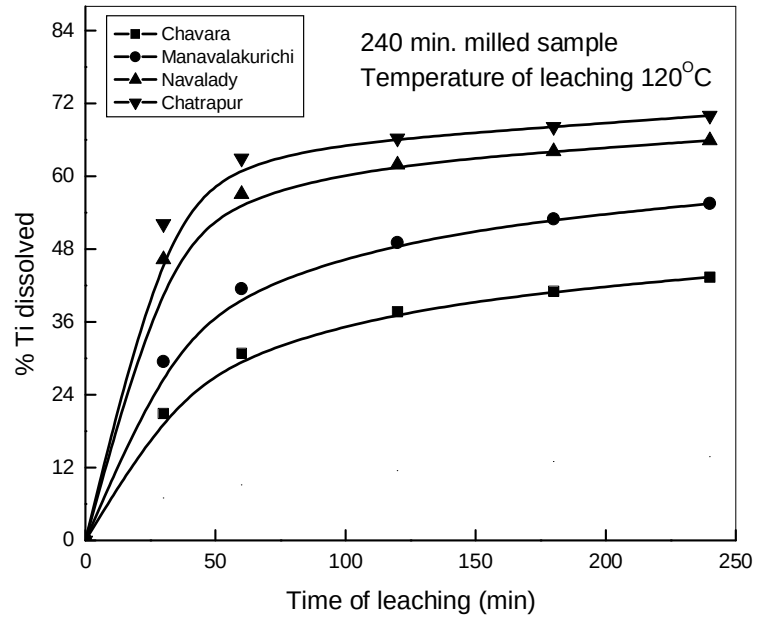

Fig.6.11: Variation of dissolution of Fe and Ti in 9.2 M sulfuric acid with time of leaching at 120^{O}C for the ilmenite samples subjected to 240 minutes of planetary milling.

The leaching behavior of both iron and titanium showed an exponetial increase with leaching time for the naturally weathered ilmenite samples as well as the mechanically activated samples at all the leaching temperatures in

.

the range of 60 to 120°C. The percentage of dissolution decresed with the extent of natural weathering, whereas the perentage of dissolution increased with milling time exponetially. The maximum dissolution of Fe and Ti in the naturally weathered samples is shown in Fig. 6.12 as a function of the Fe^{+3}/Fe^{+2} ratio.

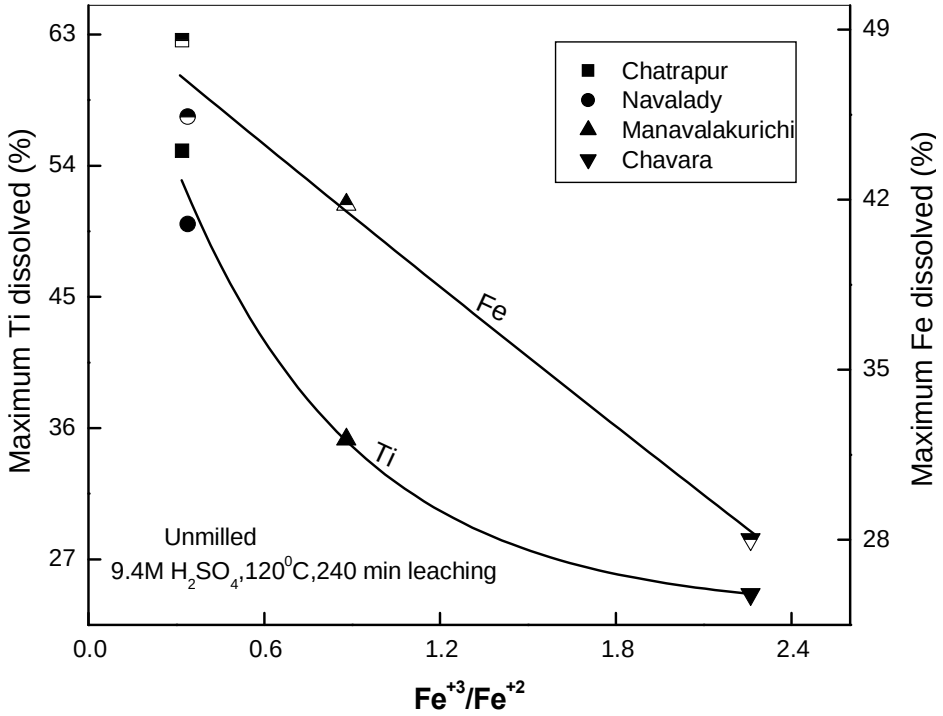

Fig.6.12: Variation of maximum dissolution of Fe and Ti in 9.2 M sulfuric acid with Fe^{+2}/Fe^{+3} ratio at 120°C for the ilmenite samples subjected natural weathering.

Despite an increase in surface area and porosity and decrease in crystallite size with increased alteration, the dissolution of both iron and titanium in the naturally weathered samples decreased with an increase in the Fe^{+3}/Fe^{+2} ratio, the dissolution being highest for the Chatrapur sample and lowest for the Chavara sample. The dissolution kinetics was also considerably enhanced at higher temperatures. About 30% Fe and 25% Ti dissolved in the case of the unmilled Chatrapur sample in four hours of leaching at 120°C compared to 54% of Ti and 63% Fe in the case of the unmilled Chavara sample under the same conditions. The decrease in dissolution with increase in Fe^{+3}/Fe^{+2} ratio can be attributed to the ready solubility of the ferrous iron at la

.

relatively low pH as compared to the ferric constituent and the resistance of the Ti-rich phases leucoxene/rutile to acid leaching (Sinha, 1979).

The dissolution of both Fe and Ti increased significantly with milling time. The maximum dissolution of Fe and Ti in 9.2 M H_2SO_4 is depicted in Figs. 6.13 for all the four ilmenite samples as a function of milling time.

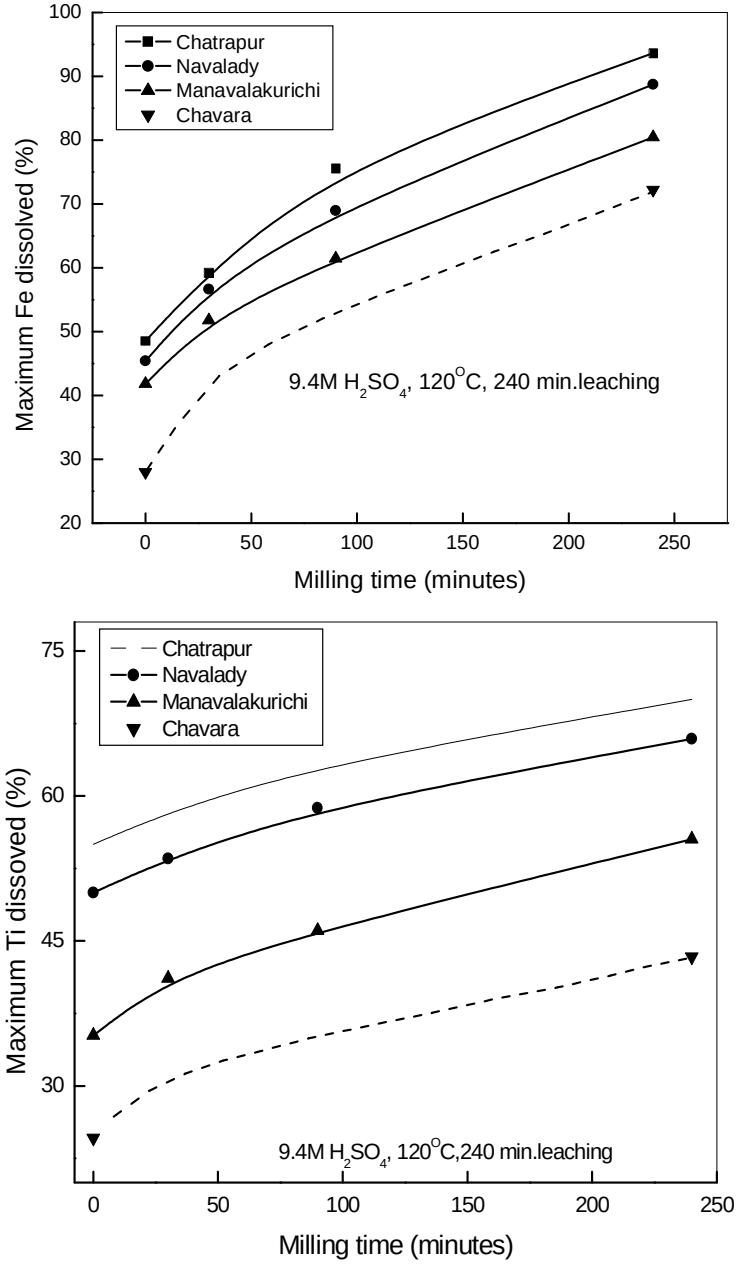

Fig.6.13: Variation of maximum dissolution of Fe and Ti in 9.2 M sulfuric acid with time of leaching at 120^{O}C for the ilmenite samples subjected to 240 minutes of planetary milling.

.

In the case of the Chatrapur ilmenite, about 65% Ti and 93% Fe has been observed to dissolve in 9.2 M H_2SO_4 at 120^oC in 4 hours of leaching. On the other hand the Chavara ilmenite exhibited a dissolution of 35% Ti and 65% Fe. under identical conditions In the unmilled as well as the activated samples, hydrolysis was not observed at any temperature even for prolonged periods of leaching. Despite the oxidation of Fe^{+2} to Fe^{+3}, an enhanced sulfuric acid dissolution of Fe and Ti from ilmenite in the mechanically activated samples is attributed to an increase in surface area as well as the non-uniform strain introduced by the defects.

6.7 Alteration in kinetics of dissolution

The method of derivation of kinetic parameters for dissolution of Fe and Ti were described in chapter 5. The calculated activation energy for dissolution of Fe and Ti in the unmilled altered samples is shown in Fig. 6.14 with respect to increasing ferric to ferrous ratio.

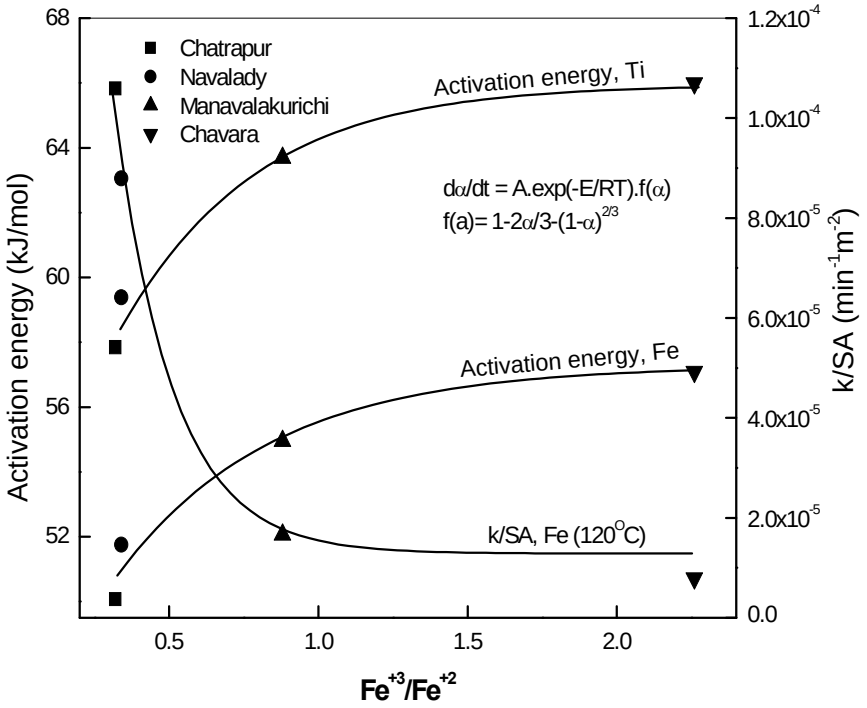

Fig 6.14: Variation of activation energy for dissolution of Fe and Ti in altered ilmenite samples and the surface area normalized rate constant for dissolution of Fe as a function of Fe^{+3}/Fe^{+2} ratio.

.

Despite the increase in surface area, the activation energy increases exponentially with increasing ferric to ferrous ratio i.e. higher degree of alteration is associated with higher activation energy. The unmilled naturally weathered samples show an activation enegy of 57 to 64 kJ/mol for dissolution of Ti and 52 to 61 kJ/mol for dissolution of Fe depending on the extent of alteration. To further clarify this aspect, the surface area normalized rate constant for both Fe and Ti is plotted as a function of the extent of alteration (characterized by the Fe^{+3}/Fe^{+2} ratio) for the four unmilled samples in Fig. 6.14. The surface area normalized rate constant decreases with increase in Fe^{+3}/Fe^{+2} ratio signifying the marginal effect of surface area *vis a vis* oxidation on the acid dissolution kinetics of altered ilmenites. The increase in activation energy with the extent of alteration is directly related to the difficulty in acid leaching of the oxidized phases; pseudorutile ($Fe_2Ti_3O_9$) and leucoxene (TiO_2).

The calculated activation energies for the sulfuric acid dissolution of Fe and Ti for the mechanically activated samples are depicted in Fig. 6.15 as a function of time of activation.

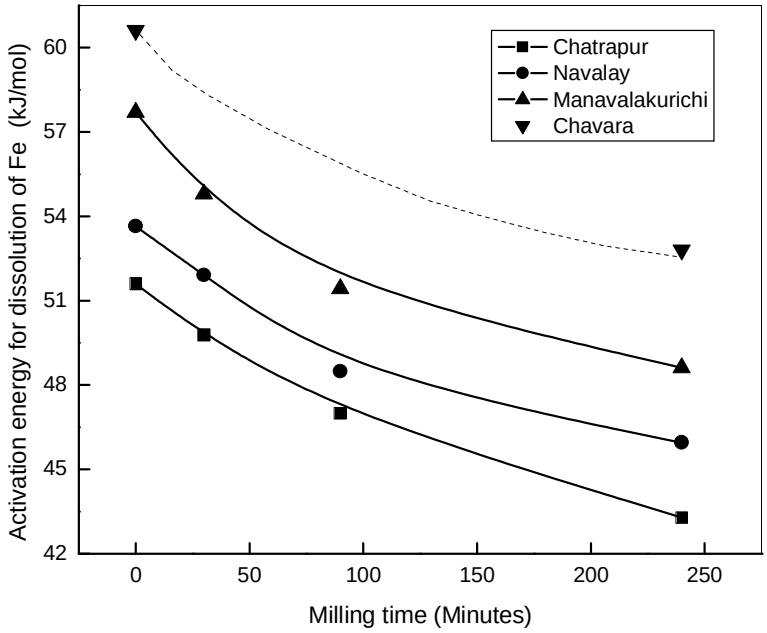

.

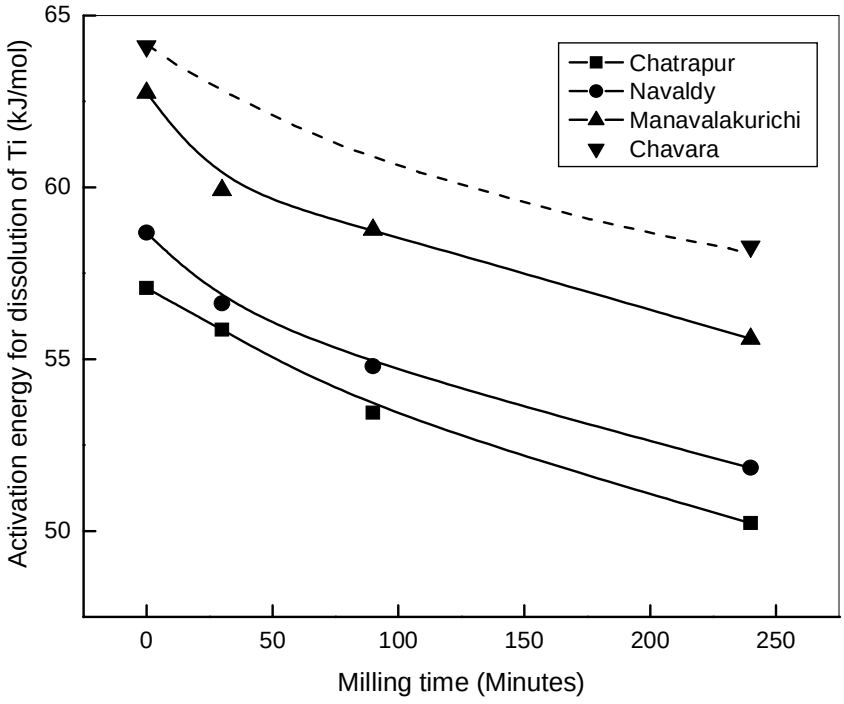

Fig.6.15: Variation of activation energy for dissolution of Fe and Ti with milling time.

In contrast to the altered samples, it is observed that the activation energy decreases monotonically with time of activation for the mechanically activated samples despite an increase in the ferric content and the refractory leucoxene phase. The enhancement in the leaching kinetics because of mechanical activation can arise because of increased surface area or structural disordering or both. A method commonly used to determine whether surface area or structural parameters are predominant for the reactivity is to plot the surface area normalized rate constant against the applied energy during activation which is proportional to time of activation or the degree of amorphization (Senna, 1989; Balaz,2000). If the surface area normalized rate constant does not vary or decreases with the applied energy/time of activation, the reaction rate may be considered to be insensitive to structural changes. An increase in the surface area normalized rate constant with the applied energy, can be considered to be a result of structural imperfections introduced during the process of mechanical activation. Fig. 6.16 shows a plot of the surface area

.

normalized rate constant with time of activation for all the four ilmenite samples subject to different degree of alteration.

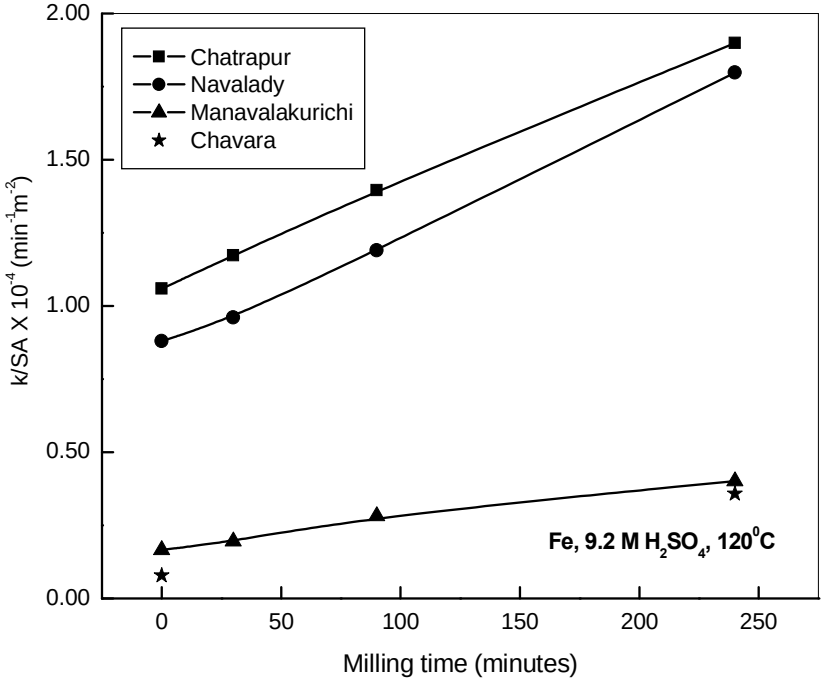

Fig.6.16: Variation of activation energy for dissolution of Fe and Ti with milling time.

It is observed that the normalized rate constant monotonically increases with time of activation clearly demonstrating the effect of structural disorder.

Conclusions

1. In terms of the physico-chemical characteristics, mechanical activation found to have a similar effect as natural weathering on ilmenite.
2. The ferric to ferrous ratio increased with both extent of alteration and time of mechanical activation, alteration resulted in the formation of new Fe^{+3} and Ti-rich phases whereas mechanical activation was found to result only in partial amorphization of some of the existing phases.
3. Both, alteration and mechanical activation resulted in a higher surface area and pore size and a decrease in specific gravity and crystallite size.

.

However, mechanical activation also resulted in non-uniform strain in the crystallite introduced due to the large concentration of defects.

4. The acid dissolution behavior was completely different between naturally altered ilmenite samples and mechanically activated samples. Despite an increase in surface area and porosity and decrease in crystallite size with increased alteration, the sulfuric acid dissolution of both iron and titania in the naturally weathered samples decreased with an increase in the Fe^{+3}/Fe^{+2} ratio, the dissolution being highest for the Chatrapur ilmenite which is least altered and lowest for the Chavara sample which has the highest alteration.
5. The activation energy for dissolution of Fe and Ti increased with the extent of alteration.
6. The decrease in the rates of dissolution in naturally weathered samples despite an increase in surface area (exemplified by the behavior surface area normalized rate constant) was found to be directly related to the difficulty in acid leaching of the oxidized phases pseudorutile and leucoxene.
7. For the mechanically activated samples, the dissolution rates of both Fe and Ti increased (activation energies decreased) significantly with time of activation despite the partial oxidation of Fe^{+2} to Fe^{+3}. The enhanced dissolution of the mechanically activated ilmenite samples despite the partial oxidation was attributed to the large concentration of defects introduced during the activation process.

.

CHAPTER 7

CONCLUSIONS AND SUGGESTIONS FOR FUTURE WORK

7.1 Conclusions

7.1.1 Effect of mechanical activation on physico-chemical, structural, thermal and magnetic properties

Mechanical activation was found to have a pronounced effect on the physical, chemical, structural, thermal and magnetic properties of ilmenite. The morphology of the particles changed from sub-rounded to subangular particles in the raw samples to angular particles upon milling. The particle size decreased exponentially from an initial size range of 100-500 μm with time of activation and remained constant in the range of 0.04 to 15 εm beyond 90 min of activation. The BET absorption surface area also showed an exponential variation with milling time and a maximum surface area of 11.6 m^2/g was achieved for Manavalakurichi ilmenite sample in 4 hours of milling. The apparent density of all the ilmenite samples decreased with milling time, partly due to the increase in lattice volume arising from creation of defects. Significant amount of structural disorder was also observed on mechanical activation. A partial amorphization or a much fined grained phases of the hematite and pseudorutile was observed for the Chatrapur Ilmenite sample after 30 minutes and 4 hours of planetary milling respectively. The ilmenite phase also showed substantial disordering (referred as xrd amorphization in literatures) and the degree of xrd amorphization exhibited an exponential variation with time of milling. The crystallite size of ilmenite samples decreased exponentially with milling time, whereas the non-uniform lattice strain showed a linear increase. The crystallite sizes and the lattice strain varied in the range of 57-131 nm and 0.14ï 0.47% for Chatrapur ilmenite sample and 38-90 nm and 0.17-0.23% for Manavalakrichi ilmenite sample in 4 hours of mechanical activation. The oxidation kinetics was also found to be

.

considerably enhanced by mechanical activation, the rate of oxidation increasing with increasing time of activation. Whereas complete oxidation (~3.5%) of Fe^{+2} to Fe^{+3} was achieved in ambient air at $850^{O}C$ for the activated samples, less than 50% oxidation occurred in the unmilled sample. The magnetic properties of Manavalakurichi ilmenite showed small variations upon mechanical activation. The magnetization of ilmenite at maximum field strength (1200 kA/m) decreased with milling time; however the coercivity of ilmenite samples increased with milling time as the variation in crystallite size and structural disorder was enhanced by mechanical activation process.

7.1.2 The effect of mechanical activation on energetics of ilmenite

The energetics of the mechanical activation process of ilmenite by high energy milling in a planetary mill was analyzed with respect to the energy stored within the material vis-à-vis the specific energy consumption and the manifestation of the stored energy in different forms such as new surfaces and interfaces, point, line and volume defects, high energy structures, uniform and non-uniform strain. The specific power consumption in the planetary mill was found to depend on the degree of alteration of ilmenite. For Chatrapur ilmenite, which was least altered, the specific power consumption was 5865 kJ/mol (10,740 wh/kg). The corresponding energy consumption in 4 hours of milling (milling of 80 g of ilmenite with 30 agate balls of net weight 320 g at a mill speed of 200 rpm)of Chavara ilmenite, which was most altered was 6193 kJ/mol (11,340 wh/kg). It was observed that the energy transferred to the material varied in the range of 3 to 8.0 % in 4 hours of milling in a planetary mill depending on the degree of alteration of the ilmenite. The specific energy transferred derived from milling with material and a blank run under identical conditions was found to be 162 kJ/mol in 4 hours of milling for Chatrapur ilmenite and 360 kJ/mol for Manavalakurichi ilmenite. It was deduced that more than half of this measured difference in energy was actually expended in the breakage of the bonds in the material, which was released mainly as heat and only the remaining energy was truly stored within the material. This energy was found to be stored in additional surfaces and interfaces, point, line and

.

volume defects, high energy structures and non-uniform strain. A large part of the stored energy was reflected as strain energy (24 and 127 kJ/mol respectively for the Chatrapur and Manavalakurichi ilmenite samples) and structural disorder (34 and 25 kJ/mol respectively for the Chatrapur and Manavalakurichi ilmenite samples respectively). Part of the defect energy stored in the activated ilmenite samples was found to relax much faster. This component determined from calorimetric studies was found to be 19 kJ/mol for Chatrapur ilmenite and 12 kJ/mol for Manavalakurichi ilmenite sample subjected to 4 hours of mechanical activation. The energy stored through additional surfaces and grain boundaries was found to be much lesser. The surface energy increased from 19 mJ/m^2 (2 J/mol) to 37 mJ/m^2 (15 J/mol) in the Chatrapur ilmenite and from 25 mJ/m^2 (11 J/mol) to 48 mJ/m^2 (40 J/mol) for the Manavalakurichi ilmenite in 4 hours of planetary milling. The grain boundary energy varied in the range of 8-15 mJ/m^2 (5-25 J/mol) in Chatrapur ilmenite and 10-19 mJ/m^2 (9-33 J/mol) in Manavalakurichi ilmenite sample.

7.1.3 The effect of mechanical activation on dissolution characteristics of ilmenite

Mechanical activation had a large effect on the dissolution kinetics of ilmenite. Although mechanical activation considerably enhanced the dissolution kinetics for both Fe and Ti, it was observed that the Ti and Fe in the ilmenite dissolves incongruently and not according to their stoichiometry in the ilmenite phase. The maximum dissolution of Fe and Ti in the Chatrapur ilmenite was restricted to 20-65% in the unmilled condition whereas, in excess of 90% Fe and % Ti could be dissolved (120^oC, 4 h leaching) from ilmenite samples subjected to 240 minutes of milling. For Manavalakurichi ilmenite, the maximum dissolution Fe and Ti in unmilled condition was restricted to 20-30% and 25-50% respectively, whereas, in excess of 80-90% Fe and 50-65% Ti could be dissolved (120^oC, 4 h leaching) for ilmenite samples milled for 240 minutes. The dissolution kinetics of ilmenite in hydrochloric acid was marginally favorable compared to that in sulfuric acid. However, the enhanced dissolution of Ti in HCl for the activated sample is affected by the hydrolysis

.

and precipitation reactions that set in at higher temperatures and lower acid concentrations for prolonged periods of leaching. The dissolution kinetics HCl (prior to significant hydrolysis) and in H_2SO_4 is found to conform to the reaction rate control model for the initial leaching period and thereafter to the shrinking core model where product layer diffusion is rate controlling. The activation energy for dissolution of Fe and Ti (in Manavalakurichi ilmenite) was higher in H_2SO_4 (68 and 70 kJ/mol respectively) compared to HCl (64 and 68 kJ/mol respectively). The activation energies for dissolution of Fe and Ti also showed a monotonic increase with time of milling.

7.1.4 A comparative study of natural weathering and mechanical activation of ilmenite

In terms of the physico-chemical characteristics, mechanical activation found to have a similar effect as natural weathering on ilmenite. The ferric to ferrous ratio increased with both extent of alteration and time of mechanical activation, alteration resulted in the formation of new Fe^{+3} and Ti-rich phases whereas mechanical activation was found to result only in partial amorphization of some of the existing phases. Both, alteration and mechanical activation resulted in a higher surface area and pore size and a decrease in specific gravity and crystallite size. However, mechanical activation also resulted in non-uniform strain in the crystallite introduced due to the large concentration of defects. The acid dissolution behavior was completely different between naturally altered ilmenite samples and mechanically activated samples. Despite an increase in surface area and porosity and decrease in crystallite size with increased alteration, the sulfuric acid dissolution of both iron and titania in the naturally weathered samples decreased with an increase in the Fe^{+3}/Fe^{+2} ratio, the dissolution being highest for the Chatrapur ilmenite which is least altered and lowest for the Chavara sample which has the highest alteration. The activation energy for dissolution of Fe and Ti increased with the extent of alteration. The decrease in the rates of dissolution in naturally weathered samples despite an increase in surface area (exemplified by the behavior surface area normalized rate constant) was found to be directly related

.

to the difficulty in acid leaching of the oxidized phases pseudorutile and leucoxene. For the mechanically activated samples, the dissolution rates of both Fe and Ti increased (activation energies decreased) significantly with time of activation despite the partial oxidation of Fe^{+2} to Fe^{+3}. The enhanced dissolution of the mechanically activated ilmenite samples despite the partial oxidation was attributed to the large concentration of defects introduced during the activation process.

7.2 Suggestions for future work

The following future work on mechanical activation has to be carried out in order to resolve the outstanding issues in this area:

1. Effective dissolution kinetics of ilmenite was observed in mechanically activated samples in a laboratory scale. However the dissolution studies have to be carried out in a pilot scale and industrial scale to find out the commercial feasibility of the present work.
2. The presence of minor phase constituents with ilmenite grains and their transformation during milling has to be studied with high resolution electron microscopy. The effect of these minor phase constituents on dissolution characteristics of ilmenite has to be evolved out to develop a better processing method.
3. The studies on mechano-chemical leaching of ilmenite (i.e. wet milling with acids) are to be carried out to investigate the extent of leaching at room temperature milling.
4. The roasting of ilmenite samples should be carried out to enhance the magnetic properties and dissolution characteristics of ilmenite samples. The effect of low temperature roasting on mechanically activated ilmenite samples has to be studied to appreciate the enhancement in magnetic separation and dissolution kinetics of ilmenite samples. .
5. A part of the energy stored in the material gets relaxed with time. The relaxation process of mechanically activated ilmenite samples has to be

.

studied with time to find out the efficient period of energy storage in the activated material.

6. Only part of the stored energy was been used to enhance the dissolution kinetics of Fe and Ti in ilmenite samples. The investigation has to be carried out to find out the actual fraction of stored energy used in reduction of activation energy of dissolution process to develop efficient processing method.
7. An attempt had been made to study the energy transferred to the material and stored as various forms in the material subjected to mechanical activation. The investigations on energetics has to be carried out in detail and a theoretical model has to be developed to find out the actual energy required for disordering of a crystal lattice, crystalline phase transformations, amorphization and for various chemical reactions.

.

REFERENCES

- Abdel-Aal, E.A., Ibrahim, I.A., Afifi, A.A.I., Ismail, A.K., 2000. Production of synthetic rutile from Egyptian ilmenite ore by a direct hydrometallurgical process. In: Mishra, B., Yamanuchi, C. (Eds.),2nd International Conference on Processing Materials for Properties. The Minerals, Metals & Materials Society, pp. 955ï 960.
- Acharya, B.C., Das, S.K., Muralidhar, J., 1999. Mineralogy, mineral chemistry and magnetic behaviour of ilmenite from Chatrapur coast, Orissa. Indian J. Earth Sci., 26, 45ï 51.
- Afifi, A.A.I., 1994. A contribution to the hydrometallurgy of Egyptian ilmenite ore for titanium dioxide production. M. Sc. Thesis, Chemistry Department, Faculty of Science, Ain Sharma University,Cairo, Egypt.
- Allen, T., 1981. Particle Size Measurement, Vol 1. 5th Ed., Chapman & Hall, London,
- Amer, A.M., 2000. Investigation of the direct hydrometallurgical processing of mechanically activated low-grade wolframite concentrate. Hydrometallurgy 58, 251- 259.
- Amer, A.M., 2002. Alkaline pressure leaching of mechanically activated Rosetta ilmenite concentrate. Hydrometallurgy, 67, 125-133.
- Anand, R.R. and Gilkes, R.J., 1984. Weathering of ilmenite in lateritic pallid zone. Clays and Clay Minerals, 32, 5, 363-374.
- Anderson, C. G., Harrison, K. D., Krys, L. E., Nordwick, S. M., 1993. The Application of Sodium Nitrite Oxidation and Fine Grinding in Refractory Precious Metal Concentrate Pressure Leaching. SME Transactions, 300, 19-25.
- Anderson, H.L., Kemmler, A., Hohne, G.W.H., Heldt, K., Strey, R.,1999. Round robin test on the kinetic evaluation of a complex solid state reaction from 13 European laboratories. Part 1.Kinetic TG-analysis. Thermochim. Acta 332, 33ï 53.

.

- Angove, J., 1993. The ACTIVOX^{TM} Process for Refractory Gold Ores. Proc.Int.Conf. Randol Gold Forum, Beaver Creek, 1-12.
- Aresta.M., Dibenedetto.A., Pastore.T., 2005. Mechanochemistry : An Old Technology With New Applications to Environmental Issues. Decontamination of Polychlorobiphenyl-Contaminated Soil by High-Energy Milling in the Solid State with Ternary Hydrides. Environmental Chemistry, Springer Berlin Heidelberg, part IV, 553-559.
- Asadov, M.M.,1975. Izv. Ak.Nauk SSSR, Neorg. Mater., 11, 324.
- Avvamkumov, E.G., 1986. Mechanical Methods of Chemical Process Activation , Nauka, Novosibirsk.
- Bade, S., Hoffmann, H., 1996. Developement of new reactor for combined communition and chemical reaction. Chem.Eng.Commun. 143, 169-193.
- Balaz, P., 1981. Intensification of oxidative leaching of chalcopyrite. PhD thesis, Mining Institute of Slovak Academy of Sciences, Kosice.
- Balaz, P., 1985. Folia Montana, 10, 49.
- Balaz, P., Briancin, V., Sepelak, V., Havlik, T., Skrobian, M., 1992. Non-oxidative leaching of mechanically activated stibnite. Hydrometallurgy 31, 201ï 212.
- Balaz, P., Briancin, J.,1993. Reactivity of mechanically activated pyrite. Solid State Ionics, 63-65, 296-300.
- Balaz, P., Balassaova, M.,1994. Thermal decomposition of mechanically activated arsenopyrite., J. Thermal Analysis and Calorimetry, 41, 1101-1107.
- Balaz, P., Briancin, and Turcaniova, L., 1995. Thermal decomposition of mechanically activated tetrahedrite. Thermochim. Acta, 249, 375-381.
- Balaz, P., 1996. Influence of solid state properties on ferric chloride leaching of mechanically activated galena. Hydrometallurgy, 40, 359-368.

.

- Balaz,P., Ficeriova,J., Sepelak,V., Kammel, R., 1996. Thiourea leaching of silver from mechanically activated tetrahedrite. Hydrometallurgy, 43, 367-377.
- Balaz, P., 1997. Mechanical Activation in Process of Extractive Metallurgy, Veda Bratislava.
- Balaz, P., 2000. Extractive Metallurgy of Activated Minerals. Elsevier, Amsterdam.
- Balaz, P., 2001. Mechanochemistry in extractive metallurgy: the modern science with an old routes (historical note). Acta Metallurgical Slovaca , 4, 23-28.
- Balaz, P., 2003. Mechanical Activation in Hydrometallurgy. Int.J.Miner.Process. 72,341-354.
- Balaz, P, Godocikova, E., Krillova, L., Lobotka, P., Gock, E., 2004. Preparation of nano-crystalline materials by high energy milling, Material Science Engineering, A386, 442-446.
- Balaz, P, Godocikova, Takacs,L., Gock, E., 2005. Mechanochemical preparation of metal/sulphide nano-composite particles. International Journal of Materials Products Technology, 23, 26-41.
- Balaz, P., 2008. Mechanochemistry in Nano Science and Minerals Engineering. Springer, Berlin.
- Balderson, G.F. and MacDonald, C.A., 1999. US Patent 5,885,324, March 23.
- Barry, A., Wechsler, Prewitt T.C., 1984. Crystal Structure of ilmenite ($FeTiO_3$) at high temperature and at high pressure. American Mineralogist, 69, 176-185.
- Barton, A.F.M., McConnel, S.R., 1979. Rotating disc dissolution rates of ionic solids: Part 3. Natural and synthetic ilmenite. J. Chem. Soc., Faraday Trans. I 75, 971ï 983.
- Becher, R.G., 1963. Improved process for the beneficiation of ores containing contaminating iron. Australian Patent 247, 110.

.

- Bernhardt, C., Heegn, H.P., 1976. Contribution to the investigation of mechanical activation in fine grinding mills. In : Rumpf, H., Schonert, K., (Eds), Proc.4th European Symp.on communition. Nunberg, 1975, 213-225.
- Berg, L.G., Burmistrova, N.P., Lisov, N.I., 1975. Investigation of reactions in solids by DTA. J. Thermal Analysis and Calorimetry, 7, 111-117.
- Berg, L.G., Sljapina, E.N., 1975. J. Them. Anal., 8, 417.
- Bin Liang, Chun Li, Zhang, Chenggang, Zhang, Yongui, 2005. Leaching kinetics of Panzhihua ilmenite in sulfuric acid. Hydrometallurgy 76, 173ï 179.
- Bogatyreva, E.V., and Ermilov, A.G., 2008. Energy Stored in Raw Materials during Mechanical Activation. Neorganicheskie Materialy, 44, 242-247.
- Boldyrev, V.V., Sakovich, G.V., Yakovlev, L.K., 1953. Zh.Vsesoyuz. Khim. O-va im. D I Mendeleeva 3, 31.
- Boldyrev, V.V., Avvakumov,E.G., 1971. Mechanochemistry of Inorganic Solids. Russ. Chem. Rev. 40, 847-859.
- Boldyrev,V.V., 1972. Kietic Factors of Mechanochemical Processes in Inorganic Systems. Kinet. Katal., 13,1411-1421.
- Boldyrev, V.V., Kolosov, A.S., Chaikina, M.V., Avvakumov, E.G., 1977. Dokl, Akad. Nauk SSSR 233, 892.
- Boldyrev, V.V., Boulens, M., and Delomon, B., 1979. The Control of Reactivity of Solids., Elsvier, Amsterdam.
- Boldyrev, V.V., 1983. Experimental Methods in Mechanochemistry of Solid State Materials. Nauka, Novosibirsk.
- Boldyrev, V.V., Pavlov, S.V., and Goldberg, E.L., 1996, Interrelation between fine grinding and mechanical activation, Int.J.Min.Process. 44-45, 181-185.
- Boldyrev,V.V., Tk´agcov´a, K., 2000. Mechanochemistry of Solids: Past, Present, and Prospects, J.Mat.Syn. and Process., 8, 121-132.

.

- Boldyrev, V.V., 2004. Mechanochemical Modification and Synthesis of Drugs. J.Mater.Sci., 39, 5117-5120.
- Boldyrev, V.V., 2006. Mechanochemistry and Mechanical activation of Solids, Russian Chemical Reviews, 75, 3, 177-189.
- Boldyreva, E.V., 2003. High pressure studies of the anisotropy of the structural distortion of molecular crystals, J.Mol. Struct., 647, 159-179.
- Bretenev,G.M., Razumovskaya,I.V., 1969. Fiz. Khim. Mekh. Mater., 5,60.
- Brunauer, S., Emmett, P.H., and Teller, E., 1938. Adsorption of gases in mutimolecular layers. J.Am.Chem.Soc., 1938, 60 , 309-19
- Butyagin,P.Yu., 1971. Butyagin, Kinetics and nature of mechanochemical reactions. Russ. Chem. Rev. 40, 11 , 901ï 915.
- Butjagin, P.J., 1984. Uspechi chimiji, 53, 1769-1788.
- Buyanov, R.A., 1987. Mechanism of deactivation of hetrogenious catalysts. Kinet. Katal., 28, 157-164.
- Carey Lea,M., 1892. Phil.Mag., 34 ,46.
- Carey Ley, 1894. Phil.Mag., 37, 31.
- Carey Lea, 1894. Phil.Mag.37, 470.
- Casey, W.H., 1995. Surface chemistry during the dissolution of oxide and silicate minerals. In: Vaughan, D.J., Patrick, R.A.D. (Eds.), Mineral Surfaces. Chapman & Hall, London, 185ï 217.
- Chaikina, M.V., 2002. Mekhanokhimiya Prirodnykh Sinteticheskikh Apatitov (Mechanoichemistry of Natural Synthetic Apatites). Novosibirsk: Nauka.
- Chakk, Y., Berger, S., Weiss, Brook, E., 1994. Solid State Amorphization by Mechanical Alloying- an atomistic Model. Acta Metall.Mat., 42, 3679-3685.
- Chaudhuri, J.N.B., Newesely, H., 1990. Transformation of ilmenite FeTiO3 to leucoxene TiO2 under the influence of weathering reactions. Indian Journal of Technology 28, 13ï 23.

.

- Chen, Y., 1997. Low-temperature oxidation of ilmenite (FeTiO3) induced by high energy ball milling at room temperature. J.Alloys Compd. 257, 156ï 160.
- Chen, Y., 1998. Different oxidation reactions of ilmenite induced by high energy ball milling. J. Alloys Compd. 266, 150ï 154.
- Chernet, T., 1999. Mineralogical and textural constraints on mineral processing of the Koivusaarenneva ilmenite ore, Kalvia, Western Finland. Int. J. Miner. Process. 57, 153ï 165.
- Chun Li, Bin Liang, Sheng-Pin Chen, 2006. Combined milling-dissolution of punzihua ilmenite in sulphuric acid. Hydrometallurgy, 82, 93-99.
- Clark,J., Rovan,R.J.,1941. J. Amer. Chem. Soc. 63**,** 1302.
- Cottrell,A.H.,1964. The Mechanical Properties of Matter. Wiley, New York, pp. 78ï 98.
- Cservenyak, T., Kelsall, G.H., Wang, W., 1996. Reduction of TiIV species in aqueous sulfuric and hydrochloric acids: I. Titanium speciation. Electrochimica Acta 41 (4), 563ï 572.
- Cullity, B.D., and Stock, S.R.,2001. Elements of X-Ray diffraction, Prentice Hall, New Jersey.
- Dachille, F., Roy, R., 1961. Reactivity of Solids, Proceedings of 4th International Symposium on the Reactivity of Solids, Elsevier, Amsterdam. p.502.
- Ding, J., Street, R., Nishio, H., 1996. Magnetic properties of Ba- and Sr-hexaferrite prepared by mechanical alloying. J.Magnetism and Magnetic Materials. 164, 385- 389.
- Dubinskya A.M., Sov.Sci. Rev, 1989. B.Chem. Pt., 3, 14, 37.
- Duncan, J.F. and Metson, J.B., 1982a. Acid attack on New Zealand ilmenite 1. The mechanism of dissolution, New Zealand Journal of Science, 25, 103-109.

.

- Duncan, J.F. and Metson, J.B., 1982b. Acid attack on New Zealand ilmenite 2. The structure and composition of the solid. New Zealand Journal of Science, 25, 111-116.
- Dwivedy, K.K., 1999. Indian ilmenite resourcesð an economic appraisal. Journal of Mines, Metals and Fuels 77ï 79 March.
- Eckert, 1992. J. Mater Sci Forum 1992, 88-90, 679-86
- Ehrhardt, H., Campbell, S.J., Hofmann, M., 2003. Magnetism of nanostructured spinel zinc ferrite. The American Minerologist, 88, 967-977.
- El-Eskandarany, M.S., Aoki, K., Suzuki, K., 1990. J Less-Common Metals, 167, 113-121.
- El-Eskandarany M.S., Aoki K, Suzuki K.,1992. Morphological and Calorimetric Studies on the Amorphization Process of Rod Milled $Al_{50}Zr_{50}$ Alloy Powders. Metall Trans., 23A, 2131-2140.
- Ermilov , A.G., Safonov, V.V., Doroshko, L.F., et al.,2002. lzv. Vyssh. Uchebn. Zaved., Tsvetn. Metall., 3, 48-53.
- Farrow, J.B., Ritchie, I.M., 1987. Reaction between reduced ilmenite and oxygen in ammonium chloride solutions. Hydrometallurgy, 18, 21-38.
- Fernandez-Bertan, J., 1999. Mechanochemistry: an overview. Pure Applied chemistry 71, 4, 581-586.
- Flavicjij,F.M., 1902. Z.rus. fiz.-chim.obsc., 34, 8.
- Flavickij, F.M, 1909. Special Methods and Reactions of Solid State Chemistry, Trudy Mendelej.siezda, SPB.
- Frost, M. T., Grey, I. E., Horrowfield, I. R. and Mason, K., 1983. The dependence of alumina and silica contents on the extend of alteration of weathered ilmenites from Western Australia. Mineral Mag., 47,201-208.
- Fokina, F.L., Budim, N.I., Kochnev, V.G., Chernik, G.G., 2004. Planetary Mills of Periodic and Continuous Action. J.Mat.Sci., 39, 5217-5222.

.

- Gibb, T.C., Greenwood, N.N. and Twist, W., 1969. The mossbauer spectra of natural ilmenites. J. Inorg. Nucl. Chem., 31, 947-954.
- Gock, E., 1977. The Influence of Vibratory Grinding on Leachability of Sulhidic Minerals by Solid State Reactions, Habilitationsschrift, Technical University Berlin.
- Gock, E., 1978. The impact on chalcopyrite dissolution by solid state reactions using vibrating milling. Erzmetall, 31 , 282-287.
- Gock, E., Kurrer, K.E., 1996. Eccentric vibratory mill-a new energy-efficient way for pulverization. Erzmetall 49, 434-442.
- Gock, E., Kurrer, K.E., 1998. Increased efficiency of vibratory milling process with eccentric vibratory mill. Aufbereitung-Technik,39, 103-111.
- Gock, E., Kurrer, K.E., 1999. Eccentric vibratory mill theory and practice. Powder Technology, 105, 302-310.
- Golosov,S.J., 1971. Introduction of ultra fine milling in planetary mills. Nauka, Novosibirsk.
- Gregoreva, T.F., Vorsina, I.A., Barinova, A.P., Lyakhov, N.Z., 2003. Khim.Inter.Ustoich.Razv. 11, 520.
- Grey, I.E., Reid, A.F., 1975. The structure of the pseudorutile and its role in the alteration of ilmenite. Am. Mineral. 60, 898ï 906.
- Gregoreva, T.F., Vorsina, I.A., Barinova, A.P., and Lyakhov, N.Z., 2003. Khim.Inter.Ustoich.Razv. 11, 520.
- Grigorêva, T.F., Boldyrev, V.V., 1995. Dokl. Akad. Nauk, 340, 195.
- Griffith, A.A., 1920. The phenomena of rupture in and flow in solids. Philosophical Transactions of the Royal Society (London), A221, 163-198.
- Han, K.N., Rubcumintara, T., Fuerstenau, M.C., 1987. Leaching behaviour of ilmenite with sulfuric acid. Metall. Trans. 18B,326ï 330.

.

- Heegn, H.P, Bernhardt, C., Gottschalk, J., Hussemann, K., 1974. Activation effect on communtion of quartz and calcite in various laboratory mills. Chemische Technik (Leipzig), 26, 696-701.
- Heegn, H., 1979. Effect of fine grinding on structure and energy content of solids, in: Proc.of 6th POWRECH, Birmingham, pp. 61-69.
- Heegn,H, 1986. Sc. D. Thesis, Research Institute of Mineral Processing of the Academy of Sciences of the GDR, Freiberg.
- Heegn, H., 1987. Model describing the resistance against structural changes and the hardness of crystalline solids. Crystal Research Technology 22, 9, 1193-1203.
- Heegn, H.P., 1989. On the connection between ultrafine grinding and mechanical activation of minerals. Chemie Ingenieur Technik, 62, 458-464.
- Heinicke, G., 1984. Tribochemistry, Akademie-Verlag, Berlin.
- John, H., 1774. Theophrastusôs History of English stones, London.(English translated from Greek).
- Hisashi, T., 1982. Bull. Chem. Soc. Jpn., 55, 1934-1938.
- http:/www.ttd.spb.ru
- http:/www.altairnano.com/documents/AltairHydro2003.pdf.
- http:/www.sturventevantinc.com
- Hussein, M.K., Kolta, G.A., El-Tawil, S.Z., 1976. Removal of iron from Egyptian ilmenite. Egyptian J. of Chem., 19, 143-152.
- Huseman, K., Wolf, R., Hermann, R., Hoffmann, B., 1976. Erhohung der Effektivitat trokener Feinstmahlprozess durch grenzflachenaktive Zusatse. Aufbereitungstechnik 35, 393-403.
- Huttenrauch, R., Fricke, S., 1985. P.Zielhe Pharm. Res. 6, 235.
- Huttig, G.F., 1943. Zwischenzustande bei Reaktionen im Festen Zustend und ihere Bedeutungfur die Katalyse, Handbuch der Katalyse IV, Spring Verlag , Wien , 318-331.

.

- Imahashi, M. and Takamatsu,N., 1976. The dissolution of titanium minerals in hydrochloric and sulphuric acid. Bull. Chem. Soc. Japan, 49, 1549-1553.
- Imamura, K., Senna, M., 1982. J.Chem.Soc., Faraday, Trans, 78, 1131.
- Isakov, P.M., 1950. Qualitative Analysis of Minerals and Ores, Gosgeolizdat, Moscow.
- Jackson, J.S., Wadsworth, M.E., 1976. A kinetic study of dissolution of Allard Lake ilmenite in hydrochloric acid. Light Metals, 1, 481.
- Jangg, G., Kuttner, F., Korb, G., 1975. Aluminium, 51, 641-646.
- Jayasekera, S., Marinovich, Y., Avraamides, J. and Bailey, S.I., 1995. Pressure leaching of reduced ilmenite: electrochemical acpects. Hydrometallurgy, 39, 183-199.
- Judd, B., Palmer, E.R., 1973. Production of titanium dioxide from ilmenite of the west coast, south island, New Zealand., Proc. Aust. Inst. Min. Metall., No. 247, 23-33.
- Juhaz , A.Z., 1974. Aufbereitungs-Technik, 10, 558.
- Juhász and Opoczky, 1990. A.Z. Juhász and L. Opoczky, Mechanical Activation of Minerals by Grinding: Pulverising and Morphology of Particles. , Academic, Budapest.
- Kalinkin, A. M., Kalinkina, E.V. Makarow, V.N., 2003. Mechanical activation of natutal titanite and its influence on mineral decomposition. Int. J. Miner. Process., 69, 143-155.
- Karasev, V. A., Krotova, N. A., Deryagin, B.V., 1953. Dokl. Akad.Nauk SSSR 88, 777.
- Kaye, B.H., 1981. Direct Characterization of Fine particles, John Wiley and Sons, New York.
- Kelsall, G.H., Robbins, D.J., 1990. Thermodynamics of Ti-H_2O-F(-Fe) systems at 298 K. Journal of Electroanalytical Chemistry, 283, 135-157.

.

- Keller, W.D., 1955. Oxidation of montmorillonite during laboratory grinding. *Am. Miner.* 40, 348.
- Kellogg, H.H., 1967. In: G.R. Fitterer (Ed.), Application of Fundamental Thermodynamics to Metallurgical Processes, Gordon and Breach, 357.
- Koach, C.C., 1993. The synthesis and structure of nanocrystalline materials produced by mechanical attrition: a review, Nanostructured Materials, 2, 109-129.
- Koach, C.C., 1995. Mater. Trans. JIM 36, 2, 85.
- Khodakov, G.S., Rebinder, P.A., 1966. Dokl. Akad. Nauk SSSR 83**,** 1316.
- Kochnev, V.G., 1992. Planetray Mill. Russian Patent 1358990.
- Kochnev, V.G., Simakin, S.A., 1994. Planetray mill feeder. Russian Patent 2094120.
- Kubo,T., 1968. J. Chem. Soc. Jpn. Ind. Sec. 71, 1301.
- Kulebakin, V.G., 1983. Sulphides Transformations by Activation, Nauka, Novosibirsk.
- Kulebakin,V.G., 1988. Primenenie Mekhanokhimii v Gidrometalluricheskikh Protsessakh (The Use of Mechanochemistry in Hydrometallurgical Process), Novosibirsk: Nauka.
- Lanyon, M.R., Win, T.L., Merritt, R.R., 1999. The dissolution of iron in hydrochloric leach of an ilmenite concentrate. Hydrometallurgy, 21, 9-21.
- Lapides, I., Yariv, S., Lahav, N., Broadshy, 1998. Colloid. Polym. Sci. 276, 601.
- Liddell, K.S.,Dunne, R.C., 1988. The Recovery of Gold from Refractory Telluride Concentrates by the Metprotech Fine Milling Process, Proc.Int.Conf. Innovations in Gold and Silver Recovery, ed. Randol, Perth, 4524-4537.
- Lin, I.J., Nadiv, S., and Grodzian, J.M., 1975. Changes in the state of solids and mechanochemical reactions in prolonged communition processes. Materials Science Engineering 7, 313-336.

.

- Ljachov, N., 1993. Mechanical activation from the viewpoint of kinetic reaction mechanisms, Int.Conf. on Mechanochemistry, ñInCoMe ó93ò. (Tkacova, ed.), Vol.1, Kosice, Cambridge Interscience Publishing, Cambridge, 1994, 59-65.
- Mahmoud, M.H.H., Afifi, A.A.I. and Ibrahim, I.A., 2004. Reductive leaching of ilmenite ore in Hydrochloric acid for preparation of synthetic rutile. Hydrometallurgy, 73, 99-109.
- Malconov, V.I., Jusupov, T.S., 1981. Physical and Chemical Properties of Fine Milled Minerals. Nedra, Moscow.
- Malcanov, V.I., Selezneva, O.G., Zirnov, E.N., 1988. Activation of Minerals by Grinding, Nedra, Moscow.
- Manna, I., Nandi, P., Nambissan, G., 2004. Mechanism and Kinetics of solid-state amorphization by mechanical alloying of $Al_{65}Cu_{35-x}Nb_x$.
- Mehrotra, S.P., 2007. Mechanochemical processing of Minerals and Wastes-Scientific curiosity to commercial reality.
- Merva, M., Kupka,J., 1973, Elektrotech.Cas., 24, 108.
- Meyer, K., 1977, Physico-Chemical Crystallography, VEB Deutscher Verlag fur Grundstoffindustrie, Leipzig.
- McEnroe et al., 2002, Geophysical Journal International 151, 890-912.
- Molchanov, V.V., Buyanov, R.A., 2000. Mechanochemistry of catalysts. Russ.Chem. Rev, 69, 435-450.
- Morad, S. and Aldahan, A. A., 1982. Authigenesis of titanium minerals in two Proterozoic sedimentary rocks from southern and central SwedenJour. Sediment. Petrol., 52, 1295.
- Mukherjee, T.K., 2000. Exploitation of heavy mineral resources in India. Handbook of Placer Mineral Deposits.
- Mullov, V., Lodejscikov, V.V.,1979. Izvestija SO AN SSSR, 3, 71.
- Murthy, B.S., Ranganathan, S., 1998. Novel Material Synthesis by Mechanical alloying/mixing, International Materials Review 43, 101-143.

.

- Murty, C.V.G.K., Asokan, S., Chatterjee, A. and Muthuraman, B., 2004, Int. Sym. On Metal and Materials from Titanium Minerals, Ed., Mohandas, P.N, Suresh Kumar, S., 82.
- Natziger, R.H. and Elger, G.W., 1987. ñPreparation of titanium feedstock from Minnesota ilmenite by smelting and sulfation-leachingò US Bureau of Mines, Report Invest No.9065.
- Ogasawara, T. and Velso de Araiya, R.V., 2000. Hydrochloric acid leaching of pre-reduced Brazilian ilmenite concentrate in an autoclave. Hydrometallurgy, 56**,** 203-216.
- Ohlberg, S.M., and Strikler, D.W., 1962. Determination of percent crystallinity of. partly devitrified glass by X-ray diffraction J.Am.Ceram.Soc., 45 , 4, 170-171.
- Olanipekun, E.O., 1999, A kinetic study of the leaching of a Nigerian ilmenite ore by hydrochloric acid. Hydrometallurgy, 53, 1-10.
- Oswald,W. Handbuch der Allgemeinen Chemie, 1.Auflabe, 2.Band, 3.Leipzig, 1887.
- Owens, D.K.,Wendt, R.C., 1969.Estimation of Surface Free Energy of Polymers. J.Appl.Polym.Sci.,13, 1741-1747.
- Parker, L.H., 1914, J.Chem.Soc. 105,1504.
- Parker, L.H., 1918, J.Chem.Soc. 113. 396.
- Pawlek, F.,1977. Verfahhren zur hydrometallurischen Aufarbeitung von Kupferkies, Kupfer-Nickel-Konzentraten und Ruckstanden, Zwischenproduckten und Flugstauben, Austria Patent No. 341231.
- Peters, K., Pajakoff, S., 1962. Microchim.Acta, 1-2, 314.
- Peters, K., 1962. Mechanochemische Reaktionen, Reaktionen, in: Proc. I.Europaischen Symp.ñZerkleinernñ (H.Rumpf, ed.), Weinheim, Frankfurt, 1962, pp.78-98.
- Pourghahramani, P., L. Thesis, 2006. Effect of Grinding Variables on Structural Changes and Energy conversion during Mechanical Activation

.

using Line Profile Analysis (LPA), Lulea Institute of Technology, Sweden.

- Putsov, L, Yu., Kaloshkin, S.D., Tcherdyntsev, V.V., Tomilin, I.A., Shelekhov, E.V., Salimon, I.A., 2001. Meter.Sci.For. 360-362:373-378.
- Rabanal, M.E., Varez, A., Levenfield, B., Torralba, J.M., 2003. Magnetic properties of Mg-ferrite after milling process. 143-144, 470-474.
- Rakesh Kumar, Alex,T.C.,Jha,M.K., Khan,Z.H.,Mahapatra,S.P., Mishra,C.R., 2004. in : Light Metals 2004, (Ed.) Tabereaux, A.T., The Minerals, Metals and Materials Society.
- Rakesh Kumar, Alex,T.C., Khan,Z.H., Mahapatra,S.P., Mehrotra,S.P., 2005. in: Light Metals 2005, (Ed.), K.Kvande, The Minerals, Metals and Materials Society.
- Rakesh Kumar, Sanjay Kumar,S., Badjena and Mehrotra,S.P., 2005. Hydration of mechanically activated balst furnace slag, Met. Mat. Trans. B, 36B ,473-484.
- Rao, D.S., Kumar, T.V.V., Prabhakar, S., Raju, G.B., 2005. Alteration characteristics of the Manavalakurichi ilmenite, Tamilnadu.Journal of Applied Chemistry 7 (2), 195ï 200.
- Rebinder,P.A.,1947. Proceedings of the Jubilee Session of the Academy of Sciences of USSR, (Izdat. Akademii Nauk SSSR), Moskva, p. 55.
- Russanov, A.I., 2000. Zh. Obshch. Khim.70, 353.
- Satyajeet Sharma, Suryanarayana, C., 2008. Effect of Nb on glass forming ability of mechanically alloyed Fe-Ni-Zr-B alloys. Scripta Materialia, 58, 508-511.
- Schaider, R., Tetzner, G., 1961. Z. Anorg. Allg. Chem. 309**,** 55.
- Schonert, K., 1982. About the particle breakage and the possibilities and limits for improving size-reduction process. In: Proceedings of Int. Symposium on Powder Technology, The Society of Powder Technology, Kyotto, pp. 331-345.

.

- Schonert, K., 1990. Physical and technical aspects of very and micro fine grinding. In: Proceedings of World Congress Particle Technology, Society of Powder Technology, Kyoto, pp.257-271.
- Schort, M.A, and Steward, E.G., Z.Phys.Chem., 13, 1957, 298.
- Schrader, R., Werner, K., 1975. Chem.Technol., 27, 156.
- Senna, M., 1989, Determination of effective surface area fro the chemical reaction of fine particular materials. Particles and Particle systems Characterization 6, 163-167.
- Senna, M., Crystal Res. Technol., 20, 1985, 209.
- Sepelak.V, Wibmann , S., Becker, K.D., 1999. Magnetism of nanostructured mechanically activated and mechanosynthesized spinal ferrites. 203, 135-137.
- Sepelak.V, Baabe.D, Mienert.D, Litterst, F.J., Becker, K.D., 2003. Enhanced magnetization in nanaocrystalline high-energy milled $MgFe_2O_3$. Scripta Materialia 48, 961-966.
- Sewry, J.D., Brown, M.E., 2002. Model-free kinetic analysis, Thermochim. Acta 390, 217ï 225.
- Shakhtshneider, T., Boldyrev,V., 1993. Drug Develop. Ind. Pharm., 19, 2055.
- Shaktshneider, T., Boldyrev, V., 1999. in Reactivity of Molecular Solids , 6400-6407. (Eds. Boldyreva, E., Boldyrev, V.), New York: Wiley, 1999, p.271.
- Sheng, H.W., Lu, K., Ma, E., 1999. Amorphization of Zr-Al solid solutions under mechanical alloying at different temperatures, J.Appl.Phys., 85,
- Shellinger, S.H., Lalkala, R.D., 1951, Min.Engg., 3, 523.
- Shellinger, S.H., 1952, Min.Eng., 4, 369.
- Shenoy, S.D., Joy, P.A., Anantharaman, M.R., 2004. Effect of mechanical milling on the structural, magnetic and dielectric properties of the co-precipitated ultrafine zinc ferrite. 269, 217-226.

.

- Sherif El-Eskandarany,M., Aoki, K., Itoth.H., and Suzuki.K., 1991. J.Less Com. Metals, 169, 235.
- Sinha,H.N.,1973. MURSO process for producing rutile substitute. Jaffe, R.I., Burte,H.M. (Eds.),Titanium Science and Technology. Cambridge, Massachusetts, pp. 233-244. May 2-5, 1972, A publication of the Metallurgical Society of AMIE, Plenum Press, New York ï London.
- Sinha H N 1984. Hydrochloric acid leaching of ilmenite. Proceeding of the Symposium on Extractive Metallurgy AusIMM Melbourne (Australia), The Australasian Institute of Mining and Metallurgy, Australia, 163-168.
- Sinha, H.N. 1979. Solubility of titanium minerals. International Conference on Advanced Chem. Metallurgy, 2(35), 16 p.
- Smekal,A., 1942. Ritzvorgang und molekulare Festigkeit. Naturwissenschaften, 30, 224-225.
- Stroiizdat Tallin, 1977. I. Hint, On Basic Problems of Mechanical Activation .
- Sukhikh, V.A., Yu, B.,1947. Khariton in Voprosy Izucheniya Vzryvchatykh Veshchestv (Studies into Explosives).Moscow, Academy of Sciences of the USSR, p.177.
- Suresh Babu, D.S., Thomas, K.A., Mohan Das, P.N., Damodaran, A.D.,1994. Alteration of ilmenite in the Manavalakurichi deposit, India.Clays and Clay Minerals 42, 567ï 571.
- Suresh Babu, D.S., Mohan Das, P.N., 1999. Mineralo-chemical assessment of ilmenites from the three Indian placers. Trans.Indian Inst. Met. 52 (2ï 3), 73ï 79.
- Suryanarayana, C., 1999. ed., Non-Equilibrium Processing of Materials, Pergamon, Oxford.
- Suryanarayana, C., 2001. Mechanical alloying and milling, Progress in Materials Science 46,1-184.
- Suryanarayana, C., 2004. Mechanical Alloying and Milling, Marcel Dekker, New York

.

- Takacks,L.,2000. Quick silver from cinnabar: the first documented mechanochemical reaction. JOM January, 12-13.
- Tamman, 1929, G. Z.Elektrochem., 35, 21.
- Temple, A. K., Econ. Geol., 1966, 61, 695.
- Theophrastus, De Lapidus, Translation and Commentary by D.E.Eichholz, Oxford University Press, 1965, p8.
- Thiessen,P.A., Meyer,K.,Heinicke,G., 1967. Grundlagen der Tribochemie, Akademie Verlag, Berlin.
- Thiessen, H., Heinicke, G., Schober, E.,1970. Z.Anorg. Allg.Chem, 377, 20.
- Tkacova,K., 1989.Mechanical Activation of Minerals, Elsevier Publishers, Amsterdam.
- Tkacova, K., Balaz, P., 1996. Reactivity of mechanically activated chalcopyrite. Int. J. Miner. Process. 44ï 45, 197ï 208.
- Tkacova, K., Balaz, P., Misuara, B., Vigdergauz, V.E. and Chanturiya, V.A. 1993. Selective leaching of zinc from mechanically activated complex Cu-Pb-Zn concentrate. Hydrometallurgy, 33, 291-300.
- Tkacova, K., Balaz., P., 1988. Structural and temperature sensitivity of leaching of chalcopyrite wit iron (III) sulphate. Hydrometallurgy 21, 103-112
- Tkacova, K., Sekula, F., Hochmanova, I., and Krupa, V.,1979. The determination of energy irreversibly accumulated in the grinding process, Preprints of Papers of the XIIIth Int.Mineral Processing Congress, J.Laskowski (ed.), Polish Sci. Publishers, Warshaw, 1979, p.499.
- Tkacova, K., Sepelak, V., Stevulova, N., Boldyrev, V.V., 1996.Structureï reactivity study of mechanically activated zinc ferrite.J. Solid State Chem. 123, 100ï 108.

.

- Tromans, D. and Meech, J.A., 1999. Enhanced dissolution of minerals: Microtopography and Mechanical Activation. Minerals Engineering,12, 609-625.
- Tromans, D., Meech, J.A., 2002. Enhanced dissolution of minerals: conjoint effects of particle size and microtopography. Miner.Eng. 15, 263ï 269.
- Tromans, D., Meech, J.A., 2004. Fracture toughness and surface energies of covalent minerals: theoretical estimates. Miner.Eng. 17, 1ï 15.
- Tsuchida, H., Narita, E., Takeuchi, H., Adachi, M. and Okabe, T., 1982. Manufacture of high pure titanium (IV) oxide by chloride process. I kinetic study on leaching ilmenite ore in concentrated hydrochloric acid solution. Bull. Chem. Soc. Japan, 55, 1934-1938.
- Turke, W., and Fischer, P., 1978. Hydrometallurgical Treatment of Complex Copper Sulphide Concentrates with Special Reference to the Lurgi-Mitterberg Process, Proc.Int. Symp. ñComplex Metallurgyõ78ò (Jones, M.J., ed.), Bad Harzburg, 101-112.
- U.S.Environmental production Agency. ñTitanium Tetrachloride Production by the Chloride Ilmenite Processò. From Technical Background Document supporting the Supplemental Proposed Rule applying phase IV Land Restriction to Newly Identified Mineral processing Wastes. Dec.1995
- Valiama, J., 1993. Research on ilmenite concentrates (in Finnish), Research Report, University of Turku, Department of Geology and Mineralogy.
- Valima, J., 1992. Research on ilmenite concentrates. MSc Thesis, University of Turku, Department of Geology and Mineralogy.
- Van Dyk, J.P., Vegter, N.M. and Pistorius, P.C., 2002. Kinetics of ilmenite dissolution in hydrochloric acid. Hydrometallurgy 65, 31-36.
- Varhegyi, G., Szabo, P., Jakab, E., Till, F., 2001. Least squares criteria for the kinetic evaluation of thermo analytical experiments. Examples from a

.

char reactivity study. Journal of Analytical and Applied Pyrolysis 57, 203ï 222.

- Vaughan, J.,Alfantazi,A., 2004. Presented at ñPressureHydrometallurgy Conferenceò held at Banff, Alberta, Canada during 23ï 27 October 2004. full paper at mmat.ubc.ca/units/bioh/people/vaughan/files/PH 2004.doc.
- Vogel, 1989. Textbook of Quantitative Chemical Analysis, ELBS Publishers, Singapore.
- Vyazovkin, S., Wight, C.A., 1999. Model-free and model-fitting approaches to kinetic analysis of isothermal and no isothermal data. Thermochim. Acta 340ï 341, 53ï 68.
- Walpole, E.A., 1997. The Austpac ERMS and EARS processes. A cost effective route to high-grade synthetic rutile and pigment grade TiO_2. Heavy Minerals, SAIMM, Johannesburg, 169-174.
- Wanetig, P., 1922. Textilforschung 4, 154.
- Wanetig, P., 1925, Texilforschung. 3, 66.
- Wanetig, P., 1927. Kolloid Z. 41**,** 152.
- Washburn, E.W., 1921. The dynamics of Capillary Flow. Phys.Rev., 17, 273-283.
- Weeber, A.W., Bakker, H., deBoer, F.R., 1986. Euro. Phys. Lett. , 2, 445-453.
- Welham, N.J., 1997. Enhancement of the dissolution of ilmenite (FeTiO3) by extended milling. Trans. Inst. Min. Metall., Sec. C,C138ï C141.
- Welham, N.J., 2001. Enhanced dissolution of tantalite/columbite following milling. Int. J. Miner. Process. 61, 145ï 154.
- Welham, N.J., Llewellyn, D.J., 1998. Mechanical enhancement of the dissolution of ilmenite. Miner. Eng. 11, 827ï 841.
- Zelikman, A.N., Voldman, G.M., Beljaevskaja, L.V., 1975. Theory of Hydrometallurgical Processes. Metallurgija, Moscow, In Russia.

.

- Zeto, R., Roy, R., in: Reactivity of Solids, Proceedings of 6th International Symposium on the Reactivity of Solids, New York: Wiley, 1969. P.803.
- Zhang, Q., Matsumotto, H., Saito, F., Baron, M,, 2002. Chemosphere 48, 787.
- Zhao, Y.H., Jin, Z.H., Lu, K., 1999.Mechanical-Milling-induced amorphization of Se: a crystallite destabilization model. Phil. Mag. Let. 79, 9, 747-74.

.

LIST OF PUBLICATIONS

PULICATIONS IN JOURNALS

1. Sasikumar,C., Rao, D.S.,Srikanth, S.,Ravikumar, B., Mukhopadhyay, N.K., and Mehrotra, S.P.,2004. Effect of mechanical activation on the kinetics of sulfuric acid leaching of beach sand ilmenite from Orissa, India. *Hydrometallurgy,* vol 75, Issue 1-4, pp.189-204.
2. Sasikumar,C., Rao, D.S.,Srikanth.,S Narashiman,B.R.V, Ravikumar, B., Mukhopadhyay, N.K., and Mehrotra, S.P.,2006. Effect of Natural Weathering and Mechanical Activation on the Acid Dissolution Kinetics of Indian Beach Sand Ilmenites. *Metals Materials and Processes,* vol 18, no3. 211-224.
3. Sasikumar,C., Rao, D.S.,Srikanth, S., Mukhopadhyay, N.K., and Mehrotra, S.P.,2007. Dissolution Studies of Mechanically Activated Manavalakurichi Ilmenite with Hcl and H_2SO_4. *Hydrometallurgy,*Vol 88, Issue 1-4, pp 154-169.
4. Sasikumar,C., S.,Srikanth, Mukhopadhyay, N.K., and Mehrotra, S.P.,2009. Energetics of Mechanical Activation- Application to Beach Sand Ilmenite. *Minerals Engineering,* (in press).

PULICATIONS IN CONFERENCE PROCEEDINGS

5. Srikanth, S., Sasikumar, C., Rakesh Kumar. Energetics and effect of mechanical activation of materials, *EMC 2007 conference proceedings*, 4th biennial international European metallurgical conference held at Düsseldorf in June 2007. Vol :4, Issue: ISBN 978-3-940276-07-p 2015.
6. Sasikumar, C, Srikanth,S., Rakesh Kumar, Alex' T.C.,Mehrotra, S.P., 2008. Where does the energy go in high energy milling?. In: VI th International Conference on Mechanochemistry and Mechanical Alloying, held at NML Jamshedpur, India.in Nov.2008, (in press).

.

LIST OF PRESENTATIONS

1. Sasikumar,C., Rao, D.S.,Srikanth, S., Mukhopadhyay, N.K., and Mehrotra, S.P., 2004. Effect of mechanical activation on kinetics of dissolution of orissa ilmenite. ISRS 2004**,** International Seminar for Research Scholars , held at Indian Institute of Technology, Chennai in Dec 2004.
2. Sasikumar,C., Rao, D.S., Srikanth, S., Mukhopadhyay, N.K., 2005. Effect of mechanical activation on liberation of TiO_2 from beach sand ilmenite. NMD-ATM 2005**,** International Annual Technical Meeting, held at Indian Institute of Technology Chennai on Nov. 2005.
3. Sasikumar, C., Mukhopadhyay, N.K., Srikanth.S. 2006. Dissolution kinetics of mechanically activated beach placer ilmenite in H_2SO_4. ETMPT 2005, A National Seminar on Emerging Trends in Metallurgical Processing and Tribochemistry, Organized by Met. Engg. Dept. IT-BHU, held at IT-BHU Varanasi on March 2006.
5. Mukhopadhyay, N.K Sasikumar,C., and Srikanth, S, 2006. An investigation of the effect of mechanical activation on leaching kinetics of ilmenite in HCl and H_2SO_4. INCOME 2006**,** International Seminar on Mechnao-chemistry and Mechanical alloying organized by scientific centre of Russian academy of sciences, held at Russia in July 2006.
6. Srikanth, S., Sasikumar, C., Rakesh Kumar. Energetics and effect of mechanical activation of materials, EMC 2007 conference proceedings**,** 4^{th} biennial international European metallurgical conference held at Düsseldorf in June 2007.
7. Sasikumar, C, Srikanth,S., Rakesh Kumar, Alex' T.C.,Mehrotra, S.P., 2008. Where does the energy go in high energy milling?. In: VI th International Conference on Mechanochemistry and Mechanical Alloying, held at NML Jamshedpur, India., Nov.2008.

.